



## Durham E-Theses

---

### *Biosynthetic studies on fluoroacetate and longianone*

Goss, Rebecca Jane Miriam

#### How to cite:

---

Goss, Rebecca Jane Miriam (2000) *Biosynthetic studies on fluoroacetate and longianone*, Durham theses, Durham University. Available at Durham E-Theses Online: <http://etheses.dur.ac.uk/4546/>

#### Use policy

---

The full-text may be used and/or reproduced, and given to third parties in any format or medium, without prior permission or charge, for personal research or study, educational, or not-for-profit purposes provided that:

- a full bibliographic reference is made to the original source
- a [link](#) is made to the metadata record in Durham E-Theses
- the full-text is not changed in any way

The full-text must not be sold in any format or medium without the formal permission of the copyright holders.

Please consult the [full Durham E-Theses policy](#) for further details.

*Blessed is the man who finds wisdom,  
the man who gains understanding,  
for she is more profitable than silver  
and yields better returns than gold.*

*Proverbs 3: 13&14*

# Biosynthetic Studies on Fluoroacetate and Longianone

*Rebecca J M Goss*

This thesis explores the biosynthesis of two secondary metabolites, fluoroacetate and longianone, and involves the synthesis and feeding of deuterated putative intermediates.

The bacterium *Streptomyces cattleya* produces fluoroacetate and 4-fluorothreonine; the mechanism by which C-F bond formation occurs is unknown. The stereochemistry of the fluorination event was investigated by feeding [2,2,3,3-<sup>2</sup>H<sub>4</sub>]-succinate and (2*R*)-[1-<sup>2</sup>H<sub>2</sub>]- and (2*S*)-[1-<sup>2</sup>H<sub>2</sub>]-glycerols. The chirality of the resultant [2-<sup>2</sup>H]-fluoroacetate was determined by chiral liquid crystal <sup>2</sup>H-NMR and the fluorination was demonstrated to proceed with retention of stereochemistry.

Longianone is produced by the slow growing fungus *Xylaria longiana*. This simple bicyclic metabolite is an isomer of the notorious fungal toxin patulin. Putative deuterated intermediates were administered to the fungus and the longianone produced analysed by <sup>2</sup>H-NMR. It was demonstrated that longianone is biosynthesised from 6-methylsalicylic acid in a pathway closely related to that found in patulin biosynthesis.

**Biosynthetic Studies on Fluoroacetate  
and Longianone**

**Rebecca Jane Miriam Goss**

**PhD Thesis 2000**

**University of Durham  
Department of Chemistry**

## *Declaration*

The work contained in this thesis was carried out by the author in the Department of Chemistry, University of Durham between October 1997 and September 2000. Part of the work was conducted in collaboration with the Institut de Chimie Moléculaire d'Orsay, Université de Paris Sud, France. Chiral liquid crystal  $^2\text{H}$ -NMR analyses, on samples submitted by the author, were performed by Dr Abdelkrim Meddour at the Institut de Chimie Moléculaire d'Orsay.

## *Copyright*

The copyright of this thesis rests with the author. No quotation from it should be published without their prior written consent, and information derived from it should be acknowledged.

## *Acknowledgements*

I would like to thank my supervisor, Professor David O'Hagan for his unfailing support and encouragement throughout the duration of the project, especially at times when the organisms refused to produce any measurable quantities of their respective secondary metabolites.

Dr Abdelkrim Meddour and Professor Jacques Courtieu at the Institut de Chimie Moléculaire d'Orsay, not only for analysing countless samples that I sent them, but also for their instruction in the use of chiral liquid crystal  $^2\text{H}$ -NMR and their generous hospitality when I visited their labs.

I would like to thank all the technical support staff within the Department of Chemistry, specifically Mr Ian McKeag and Dr Alan Kenwright for tirelessly running  $^2\text{H}$ -NMR and their enthusiasm and talent in running chiral liquid crystal  $^2\text{H}$ -NMR experiments for me.

I would like to acknowledge all my colleagues in the lab and the department for their help, advice and for making the department an interesting and stimulating working environment. The glassblowers should be recognised not only for their helpfulness and expertise, but also for their cheerful and welcoming attitude. Dr Jens Nieschalk and Dr Jens Fuchser are especially to be thanked for imparting much help and advice during my first few months in the lab.

Especially, I would like to thank Jules for the countless ways in which he has helped me in the final preparation of my thesis and for being a wonderful friend.

Finally I would like to thank the Isle of Man Education Authority for the provision of funding.

## ***List of Contents***

<b>Table of Contents</b>	<b>v</b>
<b>List of Figures</b>	<b>x</b>
<b>List of Schemes</b>	<b>xii</b>
<b>List of Tables</b>	<b>xv</b>
<b>List of Abbreviations</b>	<b>xvi</b>

### ***Chapter 1: Introduction***

<b>1.1 Secondary metabolism</b>	<b>2</b>
1.1.1 Primary and secondary metabolism	
2.1.2 Secondary metabolism in microbial systems	
<b>1.2 Methods of investigating the biosynthesis of secondary metabolites</b>	<b>6</b>
1.2.1 Inhibition of enzymes	
6.2.2 Genetic mutations	7
1.2.3 Radioisotopic labelling studies	10
1.2.4 Stable isotope labelling studies	10
<b>1.3 Stereochemical biosynthetic investigations</b>	<b>13</b>
<b>1.4 Topics addressed in this thesis</b>	<b>14</b>
<b>References</b>	<b>16</b>

**Chapter2**  
***Chiral Analysis by Chiral Liquid Crystal  $^2\text{H}$ -NMR***

<b>2.1</b>	<b>Methods of determining enantiomeric excess</b>	<b>18</b>
<b>2.2</b>	<b>The chiral analysis of labelled biosynthetic fluoroacetate</b>	<b>21</b>
<b>2.3</b>	<b>The use of chiral liquid crystal deuterium NMR for chiral resolution</b>	<b>23</b>
	2.3.1 An introduction to liquid crystals	23
	2.3.2 The use of PBLG as a solvent for NMR analysis	25
	2.3.3 Sample preparation for chiral liquid crystal NMR	
<b>2.4</b>	<b>The synthesis of (S)-[<math>^2\text{H}</math>]-fluoroacetate</b>	<b>28</b>
<b>2.5</b>	<b>Chiral analysis of (S)-[<math>^2\text{H}</math>]-fluoroacetate</b>	<b>35</b>
<b>2.6</b>	<b>Investigating the enantiomeric excess of fluoroalkanes</b>	<b>37</b>
	<b>References</b>	<b>42</b>

**Chapter3**  
***Fluorine in Bioorganic Chemistry***

<b>3.1</b>	<b>A historical perspective of fluorine</b>	<b>44</b>
<b>3.2</b>	<b>The nature of the carbon fluorine bond</b>	<b>45</b>
<b>3.3</b>	<b>Fluorine's effect upon the bioactivity of molecules</b>	<b>45</b>
<b>3.4</b>	<b>Fluorine's role in medicine</b>	<b>46</b>
<b>3.5</b>	<b>Halogenated natural products</b>	<b>48</b>
<b>3.6</b>	<b>Mechanisms for biohalogenation</b>	<b>50</b>
<b>3.7</b>	<b>Fluorinated secondary metabolites</b>	<b>52</b>
	3.7.1 Nucleocidin	53
	3.7.2 Fluoroacetate	54
	3.7.3 $\omega$ -Fluorofatty acids	55
	3.7.4 Fluoroacetone	57
	3.7.5 (2R, 3R)-2-Fluorocitrate	57
<b>3.8</b>	<b>Resistance to fluoroacetate poisoning</b>	<b>58</b>
<b>3.9</b>	<b>Proposed mechanisms of biological fluorination</b>	<b>60</b>



3.9.1	Formation of the C-F bond by addition of fluoride to a carbon-carbon multiple bond	60
3.9.1.1	Pyridoxal phosphate catalysed incorporation of fluoride	60
3.9.1.2	Fluorination of ethylene	62
3.9.2	Nucleophilic substitution by fluoride	63
3.9.3	Nucleophilic attack by fluoride on a halonium ion	63
<b>3.10</b>	<b>Contemporary studies into biological fluorination</b>	<b>65</b>
<b>3.11</b>	<b>The Biosynthesis of fluoroacetate and 4-fluorothreonine</b>	<b>66</b>
	<b>References</b>	<b>72</b>

## **CHAPTER 4**

### ***The Stereochemical Course of Biological Fluorination in Streptomyces cattleya***

<b>4.1</b>	<b>Introduction</b>	<b>78</b>
<b>4.2</b>	<b>The stereochemical processing of succinate through the Krebs cycle and glycolysis</b>	<b>80</b>
4.2.1	The conversion of succinate to fumarate	80
4.2.2	The conversion of fumarate to malate	82
4.2.3	The Conversion of malate to phosphoenol pyruvate	82
4.2.4	Metabolic processing of [2,2,3,3- <sup>2</sup> H <sub>4</sub> ]-succinate	83
4.2.5	[2,2,3,3- <sup>2</sup> H <sub>4</sub> ]-Succinate feeding experiments	85
4.2.6	Conclusion	87
<b>4.3</b>	<b>Experiments with (2R)-[1-<sup>2</sup>H<sub>2</sub>]- and (2S)-[1-<sup>2</sup>H<sub>2</sub>]-glycerols</b>	<b>87</b>
4.3.1	Synthesis of chiral glycerols	88
4.3.2	Synthesis and feeding of (1S, 2R)-[1- <sup>2</sup> H]-glycerol	91
4.3.3	Synthesis of (1R, 2R)-[1- <sup>2</sup> H]-glycerol	95
4.3.5	Results from the feeding of the chiral glycerols	97
<b>4.4</b>	<b>Conclusions</b>	<b>98</b>
<b>4.5</b>	<b>Possible mechanisms of fluorination</b>	<b>99</b>
	<b>References</b>	<b>100</b>

**CHAPTER 5**  
***The Biosynthesis of Longianone***

5.1	Introduction	102
5.2	Naturally occurring analogues of longianone	103
5.3	Fatty acids and polyketides	104
5.4	Fatty acid biosynthesis	105
5.5	Polyketide biosynthesis	108
5.6	Patulin and its biosynthesis	109
5.7	Initial investigations into the biosynthesis of longianone in <i>X. longiana</i>	113
5.8	Synthesis of [3,5- <sup>2</sup> H <sub>2</sub> ]-6-methylsalicylic acid	116
5.9	Synthesis of [2,4,6- <sup>2</sup> H <sub>3</sub> ] <i>m</i> -cresol	118
5.10	Synthesis of [7,7- <sup>2</sup> H <sub>2</sub> ] <i>m</i> -hydroxybenzylalcohol	118
5.11	Feeding experiments with [3,5- <sup>2</sup> H <sub>2</sub> ]-6-methylsalicylic acid, [2,4,6- <sup>2</sup> H <sub>3</sub> ] <i>m</i> -cresol and [7,7- <sup>2</sup> H <sub>2</sub> ] <i>m</i> -hydroxybenzylalcohol	118 121
5.12	Synthesis of [2,4,6,7,7- <sup>2</sup> H <sub>5</sub> ] <i>m</i> -hydroxybenzylalcohol	122
5.13	Feeding experiment with [2,4,6,7,7- <sup>2</sup> H <sub>5</sub> ] <i>m</i> -hydroxybenzylalcohol	123
5.14	Levels of incorporation of the deuterated intermediates	123
5.15	Discussion	123
	References	124

**CHAPTER 6 : Experimental**

6.1	Chemical Synthesis	127
6.1.1	General	127
6.1.2	Preparation of ( <i>S</i> )-hexyl-[ <sup>2</sup> H]-fluoroacetate (2.17a)	128
6.1.3	Preparation of various fluoro- deutero-alkanes	132
6.1.3.1	Preparation of 2-fluoro[2- <sup>2</sup> H]-hexane (2.28)	
6.1.3.2	Preparation of 3-fluoro[3- <sup>2</sup> H]-hexane (2.30)	
6.1.3.3	Preparation of 2-fluoro[2- <sup>2</sup> H]-heptane (2.32)	134
6.1.3.4	Preparation of 3-fluoro[3- <sup>2</sup> H]-heptane (2.34)	135

6.1.3.5	Preparation of 3-fluoro[3- <sup>2</sup> H]-octane (2.36)	136
6.1.3.6	Preparation of 4-fluoro[4- <sup>2</sup> H]-octane (2.39)	137
<b>6.1.4</b>	<b>Preparation of deuterated chiral glycerols</b>	<b>144</b>
<b>6.1.5</b>	<b>Preparation of deuterated compounds with which to investigate the biosynthesis of longianone</b>	
6.1.5.1	Preparation of [3,5- <sup>2</sup> H <sub>2</sub> ]-6-methylsalicylic acid (5.27a)	144
6.1.5.2	Preparation of [2,4,6- <sup>2</sup> H <sub>3</sub> ] <i>m</i> -cresol (5.28a)	150
6.1.5.2	Preparation of [7,7- <sup>2</sup> H <sub>2</sub> ] <i>m</i> -hydroxybenzylalcohol	148
6.1.5.4	Preparation of [2,4,6,7,7- <sup>2</sup> H <sub>5</sub> ] <i>m</i> -hydroxybenzylalcohol	149
 <b>6.2 Biological</b>		
<b>6.2.1</b>	<b>General details</b>	<b>150</b>
<b>6.2.2</b>	<b><i>Streptomyces cattleya</i></b>	<b>150</b>
6.2.2.1	Agar	150
6.2.2.2	Starter and batch cultures	151
6.2.2.3	Resting cell experiments with <i>S. cattleya</i>	152
6.2.2.4	Harvesting fluoroacetate	152
<b>6.2.3</b>	<b><i>Xylaria longiana</i></b>	<b>153</b>
6.2.3.1	Agar	153
6.2.3.2	Culture medium	153
6.2.3.3	Feeding of labelled precursors to <i>X. longiana</i>	154
6.2.3.4	Extraction of longianone from <i>X. longiana</i>	154
 <b>6.3</b>	 <b>Analysis of samples by chiral liquid crystal <sup>2</sup>H-NMR</b>	 <b>155</b>
 <b>References</b>		 <b>156</b>

### *Appendices*

<b>Appendix I:</b>	<b>List of conferences attended</b>	<b>157</b>
<b>Appendix II:</b>	<b>Publication</b>	<b>158</b>

## *List of Figures*

Fig 1.1	Chaetoglobosin A and metyrapone	6
Fig. 1.2	Blasticidin S	7
Fig 1.3	Novel lactones produced by incorporating the loading module from the avermectin PKS into the DEBS 1 TE construct	9
Fig. 2.1	$\alpha$ -Methoxy- $\alpha$ -(trifluoromethyl)phenyl-acetic acid	21
Fig. 2.2	Chiral derivatives of fluoroacetate	21
Fig. 2.3	Retey's analysis of ( <i>S</i> )- and ( <i>R</i> )-[ $^2\text{H}$ ]-fluoroacetate by CD in $\text{CF}_3\text{CH}_2\text{OH}$	22
Fig. 2.4	The molecular ordering in the three liquid crystalline phases	24
Fig. 2.5	The $^2\text{H}$ NMR of a racemic RCHDOH in a) an isotropic solvent, b) a nematic liquid crystalline solvent, c) a chiral nematic liquid crystalline solvent	26
Fig. 2.6	Modified conical flask used to centrifuge the liquid crystalline material within an NMR tube	28
Fig 2.7a	$^2\text{H}$ NMR of ( <i>R</i> )-[7- $^2\text{H}$ ]-benzyl alcohol displaying an e.e. of 88%	33
Fig 2.7b	$^2\text{H}$ NMR of ( <i>S</i> )-[7- $^2\text{H}$ ]-benzyl fluoride, displaying an e.e. of 38%.	34
Fig 2.8	$^2\text{H}$ NMR of hexyl (2 <i>S</i> )-[2- $^2\text{H}$ ]- fluoroacetate in PBLG and chloroform, displaying an e.e. of 38%.	36
Fig 2.9a-e	$^2\text{H}$ NMR of fluoro alkanes in PBLG and chloroform	38
Fig. 3.1	9- $\alpha$ -Fluoro-hydrocortisone acetate	46
Fig. 3.2	Fluorine containing drugs	46
Fig 3.3	7-Fluoro-PGI <sub>2</sub>	
Fig 3.4 48	Halogenated natural products	
Fig 3.5 49	Nucleocidin	54
Fig 3.6	Fluoroacetate	
Fig 3.7 54	Thienamycin and 4-fluorothreonine	
		65

Fig 4.1a	$^2\text{H}$ NMR of hexyl-[2- $^2\text{H}$ ]-fluoroacetate ee 25% in favour of ( <i>R</i> )-configuration, after incubation of <i>S. cattleya</i> with [2,2,3,3- $^2\text{H}_4$ ]-succinate	86
Fig 4.1b	$^2\text{H}$ NMR of synthetic hexyl-[2- $^2\text{H}$ ]- fluoroacetate 38 % ee in favour of ( <i>S</i> )-configuration.	86
Fig. 4.2	The four stereoisomers of mono-deuterated glycerol	
Fig 4.3 88	$^2\text{H}$ NMR of synthetic (1 <i>S</i> , 2 <i>R</i> )-[1- $^2\text{H}$ ]-glycerol using PCBL in dimethyl formamide as the chiral solvent	94
Fig 4.4	$^2\text{H}$ NMR of synthetic (1 <i>R</i> , 2 <i>R</i> )-[1- $^2\text{H}$ ]-glycerol using PCBL in dimethyl formamide as the chiral solvent	96
Fig 4.5a	$^2\text{H}$ NMR of hexyl-[2- $^2\text{H}$ ]-fluoroacetate, from <i>S. cattleya</i> fed (1 <i>S</i> , 2 <i>R</i> )-[1- $^2\text{H}$ ]-glycerol	97
Fig 4.5b	$^2\text{H}$ NMR of hexyl-[2- $^2\text{H}$ ]-fluoroacetate, from <i>S. cattleya</i> fed (1 <i>R</i> , 2 <i>R</i> )-[1- $^2\text{H}$ ]-glycerol	97
Fig 4.5c	$^2\text{H}$ NMR of synthetic (2 <i>S</i> )-[2- $^2\text{H}$ ]-hexylfluoroacetate	97
Fig. 5.1	Metabolites of <i>X. longiana</i>	102
Fig. 5.2	Chilenones	103
Fig. 5.3	Natural products containing furane-3-one	103
Fig. 5.4	Secosyrins and syringolides	104
Fig. 5.5	Maitotoxin	105
Fig 5.6	Fatty acids	106
Fig. 5.7	$^{13}\text{C}$ NMR of [1,2- $^{13}\text{C}_2$ ]-acetate fed longianone	114
Fig 5.7	$^2\text{H}$ NMR Results from the feeding of the labelled aromatics	
Fig 5.9 119	$^2\text{H}$ NMR After feeding [2,4,6,7,7- $^2\text{H}$ ] <i>m</i> -hydroxybenzylalcohol	122

## *List of Schemes*

Scheme 1.1	The assembly of 6-deoxythronolide B	8
Scheme 1.2	The truncated erythromycin polyketide synthase DEBS 1 TE	9
Scheme 1.3	The alcohol dehydrogenase mediated conversion of ethanol to acetaldehyde	13
Scheme 1.4	The conversion of 2 <i>S</i> -[2- <sup>2</sup> H, 2- <sup>3</sup> H] acetyl-CoA to 2 <i>S</i> -[2- <sup>2</sup> H, 2- <sup>3</sup> H] malonyl-CoA, mediated by acetyl-CoA carboxylase	14
Scheme 2.1	The reaction of chiral acetyl-CoA with glyoxylic acid	19
Scheme 2.2	The resolution of chiral methyl groups using the kinetic isotope effect	20
Scheme 2.3	The condensation of fluoroacetyl-CoA with oxaloacetate	22
Scheme 2.4	The synthesis of fluoroacetate from glycine	28
Scheme 2.5	Réte's synthesis of chiral [2- <sup>2</sup> H]-fluoroacetate	30
Scheme 2.6	The synthesis of ( <i>S</i> )-[2- <sup>2</sup> H]-fluoroacetate from [7- <sup>2</sup> H]-benzaldehyde	31
Scheme 2.7	The stereoselective reduction of [7- <sup>2</sup> H]-benzaldehyde with ( <i>S</i> )-Alpine-Borane	32
Scheme 2.8	The steric course of an alcohol's reaction with DAST	32
Scheme 2.9	Derivatisation of ( <i>S</i> )-[ <sup>2</sup> H]-fluoroacetate as its hexyl ester	35
Scheme 3.1	Mode of action of 5-fluorouracil	47
Scheme 3.2	The haloperoxidase reaction	50
Scheme 3.3	Activation of halogens by peracetic acid formed from acetic acid and hydrogen peroxide	51
Scheme 3.4	Pyrrrolnitrin biosynthesis	52
Scheme 3.5	Biosynthesis of <i>threo</i> -18-fluoro-9,10 -dihydroxystearic acid	56
Scheme 3.6	Hypothetical biosynthesis of fluoroacetone	57
Scheme 3.7	Biosynthesis of fluorocitrate	58
Scheme 3.8	Putative mechanism for the defluorination of fluoroacetate	59

Scheme 3.9	The putative biosynthesis of $\beta$ -substituted alanines	60
Scheme 3.10	A proposed mechanism by which pyridoxal phosphate catalyses the incorporation of fluoride	61
Scheme 3.11	A putative biosynthesis of fluoroacetate from ethylene	62
Scheme 3.12	Reaction of a haloperoxidase with an alkene to form a 1,2-dihalo species	63
Scheme 3.13	The horseradish peroxidase catalysed formation of 2,3-fluoroiodopropan-1-ol from allyl alcohol	64
Scheme 3.14	Neidleman and Geigert's proposed biosynthesis of fluoroacetate by iodofluorination of an $\omega$ -unsaturated fatty acid	64
Scheme 3.15	A proposed biosynthesis of 4-fluorothreonine from fluoroacetate	66
Scheme 3.16	Incorporation of glycerol into fluoroacetate	67
Scheme 3.17	Possible biosynthetic routes to fluoroacetate through $\beta$ -hydroxypyruvate	68
Scheme 3.18	Incorporation of labelled glycine into fluoroacetate	69
Scheme 3.19	An explanation for the incorporation pattern resulting from the feeding of labelled glycine	70
Scheme 3.20	Results from the incubation of (2 <i>R</i> )-[1- <sup>2</sup> H <sub>2</sub> ]- and (2 <i>S</i> )-[1- <sup>2</sup> H <sub>2</sub> ]-glycerol with resting cell cultures of <i>S. cattleya</i>	71
Scheme 4.1	Glycolytic intermediates as candidate substrates for biological fluorination	79
Scheme 4.2	The succinate dehydrogenase mediated conversion of [2,2,3,3- <sup>2</sup> H <sub>4</sub> ]-succinate to [2,3- <sup>2</sup> H <sub>2</sub> ]-fumarate	80
Scheme 4.3	Tchen and van Milligan's demonstration of the steric course of the conversion of succinic acid to fumaric acid, mediated by the enzyme succinate dehydrogenase	81
Scheme 4.4	The fumarase mediated conversion of fumaric acid, in the presence of <sup>2</sup> H <sub>2</sub> O, to (2 <i>S</i> , 3 <i>R</i> )-[3- <sup>2</sup> H <sub>1</sub> ]-malic acid	82
Scheme 4.5	The malate dehydrogenase mediated conversion of malate to oxaloacetate	82
Scheme 4.6	The stereochemical course of the phosphoenol pyruvate	83

	carboxylase mediated conversion of phosphoenol pyruvate to oxaloacetate	
Scheme 4.7	Metabolic processing of [2,2,3,3- <sup>2</sup> H <sub>4</sub> ]-succinate	84
Scheme 4.8	The reaction of lithium aluminium hydride with propargyl alcohol <del>89</del> Lewis basic and Lewis acidic solvents	
Scheme 4.9	The <i>trans</i> reduction of propargyl alcohol and 3-[ <sup>2</sup> H <sub>1</sub> ]-propargyl alcohol	90
Scheme 4.10	The synthesis of (1 <i>S</i> , 2 <i>R</i> )-[1- <sup>2</sup> H]-glycerol	91
Scheme 4.11	(1 <i>S</i> , 2 <i>R</i> )-[1- <sup>2</sup> H]-Glycerol and the other minor components of the 92 glycerol mixture	
Scheme 4.12	The synthesis of (1 <i>R</i> , 2 <i>R</i> )-[1- <sup>2</sup> H]-glycerol	95
Scheme 4.13	The stereochemical outcome of administering [2,2,3,3- <sup>2</sup> H <sub>4</sub> ]-succinate, (1 <i>S</i> , 2 <i>R</i> )-[1- <sup>2</sup> H]-glycerol and (1 <i>R</i> , 2 <i>R</i> )-[1- <sup>2</sup> H]-glycerol to <i>Streptomyces cattleya</i>	98
Scheme 4.14	Possible mechanism of fluorination involving two inversion processes	99
Scheme 5.1	Biomimetic study of the formation of syringolide	104
Scheme 5.2	Activation of acetyl-CoA to malonyl-ACP	106
Scheme 5.3	Fatty acid biosynthesis	107
Scheme 5.4	Polyketide biosynthesis	108
Scheme 5.5	The biosynthesis of patulin	109
Scheme 5.6	Ring hydroxylation in the biosynthesis of patulin	110
Scheme 5.7	Processing of the aromatic ring in the biosynthesis of patulin	111
Scheme 5.8	Oxygen-18 Labelling experiments	112
Scheme 5.9	A hypothetical biosynthesis of longianone, which accounts for the 115 observed labelling pattern following the feeding of [1,2- <sup>13</sup> C <sub>2</sub> ]-acetate	
Scheme 5.10	The synthesis of [3,5- <sup>2</sup> H <sub>2</sub> ]- 6-methylsalicylic acid	116
Scheme 5.11	Synthesis of [2,4,6- <sup>2</sup> H <sub>3</sub> ] <i>m</i> -cresol	118
Scheme 5.12	Synthesis of [7,7- <sup>2</sup> H <sub>2</sub> ] <i>m</i> - hydroxybenzylalcohol	118
Scheme 5.13	Biosynthetic pathway to longianone accounting for the observed labelling patterns	120
Scheme 5.14	Synthesis of [2,4,6,7,7- <sup>2</sup> H <sub>5</sub> ] <i>m</i> -hydroxybenzylalcohol	121



### *List of Tables*

Table 2.1	Comparative e.e.s of [7- <sup>2</sup> H]-benzyl fluoride formed from ( <i>R</i> )-[7- <sup>2</sup> H]-benzyl alcohol (88% e.e) subjected to different fluorinating conditions	33
Table 2.2	Racemic fluoroalkanes	37
Table 2.3	The resolution of racemic fluoroalkanes by <sup>2</sup> H chiral liquid crystal NMR	41
Table 3.1	A comparison of the halogens	
Table 3.45	Relative concentrations of fluorine and chlorine upon earth	
Table 3.53	Comparative heats of hydration and redox potentials of the halogens	53
Table 5.1	Incorporation of [1,2- <sup>13</sup> C <sub>2</sub> ]-acetate into longianone	
Table 5.2	Incorporation levels of the deuterated intermediates	
	123	

## *List of Abbreviations*

●	Carbon-13 label
ACP	Acyl carrier protein
AT	Acyl transferase
ATP	Adenosine triphosphate
9-BBN	9-Borabicyclo[3.3.1] nonane
br	Broad
CI	Chemical ionisation
CoA	Coenzyme A
d	doublet
DCM	Dichloromethane
DEBS	6-Deoxyerythronolide B synthase
DH	Dehydrogenase
EI	Electron impact
ER	Enoyl reductase
FAS	Fatty acid synthase
GC-MS	Gas chromatography-mass spectrometry
HP	Hewlett Packard
KS	$\beta$ -keto ACP synthase
KR	$\beta$ -keto ACP reductase
m	multiplet
MES	2-( <i>N</i> -Morpholino)ethanesulphonic acid
MS	Mass spectrometry
6MSA	6-Methylsalicylic acid
NAD <sup>+</sup>	Nicotinamide adenine dinucleotide
NMR	Nuclear magnetic resonance spectroscopy
PBLG	Poly $\gamma$ -benzyl L-glutamate
PCBL	poly- $\epsilon$ -carbobenzoxy-L-lysine
PCC	Pyridinium chlorochromate
PKS	Polyketide synthase
ppm	Parts per million
rpm	Revolutions per minute

s	Singlet
Sp.	Species
Spp.	Species (plural)
t	triplet
TE	Thioesterase
THF	Tetrahydrofuran
TLC	Thin layer chromatography
UV	Ultra violet

# **CHAPTER 1**

## **Introduction**



# **CHAPTER 1**

## **Introduction**

### **1.1 Secondary metabolism**

#### **1.1.1 Primary and secondary metabolism**

In the early 19<sup>th</sup> century, at the birth of biochemistry as a distinct field of study, the scientific community believed that living matter was composed of a substance that was qualitatively very different to that of non-living matter. There existed a notion that the substance of living matter disobeyed the known laws of physics and chemistry. It must have come as something of a surprise to a colleague of Friedrich Wöhler, when in 1828 he received a letter from the aforementioned, excitedly stating: “I must tell you that I can prepare urea without requiring a kidney or an animal, either man or dog.”<sup>1</sup> Wöhler’s laboratory preparation of urea, by heating ammonium cyanate, is the first documented example of an organic compound, a substance previously only found in living systems, being formed from an inorganic salt which had not originated from an organism. At the time, this novel discovery had little effect in dispelling the persistent belief in vitalism, a theory which held that certain reactions could only take place in living organisms.

Today, primary metabolism has been almost fully elucidated. It exists as an intricate network of enzyme-catalysed cycles and pathways driven by adenosine triphosphate (ATP), the universal energy currency of the cell. From the meagre beginning of carbon dioxide, photosynthesis generates glucose, which is converted by the plant and its consumers to a wealth of diverse compounds known as primary metabolites. Primary metabolites include amino acids, sugars, acetyl-coenzyme A, fatty acids, mevalonic acid, and nucleotides. These compounds are essential to the growth and existence of the organism that produces them. The pathways producing the primary metabolites may be found in similar, though not identical forms, in all living organisms; the obvious exception being photosynthesis, which is unique to plants and phototrophic bacteria.

The mystery that once surrounded “organic” molecules as a whole, to some extent remains with secondary metabolites. Though named “secondary metabolites”,

idiolites or natural products, are perhaps more suitable names. There is nothing secondary in terms of these compounds' biological significance and their usefulness to mankind. Since prehistoric times plant extracts have been used to drug, heal and kill. Calabar beans and hemlock were used as judicial poisons and curare on the tips of poisoned arrows. In Shakespeare's play, "Romeo and Juliet", a visit to an apothecary is made to purchase a fatal poison,<sup>2</sup> whilst Friar Laurence supplies Juliet with a plant extract which sends her into a death like coma.<sup>3</sup> Famously, frankincense, the sweet resin from a spruce tree, and myrrh, a bitter aromatic transparent gum of use as a perfume and a medicine were presented by the magi at the birth of Christ.<sup>4</sup> The use of natural products is not restricted to history and folk law. Today, we rely upon many natural products as medicines to combat a range of illnesses.

The definition of a secondary metabolite has stimulated considerable debate. The compounds perform a variety of different roles from antibiotics to sex attractants, trail markers and antifoulants and antifeedants. Unlike primary metabolites, they have a restricted distribution and are often characteristic of individual species or strains. Their structure and size range from small simple molecules to the large and extremely elaborate.

A. L. Demain proposes that the simplest criterion by which to classify a secondary metabolite is that if you eliminate a secondary metabolic pathway, the organism will continue to grow.<sup>5</sup> In contradiction to this definition is the compound lanosterol, biosynthesised by sheep and excreted as a waterproofing agent. By itself, lanosterol is not essential to the existence of the sheep but it is an intermediate on the biosynthetic pathway to cholesterol, without which the sheep would die. Though secondary metabolites are biosynthesised from compounds produced in primary metabolism, it is not always the case that their synthesis is delayed until the cessation of growth, one notable example would be the production of idiolites by immature plants. In general, primary metabolites do not accumulate but are present in the organism at a low steady state concentration. However, the use of such a definition becomes contradictory in the case of yeasts, which produce alcohol as part of their growth process and yet use it to inhibit other forms of life.

To use Occam's razor, it should be stated that a secondary metabolite, whilst having no significant role in the internal economy of the producing organism, imparts the producer with an increased evolutionary fitness by its ability to protect itself and interact with its external surroundings.

So how did these natural products arise? Some theories suggest that natural products are merely shunt metabolites, an organism's method of removing toxins arising from secondary metabolism,<sup>6</sup> whilst others propose that they are designed in an organism's molecular playground.<sup>7</sup> However, many idiolites are highly complex and energetically very costly to produce, being encoded by many thousands of kilobases. The genetic code for "successful" natural products, has, in cases, been conserved for thousands of millions of years.<sup>8</sup> One would expect natural selection to work to obtain the desired physiological response at the minimum cost to the producer, but in some cases the natural products are so sophisticated that their interaction with the target sites mirror those between enzymes and their substrates. Such relationships are clearly not accidental.

The various groups of secondary metabolites may be classified by their biosynthetic origin. Fatty acids and their derivatives (e.g. prostaglandins) originate from the iterated decarboxylative condensation of malonyl extender units followed by a reduction an elimination and a further reduction, consecutively. The keto group is reduced to a hydroxyl, water is eliminated producing a double bond in the carbon chain which is then saturated (see section 5.4). Polyketides are formed in a very similar manner, although the reduction of the polyketone backbone is not complete as in the case of the fatty acids; it may stop at any one of the three stages (see section 5.5). The intermediates formed by the partial reductions may undergo cyclisations and aromatisations. The fact that most polyketide synthase (PKS) and fatty acid synthase (FAS) genes have a common evolutionary origin is suggested by a significant level of sequence homology, irrespective of their host. Some surprising findings have been made, however, in that the *P. patulum* PKS is genetically closer to a vertebrate FAS than its own fungal FAS.<sup>9</sup> This is not a case in isolation as the erythromycin producing PKS from *Saccharopolyspora erythraea* has the same order of active sites and general organisation as a vertebrate FAS.

Other classes of secondary metabolites include the alkaloids and non ribosomal polypeptides, which both originate from the pool of aminoacids supplied by primary metabolism, and isoprenoids, which are formed by two discrete pathways utilising either deoxyxylulose or mevalonic acid as the starting material.

### **1.1.2 Secondary metabolism in microbial systems**

Phase dependent biosynthesis of secondary metabolites is particularly apparent in micro-organisms. When the micro-organism is first introduced into a complex growth media there is a lag period before cell growth commences. Once the cells from the initial inoculum are established in primary metabolism, cell division and exponential growth occur, this is known as the trophophase. The trophophase continues until most of the available nutrients have been consumed. At this stage cell death begins and the idiophase has been entered. The factors instigating the production of the idiolites are complex and not well understood. The rate of growth is known to be important. A deficiency in nutrients is also significant, one piece of evidence for this is that few secondary metabolites are produced by bacteria living within the gut where there is a continuous and plentiful supply of nutrients. It is highly likely that other different factors stimulate various organisms into secondary metabolite production, for instance, *Streptomyces cattleya* requires both a reduced growth rate and a phosphate deficiency to produce its antibiotic, thienamycin.

Once faced by these unfavourable conditions, the organism seeks to maximise its chances of survival by becoming involved in secondary metabolism and sporulation. Secondary metabolism provides the chemical weapons with which to eliminate any other microorganism competing for the dwindling nutrient supply, whilst sporulation produces heat resistant cells, which may remain dormant until the organism is, once more, in a favourable growth environment. These two events occur concomitantly and in the *Streptomyces* spp. there is evidence that this is not just a coincidence as both are controlled by the same genes, known as “pleiotropic switches”.

It is likely that evolution dictates that such organisms only produce their natural products in the idiophase as many have antibiotic activity. Often resistance genes are clustered next to those encoding for the toxin, but these resistance mechanisms are inducible, and it is possible that the antibiotic could kill the producing culture if manufactured too early.



## 1.2 Methods of investigating the biosynthesis of secondary metabolites

There are two questions to be asked when investigating the biosynthesis of a secondary metabolite; firstly, from which primary metabolite does it have its origin and secondly, by what mechanisms and through which intermediates is it processed?

The structures of the secondary metabolites often hold many clues which allow speculation to the answers of both these questions. Large numbers of secondary metabolites are formed from one or two repeating units and compounds of polyketide or terpenoid origin are often easily identified. Other metabolites of similar structure, produced by the same or related species, are also helpful in predicting a possible biosynthesis. These speculations may be tested by a variety of methods now available to the chemist and biochemist.

### 1.2.1 Inhibition of enzymes

One method of determining the unknown intermediates upon a biosynthetic pathway is by using enzymatic inhibitors. A biosynthetic sequence may be summarised as:-  $A \rightarrow B \rightarrow C \rightarrow D$  where D is the secondary metabolite under investigation and A, B and C are the unknown intermediates. If an enzyme that is responsible for catalysing the conversion of C to D is inhibited, it is probable that unknown intermediate C will accumulate in sufficient quantities to be analysed, providing that C is not too unstable.

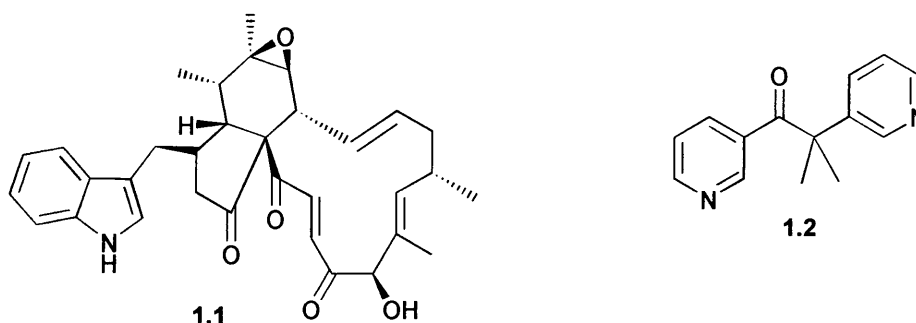


Fig 1.1 Chaetoglobosin A (1.1) and metyrapone (1.2)

In this manner the biosynthesis of chaetoglobosin A (1.1), produced by *Chaetomium subaffine*, was investigated. Chaetoglobosin A exhibits a considerable degree of oxidation, the workers thought it likely that the oxidative enzyme responsible was a cytochrome *P*-450. By using metyrapone (1.2), an inhibitor that blocks the *P*-450 enzyme, though not completely, a range of precursors accumulated in quantities large enough to be analysed, and the respective levels of each of the partially oxidised

precursors provided information as to the sequence of the oxidations.<sup>10</sup> The same approach was used by Steven J Gould and co-workers in isolating the precursors of blasticidin S (**1.3**) in *Streptomyces griseochromogenes*.<sup>11</sup> The bioavailability of L- $\alpha$ -arginine was reduced by using L- $\alpha$ -arginine biosynthetic inhibitors. Transaminase and methyl transferase inhibitors were also employed to block transamination and N-methylation, respectively. Using this strategy, it was possible for the workers to observe and identify previously unknown intermediates and thereby elucidate the biosynthesis of the compound.

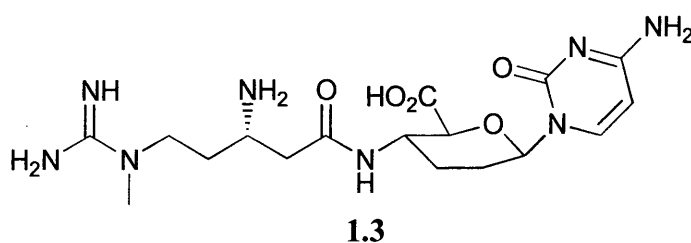


Fig. 1.2 Blasticidin S (1.3)

### 1.2.2 Genetic mutations

Rather than using an enzymatic inhibitor to block the biosynthetic pathway and accumulate precursors of the compound being investigated, it is also possible to disable enzyme expression at the genetic level. Mutations of the wild type organism may be effected by using UV, X-ray or chemical mutagenesis. The mutations generated by these methods are random and genes encoding for the enzymes involved in primary metabolism may also undergo mutations leading to the death of the organism. As the genes encoding for a polyketide are often clustered, more sophisticated techniques may be employed to cause mutations to specific genes, disabling specific enzymes so that their substrates may be elucidated.

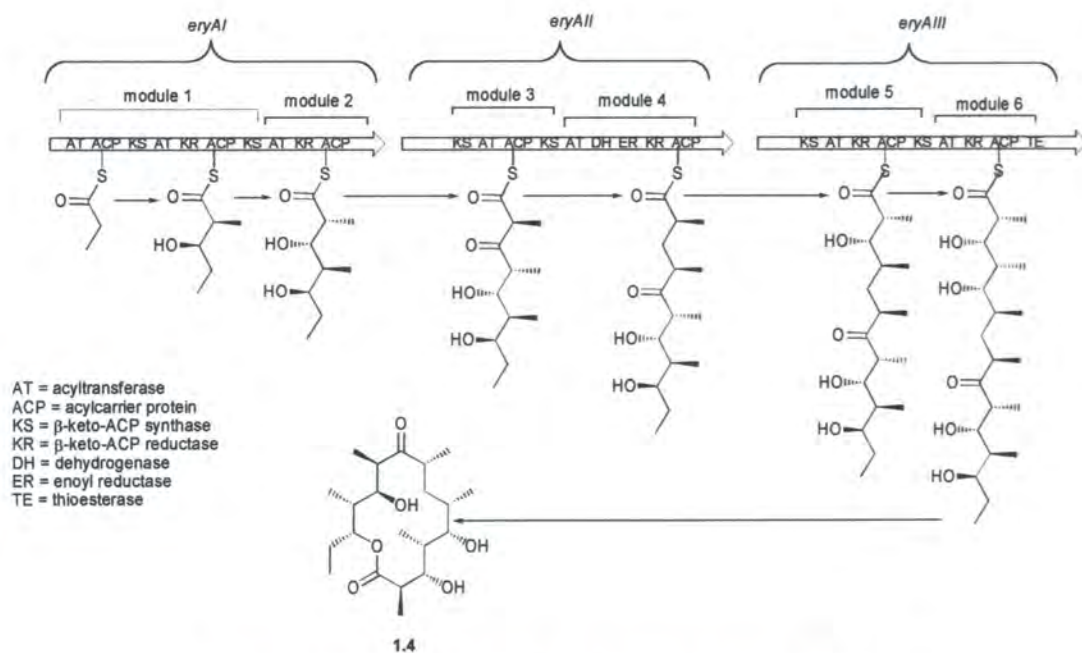
Polyketides have been subject to significant investigation at the genetic level. One reason for this is the desire for a thorough understanding of how these complex and often bioactive molecules are constructed such that further molecules, of potential pharmaceutical use, may be made using a combinatorial genetic approach.

Though the fungal polyketide synthase (PKS), 6-methylsalicylic acid (6MSA) synthase, was the first functional polyketide synthase to be isolated, the majority of the genetic studies on the PKSs have involved bacterial systems. These investigations have revealed that all of the genes encoding for the antibiotic, and resistance to it,

tend to be clustered together. These systems, therefore, readily facilitate over expression and cloning.

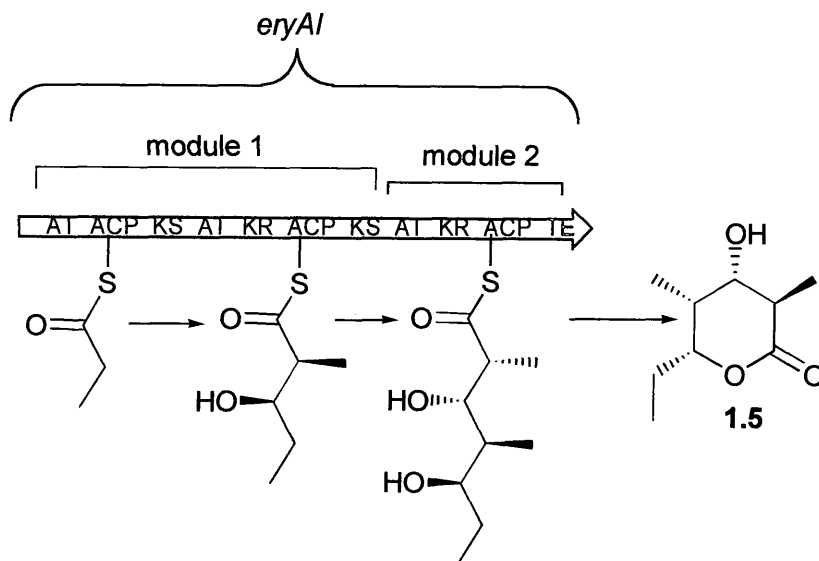
As with fatty acid synthases (FASs), PKSs may be classified as type I or type II. Type I PKSs are giant multifunctional enzymes containing different sets of active sites for each round of polyketide chain extension; type II PKSs consist of a few largely monofunctional enzyme subunits which cluster together into a complex.

The erythromycin PKS (6-deoxyerythronolide B synthase (DEBS)), has become the workhorse of many chemists and geneticists trying to develop a greater understanding as to how the PKSs function. DEBS, a type I PKS, is responsible for the sequential condensation and reduction cycles of propionyl Co-A with six units of malonyl Co-A generating the enzyme free intermediate 6-deoxyerythronolide B (1.4). This macrolide is further tailored to generate a series of active antibiotics. Genetic sequencing has revealed three large open reading frames (ORFs) *eryAI*, *eryAII*, and *eryAIII* encoding for the giant multifunctional proteins (“cassettes”) DEBS1, DEBS2 and DEBS3, respectively.<sup>12</sup> Each cassette of DEBS contains two modules, each of which is able to mediate a condensation event followed by the appropriate number of reductive transformations. The three cassettes function together as an assembly line to which the intermediates remain bound by thioester links.



Scheme 1.1 The assembly of 6-deoxyerythronolide B (1.4)

To investigate how the PKS functions, domains have been relocated along the gene. The first experiment of this type was the repositioning of the thioesterase, the final catalytic site on DEBS3, to the terminus of DEBS1.<sup>13</sup> This modified PKS resulted in the termination of the biosynthesis at the end of module 2, the polyketide chain was lactonised and released by the thioesterase domain to form the novel metabolite (3*S*,5*R*)-dihydroxy-(2*R*, 4*R*)-dimethyl-*n*-heptanoic acid- $\delta$ -lactone (**1.5**). This truncated form of the erythromycin polyketide synthase is known as “DEBS 1-TE” and is a useful tool with which to perform *in-vitro* mechanistic studies.



Scheme 1.2 The truncated erythromycin polyketide synthase DEBS 1 TE

Other genetic manipulations of the PKSs include substituting the loading modules to facilitate the production of a range of molecules with different starter units. One example of this is the incorporation of the loading module from the avermectin PKS into the DEBS 1 TE construct to produce lactones **1.6** and **1.7**.<sup>14</sup>

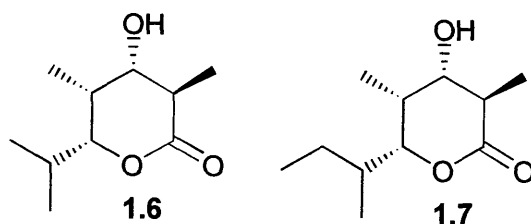


Fig 1.3 Novel lactones **1.6** and **1.7** produced by incorporating the loading module from the avermectin PKS into the DEBS 1 TE construct

### **1.2.3 Radioisotopic labelling studies**

One of the more classical methods of investigating the biosynthesis of secondary metabolites has involved using radioisotopes. A compound, which is thought to be an intermediate on a biosynthetic pathway, is synthesised containing a radioisotope such as  $^{14}\text{C}$ ,  $^3\text{H}$ , or  $^{32}\text{P}$ . After feeding of the “labelled” putative precursor to the producing organism, the resultant secondary metabolite is analysed by scintillation counting to determine whether the fed material has become incorporated.

One particular advantage of this technique is that it is very sensitive and even very low levels of incorporation may be recorded. In addition, the half life of  $^{14}\text{C}$  is 5600 years and that for  $^3\text{H}$  is 12.26 years so a reduction in the count due to decay may be neglected.

However, the feeding of radiolabelled precursors does not directly yield site specific information. In order to determine where the radiolabel is incorporated in the metabolite, each carbon (hydrogen, or phosphorus) must be essentially carved out from the metabolite, by a series of degradation reactions, and then analysed. Because the degree of sensitivity is so high, the metabolite and any degradation products must be rigorously purified prior to analysis to prevent any cross contamination of radiolabel. In addition to this disadvantage, the risk to the health of the individuals carrying out the investigations may also be a concern.

### **1.2.4 Stable isotope labelling studies**

Due to the considerable advances that have been made in the fields of high field nuclear magnetic resonance spectroscopy (NMR) and mass spectrometry (MS), the use of stable isotopic labels such as  $^2\text{H}$  and  $^{13}\text{C}$  in biosynthetic studies, has substantially replaced the use of radioisotopes.

Compounds that have been synthesised with isotopic labels incorporated at specific sites are fed to the organism. The compound whose biosynthesis is being investigated is harvested, purified and then analysed by either NMR or mass spectrometry.

#### **Single label feeding studies**

$^{13}\text{C}$  may also be used as a single label within a putative precursor. Comparison of the peak integrals from a natural abundance  $^{13}\text{C}$  spectrum of the metabolite with those resulting from the feeding of the labelled compound, readily demonstrates the level of incorporation. The wide chemical shift range observed in a  $^{13}\text{C}$  NMR spectrum and

the low natural abundance of  $^{13}\text{C}$  make this a particularly useful tool for examining site specific incorporations.

$^2\text{H}$  has an even lower natural abundance of 0.016 % meaning that it is possible to detect even smaller levels of incorporation accurately. The chemical shifts in a  $^2\text{H}$  NMR spectrum closely correspond to those of the proton, making assignment of the peaks simple. The peaks may also be readily integrated to provide precise information about the levels of incorporation of the labelled precursor. However, deuterium has a low gyromagnetic ratio meaning that detection of the nucleus is less sensitive; it is often necessary to run the NMR analysis experiments on high field spectrometers and for extensive periods of time. Deuterium possesses a quadrupolar nucleus with nuclear spin ( $I$ ) =1, this leads to an increased nuclear relaxation time and thus broadening of the signals.

$^3\text{H}$ . The sophistication of modern NMR techniques has also brought about a resurgence in the use of tritium. Tritium lends itself particularly well to NMR analysis as it has the highest gyromagnetic ratio of any element and is thus readily detected. It has a very low natural abundance of  $10^{-15}\%$ , so it is possible to detect very low levels of incorporation. Though detection of tritium by scintillation counting is the more sensitive technique, the use of NMR for analysis can provide site specific information about the incorporations.

#### Double label feeding studies "bond labelling"

Often in a biosynthetic investigation, the first labelled molecule to be administered to the organism is  $[1,2-^{13}\text{C}_2]$ -acetate. The two carbon nuclei couple to each other and if the acetate bond is not broken during the biosynthetic process then the coupling is retained in the final metabolite and may be observed by  $^{13}\text{C}$  NMR. This provides a useful method of investigating how the carbon skeleton of the molecule is formed. As the natural abundance of  $^{13}\text{C}$  is only 1.1 %, the possibility of two  $^{13}\text{C}$ s naturally occurring together in the metabolite may be calculated as  $1.1\% \times 1.1\%$ . The technique is, therefore, highly sensitive.

### Using “reporter” nuclei in $^{13}\text{C}$ NMR analysis

#### **$^2\text{H}$ and $^{13}\text{C}$**

The fate of a deuterium label may also be followed by  $^{13}\text{C}$  NMR as the  $^2\text{H}$  and  $^{13}\text{C}$  will couple together. Furthermore, a carbon will be shifted upfield by between 0.25 and 0.3 ppm per deuterium attached to it ( this is known as the  $\alpha$  effect). A deuterium decoupled  $^{13}\text{C}$  NMR spectrum may be used to determine how many deuteria are incorporated at one site. The feeding of  $^{13}\text{C}$ - $^2\text{H}$  labelled material may also be used to determine whether a particular C-H bond is broken during the biosynthesis of a particular metabolite.

A carbon atom can also report on the number of deuteria attached to the directly neighbouring carbon atoms. The  $\beta$  effect is also additive, with one deuterium leading to an upfield shift of 0.05-0.08 ppm. It is not necessary to employ  $^2\text{H}$  decoupling to clearly observe the  $\beta$  effect, as there is no  $^2J_{^{13}\text{C}-^2\text{H}}$ .

#### **$^{18}\text{O}$ and $^{13}\text{C}$**

Though  $^{18}\text{O}$  itself, may not be observed directly by NMR, its incorporation into a molecule may also be witnessed by monitoring the induced chemical shift on an adjacent carbon-13 atom.

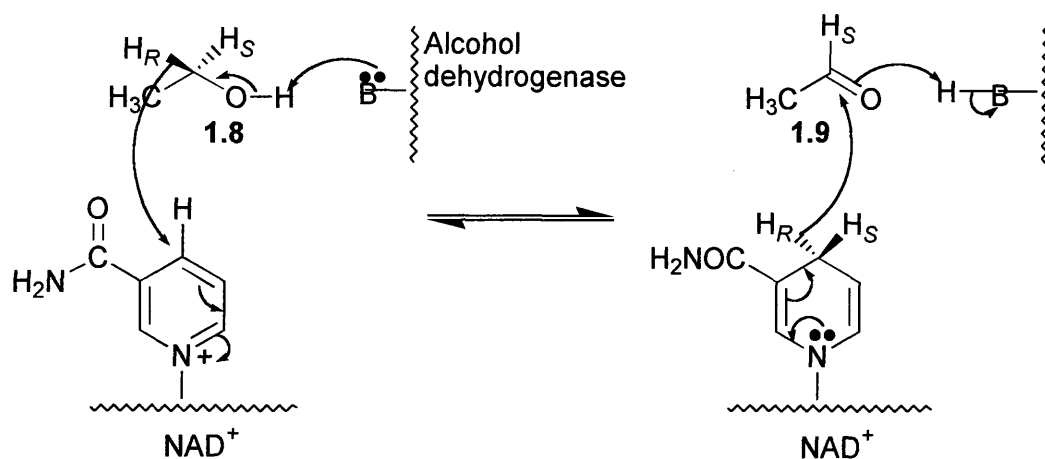
### Mass spectrometry analysis

Mass spectrometry is often an attractive alternative to NMR analysis as much smaller amounts of metabolite may be analysed. If the fragmentation pattern of the metabolite is easily identified it is sometimes possible to assign the isotopic incorporation to a particular site.

Though the use of stable isotope labelling experiments is, on the whole, preferable to radioisotopic labelling, due to the decreased sensitivity of detection, it is often necessary to feed the labelled putative precursor at a much higher concentration. There is a danger of the ordinary metabolism of the organism being perturbed, or at worst, the death of the organism resulting.

### 1.3 Stereochemical biosynthetic investigations

Almost all enzyme catalysed reactions proceed with very high stereospecificity. The substrates utilised by the enzyme must be of a strictly defined configuration and the products, in turn, are formed with a particular stereochemistry. In some cases the stereochemistry of the enzymatic reaction is immediately apparent as it occurs at a chiral centre. However, enzymes may also act stereospecifically at achiral centres or prochiral groups within a molecule. One such example is the alcohol dehydrogenase mediated conversion of ethanol (1.8) to acetaldehyde (1.9), using nicotinamide adenine dinucleotide (NAD<sup>+</sup>) as the co-enzyme (Scheme 1.3). Although the enzyme is presented with the possibility of removing one of two chemically equivalent hydrogens, in the oxidation of the ethanol, only the *pro-R* is abstracted. This may be demonstrated by isotopically labelling the *pro-R* position with deuterium and noting the absence of label in the acetaldehyde produced.



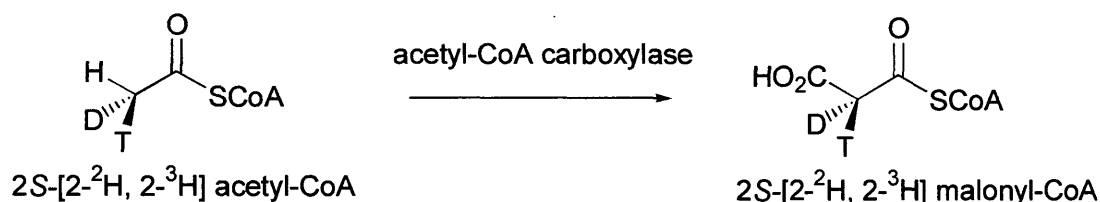
Scheme 1.3 The alcohol dehydrogenase mediated conversion of ethanol (1.8) to acetaldehyde (1.9)

Although within a methyl group the three hydrogens are homotopic, the biochemical reactions generating the methyl group may be stereospecific. For example, the methyl group may be formed by the protonation of a methylene group operating on one side of the molecule only. The steric course of the reaction, in such cases, is not evident from the inspection of the substrates and to elucidate the stereochemical course by which the enzyme is operating it is often necessary to prepare chiral versions of the methyl group by using heavy isotopes.



The “chiral methyl group” is frequently used in the elucidation of the stereochemistry of biosynthetic transformations.<sup>15</sup> The methodology relies upon the kinetic isotope effect which dictates that a C-H bond is more readily broken than a C-D bond, which is, in turn, more readily broken than a C-T bond (see section 2.1).

The activation of acetyl-CoA to malonyl-Co, mediated by acetyl-CoA carboxylase, was demonstrated to proceed with retention of stereochemistry, by Sedgwick and Cornforth’s use of chiral acetyl-CoA.<sup>16, 17</sup>



Scheme 1.4 The conversion of 2S-[2-<sup>2</sup>H, 2-<sup>3</sup>H] acetyl-CoA to 2S-[2-<sup>2</sup>H, 2-<sup>3</sup>H] malonyl-CoA mediated by acetyl-CoA carboxylase

Studies into the manner in which a substrate is stereochemically processed can provide mechanistic information about the way in which the enzyme functions (Chapter 4).

#### 1.4 Topics addressed in this thesis

This thesis investigates the biosynthesis of two idiolites, longianone and fluoroacetate, using stable isotope labelling techniques (section 1.2.3).

Longianone is an intriguing, highly functionalised metabolite of the fungus *Xylaria longiana*. It is an isomer of the notorious fungal toxin, patulin. The biosynthesis of patulin is examined to provide clues as to the biosynthesis of longianone. Intermediates on the patulin pathway are synthesised carrying an isotopic label and incubated with the *X. longiana*, to determine whether they are intermediates upon the biosynthetic pathway to longianone as well.

Although fluoroacetate, the most common of the fluorinated metabolites, was discovered by Marais in 1943 as the toxic component of the South African plant *Dichapetalum cymosum*,<sup>18</sup> the simple compound’s biosynthesis has not yet been fully elucidated. This thesis addresses the stereochemistry of the fluorination event, in order to gain insight into the mechanism by which the biological fluorination occurs.

This problem is approached by the feeding of stereoselectively deuterated, known precursors of fluoroacetate. Chiral liquid crystal  $^2\text{H}$  NMR is used to determine the chirality of the fluoroacetate produced from these deuterated biosynthetic intermediates, and a sample of sodium (*S*)-[ $^2\text{H}$ ]-fluoroacetate is biosynthesised as a standard.

The power of chiral liquid crystal NMR as a tool for resolving enantiomers, chiral by virtue only of the substitution of a proton by a deuterium is further investigated. Fluoro-deutero-alkanes are synthesised and examined by chiral liquid crystal NMR to determine the limit of the techniques resolution, where only a subtle difference in the chirality of each enantiomer exists.

## References

- 1 C. K. Mathews, K. E. van Holde, *Biochemistry*, 1<sup>st</sup> Ed., The Benjamin/ Cummings Publishing Company, Inc. p4.
- 2 W. Shakespeare, "*Romeo and Juliet*", 5.1
- 3 W. Shakespeare, "*Romeo and Juliet*", 4.1.91
- 4 The Gospel According to St Matthew, 2:11
- 5 A. L. Demain, *Secondary Metabolites: Their Structure Function And Evolution*, Ciba Foundation Symposium 171, J. Wiley and sons, p21.
- 6 J. W. Bennett, R. Bently, *Adv. Appl. Microbiol.*, 1989, **34**, 1.
- 7 H. Zahner, *Folia Microbiol*, 1979, **24**, 435
- 8 L. C. Vining, *Annu. Rev. Microbiol.* 1990, **44**, 395.
- 9 D. A. Hopwood, C. Khosla, *Secondary Metabolites: Their Structure Function And Evolution*, Ciba Foundation Symposium 171, J. Wiley and sons, p103.
- 10 H. Oikawa, Y. Murakami, A. Ichihara, *J. Chem Soc., Perkin Trans.*, 1992, 2949.
- 11 S. J. Gould, J. Guo, A. Geitmann, K. Dejesus, *Can. J. Chem.*, 1994, **72**, 6.
- 12 S. Donadio, L. Katz, *Gene*, 1992, **111**, 51; S. Donadio, M. J. Staver, J. B. McAlpine, S. J. Swanson, L. Katz, *Science*, 1991, **252**, 675; J. Staunton, *Agew. Chem. Int. Ed. Engl.*, 1991, **30**, 1302.; J. Cortés, S. F. Haydock, G. A. Roberts, D. J. Bevitt and P. F. Leadlay, *Nature*, 1990, **348**, 176; D. J. Bevitt, J. Cortés, S. F. Haydock, P. F. Leadlay, *Eur. J. Biochem*, 1992, **204**, 39.
- 13 J. Cortés, K. E. H. Wiesmann, G. A. Roberts, M. J. B. Brown, J. Staunton and P. F. Leadlay, *Science*, 1995, **268**, 1487.
- 14 J. Staunton, B. Wilkinson, *Chem. Rev.*, 1997, **97**, 2611.
- 15 H. G. Floss in *Methods in Enzymology*, **87**, part C, Ed. D. L. Purich, Academic Press, New York, London, Paris, San Diego, São Paulo, Sydney, Tokyo, Toronto, 1982, p126.
- 16 B. Sedgwick, J. W. Cornforth, *Eur. J. Biochem.*, 1977, **75**, 465.
- 17 B. Sedgwick, J. W. Cornforth, S. J. French, R. T. Gray, E. Kelstrup, P. Willadsen, *Eur. J. Biochem.*, 1977, **75**, 481.
- 18 J. S. C. Marais, *Onderstepoort J. Vet. Sci. Anim. Ind.* 1944, **20**, 67.

## **CHAPTER 2**

### **Chiral Analysis by Chiral Liquid Crystal $^2\text{H}$ -NMR**

## CHAPTER 2

### **Chiral Analysis by Chiral Liquid Crystal Deuterium NMR**

#### Introduction and Background

##### 2.1 Methods of determining enantiomeric excess

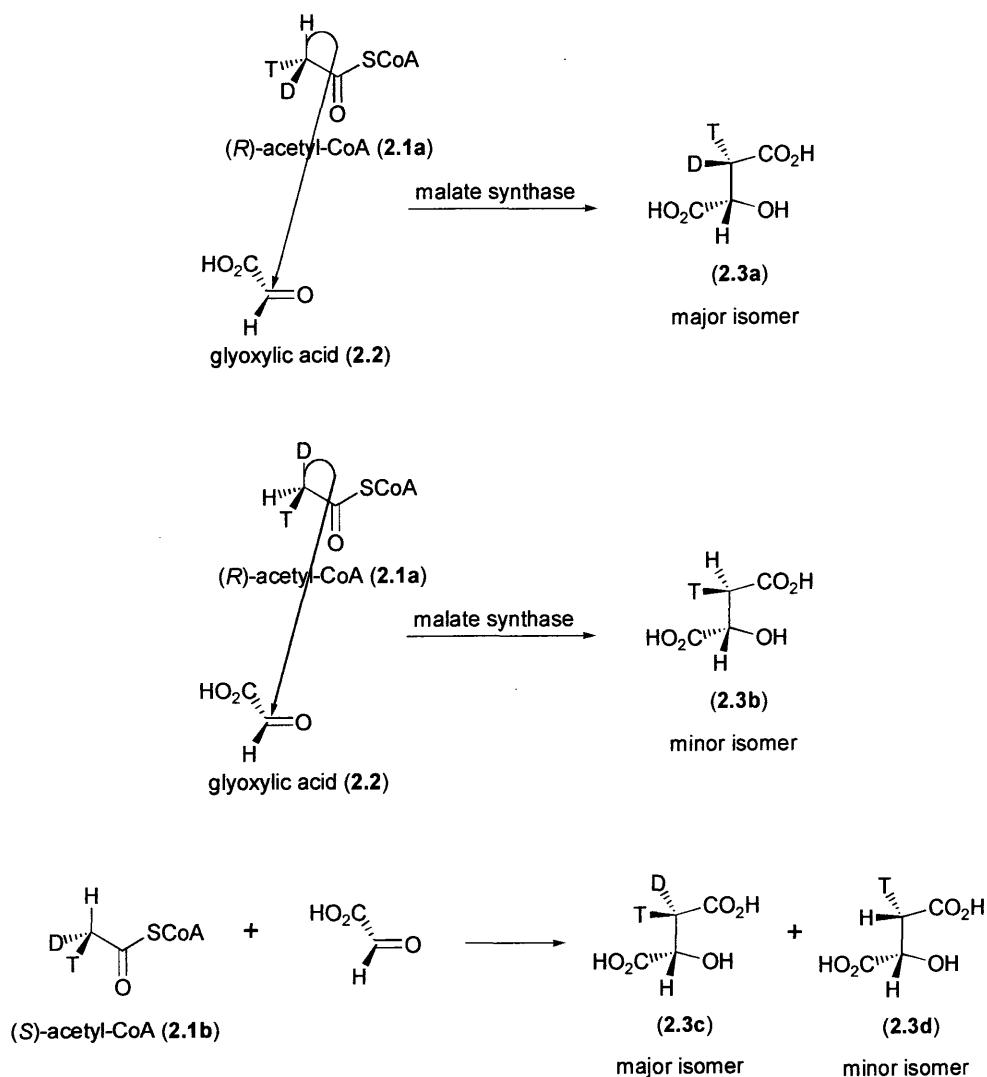
There are many occasions when it is highly important that a chemist should be able to measure the enantiomeric excess (ee) of a chiral compound. Sometimes, the reason for doing so is promoted by a desire to understand the mechanism of a reaction; on other occasions it may be necessary to test that the material contains only one enantiomer so that it may be used in the synthesis of pharmaceutical or agrochemical products.

When determining the ee of molecules that are chiral by virtue only of isotopic substitution, such as with deuterium for hydrogen, the methods available to the chemist are very limited. The shape of the molecule is little altered and thus separation of the two enantiomers by gas chromatography (GC) or high pressure liquid chromatography (HPLC) with a chiral column, is not viable. Additional problems arise if the material to be analysed is of biosynthetic origin and thus available only in milligram quantities with, often, an isotopic enrichment well below 100 %.

An elegant, though rather time consuming, means of measuring the chirality of methyl groups, chiral by virtue of tritium and deuterium substitution, has been used for many years to investigate the chirality of biosynthetic acetate.<sup>1</sup> The method employs two enzymes and takes advantage of the kinetic isotope effect. The analysis was initially developed with synthetic (*R*)- and (*S*)-[<sup>2</sup>H, <sup>3</sup>H]-acetic acid.<sup>2</sup>

Malate synthase mediates the irreversible condensation of acetyl-CoA (**2.1**) with glyoxylic acid (**2.2**). The condensation occurs with the loss of a hydrogen atom. The hydrogen or the isotope that is lost is dictated by the primary isotope effect ( $k_H > k_D > k_T$ ). This means that the loss of hydrogen is favoured over deuterium, which, in turn,

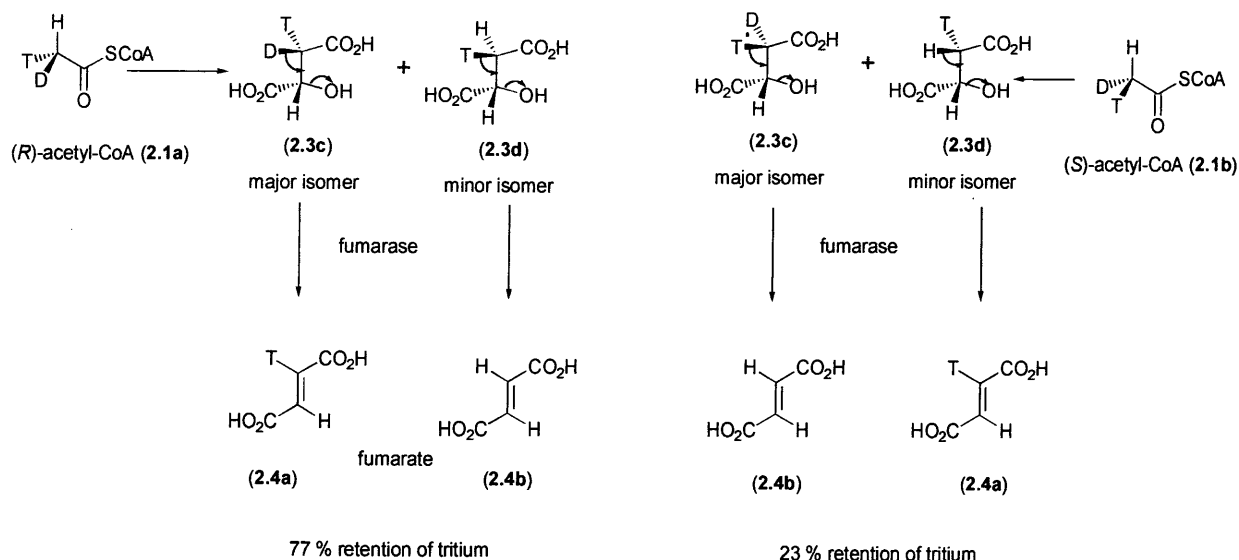
is favoured over tritium. When (*R*)-[<sup>2</sup>H, <sup>3</sup>H]-acetyl-CoA (**2.1a**) is condensed with glyoxylic acid, malic acid (**2.3a**), resulting from the loss of a proton, is generated as the major isomer (77%). A small amount of the minor isomer (**2.3b**) (23%) is generated by the less kinetically favourable loss of a deuteron. Similarly, when (*S*)-[<sup>2</sup>H, <sup>3</sup>H]-acetyl-CoA (**2.1b**) is condensed with glyoxylic acid, malic acids **2.3c** and **2.3d** are generated as the major and minor isomers, respectively (**Scheme 2.1**).



**Scheme 2.1** The reaction of chiral acetyl-CoA (**2.1**) with glyoxylic acid (**2.2**)

The resultant malic acid is subsequently isolated and incubated with fumarase. Fumarase mediates the loss of water from malic acid, in a stereospecific manner, to generate fumaric acid (**2.4**). The material is incubated until no further TOH is lost: the levels of tritium remaining within the material are then measured. From the original investigation, using synthetic (*R*)- and (*S*)-[<sup>2</sup>H, <sup>3</sup>H]-acetic acid, it was observed that (*R*)-[<sup>2</sup>H, <sup>3</sup>H]-acetic acid incubated with malate synthase and then fumarase led to a 77% retention of tritium, whereas only 23% retention of tritium resulted from the incubation of (*S*)-[<sup>2</sup>H, <sup>3</sup>H]-acetic acid with the two enzymes (**Scheme 2.2**). From this

information, the technique could be used to deduce the chirality of many biosynthetic acetic acid samples.



### Scheme 2.2 The resolution of chiral methyl groups using the kinetic isotope effect

In certain cases, it has been shown possible to discriminate between two enantiomers whose chirality results from the substitution of a proton with a deuteron, by chiral optical methods. Such techniques are difficult due to the weak circular dichroism response elicited. Another method of enantiomeric resolution is the use of chiral derivatising reagents. This involves derivatising the compound with an enantiomerically pure material. The resultant diastereoisomeric compound will have a chemical shift non-equivalence. However, not only may manipulation of the sample be tricky and time consuming, especially when only small amounts of the biosynthetic compound are available for derivatisation, but also, retrieval of the product for further analysis may be problematic. To ensure an accurate analysis of the ee, using this method, the derivatising agent must be enantiomerically pure. The formation of the diastereoisomer must occur under conditions that exclude racemisation, and an excess of the derivatising agent used to minimise kinetic resolution due to differences in reaction rates between the enantiomers. Care must be taken, throughout the purification, not to include any techniques, such as crystallisation, which might favour the enrichment of one diastereoisomer.

One of the most frequently used chiral derivatising agents is  $\alpha$ -methoxy- $\alpha$ -(trifluoromethyl)phenyl-acetic acid (MTPA) (**2.5**).<sup>3</sup> Introduced by Mosher,<sup>4</sup> this compound is highly favoured as the absence of a proton  $\alpha$  to the carboxy group prohibits racemisation. The presence of the trifluoromethyl group allows analysis by integrating the signals for the two diastereoisomers in the  $^{19}\text{F}$  NMR spectra.

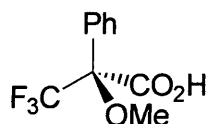


Fig 2.1  $\alpha$ -methoxy- $\alpha$ -(trifluoromethyl)phenyl-acetic acid (**2.5**)

## 2.2 The chiral analysis of labelled biosynthetic fluoroacetate

To gain a better understanding of the mechanism of biological fluorination by the bacterium *Streptomyces cattleya*, it became appropriate to assay the enantiomeric excess of a biosynthetic sample of fluoroacetate, chiral by virtue of deuterium substitution alone (Chapter 4).

Analysis of the enantiomeric excess of  $\alpha$ -deuterated carboxylic acids, alcohols and amines by first forming their MTPA derivative has been shown to be largely unsuccessful and other derivatising agents must be employed.<sup>5</sup> In the past, workers at Durham have attempted to analyse the ee of  $[2\text{-}^2\text{H}]$ -fluoroacetate by derivatising it as the methyl mandelate ester (**2.6**) and also as the amide of  $\alpha$ -methyl benzylamine (**2.7**). However,  $^1\text{H}$  NMR analysis of the two derivatives using a 500 MHz spectrometer failed to resolve the diastereotopic hydrogens of the fluoromethyl groups.

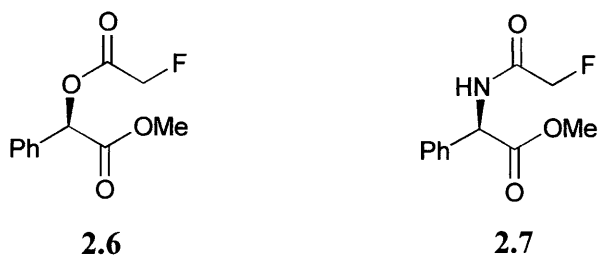
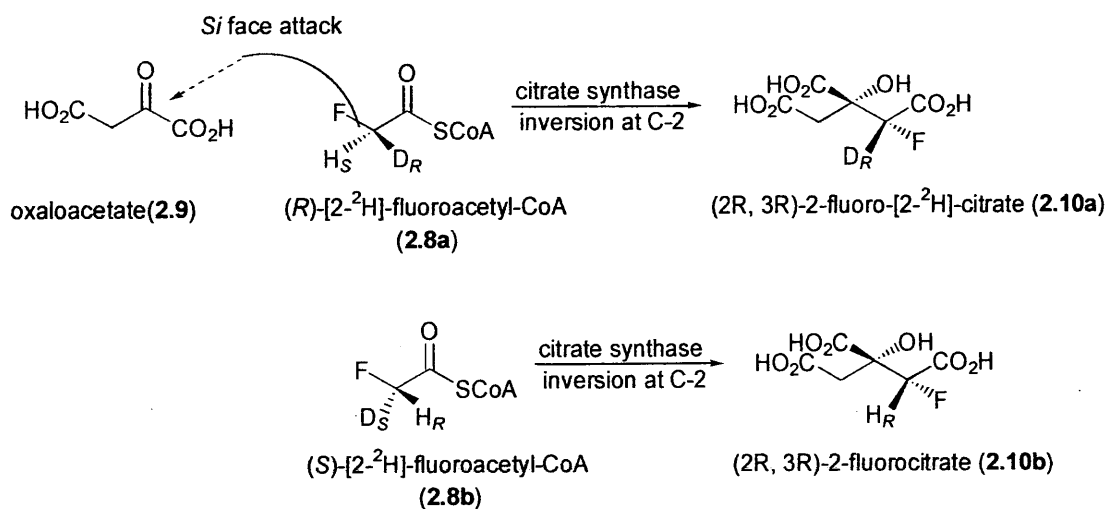


Fig 2.2 Chiral derivatives of fluoroacetate

The condensation of fluoroacetyl-CoA (**2.8**) with oxaloacetate (**2.9**) in the fatal conversion to fluorocitrate (**2.10**) mediated by citrate synthase, is known to be highly stereospecific.<sup>11</sup> The 2-*pro-S* proton of fluoroacetyl-CoA is abstracted exclusively to afford (2*R*, 3*R*)-2-fluorocitrate as the only isomer (section 3.7.4). It was anticipated



that by incubating the biosynthetically derived  $[^2\text{H}_1]$ -fluoroacetate with citrate synthase, the presence, or absence, of deuterium in the resultant fluorocitrate would provide an assay for the *R* or *S* configuration. Mass spectral data indicating the percentage of fluorocitrate molecules containing deuterium could then be used to calculate an enantiomeric excess. However, development of this methodology in Durham was unsuccessful.



Scheme 2.3 The condensation of fluoroacetyl-CoA (2.8) with oxaloacetate (2.9)

Rétey reported the synthesis of both (*S*)- and (*R*)- $[^2\text{H}]$ -fluoroacetate and distinguished the enantiomers analytically by circular dichroism (Fig 2.3).<sup>6</sup> Accordingly, attempts were made to similarly analyse the  $[^2\text{H}_1]$ -fluoroacetate recovered from *Streptomyces cattleya*. Due to the milligram quantities of the metabolite, which were no more than 15 % deuterated and which contained inorganic impurities, analysis by this method was frustrated. (Samples were analysed at King's College London.)

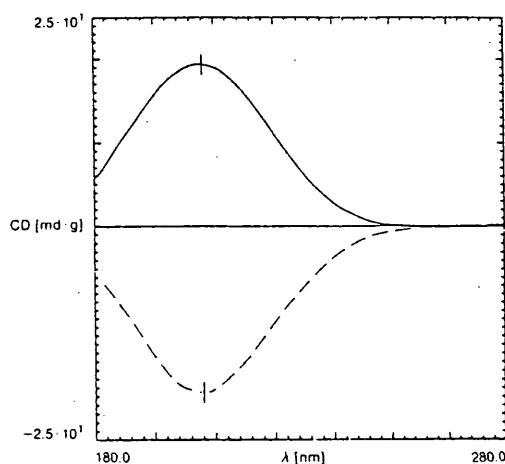


Fig. 2.3 Rétey's analysis of (*S*)- and (*R*)- $[^2\text{H}]$ -fluoroacetate by CD in  $\text{CF}_3\text{CH}_2\text{OH}$ <sup>6</sup>

## **2.3 The use of chiral liquid crystal deuterium NMR for chiral resolution**

In recent years, a novel and extremely sensitive technique for enantiomeric assay has emerged in the literature. The observation by NMR analysis of a range of nuclei ( $^2\text{H}$ ,  $^{19}\text{F}$ , and  $^{13}\text{C}$  included) of compounds solvated in a chiral liquid crystalline medium, can be used to discriminate between enantiomers. The resolution of the two enantiomers may be particularly pronounced for quadrupolar nuclei, such as deuterium, where the nuclear spin  $I > \frac{1}{2}$ .<sup>7, 8</sup>

### **2.3.1 An introduction to liquid crystals**

The liquid crystalline phase, a state occurring between solid and liquid, was first discovered by Reintzer in 1888.<sup>9</sup> He observed that a cholesteryl ester existing as an opaque liquid at room temperature, became a clear isotropic liquid upon heating. This new state he termed a “mesophase”, meaning “in between phases”.

In 1956 Flory postulated that concentrated solutions of rigid rod like polymers should form ordered structures when in solution at a critical concentration.<sup>9</sup> This was subsequently found to be the case. These two instances refer to two different types of liquid crystalline state, termed thermotropic and lyotropic, respectively.

The mesophase may be further broken down into three main categories determined by the level of ordering of the liquid crystal:-

The smectic state (smegma ~ Greek for soap) is very highly ordered. The molecules arrange themselves in parallel lines, and the centres of gravity of the molecules are confined to layers (Fig 2.4a). The nematic, or thread like, phase is slightly less ordered, and although the molecules are arranged in parallel lines, the centres of gravity of the molecules are randomly distributed through space. As a consequence of this lesser degree of ordering, the nematic phase is far more fluid than the smectic phase, though, still exhibiting birefringence (Fig. 2.4 b).

When a lyotropic liquid crystalline phase is formed by the addition of polymer to a solvent, initially the viscosity increases whilst the solution remains isotropic and clear. At a critical concentration, determined by temperature, solvent and molecular weight of the polymer, the viscosity of the material sharply decreases. At this stage the formation of orientated nematic domains occurs, in which the chains are lined parallel to the direction of flow thereby reducing the frictional drag on the molecules and thus the viscosity of the material.

In the third type of mesophase, the “chiral nematic state”, the mesogens have a chiral centre. In each layer of the material there is directional ordering, as in the case of the nematic phase. The presence of the chiral centre causes the director of each layer to be displaced, each time, by an angle  $\theta$ , thus giving a helical twist to the material. The result of this effect is a liquid crystal of high optical activity with the ability to reflect circularly polarised light of a particular wavelength (Fig 2.4c). The solvation of poly  $\gamma$ -benzyl L-glutamate (PBLG), gives rise to such a material as this.

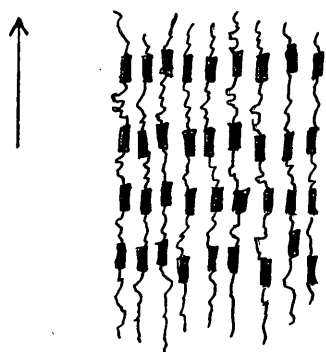


Fig. 2.4a

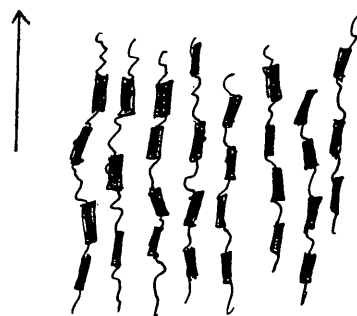


Fig. 2.4b

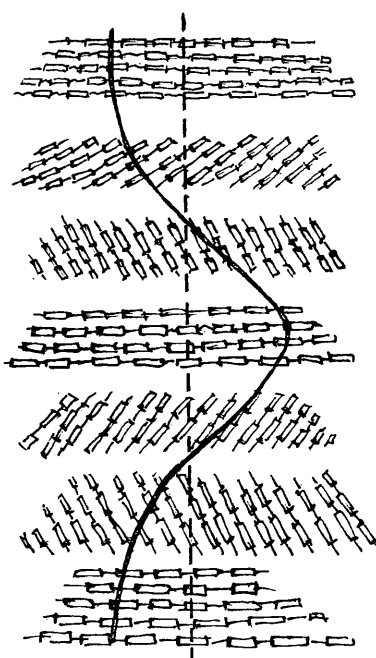


Fig. 2.4c

Fig. 2.4 The molecular ordering in the three liquid crystalline phases

### **2. 3. 2 The use of PBLG as a solvent for NMR analysis**

The presence of a chiral environment created by the liquid crystalline PBLG in chloroform leads to differing orientations of the different enantiomers of a molecule solvated by the material. The differential ordering induces different magnetic environments.

For ordinary enantiomers, it is the difference in shape which leads to the different solvent/solute interactions. For molecules that are chiral only by virtue of isotopic substitution and for prochiral groups, the chiral environment of the PBLG helices can, perhaps, be compared to the  $\alpha$  helices present at the active site of an enzyme, imparting diastereotopicity to the substrate. In such a manner, the two nuclei or groups are induced into magnetic non equivalence. The differential ordering effects, caused by the presence of the chiral environment, induces different chemical shifts and different quadrupolar interactions for each enantiomer.

Quadrupolar couplings may be observed for nuclei with spins  $I > \frac{1}{2}$ . In such nuclei there exists an anisotropic distribution of charge. The interaction of this nuclear quadrupole moment with the electric field gradient of the molecule (caused by the molecule's asymmetry) leads to quadrupolar coupling.

When a racemic mixture of a compound, bearing an atom with a quadrupolar nuclei, such as deuterium, is solvated in an isotropic medium, tumbling of the molecule can occur. The electric field gradients of the molecules are averaged out, and a single broad line is observed in the NMR spectrum (Fig 2.5a). If the same material is dissolved in a nematic liquid crystal, the solute molecules become partially orientated and the average quadrupolar coupling becomes non zero: a doublet is observed with a quadrupolar splitting of  $\Delta\nu_Q$  (Fig 2.5b). When the same material is dissolved in a chiral nematic liquid crystalline solvent, such as poly  $\gamma$ -benzyl L-glutamate, due to the difference of ordering of each enantiomer within the chiral environment, two doublets are observed whose intensity is equal to the concentration of each enantiomer present (Fig 2.5c).

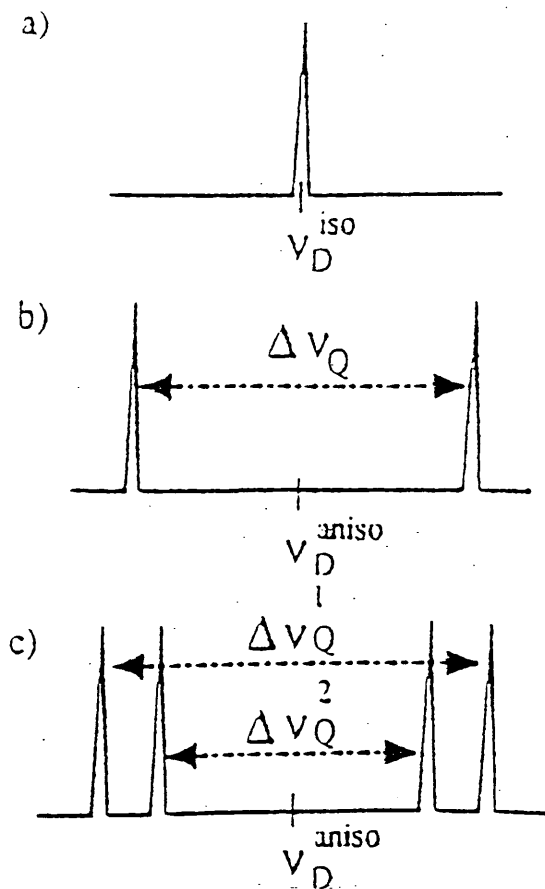


Figure 2.5 The  $^2\text{H}$  NMR of a racemic RCHDOH in a) an isotropic solvent, b) a nematic liquid crystalline solvent, c) a chiral nematic liquid crystalline solvent<sup>10</sup>

Even though the differences in ordering for the two enantiomers may be very small; due to the large values for the quadrupolar coupling, discernable differences in the quadrupolar splittings may be observed (Equation 2.1).

$$\Delta V_Q = \frac{3 Q_D V_{CD}}{2 h} S_{CD}$$

$$S_{CD} = \frac{1}{2} \langle 3 \cos^2 \theta_{CD}^Z - 1 \rangle$$

$Q_D$  = deuterium quadrupolar moment

$V_{CD}$  = the electric field gradient along the carbon deuterium bond

$S_{CD}$  = the order parameter along the carbon deuterium axis

$\theta_{CD}^Z$  = the angle between the electric field gradient and the external magnetic field

$\langle \rangle$  denotes an average value over the anisotropic molecular reorientations

Equation 2.1

The differences in  $\Delta\nu_Q$  produced by the technique means that it is particularly good for examining the ee in cases when the molecule is chiral only by virtue of deuterium incorporation, even when the degree of incorporation is extremely low, as for the case of many biosynthetic materials.

### **2.3.3 Sample preparation for chiral liquid crystal NMR**

Samples for chiral liquid crystal NMR analysis are prepared by weighing, accurately, PBLG (120 mg, 13%, DP $\approx$ 800, MW 150,000-350,000) into a 5mm diameter NMR tube. A noted mass of material to be analysed is added to the NMR tube, and finally chloroform (803 mg, 87%) is added. The contents of the tube are left to dissolve in the chloroform before being thoroughly mixed. Mixing is achieved by drawing the material from one end of the tube to the other at least 40 times. As the material is very viscous, it is beneficial to introduce a centrifugal force to drag the material from one end of the tube to the other. After centrifugation, the NMR tube is reweighed so that any loss of chloroform, due to evaporation, may be accounted for. The NMR of the sample is immediately run so that the homogeneity of the sample is not lost by further evaporation of chloroform.

Initially, all chiral liquid crystalline deuterium NMR analysis were performed on a Bruker AC-250 at the Institut de Chimie Moléculaire d'Orsay, Université de Paris Sud, France. Experiments were performed in our laboratories to adapt the technique to our equipment. The greatest challenge lay in the sample preparation, and our ability to thoroughly mix the liquid crystal. In our initial experiments, the NMR tube was placed at an angle of 60°, in a specially designed conical flask (Fig 2.6) and spun on an orbital shaker at 500 rpm. Using this technique, it took almost ten minutes for the material to be spun from the top to the bottom of the tube. Finally, a MSE Chilspin centrifuge, fitted with an 8 x 100 ml angle head rotor, was employed to spin the tubes. This model of centrifuge has sufficient head-space to allow for the height of an NMR tube, with the lid closed. The deuterium NMR were obtained on a Unity Inova 500 MHz. Gradient shimming was employed to increase the resolution of the spectra.

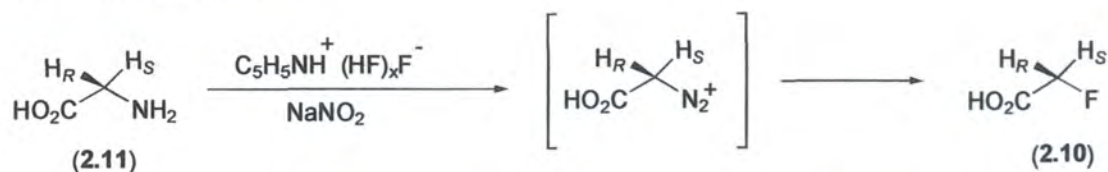


Fig. 2.6 Modified conical flask used to centrifuge the liquid crystalline material within the NMR tube

#### 2.4 The synthesis of (*S*)-[<sup>2</sup>H]-fluoroacetate

In order to determine whether chiral liquid crystal <sup>2</sup>H NMR would be a suitable technique by which to resolve the *S* and *R* enantiomers of [<sup>2</sup>H]-fluoroacetate (2.10), it was necessary to synthesise a reference sample. To provide a standard against which the biosynthetic material could be compared, it was decided to prepare [<sup>2</sup>H]-fluoroacetate with an ee in favour of the *S* configuration.

Keck has reported the synthesis of (*R*)-[<sup>2</sup>H]-fluoroacetate.<sup>11</sup> Using (*R*)-[<sup>2</sup>H]-glycine, the synthesis was based upon deaminative halogenation methodology established by Pattison *et al.*, the substitution proceeding with retention of configuration.<sup>12</sup> In this synthesis glycine (2.11) is reacted in a pyridinium poly(hydrogen fluoride) solution containing an excess of sodium nitrite. Initially, *in situ* diazotisation generates an intermediate diazonium salt, this is followed by a subsequent dediazonization to furnish fluoroacetate.



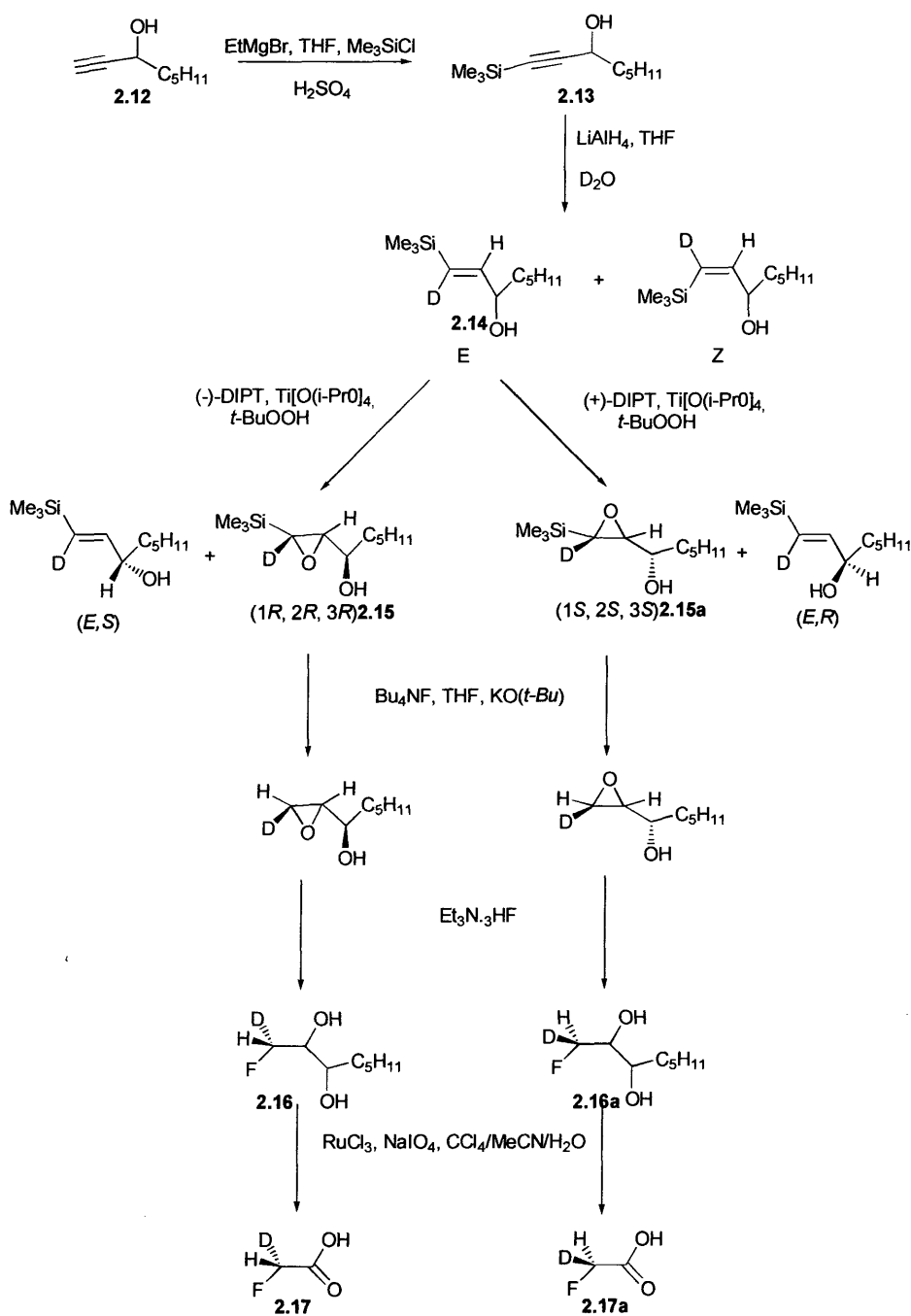
Scheme 2.4 The synthesis of fluoroacetate (2.10) from glycine (2.11)

This synthesis was employed by Walsh to obtain a sample of (*R*)-[<sup>2</sup>H]-fluoroacetate with which to test the stereochemistry of the dehalogenation of fluoroacetate to glycolate by a halidohydrolase enzyme.<sup>13</sup>

starting material. Ethyl magnesium bromide is then used to deprotonate the alkyne at the terminal position, and the resultant anion reacted with trimethylsilyl chloride to furnish 1-(trimethylsilyl)oct-1-yn-3-ol (**2.13**). The reduction, of this material, with lithium aluminium hydride followed by a deuterium oxide quench yields 1-(trimethylsilyl)[1-<sup>2</sup>H]oct-1-en-3-ol (*E*)/(*Z*) 5:1 (**2.14**). Rétey reports the selective epoxidation of the (*E*)-isomer, alone, under Sharpless conditions using both enantiomers of diisopropyl tartrate as the chiral ligand to generate either (1*R*, 2*R*, 3*R*)- or (1*S*, 2*S*, 3*S*)-1-(trimethylsilyl)-1,2-epoxy[1-<sup>2</sup>H]octan-3-ols (**2.15**, **2.15a**). Deprotection of the trimethyl silyl group was achieved by reaction with KO(*t*-Bu) and with Bu<sub>4</sub>NF. The oxirane ring was opened with Et<sub>3</sub>N.3HF to afford the two fluoro-octane diols (**2.16**, **2.16a**), which were subsequently cleaved with sodium metaperiodate to furnish both isomers of fluoroacetic acid (**2.17**, **2.17a**).

Rétey's synthesis is lengthy and not so efficient particularly as one sixth of the lithium aluminium hydride reduction proceeds in a *cis*-fashion to yield *Z*-allyl alcohol, which is discarded. Also, 50% of the material becomes redundant following the Sharpless kinetic resolution.

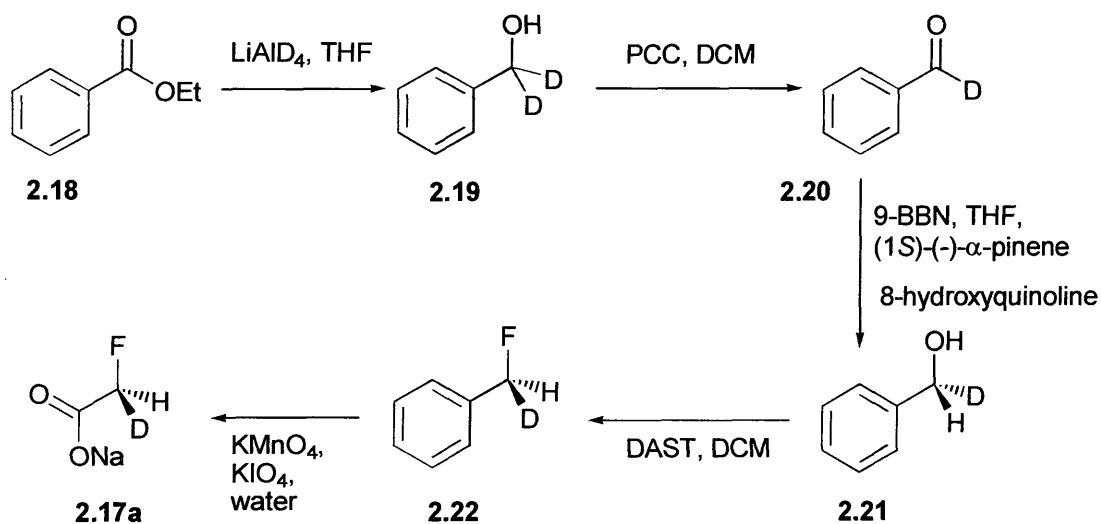




**Scheme 2.5 Rétey's synthesis of chiral [2-<sup>2</sup>H]-fluoroacetate**

At the outset of the project this route was considered, however, the Sharpless epoxidation of 1-(trimethylsilyl)[1-<sup>2</sup>H]octan-3-ol (**2.14**) was unsuccessful in my hands.

An alternative route for the synthesis of chiral deuterated sodium fluoroacetate was investigated. It was chosen to utilise the well known Midland methodology<sup>14</sup> for the asymmetric reduction of benzaldehyde, to introduce the stereogenic centre.

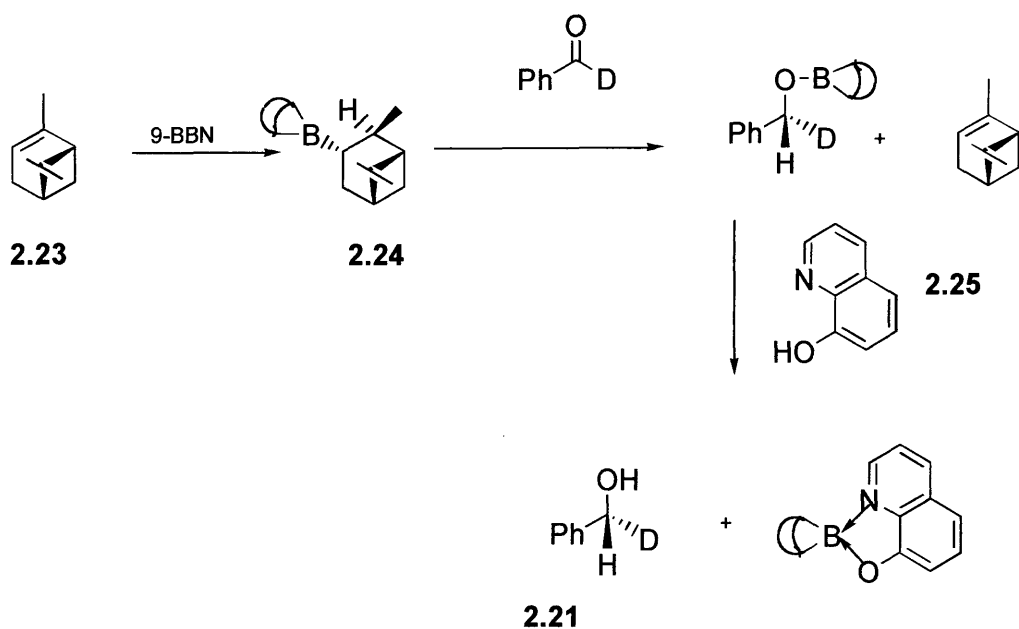


**Scheme 2.6** The synthesis of (*S*)-[2-<sup>2</sup>H]-fluoroacetate (**2.17a**) from [7-<sup>2</sup>H]-benzaldehyde (**2.20**)

Although the starting material, [7-<sup>2</sup>H]-benzaldehyde (**2.20**), may be purchased from Aldrich, it is expensive. [7-<sup>2</sup>H]-Benzaldehyde may be made, in a straightforward manner and in good yield, by a two-step process involving the lithium aluminium deuteride reduction of ethyl benzoate (**2.18**), followed by the pyridinium chloro chromate (PCC) oxidation of the resulting alcohol (**2.19**).

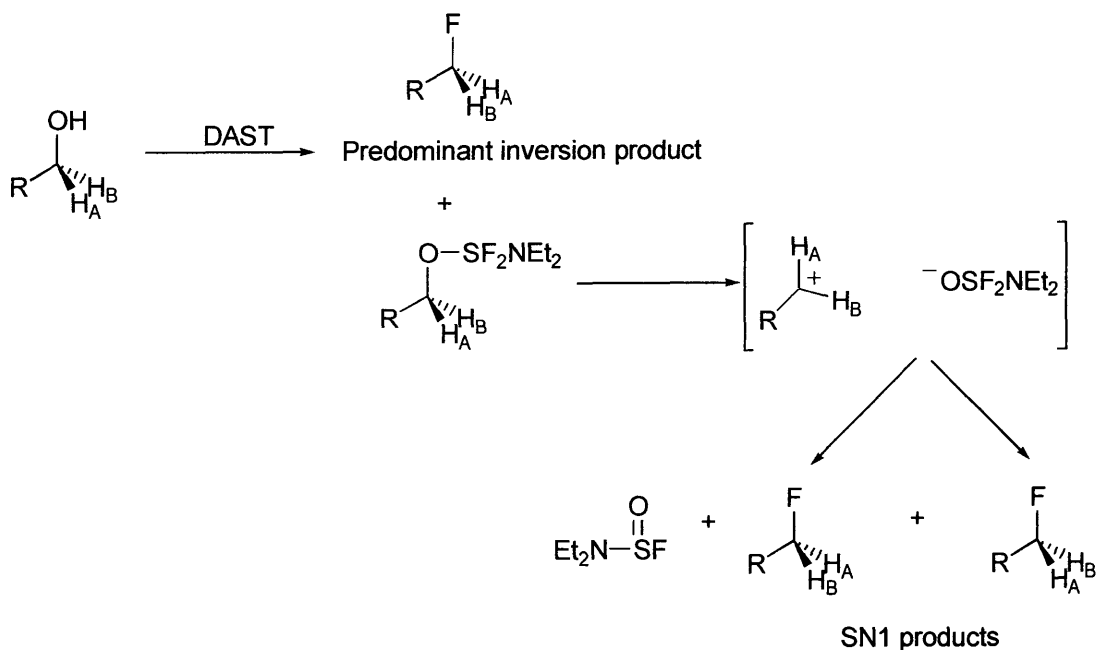
*S*-Alpine-Borane ( $\beta$ -isopinocampheyl-9-borabicyclo[3.3.1]nonane) (**2.24**), the asymmetric reducing agent, is created *in situ* by the addition of (1*S*)-(-)- $\alpha$ -pinene to a solution of 9-BBN in THF. The 9-BBN adds *syn* across the double bond, on the opposite side of the ring to the isopropyl moiety (scheme 2.7).

The *S*-Alpine-Borane stereoselectively hydroborates the *pro-S* face of the benzaldehyde concomitantly releasing the chiral template, (1*S*)-(-)- $\alpha$ -pinene. In order to ensure that all of the *S*-Alpine-Borane has been consumed, acetaldehyde is added to the reaction mixture. The pinene and ethanol generated are removed under vacuum. Midland details the use of ethanolamine to precipitate the 9-BBN as an adduct, thus liberating the benzyl alcohol. Ethanolamine has a boiling point of 170 °C, whereas benzyl alcohol boils at 205 °C. To increase the ease of purification, it was decided to use 8-hydroxyquinoline (**2.25**) (b.p. 267°C) to precipitate the 9-BBN. The enantiomeric excess of the resultant (*R*)-[7-<sup>2</sup>H]-benzyl alcohol was shown to be 88%, by chiral liquid crystal <sup>2</sup>D NMR, using PBLG and chloroform as solvent (Fig. 2.7a).



Scheme 2.7 The stereoselective reduction of [7-<sup>2</sup>H]-benzaldehyde with *S*-Alpine-Borane

The (*R*)-[7-<sup>2</sup>H]-benzyl alcohol (**2.21**) was converted to (*S*)-[7-<sup>2</sup>H]-benzyl fluoride (**2.22**), using DAST (diethylaminosulphur trifluoride) as the fluorinating agent. The enantiomeric excess of the benzyl fluoride was shown, by chiral liquid crystal <sup>2</sup>D NMR, to be 38% (Fig.2.7b).



Scheme 2.8 The steric course of an alcohol's reaction with DAST

Although the fluorination by DAST proceeds predominantly by an inversion process, DAST is renowned for its ability to stabilise carbocations (scheme 2.8). The aromatic group will stabilise carbocation character at the benzylic position. These two factors lead to the reaction proceeding with a considerable degree of S<sub>N</sub>1 character, and thus a loss in enantiomeric excess of the resultant benzyl fluoride. There are reports in the literature of greater steric control with DAST reactions at lower temperatures, such as -50°C.<sup>15</sup> This was investigated in the case of (*R*)-[7-<sup>2</sup>H]-benzyl alcohol; however, although the reaction took longer at the lower temperature, the resultant material showed no increase in enantiomeric purity when examined by chiral liquid crystal <sup>2</sup>D NMR. In a further attempt to increase the stereospecificity of the fluorination reaction, Ishikawa's reagent, N, N-diethyl-1,1,2,3,3,3-hexafluoropropylamine,<sup>16</sup> was also investigated; the product of this reaction showed no greater enantiomeric excess either. It may be concluded that the aromatic ring plays a considerable role in stabilising a benzylic carbocation. For the purpose of a chiral standard for chiral liquid crystal NMR analysis, an enantiomeric excess of 38 % was considered sufficient.

Fluorinating Reagent	% ee
DAST	38%
DAST (-50 °C)	38%
Ishikawa's reagent	38%

Table 2.1 Comparative ee s of [7-<sup>2</sup>H]-benzyl fluoride formed from (*R*)-[7-<sup>2</sup>H]-benzyl alcohol (88% ee) subjected to different fluorinating conditions

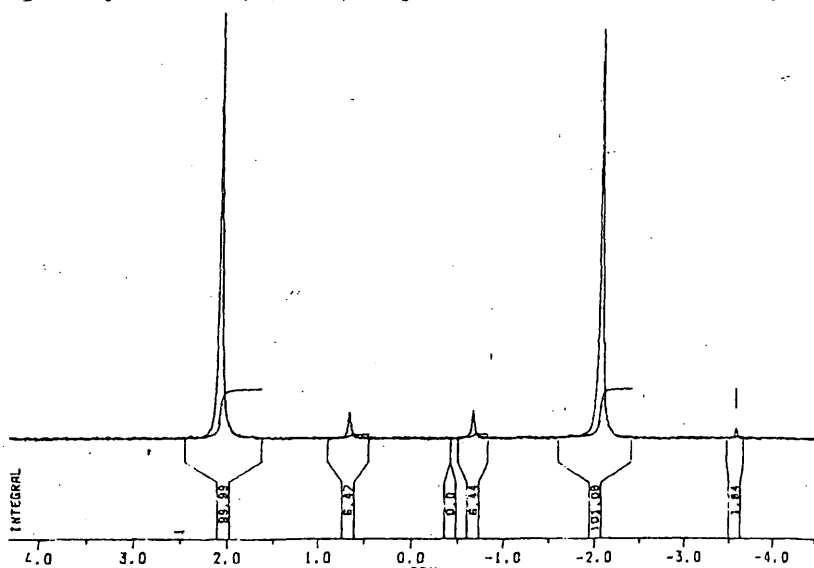


Fig 2.7a <sup>2</sup>H NMR of (*R*)-[7-<sup>2</sup>H]-benzyl alcohol displaying an ee of 88% (Bruker AC-250, 250.133 MHz)

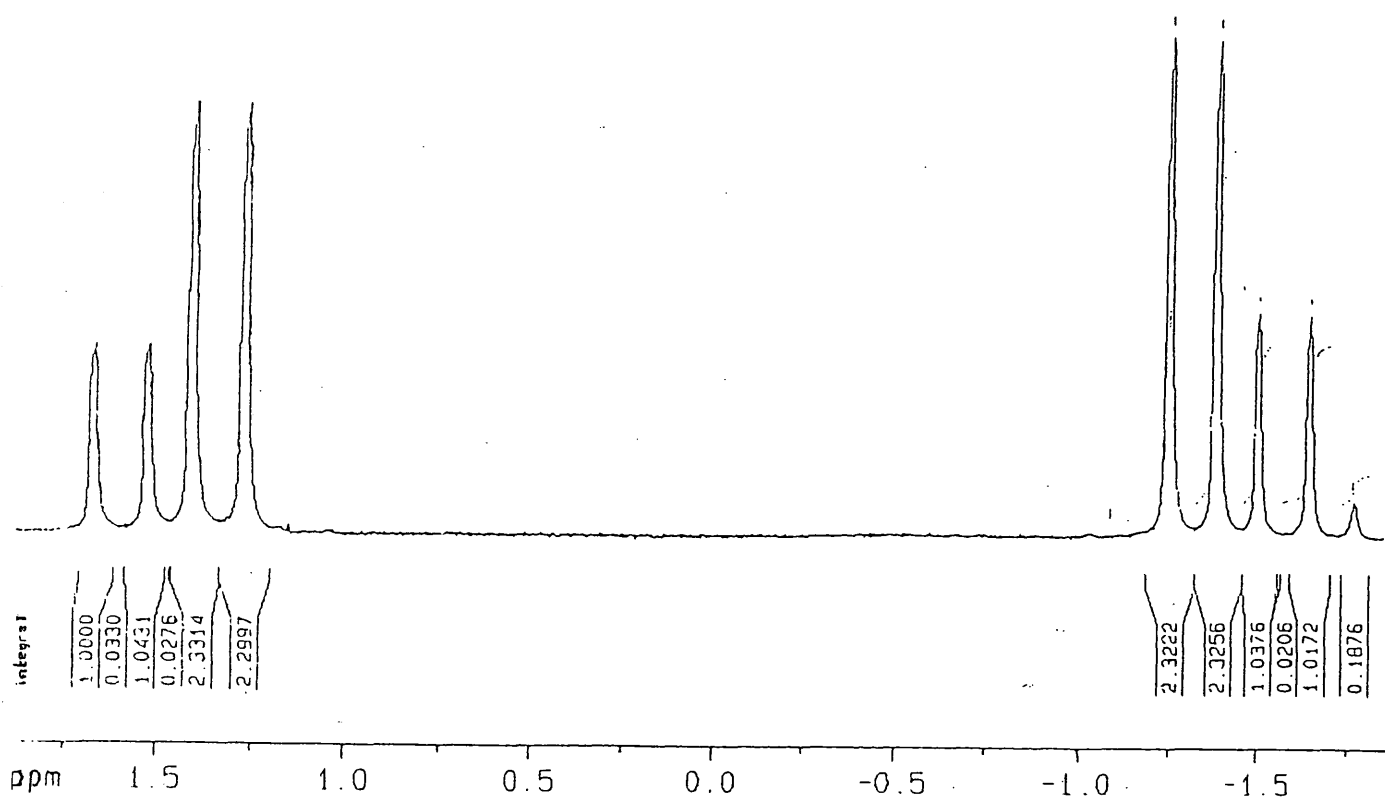


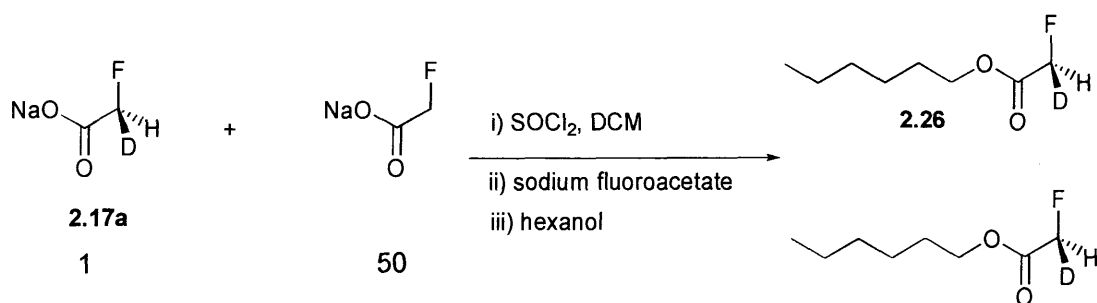
Fig 2.7b  $^2\text{H}$  NMR of (*S*)-[7- $^2\text{H}$ ]-benzylfluoride, displaying an ee of 38%. (Bruker AC-250, 250.133 MHz)

Fig2.7

(materials are analysed in a liquid crystalline solvent of PBLG and chloroform)

O'Hagan reported the preparation of a series of fluorinated carboxylic acids, including 3-fluoropropanoic acid,<sup>17</sup> by the oxidation of their corresponding aromatics, under Sharpless conditions.<sup>18</sup> Accordingly, benzyl fluoride was added to a solution of ruthenium trichloride and potassium periodate in water, acetonitrile and carbon tetrachloride (3:1:1). After 48 hours, no fluoroacetate was observed in the aqueous phase by  $^{19}\text{F}$  NMR. The reaction was repeated, replacing the ruthenium trichloride with ruthenium tetraoxide; once more, no reaction was observed. Finally, potassium permanganate and potassium periodate, in aqueous solution, was shown to effectively convert the benzyl fluoride to fluoroacetate. Purification of the fluoroacetate was achieved by acidifying the supernatant and lyophilizing the fluoroacetic acid, which was subsequently neutralised and freeze dried.

## 2.5 Chiral analysis of (*S*)-[<sup>2</sup>H]-fluoroacetate



Scheme 2.9 Derivatisation of (*S*)-[<sup>2</sup>H]-fluoroacetate as its hexyl ester

Due to its poor solubility, in the PBLG solvent system required for the chiral liquid crystal NMR analysis, (*S*)-[<sup>2</sup>H]-fluoroacetate was converted to its hexyl ester. As the biosynthetic fluoroacetate from *Streptomyces cattleya* had only a low level of deuterium incorporation, a similar system was required to determine whether chiral liquid crystal NMR could be a suitable technique for the analysis. Commercial, unlabelled sodium fluoroacetate was added to the synthetic material to dilute the deuterium label to a level comparable with that of the biosynthetic material. Accordingly, a 50-fold excess of undeuterated fluoroacetate was added to the (*S*)-[<sup>2</sup>H]-fluoroacetate and one equivalent of thionyl chloride introduced to the mixture to form fluoroacetyl chloride. To ensure that all of the thionyl chloride had been consumed an additional aliquot of unlabeled fluoroacetate was added to the reaction mixture. Addition of hexanol to the reaction mixture and flash silica chromatography furnished the hexyl fluoroacetate (scheme 2.9), which was analysed by <sup>2</sup>H chiral liquid crystal NMR (Fig 2.8).

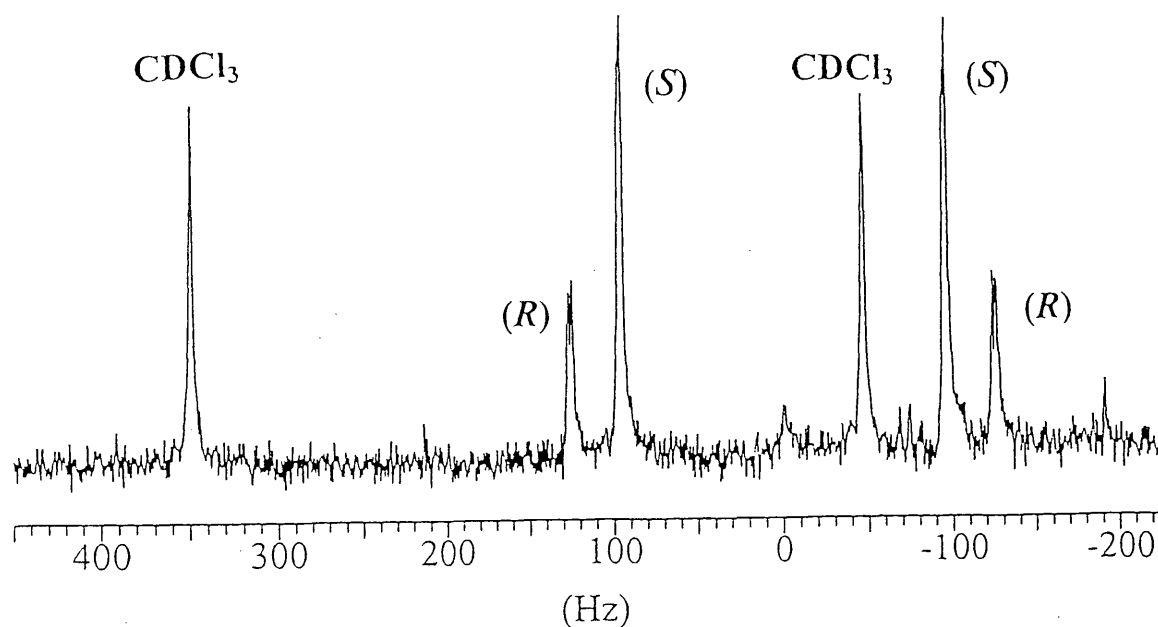


Fig 2.8  $^2\text{H}$  NMR of hexyl (2*S*)-[2- $^2\text{H}$ ]-fluoroacetate in PBLG and chloroform, displaying an ee of 38% (Bruker AC-250 , 250.133 MHz)

The  $^2\text{H}$  NMR of hexyl (2*S*)-[2- $^2\text{H}$ ]-fluoroacetate in poly  $\gamma$ -benzyl L-glutamate and chloroform exhibits a considerable difference in the quadrupolar splittings of the *S* and *R* enantiomers. The difference in splittings is very striking particularly as the molecules are only chiral by virtue of deuterium substitution. Only 2% of the hexyl fluoroacetate molecules analysed contained deuterium, this level of incorporation is comparable with the material that could be prepared from the biosynthetic fluoroacetate. It may be concluded that chiral liquid crystal  $^2\text{H}$  NMR is a powerful technique for examining the chirality of biosynthetically derived [ $^2\text{H}_1$ ]- fluoroacetate.

A number of mid chain, fluorinated, alkanes have found applications in the liquid crystal industry particularly as ferroelectric liquid crystals. To date, no analytical technique has been capable of demonstrating the enantiomeric excess of such compounds with fluorine at a remote chiral centre. Impressed by chiral liquid crystal  $^2\text{H}$  NMR's ability to discriminate between (2*R*)- and (2*S*)-[2- $^2\text{H}$ ]-hexylfluoroacetate, an example of an exceptional chiral resolution, we decided to explore the limits of this technique when applied to fluoroalkanes. To accomplish this, it was necessary to synthesise racemic *n*-fluoro[*n*- $^2\text{H}$ ]-alkanes, gradually increasing *n*, and the chain length, such that the fluorine atom was gradually moved towards the centre of a alkyl chain (table 2.2). Appropriate racemic fluorodeutero alkanes were prepared by firstly reducing the corresponding ketone with lithium aluminium deuteride and then fluorinating the resultant deuterioalcohols with DAST. All ketones, except 4-octanone are commercially available. 4-Octanone may, however, be prepared by the oxidation of 4-octanol with PCC.

<b>Fluoroalkane</b>	Structure	$\text{CH}_3(\text{CH}_2)_x\text{CDF}(\text{CH}_2)_y\text{CH}_3$ x, y
2-Fluoro[2- $^2\text{H}$ ]-hexane		0, 3
3-Fluoro[3- $^2\text{H}$ ]-hexane		1, 2
2-Fluoro[2- $^2\text{H}$ ]-heptane		0, 4
3-Fluoro[3- $^2\text{H}$ ]-heptane		1, 3
3-Fluoro[3- $^2\text{H}$ ]-octane		1, 4
4-Fluoro[4- $^2\text{H}$ ]-octane		2, 3

Table 2.2 Racemic fluoroalkanes

The fluorodeutero alkanes were analysed by chiral liquid crystal  $^2\text{H}$  NMR to investigate whether the enantiomers could be resolved (Fig 2.9).



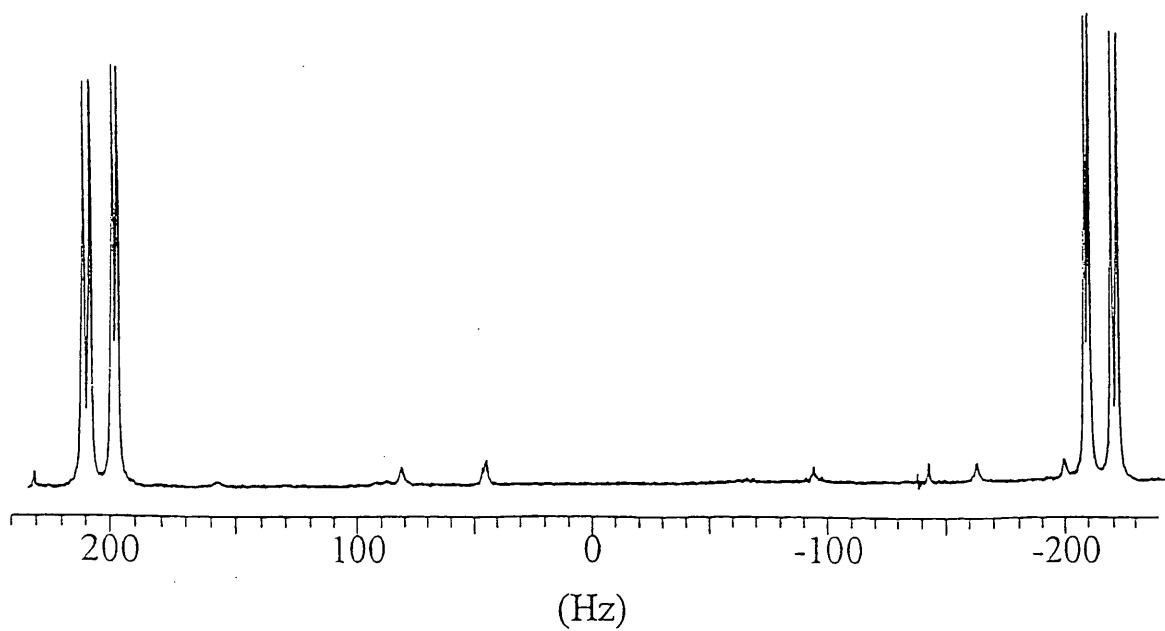


Fig 2.9a  $^2\text{H}$  NMR of 2-fluoro[2- $^2\text{H}$ ]-hexane in PBLG and chloroform (Bruker AC-250, 250.133 MHz)

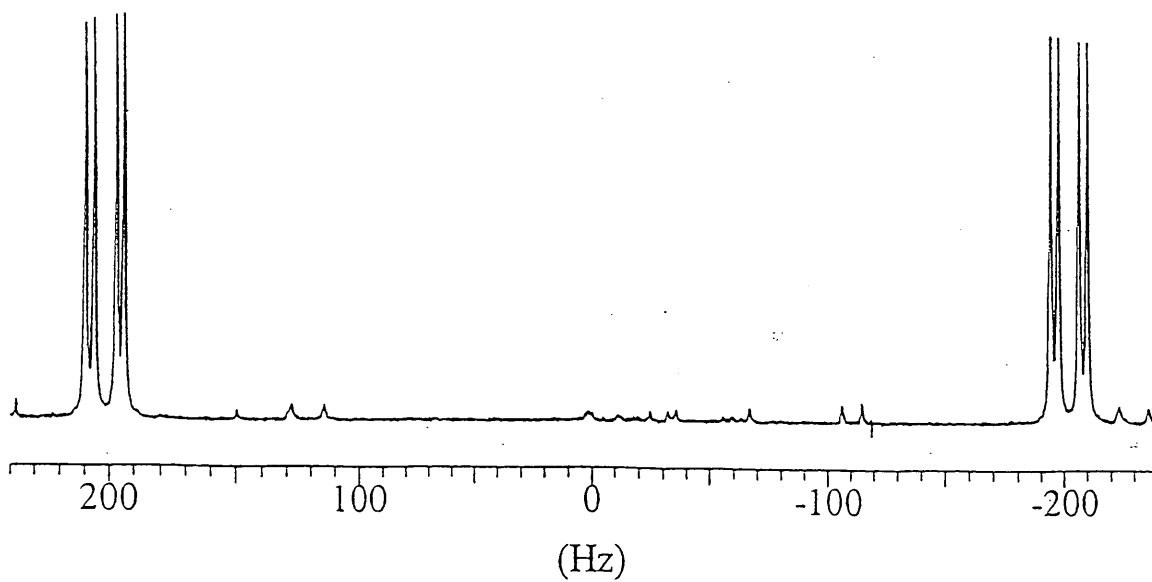


Fig 2.9b  $^2\text{H}$  NMR of 3-fluoro[3- $^2\text{H}$ ]-hexane in PBLG and chloroform (Bruker AC-250, 250.133 MHz)

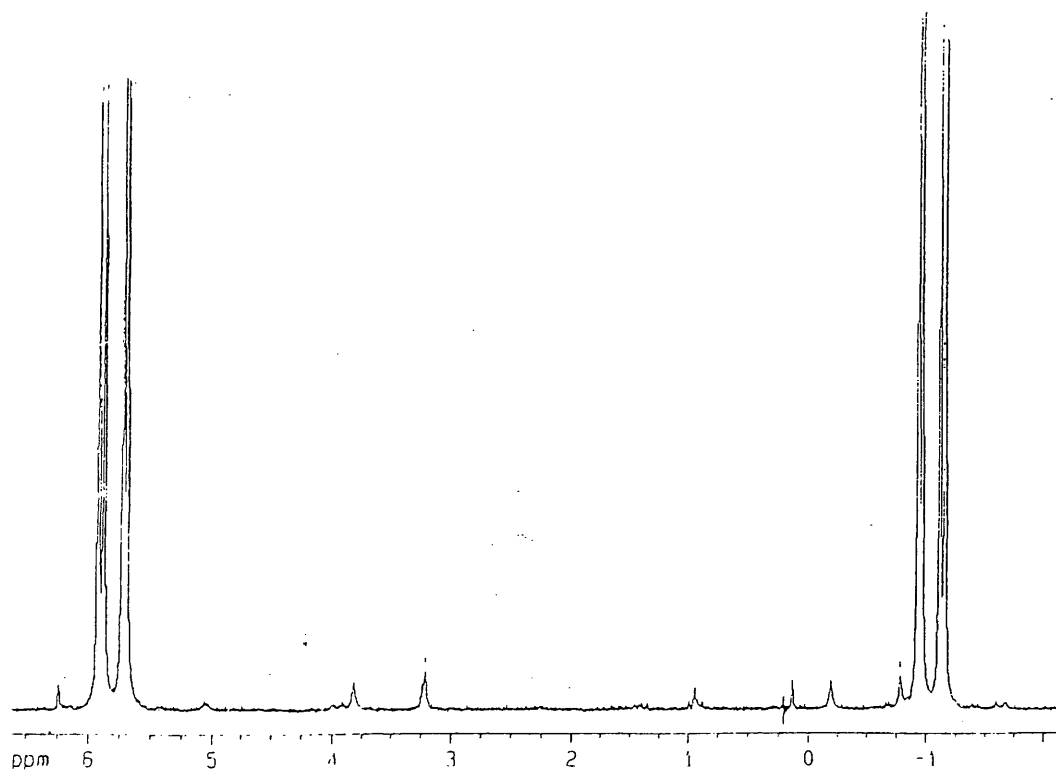


Fig. 2.9c  $^2\text{H}$  NMR of 2-fluoro[2- $^2\text{H}$ ]-heptane in PBLG and chloroform (Unity Inova 500 MHz)

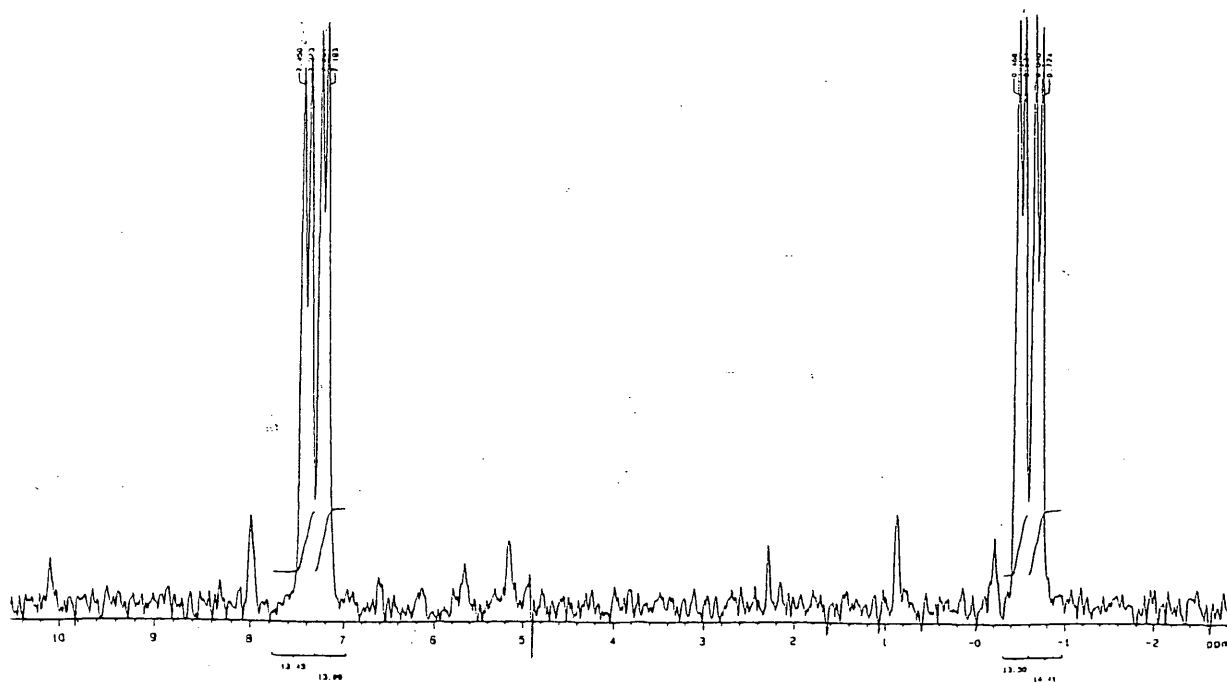


Fig 2.9d  $^2\text{H}$  NMR of 3-fluoro[3- $^2\text{H}$ ]-heptane in PBLG and chloroform (Unity Inova 500 MHz)

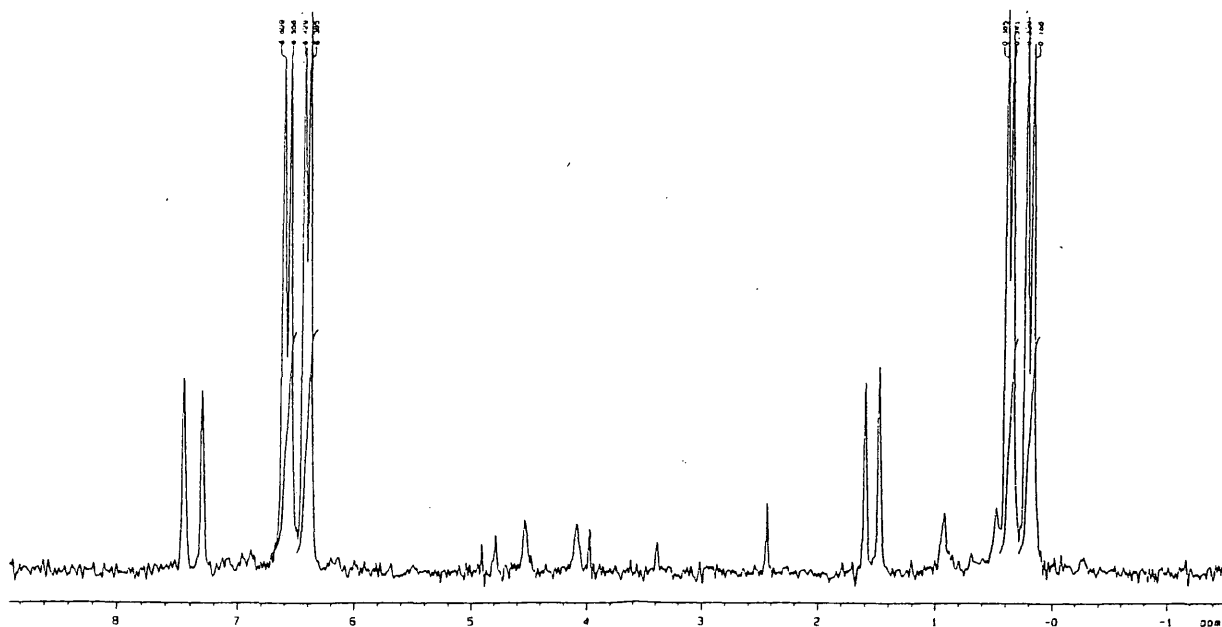


Fig 2.9e  $^2\text{H}$  NMR of 3-fluoro[3- $^2\text{H}$ ]-octane in PBLG and chloroform (Unity Inova 500 MHz)

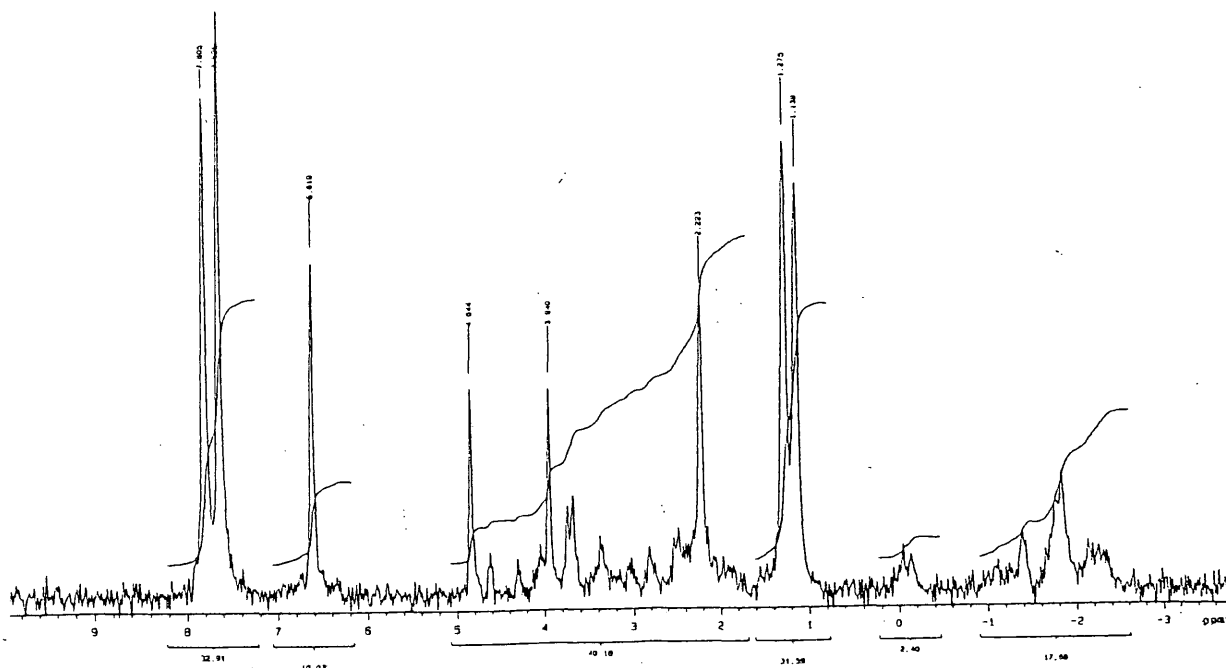


Fig 2.9f  $^2\text{H}$  NMR of 4-fluoro[4- $^2\text{H}$ ]-octane in PBLG and chloroform (Unity Inova 500 MHz)

The two enantiomers of the 2-fluoro[2- $^2\text{H}$ ]-hexane, 3-fluoro[3- $^2\text{H}$ ]-hexane, 2-fluoro[2- $^2\text{H}$ ]-heptane, 3-fluoro[3- $^2\text{H}$ ]-heptane and 3-fluoro[3- $^2\text{H}$ ]-octane are clearly resolved and the resultant spectra are shown in figures. 2.89a- 2.9e. In the NMR spectra of the 4-fluoro[4- $^2\text{H}$ ]-octane only the deuterium-fluorine coupling is

<b>Fluoroalkane</b>	$\Delta\nu_{Q1} - \Delta\nu_{Q2}$ (Hz)	Machine and Field
2-Fluoro[2- <sup>2</sup> H]-hexane	2.3	(Bruker AC-250, 250.133 MHz)
3-Fluoro[3- <sup>2</sup> H]-hexane	3.5	(Bruker AC-250, 250.133 MHz)
2-Fluoro[2- <sup>2</sup> H]-heptane	4.7	(Unity Inova 500 MHz)
3-Fluoro[3- <sup>2</sup> H]-heptane	5.6	(Unity Inova 500 MHz)
3-Fluoro[3- <sup>2</sup> H]-octane	3.7	(Unity Inova 500 MHz)
4-Fluoro[4- <sup>2</sup> H]-octane	Not Resolved	(Unity Inova 500 MHz)

Table 2.3 Resolution of racemic fluoroalkanes by <sup>2</sup>H chiral liquid crystal NMR

It may be concluded that <sup>2</sup>H chiral liquid crystal NMR is a very powerful tool for examining the enantiomeric excess of fluoroalkanes. It is demonstrated that it is possible to resolve the enantiomers of systems chiral by virtue of deuterium substitution, such as of 3-fluoro[3-<sup>2</sup>H]-heptane and 3-fluoro[3-<sup>2</sup>H]-hexane. This, at present, must be viewed as the upper limit of the technique, as when the fluorine is moved towards the centre of a slightly longer alkyl chain (e.g. 4-fluoro[4-<sup>2</sup>H]-octane), the two enantiomers are no longer resolved.

## References

- 1 H. G. Floss in *Methods in Enzymology*, **87**, part C, Ed. D. L. Purich, Academic Press, New York, London, Paris, San Diego, São Paulo, Sydney, Tokyo, Toronto, 1982, p126.
- 2 B. Sedgwick, J. W. Cornforth, *Eur. J. Biochem.*, 1977, **75**, 465.
- 3 D. Parker, *Chem Rev.*, 1991, **91**, 1441.
- 4 J. A. Dale, D. L. Dull, H. S. Mosher, *J. Org. Chem*, 1969, **34**, 2543.
- 5 D. Parker, *J. Chem. Soc., Perkin Trans 2*, 1983, 83
- 6 D. Gartz, J. Reed, J. Rétey, *Helv. Chim. Acta*, 1996, 1021
- 7 M. Jakubcora, A. Meddour, J. M. Péchiné, A. Baklouti, J. Courtieu, *J. Fluor. Chem.*, 1997, **86**, 149
- 8 P. Lesot, D. Merlet, A. Loewenstein, J. Courtieu, *Tet. Assym.*, 1998, **9**, 1871.
- 9 J. M. G. Cowie, *Polymers: Chemistry and Physics of Modern Materials*, 2<sup>nd</sup> Ed. (1991)Blackie and Sons Ltd., London, p 362.
- 10 A. Meddour, D. Atkinson, A. Loewenstein, J. Courtieu, *Chem. Eur. J.*, 1998, **4**, 1142.
- 11 R. Keck, H. Haas, J. Rétey, *FEBS Lett.*, 1980, **114**, 287.
- 12 F. L. M. Pattison, R. L. Buchanana, F. H. Dean, *Can. J. Chem.*, 1965, **43**, 1700.
- 13 K. G. Au, C. T. Walsh, *Bio. Org. Chem.*, 1984, **12**, 197.
- 14 M. M. Midland, S. Greer, A. Tramontano, S. A. Zderic, *J. Am. Chem. Soc*, 1979, **101**, 2352.
- 15 V. Madiot, P. Lesot, D. Gree, J. Courtieu, R. Gree, *Chem Commun.*, 1999, 169.
- 16 A. Takaoka, H. Iwakiri, N. Isikawa, *Bull. Chem Soc. Jpn.*, 1979, **52**, 3377.
- 17 D. O'Hagan, *J. Fluorine Chem.*, 1988, **43**, 371
- 18 K. B. Sharpless, *J. Org. Chem.*, 1981, **46**, 3936

## **CHAPTER 3**

### **Fluorine in Bioorganic Chemistry**

## CHAPTER 3

### **Fluorine in Bioorganic Chemistry**

#### Introduction and Background

##### 3.1 A historical perspective of fluorine

The use of the mineral fluorospar ( $\text{CaF}_2$ ) as a flux (an additive to aid the soldering of a material), was first described in 1529 by Georgius Agricola. It was due to this early application that A.M. Ampere suggested to Sir Humphrey Davy, in 1812, that the element be named *le fluor* (Latin *fluor*, flowing). In the 17<sup>th</sup> century, scientists discovered the curious property that fluorospar has of emitting light when heated and, in 1670, H. Schwanhard found that if a strong acid was mixed with fluorospar corrosive vapours were evolved which could be used to decoratively etch glass. However, it was not until 1771 that C. W. Scheele was able to produce a crude solution of hydrofluoric acid. All attempts to isolate the free element by either chemical reactions or electrolysis were frustrated due to the extremely reactive nature of free fluorine. Eventually, in 1886, it was H. M. Moissan who succeeded in electrolysing a solution of  $\text{KHF}_2$  in HF to produce a gas which caused crystalline silicon to burst into flames. He cautiously reported the result "One can indeed make various hypotheses on the nature of the liberated gas; the simplest would be that we are in the presence of fluorine". Moissan was rewarded for his efforts by being given the Nobel Prize for Chemistry in 1906.

### 3.2 The nature of the carbon fluorine bond

It has been said that if a man were to have the features of fluorine, he would be small, greedy and violent, and would therefore be either ostracised by society or governing it.<sup>1</sup> Fluorine has the smallest van der Waals radius of all the halogens (135 pm) and is comparable in size to the smallest atom, hydrogen (120 pm). Fluorine also has the property of being the most electronegative of the elements. These two features combined lead to the C-F bond being the strongest single bond involving carbon, 10% stronger than the C-H bond and considerably stronger than a C-C bond, which has a bond dissociation energy of 243 kJmol<sup>-1</sup>. The C-F bond length lies between that of C-H and C-OH in magnitude (Table 3.1).

X	Van der Waals Radius (pm)	Electronegativity (Pauling scale)	Bond length C-X (pm)	CH <sub>3</sub> X bond dissociation energy (kJmol <sup>-1</sup> )
F	135	4.0	139	460
Cl	180	3.0	178	356
Br	195	2.8	193	297
I	215	2.5	214	238
H	120	2.2	109	414
O	140	3.5	143 (in OH)	

Table 3.1 A comparison of the halogens

### 3.3 Fluorine's effect upon the bioactivity of molecules

The small size and high electronegativity of fluorine have implications for its use in altering the biological activity of molecules. The substitution of fluorine into a molecule in the place of hydrogen introduces minimal steric alterations. This is particularly advantageous when the conformation of a molecule is important to its biological role, for example, in the way in which the molecule interacts with the active site of an enzyme. Once introduced into a molecule, the high C-F bond energy renders the substituents relatively resistant to metabolic transformations. In addition to this, fluorine's high electronegativity can have pronounced effects upon the electron distribution within the molecule. Other substituents will thus be rendered more or less reactive. Fluorine, having a high electron density, may act as a weak



hydrogen bond acceptor. It is also noteworthy that the C-F bond length (139 pm) is very similar in magnitude to the C-OH bond length (143 pm), and thus fluorine may be used as a hydroxyl substitute.

The many different outcomes of substituting fluorine into a bioactive molecule make it difficult to predict to what extent the molecule's activity will be enhanced. The first significant report of the biological activity of a molecule being successfully modified by selective fluorination was Fried's preparation of 9- $\alpha$ -fluoro-hydrocortisone acetate (3.1).<sup>2</sup>

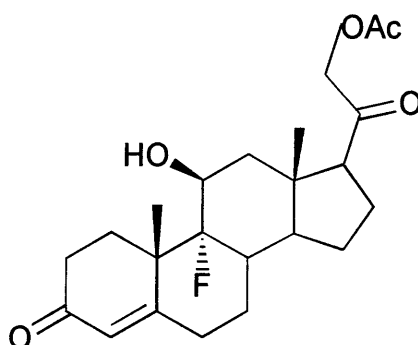
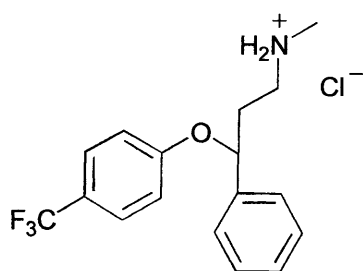


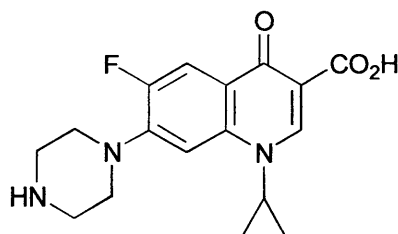
Fig. 3.1 9- $\alpha$ -Fluoro-hydrocortisone acetate (3.1)

### 3.4 Fluorine's role in medicine

The number of commercially available drugs containing fluorine is rapidly increasing. Many of the current blockbuster medicines such as Eli Lilly's Prozac (fluoxetine) (3.2), the world's most prominent antidepressant in terms of both volume and sales, and Ciprofloxacin (3.3), a broad spectrum antibacterial which earns almost \$200 m a year for Bayer, contain the element.



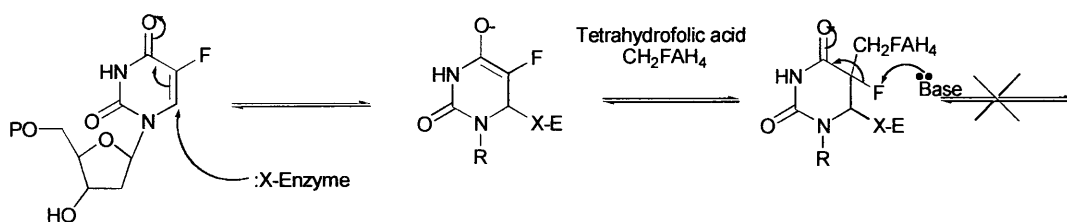
Prozac (3.2)



Ciprofloxacin (3.3)

Fig. 3.2 Fluorine containing drugs

The modes of action of fluorine containing drugs are many and varied. One common use of the element is in deceptor molecules. A common theme in enzyme-catalysed reactions is the loss of a proton. In many medicines, for example the anticancer drug 5-fluorouracil (3.4), the therapy takes advantage of the fact that the substitution of fluorine for hydrogen does not alter the size and shape of the molecule. The fluorine effectively acts as a deceptor. The enzyme thymidine synthase mediates the conversion of deoxyuridine monophosphate to thymidine monophosphate. The reaction proceeds with the substrate, enzyme and tetrahydrofolic acid ( $\text{CH}_2\text{FAH}_4$ ) forming a ternary complex; the dissociation of this complex by the elimination of  $\text{FAH}_4$  to form the product requires the loss of the C-5 proton. The analogous reaction cannot proceed with 5-fluorouracil as this would involve the loss of a fluoro cation, an energetically unlikely event. Instead, the 5-fluorouracil is converted *in vivo* only to 5-fluorodeoxyuridine monophosphate and DNA and RNA directed cytotoxicity result (Scheme 3.1).<sup>3, 4</sup>



5-fluorouracil (3.4)

### Scheme 3.1 Mode of action of 5-fluorouracil

Another role of fluorine in medicinal chemistry is to impart increased hydrolytic stability to compounds. There are many bioactive molecules which contain readily hydrolysed functional groups such as enol ethers, ketals and glycosidic bonds. This is a particular problem when orally administered medicines come into contact with the strongly acidic environment of the stomach. The electron withdrawing properties of fluorine can be exploited by introducing the element proximal to the site where protonation initiates hydrolysis. This has been successfully used to increase the half life of certain drug candidates.

One notable case has been the increase in the hydrolytic stability of prostacyclin ( $\text{PGI}_2$ ) an inhibitor of platelet aggregation. The native molecule has a  $t_{1/2} = 2\text{-}3$  minutes, in contrast to 7-fluoro- $\text{PGI}_2$  (3.5) with a  $t_{1/2} = 1$  month.<sup>5</sup>

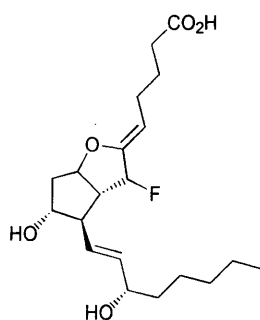


**Fig 3.3 7-Fluoro-PGL<sub>2</sub> (3.5)**

The exact modes of action of other drugs are less clear-cut and understood, for example, although it is known that the trifluoromethyl group in Prozac (3.2) increases the molecule's lipophilicity its function as a serotonin uptake inhibitor is not well documented.

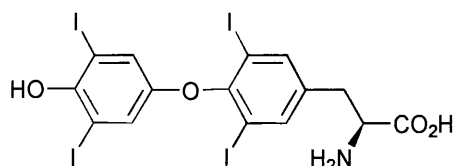
### **3.5 Halogenated natural products**

Until 1954 only a dozen halogenated natural products were known. In 1968, Fowden wrote: "present information suggests that organic compounds containing covalently bound halogens are found only infrequently in living organisms".<sup>6</sup> The past half-century has shown this to be a misconception, as today more than 3000 such compounds are known. This vast number may be attributed, almost equally, to bromine and chlorine containing compounds, though there are almost 100 known iodinated natural products. The majority of iodinated natural products known to date occur as compounds such as the thyroid hormone thyroxine (3.6). This smaller number may not be a true representation of the quantity of existing organoiodides, as the relatively unstable C-I bond may lead to difficulties in isolating such compounds.

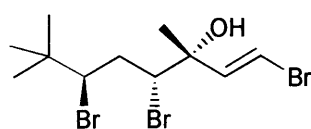
Over 1000 organohalogens have been isolated from marine plants. One species alone, the favourite edible seaweed of most native Hawaiians "limu kohu" (*Asparagopsis taxiformis*), contains almost 100 organohalogen compounds, and 80% of its weight is composed of bromoform (CHBr<sub>3</sub>).

The organohalogens are structurally diverse, some of the simpler structures are those of the halogenated monoterpenes produced by marine algae. Compounds 3.7 and 3.8 were first isolated from the sea hare, *Aplysia californica* which grazes upon algae containing these metabolites. The sea hare is thereby not only using the algae as a source of nutrition but also as a provider of chemical protection.<sup>7</sup> The sea hare shares this technique of stealing its chemical defence with the sea slug *Chromodoris*

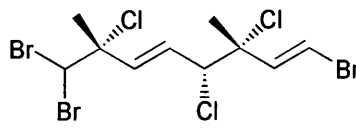
*hamiltoni*. The sea slug contains four chlorinated homo-diterpenes, one of which is hamiltonin C (3.9), as a consequence of feeding upon sponges. Halogenated terpenes are also biosynthesised by terrestrial plants, for example, Asian bracken ferns contain various chlorinated pterosins such as pterosin F (3.10) an anti-feedant responsible for cattle poisoning.<sup>8</sup> One historically noteworthy compound is the ancient Egyptian dye, Tyrian purple (3.11), the brominated analogue of indigo.<sup>9</sup>



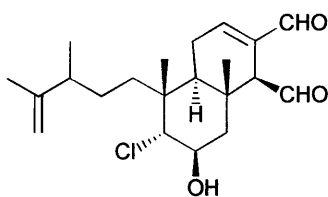
thyroxine (3.6)



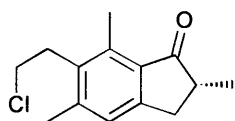
(3.7)



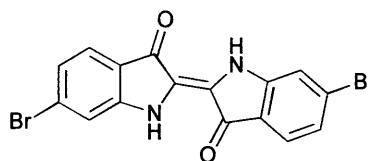
(3.8)



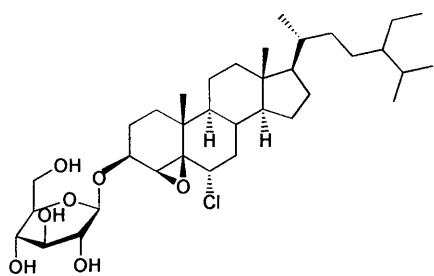
hamiltonin C (3.9)



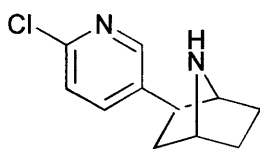
pterosin F (3.10)



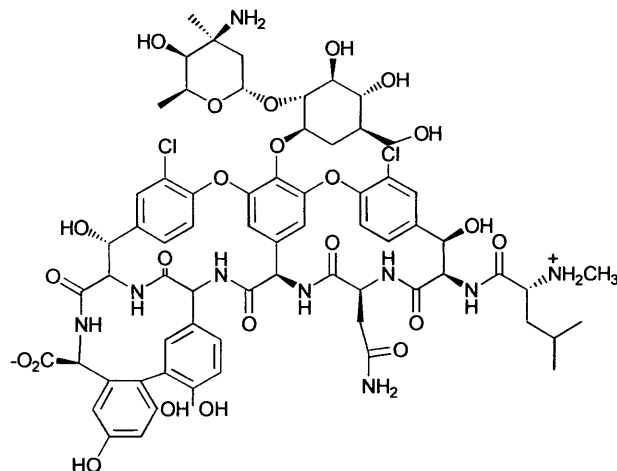
Tyrian purple (3.11),



blattellastonide (3.12),



epibatidine (3.13),



vancomycin (3.14)

**Fig 3.4 Halogenated natural products**

Various halogenated steroids have been isolated from an assortment of sources including sponges and terrestrial plants. One particularly interesting example is that of blattellastonide (3.12), the German cockroach pheromone.<sup>10</sup>

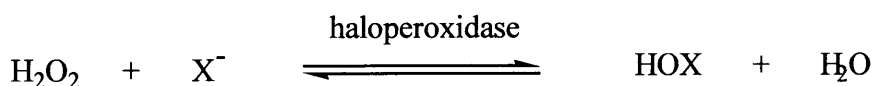
Although there exist a huge number of known alkaloids, so far only a few halogenated examples have been discovered. One such compound is epibatidine (3.13), a potent analgesic secreted by the Equidorian frog *Epipedobates tricolor*.<sup>11</sup>

Vancomycin (3.14) is one of the most medicinally important of the halogenated natural products and also one of the most structurally complex. This huge glycopeptide antibiotic is the drug of choice to treat methicillin-resistant *Staphylococcus aureus* infections, particularly those occurring in hospitals.<sup>12</sup> The chlorine atoms are essential for enforcing the molecule into the required conformation for receptor binding.

### 3.6 Mechanisms for biohalogenation

The biohalogenation of secondary metabolites has traditionally been thought to proceed *via* a haloperoxidase type mechanism. The haloperoxidase enzyme catalyses the oxidation of a halide ion to the corresponding hypohalous acid. The halogen is thus activated as an electrophile and may halogenate the organic substrate.

(Scheme 3.2)



#### Scheme 3.2 The haloperoxidase reaction

The various haloperoxidases are classified firstly with respect to their oxidising capabilities:-

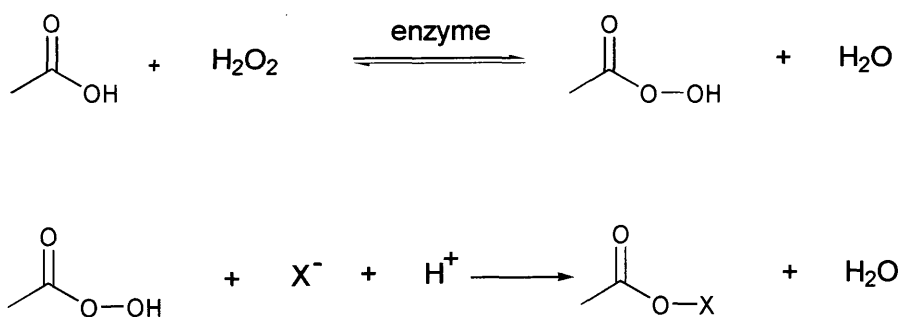
Chloroperoxidases may oxidise Cl, Br and I.

Bromoperoxidases may oxidise Br and I

Iodoperoxidases may oxidise only iodine.

Secondly, the enzymes are categorised with respect to the nature of their active site. Three different classes emerge :- haem-containing, vanadium-containing and metal-free haloperoxidases. It has been suggested that the mode of action of the metal-free haloperoxidases is firstly the perhydrolysis (lysis with hydrogen peroxide) of acetic

acid to form peracetic acid. The peracetic acid then diffuses away from the active site of the enzyme and oxidises a halide. (Scheme 3.3)<sup>13</sup>

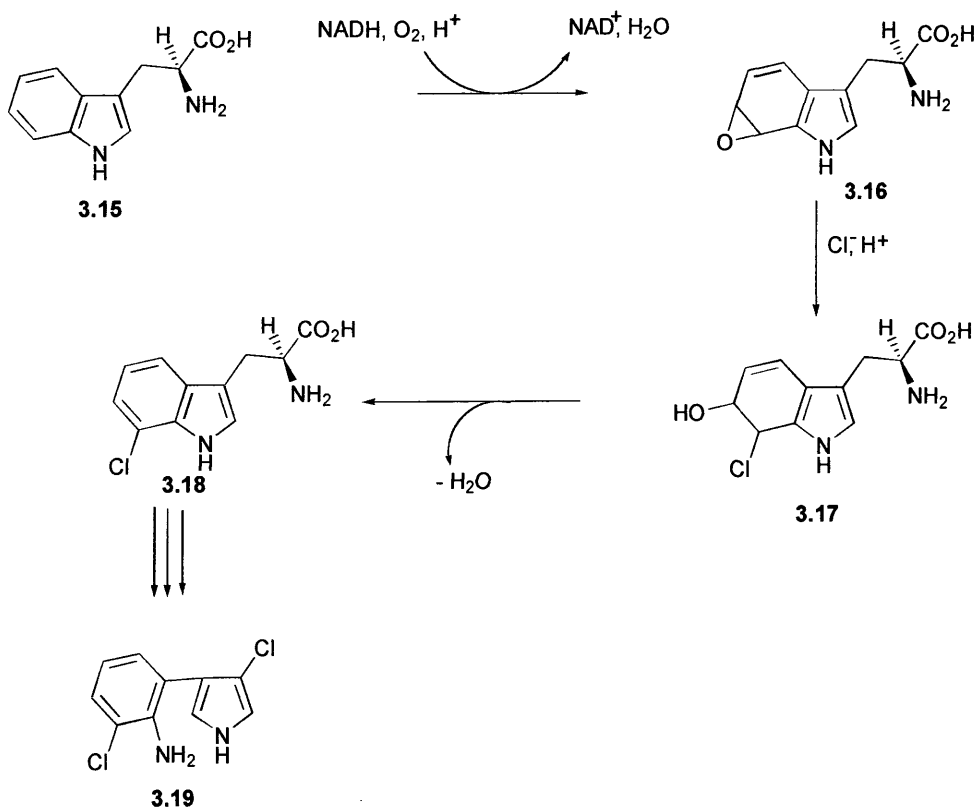


Scheme 3.3 Activation of halogens by peracetic acid formed from acetic acid and hydrogen peroxide

There exists some dispute within the literature as to whether these enzymes are true haloperoxidases. The enzymatic ability to catalyse perhydrolysis is not as rare as initially thought, and is not limited to haloperoxidases. It has been shown, using the same *in vitro* conditions employed in the study of metal free haloperoxidases, that lipases are able to catalyse the perhydrolysis of the corresponding long chain carboxylic acids. Esterases were also shown to catalyse the perhydrolysis of acetic acid. In addition, it has been demonstrated that the rates of halogenation catalysed by the metal free haloperoxidases are significantly lower than those displayed by the metal-containing microbial haloperoxidase derived from *Curvularia verruculosa*.<sup>14</sup>

The literature also raises the question as to whether it is more likely that NADH dependant halogenases are responsible for biohalogenation than haloperoxidases.

The analysis of the genes responsible for pyrrolnitrin biosynthesis (3.19) showed no evidence for the presence of a haloperoxidase on the biosynthetic pathway.<sup>15</sup> An alternative mechanism, that would lead to greater substrate specificity and regiospecificity, has been proposed. In this hypothesis, the enzyme would react first with the substrate to be halogenated, activating it as the epoxide for subsequent nucleophilic attack by a halide anion. (Scheme 3.4)<sup>16</sup>



Scheme 3.4 Pyrrrolnitrin biosynthesis

### 3.7 Fluorinated secondary metabolites

Fluorine is the most abundant halogen in the earth's crust, however, paradoxically there exist only a few known fluorinated natural products; these include fluoroacetate (section 3.7.2), the  $\omega$ -fluorofatty acids (section 3.7.3), fluoroacetone (section 3.7.4), fluorocitrate (section 3.7.5) and nucleocidin (section 3.7.1). The fluorinated metabolites have been predominantly isolated from tropical and sub-tropical plant species and, to date, there are no known examples biosynthesised in the marine environment or by members of the animal kingdom.

One reason for the dearth of fluorinated secondary metabolites is fluorine's poor bio-availability. Although fluorine is the 13<sup>th</sup> most abundant element in the earth's crust, many of the mineral fluorides (e.g. fluorospar) are insoluble in water. This becomes very apparent when examining the relative concentrations of fluoride and chloride present in the earth's crust and in sea-water.

X	Concentration in the earth's crust (ppm)	Concentration in sea water (ppm)
F	544	1.3
Cl	126	19 000

Table 3.2 Concentrations of fluorine and chlorine in the earth's crust and in sea water

Another reason for the low occurrence of fluorinated secondary metabolites is the difficulty of activating fluorine so that it may become involved in biochemical processes.

The fluoride anion is a poor nucleophile, fluoride also has a high enthalpy of hydration and a sphere of surrounding water molecules further compromise the anion's nucleophilicity. Activation of fluorine for electrophilic chemistry, by a haloperoxidase reaction, also appears unlikely as this would require overcoming an extremely high redox potential.

X	Heat of hydration of X <sup>-</sup> (kJmol <sup>-1</sup> )	Standard redox potential E <sup>o</sup> (V)
F	490	-3.06
Cl	351	-1.36
Br	326	-1.07
I	285	-0.54

Table 3.3 Comparative heats of hydration and redox potentials of the halogens

### 3.7.1 Nucleocidin

In 1957, a culture of the bacterium *Streptomyces calvus*, that had been isolated from an Indian soil sample, was observed to produce a novel secondary metabolite. The natural product displayed broad spectrum antibiotic activity, and was an especially effective antitrypanosomal agent.<sup>17</sup> Clinical use of this antibiotic was curtailed by its extreme toxicity. The empirical formula of C<sub>11</sub>H<sub>16</sub>N<sub>6</sub>SO<sub>8</sub> was initially ascribed to the compound. During the 1960's the formula was revised twice, and it was eventually realised that some of the complexity in the <sup>1</sup>H NMR was due to protons coupling with fluorine rather than hindered rotation, as previously believed. Total synthesis of the compound, in 1976, finally confirmed it to be 4'-fluoro-5'-O-sulfamoyl-adenosine



(3.20).<sup>18</sup> The presence of fluorine in the metabolite was rather a surprise as the medium in which the micro-organism had been grown had not been supplemented with fluoride. However, levels of the antibiotic produced were low, and it was discovered that the fluoride was present as a trace impurity in the corn liquor used to culture the bacterium. 4'-Fluoro-5'-*O*-sulfamoyl-adenisine (nucleocidin) is the only metabolite known to display a fluoro-sugar moiety. Subsequent attempts to encourage the organism to produce the compound again have failed, and the compound's biosynthesis remains a mystery.

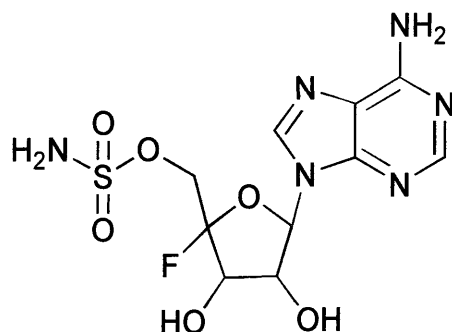


Fig 3.5 Nucleocidin (3.20)

### 3.7.2 Fluoroacetate

Fluoroacetate is by far the most abundant of the fluorometabolites. To date, at least 30 plant species, principally leguminous varieties, have been found to accumulate considerable quantities of the compound.<sup>19</sup> Fluoroacetate was first identified by Marais, in 1943, as the toxic component in the South African plant *Dichapetalum cymosum*.<sup>20</sup> This plant is responsible for considerable cattle death in the Transvaal region. The plant is most toxic in the early spring, having the capability to accumulate up to 2500  $\mu\text{g g}^{-1}$  dry weight, in the young leaves.

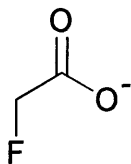


Fig 3.6 Fluoroacetate (3.21)

To date, the highest levels of fluoroacetate accumulation have been observed in the Brazilian plant *Palicourea margravii* and the seeds of the Tanzanian plant *Dichapetalum braunii*. The flower stalk and seeds of the former plant can accumulate

fluoroacetate up to  $5000\mu\text{g g}^{-1}$  dry weight,<sup>21</sup> whereas the latter has the ability to accumulate a very high level of  $8000\mu\text{g g}^{-1}$  dry weight.<sup>22</sup>

The level of fluoroacetate has been observed to vary considerably between the different organs of one particular species of plant, the leaves and the seeds tending to accumulate the compound to a higher concentration.<sup>23</sup> Fluoroacetate concentrations have also been shown to fluctuate through the seasons, the maximum protection being afforded to the young leaves, in the spring, to deter grazers. Geographical location, also, impacts upon the levels of fluoroacetate found within the same species. This may reflect the amount of fluoride present in the soil, but also suggests considerable genetic variability exists within the species in its ability to produce fluoroacetate.

Many plants have the capacity to biosynthesise and bioaccumulate fluoroacetate and fluorocitrate, to some level, when grown in soils with a sufficient fluoride concentration. For example, commercial tea from the plant *Thea sinensis* can contain as much as  $30\mu\text{g g}^{-1}$  dry weight of fluorocitrate, and levels of  $60\mu\text{g g}^{-1}$  have been reported in oatmeal. (Such levels are well below toxicological significance.<sup>24</sup>)

This finding suggests that plants, in general, have the latent ability to biosynthesise and store the fluorometabolite toxins to some extent. It is an evolutionary refinement that has amplified this ability, in some plants, for use as a defence mechanism.

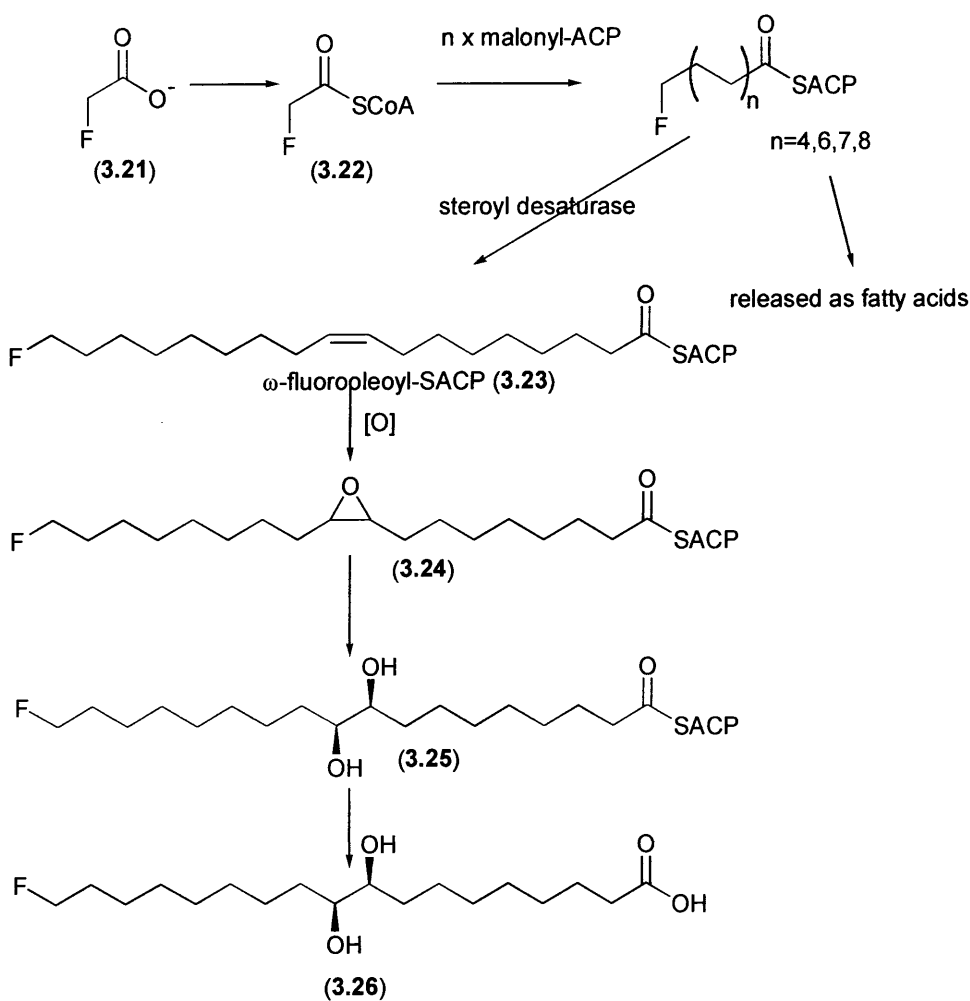
### **3.7.3 $\omega$ -Fluorofatty acids**

*Dichapetalum toxicarium* is a shrubby plant from Sierra Leone which is known to accumulate fluoroacetate in its leaves. It has also been shown to store various  $\omega$ -fluorofatty acids in its seeds (concentrations in the region of  $1800\mu\text{g g}^{-1}$  dry weight). Up to 3 % of the lipids within the seed are fluorinated, the most abundant being  $\omega$ -fluoro-oleic acid ( $\text{C}_{18:1\text{F}}$ ).<sup>25, 26, 27</sup> Eight other  $\omega$ -fluoro compounds including saturated and unsaturated acids have been identified:-  $\text{C}_{10:0\text{F}}$ ,  $\text{C}_{14:0\text{F}}$ ,  $\text{C}_{16:0\text{F}}$ ,  $\text{C}_{16:1\text{F}}$ ,  $\text{C}_{18:0\text{F}}$ ,  $\text{C}_{18:2\text{F}}$ ,  $\text{C}_{20:0\text{F}}$ , and  $\text{C}_{20:1\text{F}}$ .

The relative concentrations of these  $\omega$ -fatty acids mirror those of the unfluorinated analogues. This suggests that the  $\omega$ -fluorofatty acids are processed *via* the enzymes associated with fatty acid metabolism. Fatty acid synthases (FASs) have broad substrate specificity and may utilise a range of different starter units. The fluorofatty acids identified to date all have fluorine at the  $\omega$ -position, implying that enzymatic constraints operate at subsequent stages of the biosynthetic process. It would appear that fluoroacetate incorporated as the starter unit into these  $\omega$ -fluorofatty acids, is not

biosynthesised within the seed. Results from a study of the distribution of fluoroacetate within the plant, point to fluoroacetate first being biosynthesised within the young leaves and then being transported, after fertilization of the flower, to the developing embryo where fluoroacetyl-CoA is then incorporated into the fatty acids.

*Threo*-18-fluoro-9,10-dihydroxystearic acid (3.26) has been isolated from the saponified seed oil of *D. toxicarium*. It is envisaged that this compound is biosynthesised from  $\omega$ -fluorooleic acid (3.23) via an intermediate 9, 10-epoxide (3.24). The diol may be an artefact, having arisen from hydrolysis of the epoxide during the isolation process.

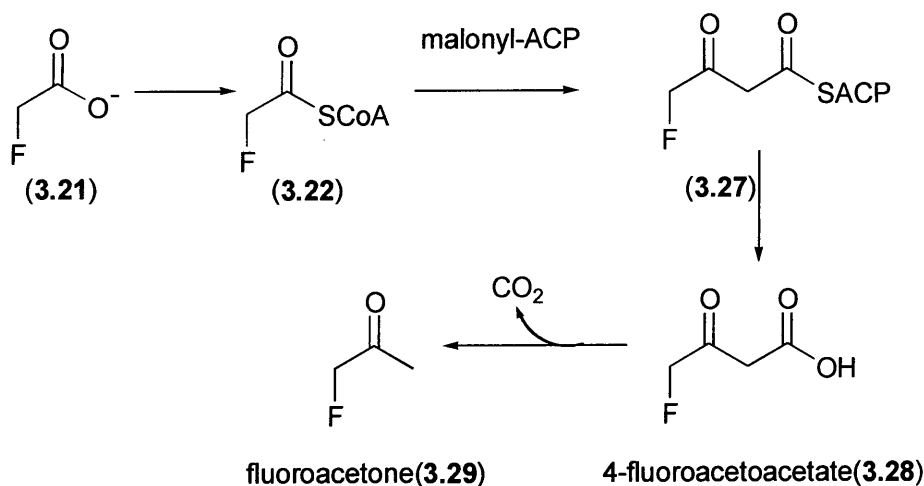


Scheme 3.5 Biosynthesis of *threo*-18-fluoro-9,10-dihydroxystearic acid (3.26)

### 3.7.4 Fluoroacetone

In 1967, Peters and Shorthouse discovered that when they incubated various plants, including *Acacia georginae*, with a source of inorganic fluoride, the total level of fluorine present was diminished. The volatiles from these tissue cultures were bubbled through a solution of 2,4-dinitrophenylhydrazine and the 2,4-dinitrophenylhydrazone derivative of fluoroacetone was identified. The amount of 2,4-dinitrophenylhydrazone derivative collected accounted for only 13% of the total fluorine lost, the remainder, they postulated, was lost as other volatile organofluorine compounds that were co-produced.<sup>28</sup> This study on fluoroacetone stands alone in the literature, and the compound's biosynthesis was never investigated.

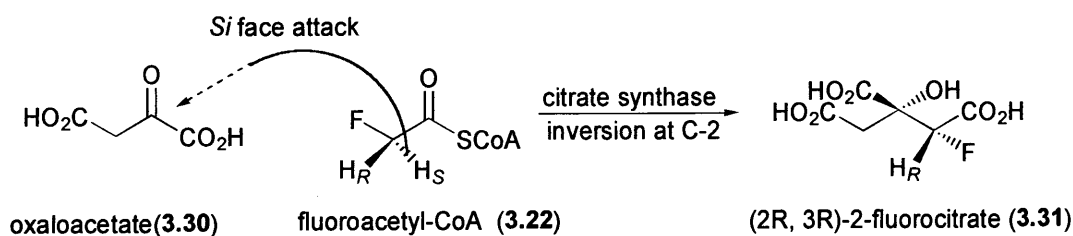
A hypothetical biosynthesis of fluoroacetone (3.29) has been proposed from the decarboxylation of 4-fluoroacetoacetate (3.28).<sup>29</sup>



Scheme 3.6 Hypothetical biosynthesis of fluoroacetone

### 3.7.5 (2*R*, 3*R*)-2-Fluorocitrate

A common co-metabolite of fluoroacetate is fluorocitrate (3.31). Citrate synthase on the citric acid cycle, mediates the condensation of fluoroacetyl-CoA (3.22) with oxaloacetate (3.30). This reaction is highly stereospecific, and the 2-*pro-S* proton of fluoroacetyl-CoA is abstracted exclusively. This implies that the C-C bond of the fluoroacetyl-CoA is locked from rotation either because of constraints induced by the active site of the enzyme or because of stereoelectronic control imparted by the presence of the fluorine atom. The condensation proceeds with inversion of stereochemistry affording (2*R*, 3*R*)-2-fluorocitrate as the only stereoisomer.<sup>30, 31, 32, 33</sup>



Scheme 3.7 Biosynthesis of fluorocitrate (3.31)

The toxicity of fluoroacetate arises from its conversion to (2R, 3R)-2-fluorocitrate (the other 3 isomers are not toxic). Fluorocitrate is an inhibitor of aconitase the ensuing enzyme on the citric acid cycle, which is responsible for the interconversion of citrate and isocitrate.<sup>34</sup> Kinetic studies on the enzymatic inhibition of aconitase by (2R, 3R)-2-fluorocitrate present a  $K_i$  value of 1  $\mu\text{M}$ , a value which is inconsistent with the observation that fluorocitrate is toxic at the level of  $10^{-4}$   $\mu\text{M}$ . The discrepancy can be explained by the fact that (2R, 3R)-2-fluorocitrate also inhibits citrate transport across the mitochondrial membrane. It has been demonstrated that  $^{14}\text{C}$ -radiolabelled fluorocitrate forms a covalent bond with the citrate carrier protein.<sup>35, 36, 37, 38, 39.</sup> Accumulation of (2R, 3R)-2-fluorocitrate ultimately arrests the citric acid cycle (the energy pathway of all living organisms). In mammals, this leads to convulsions and ultimately heart failure and death.

### 3.8 Resistance to fluoroacetate poisoning

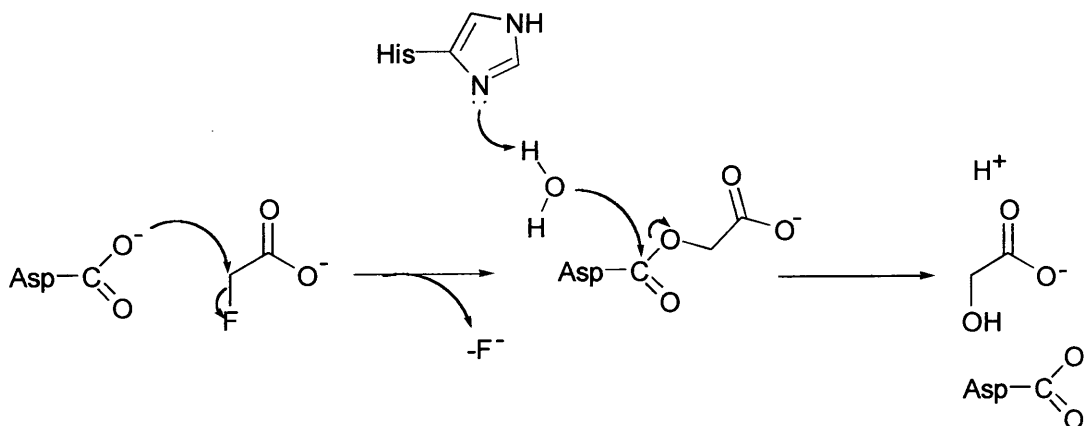
Fluoroacetate is not especially toxic; it is the compound's conversion *via* fluoroacetyl-CoA to (2R, 3R)-2-fluorocitrate in "the lethal synthesis", which has the fatal effect. *In vitro* studies have shown that protein extracts of the plant *D. cymosum* are capable of selectively hydrolysing fluoroacetyl-CoA over acetyl-CoA thus preventing the formation of (2R, 3R)-2-fluorocitrate.<sup>40</sup> It has also been postulated that host plants have evolved so that their citrate synthase enzyme will not accept fluoroacetyl-CoA.<sup>41</sup> Alternatively, some plants may have developed the ability to segregate any fluoroacetate produced, removing it from the mitochondria so that it cannot be processed to (2R, 3R)-2-fluorocitrate.<sup>42</sup> There are very little experimental data to support this hypothesis.

The ability of some micro-organisms, such as the fungus *Fusarium solani* and various *Pseudomonas* Spp., to grow on fluoroacetate producing plants has been known for many years.<sup>43, 44</sup> The micro-organisms are capable of utilising fluoroacetate as their

sole carbon source. Such organisms have the unique ability to enzymatically cleave the exceptionally strong C-F bond. Initial reports ascribed the defluorination ability to the presence of a thiol group at the active site of the enzyme. However, it is noted that iodoacetate and iodoacetamide, classical thiol poisons, fail to inhibit the enzyme's defluorination activity.<sup>44</sup>

More recently, a number of dehalogenating enzymes have been studied in detail, and their modes of action are better understood.<sup>45</sup> Fluoroacetate dehalogenase from *Moraxella* sp. B. has an amino acid sequence that is significantly similar to that of haloalkane dehydrogenase from *X. autotrophicus* GJ10, in the regions corresponding to the active site. The active site of the dehalogenase and the defluorinating enzyme both contain histidine and aspartate side chains as catalytic residues,<sup>46, 47</sup> in contrast to the thiol residue initially proposed.<sup>43</sup>

It has been suggested that the catalytic mechanism proceeds with the aspartate carboxylate, acting as a nucleophile, displacing the fluoride ion and forming a covalently bound ester intermediate. The ester is subsequently hydrolysed by water that has been activated by the histidine residue.



Scheme 3.8 Putative mechanism for the defluorination of fluoroacetate

This hypothesis was investigated by incubating the enzyme with fluoroacetate and [<sup>18</sup>O] water. The enzyme was digested and the fragments examined by mass spectrometry. The aspartate residue from the active site was found to have incorporated two <sup>18</sup>O atoms,<sup>46</sup> consistent with the hydrolysis of the proposed aspartate ester intermediate.

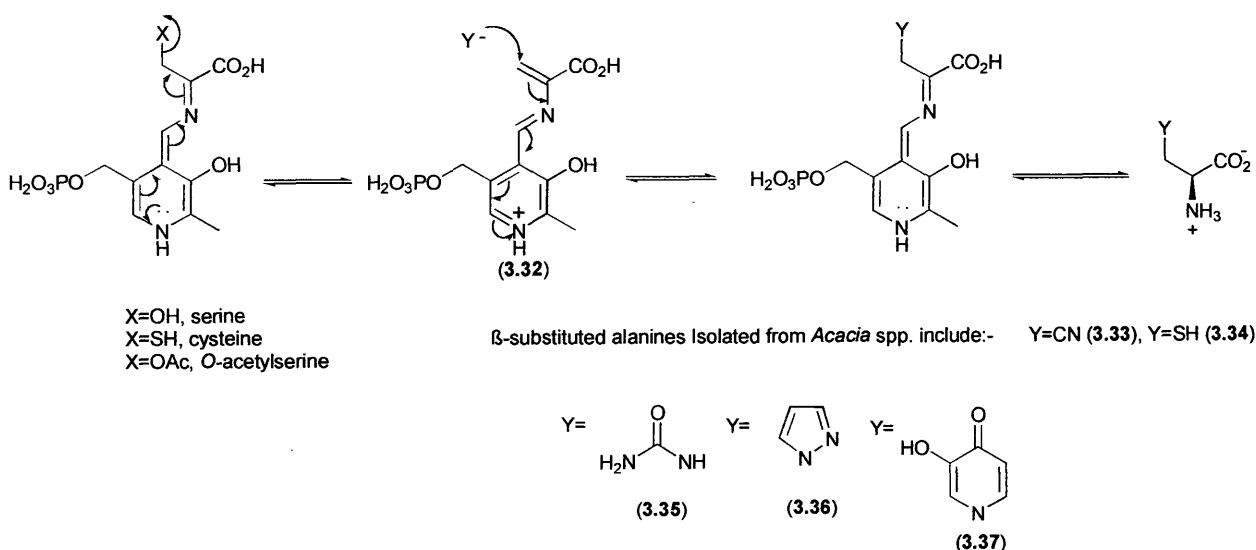
### 3.9 Proposed mechanisms of biological fluorination

Although more than 50 years have past since Marais discovered the first fluorometabolite,<sup>20</sup> we know little more today than then about the mechanism by which nature forms the C-F bond. The literature, however, contains many unsubstantiated proposals as to how the fluorination event may proceed.

#### 3.9.1 Formation of the C-F bond by addition of fluoride to a carbon-carbon multiple bond

##### 3.9.1.1 Pyridoxal phosphate catalysed incorporation of fluoride

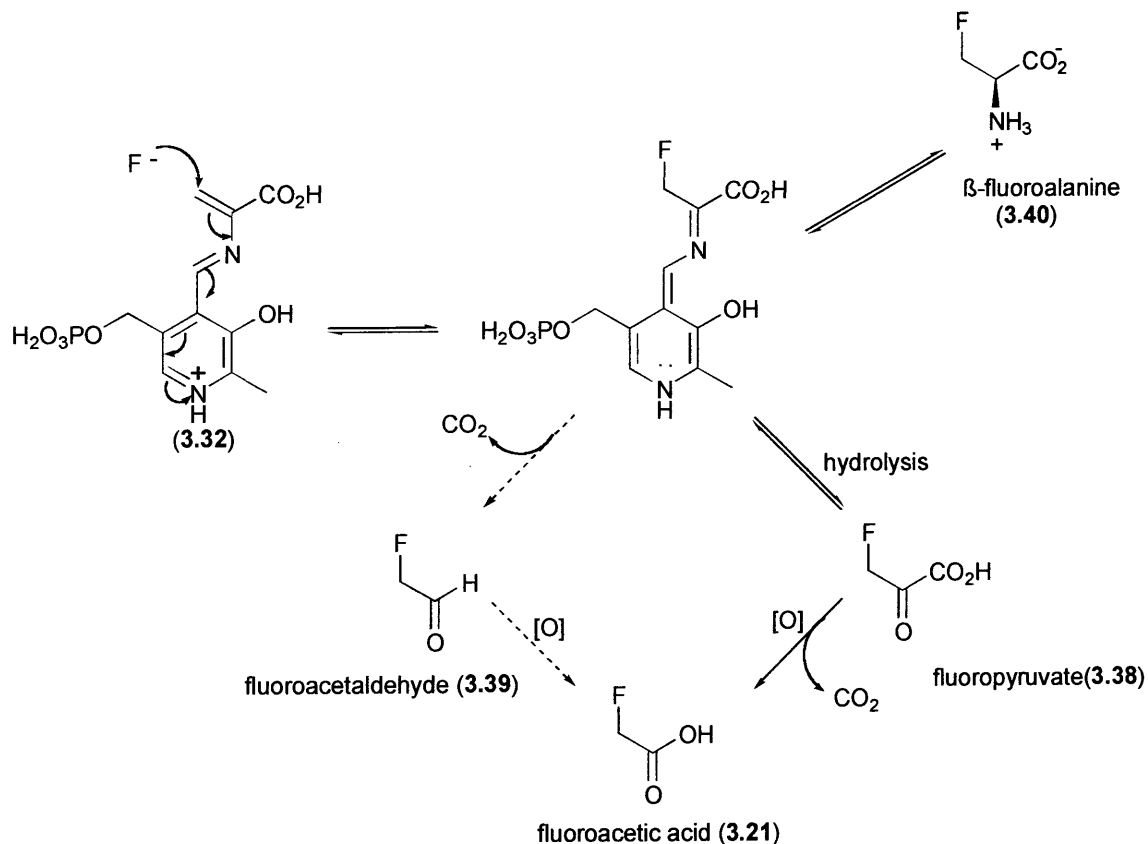
Mead and Segal recognised that many plants contain a wide variety of  $\beta$ -substituted alanines. The biosynthesis of these compounds may proceed by the nucleophilic attack to C-3 of the pyridoxal phosphate enamine adduct (3.32), formed after the elimination of the  $\beta$ -substituent from either serine or cysteine.<sup>48, 49, 50</sup>



Scheme 3.9 The putative biosynthesis of  $\beta$ -substituted alanines

The fact that many different  $\beta$ -substituted alanines have been identified in plants (e.g. 3.33-3.37) implied that the enzyme regulating the nucleophilic addition to the enamine adduct, had low substrate specificity. Mead and Segal questioned whether this enzyme would accept fluoride as a nucleophile. Were this the case, attack of fluoride at C-3 of the pyridoxal phosphate enamine adduct would generate fluoropyruvate bound to pyridoxamine phosphate. Conversion to fluoroacetate could then proceed either by hydrolysis to fluoropyruvate (3.38) and then oxidative

decarboxylation to fluoroacetic acid, or by direct decarboxylation and hydrolysis to fluoroacetaldehyde (3.39) which could be subsequently oxidised to fluoroacetic acid.<sup>51</sup> There is some evidence for the former mechanism as intact cells of *D. cymosum* have been shown to mediate the oxidative decarboxylation of fluoropyruvate to fluoroacetate.<sup>52</sup>



Scheme 3.10 A proposed mechanism by which pyridoxal phosphate catalyses the incorporation of fluoride

To investigate their hypothesis, Mead and Segal examined the conversion of L-cysteine to pyruvate, in acetone powders of *A. georginae*. They discovered that when cyanide was added the conversion was inhibited and  $\beta$ -cyanoalanine (3.33) was produced instead. This suggested that the pyridoxal phosphate enamine adduct had undergone nucleophilic addition by  $CN^-$ , and implied a lack of substrate specificity by the enzyme. Unfortunately, when they repeated the experiment, using fluoride in

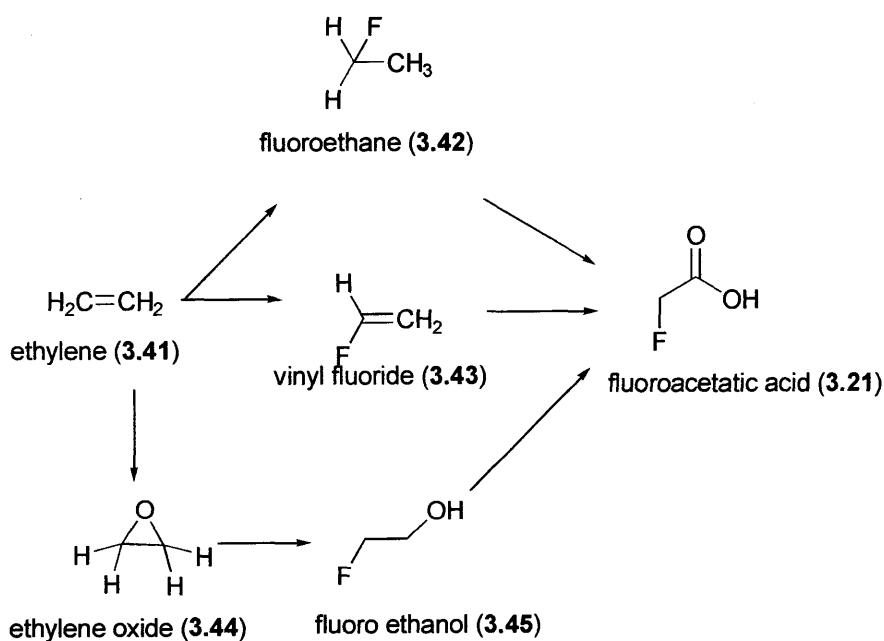


place of cyanide, no fluoride uptake was evident and no fluoropyruvate was observed.<sup>53</sup>

### 3.9.1.2 Fluorination of ethylene

Peters and Shorthouse observed the ability of *Acacia georginae* to diminish the levels of fluoride administered to it. They were able to trace 13% of this fluoride being converted to fluoroacetone but, clearly, 87% remained unaccounted for. Noting the plants capacity to produce the hormone ethylene (3.41), Peters questioned whether the plant was able to fluorinate the ethylene and loose the resultant volatile. He speculated that the ethylene was converted to either vinyl fluoride (3.43) or fluoroethane (3.42) and then these compounds were converted to fluoroacetate. No plausible mechanism was proposed for these reactions and the proposals remain speculative.<sup>54</sup>

Ethylene oxide (3.44) is known to be a major product of ethylene metabolism in plants.<sup>55, 56</sup> Fluorination of this activated compound would provide another explanation as to how fluorine is incorporated into the organic system.



Scheme 3.11 A Putative biosynthesis of fluoroacetic acid from ethylene

However, it should be noted that Peters and Shorthouse also demonstrated that non-fluoroacetone / fluoroacetate producing plants were also able to lose fluoride. To explain this, one has to argue that these plants are unable to convert the volatile intermediates to fluoroacetone or fluoroacetate. In addition, concentrations of vinyl fluoride and fluoroethane should be significant in the atmosphere. Extensive research

into the atmospheric composition, in relation to studies on the diminution of the ozone layer, has not revealed any fluorocarbons for which an anthropogenic source has not been clearly identified.<sup>57, 58</sup>

### **3.9.2 Nucleophilic substitution by fluoride**

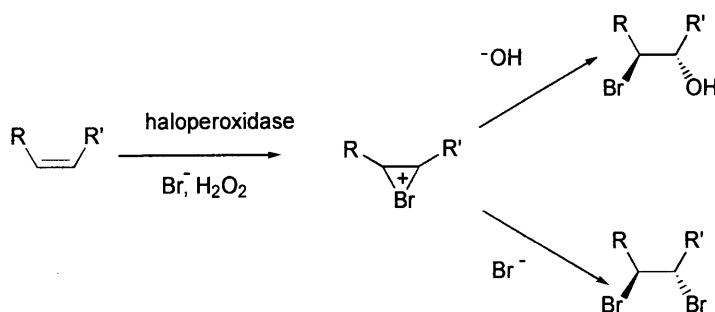
A number of micro-organisms have the capability of utilising fluoroacetate as their sole source of carbon. This requires a defluorination process (see section 3.8). Enzymes catalysing the conversion of fluoroacetate to glycolate and fluoride, have been isolated from several micro-organisms.<sup>43</sup>

The reactions catalysed by enzymes are, by definition, reversible; thus it is possible that the mechanism of defluorination might hold the key to biological fluorination. The substitution of a hydroxyl group of a glycolate, by fluoride is not energetically demanding and could, in theory, occur under normal physiological conditions if coupled energetically to a reaction that proceeds spontaneously. Though the hydroxyl moiety is not a good leaving group, it could be activated, for example, as a phosphate moiety, which could be more readily displaced by fluoride.

Goldman and Milne, investigated whether the defluorination enzyme from a *Pseudomonas* sp. could mediate the reverse reaction. They incubated the enzyme with fluoride and glycolate in the presence of [<sup>18</sup>O] water, and argued that even if the amount of fluoroacetate produced was chemically undetectable, the reversibility of the reaction should be reflected by a level of uptake of <sup>18</sup>O into the glycolate. However, no significant uptake of <sup>18</sup>O was detected in the glycolate, by mass spectrometry.<sup>59</sup>

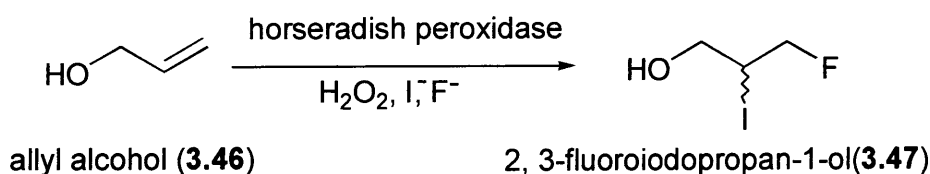
### **3.9.3 Nucleophilic attack by fluoride on a halonium ion**

Haloperoxidase reactions with alkenes have been shown to be dependent upon the relative concentrations of the anions. If there is a sufficiently high concentration of the anion a 1,2-dihalo species may be formed.<sup>60</sup>



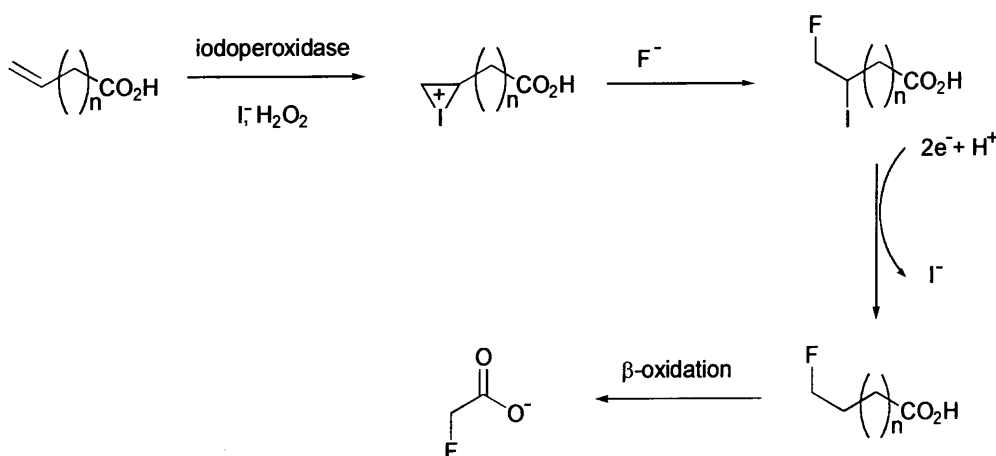
**Scheme 3.12 Reaction of a haloperoxidase with an alkene to form a 1,2-dihalo species**

Neidleman and Geigert were able to exploit this idea. Using equivalent concentrations of fluoride and iodide in the presence of horseradish peroxidase and  $H_2O_2$ , they demonstrated the conversion of allyl alcohol (3.46) to 2,3-fluoriodopropan-1-ol (3.47).<sup>56</sup>



Scheme 3.13 The horseradish peroxidase catalysed formation of 2,3-fluoriodopropan-1-ol from allyl alcohol

On the basis of this experiment, Neidleman and Geigert, proposed that fluoroacetate could be biosynthesised by the iodofluorination of an  $\omega$ -unsaturated fatty acid; the fatty acid subsequently undergoing de-iodination and  $\beta$ -oxidation.



Scheme 3.14 Neidleman and Geigert's proposed biosynthesis of fluoroacetate by iodofluorination of an  $\omega$ -unsaturated fatty acid

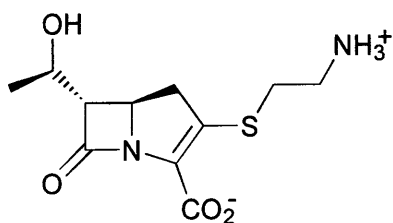
This hypothesis would have contradicted the role of fluoroacetate as a starter unit in  $\omega$ -fluorofatty acid biosynthesis, and is, therefore, weakened. In addition, the study provided no evidence to substantiate this theory, but suggested that the examination of the iodine content of fluoroacetate producing plants might be revealing.<sup>61</sup> Detailed GCMS studies have not revealed the presence of any  $\omega$ -iodofatty acids in the extracts of *D. toxicarum* seeds.

### 3.10 Contemporary studies into biological fluorination

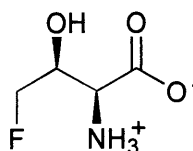
In order to arrive at a better understanding of the mechanism of biological fluorination, fluoroacetate emerges as the most obvious system to study. Not only is it the most common of the fluorinated natural products, but it is also, structurally, the least complex.

Investigations into the biosynthesis of fluoroacetate have been thwarted by many factors, which one by one are gradually being overcome. Initial problems with detection and analysis of fluorinated compounds have, to some extent, been solved by the advent of more sensitive GCMS techniques and the use of  $^{19}\text{F}$  NMR. There are also many problems associated with working with whole plant systems. Difficulties arise in acquiring fresh supplies of uniform genotype of the plants capable of biosynthesising fluoroacetate. Such species tend to be native to the less accessible areas of Australia, Africa and South America. The development of a callus tissue culture of *D. cymosum* provided a more amenable system in which to study biological fluorination, however the levels of fluoroacetate production were very low.

In 1985, a significant breakthrough was achieved. Workers investigating ways in which to improve the production of the  $\beta$ -lactam antibiotic, thienamycin (3.48), by the bacterium *Streptomyces cattleya*, discovered that the organism had produced two new metabolites. The metabolites were fluoroacetate, and the previously unknown amino acid, 4-fluorothreonine (3.49). The workers were particularly surprised, as the growth media had not been supplemented with any fluoride. On analysis of the broth components, the soy bean casein that had been employed was revealed to have a fluoride content of 0.7%.<sup>62</sup>



thienamycin (3.48)



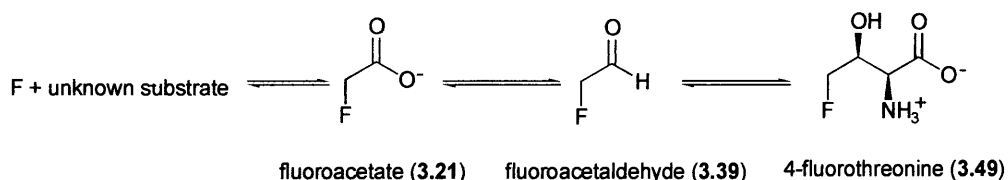
4-fluorothreonine (3.49)

Fig 3.7 Thienamycin and 4-fluorothreonine

### 3.11 The Biosynthesis of fluoroacetate and 4-fluorothreonine

The biosynthesis of fluoroacetate and 4-fluorothreonine has been extensively investigated in resting cells of *S. cattleya*. The resting cell systems are prepared from batch cells of the organism that has just reached the idiophase. The organism is no longer involved in primary metabolism and cell growth, but in sporulation and secondary metabolism (see section 1.1.2). The cells are harvested and suspended in buffer. A system is used in which the putative intermediates administered are the only carbon source available to the organism.

Initial studies by Sanada *et al.*, demonstrated that 4-fluoroglutamate, fluoroacetate, and KF could all be utilised as a source of fluorine for the biosynthesis of 4-fluorothreonine, whereas fluorocitrate was ineffectual. It was noted that when fluoroacetate was utilised as the source of fluoride, after 48 hours, there was a diminution of 4-fluorothreonine. The workers also showed the conversion of fluoroglutamate and 4-fluorothreonine to fluoroacetate, by resting cells of *S. cattleya*. From this information, a biosynthesis was proposed in which an unknown substrate is fluorinated and then converted to fluoroacetate. The fluoroacetate (3.21) is subsequently converted to fluoroacetaldehyde (3.39), which in turn undergoes a condensation reaction with glycine to yield 4-fluorothreonine (3.49) (Scheme 3.15).<sup>61</sup>



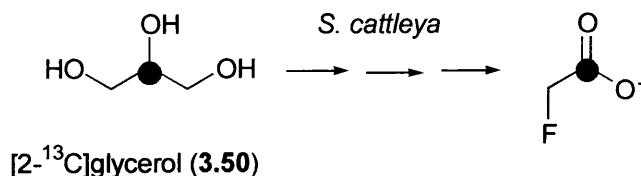
Scheme 3.15 A proposed biosynthesis of 4-fluorothreonine from fluoroacetate

In 1995, Soda *et al.* published an account of their investigations into the biosynthesis of fluoroacetate and 4-fluorothreonine in *S. cattleya*.<sup>63</sup> Using  $^{19}\text{F}$  NMR to measure the relative concentrations of the two fluorometabolites, they observed that fluoroacetate accumulated first, in the resting cells, and 4-fluorothreonine became visible three days later. From this finding, it was concluded that fluoroacetate is a precursor of 4-fluorothreonine. Such concentration studies are not necessarily a reliable method of determining a metabolite's position on a biosynthetic pathway. It cannot be ruled out that 4-fluorothreonine formed first but existed in a low steady state concentration, due

to its rapid conversion to fluoroacetate, and as such was not detectable by the relatively insensitive  $^{19}\text{F}$  NMR technique employed to measure the concentrations. Studies by Reid *et al.*<sup>64</sup> contradict the findings of Soda,<sup>62</sup> stating that 4-fluorothreonine was detectable in the culture medium 24 hours before fluoroacetate.

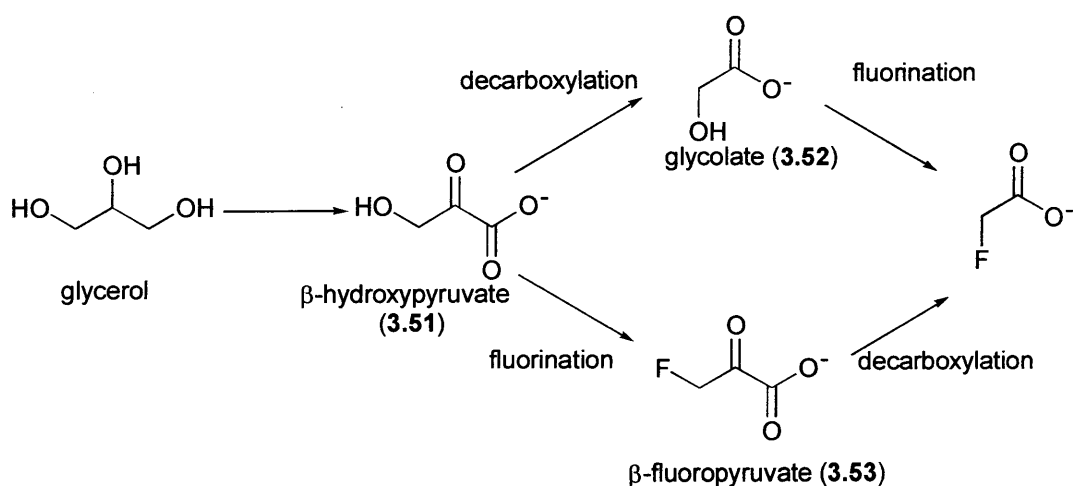
Soda *et al.* sought to determine the origin of the carbon skeleton of fluoroacetate by administering various radio-labelled, putative intermediates to resting cells of *S. cattleya*. [ $\text{U-}^{14}\text{C}$ ]Glycerol, glucose,  $\beta$ -hydroxypyruvate and L-serine were seen to be incorporated at a level of 0.2-0.4%, whereas [ $3\text{-}^{14}\text{C}$ ]pyruvate, [ $2,3\text{-}^{14}\text{C}$ ]succinate and [ $\text{U-}^{14}\text{C}$ ] aspartate were only incorporated to an extent of 0.04-0.08% implying that these latter metabolites are more remote from the fluorination event.

A key experiment was performed, incubating [ $2\text{-}^{13}\text{C}$ ]glycerol (**3.50**) with resting cells of a mutant organism, *S. cattleya* NTG29 that had been generated by treating the wild type, *S. cattleya* NRRL 8057, with N-methyl-N'-nitro-N-nitrosoguanidine, a chemical mutagen. Analysis of the resultant fluoroacetate by  $^1\text{H}$ ,  $^{13}\text{C}$  and  $^{19}\text{F}$  NMR indicated that the label was incorporated exclusively into the carbonyl carbon of the fluoroacetate at a level of 40%.



#### Scheme 3.16 Incorporation of glycerol into fluoroacetate

The study was extended to incorporation experiments with [ $\text{U-}^{14}\text{C}$ ], [ $3\text{-}^{14}\text{C}$ ] and [ $1\text{-}^{14}\text{C}$ ]- $\beta$ -hydroxypyruvate. Incorporation of the label from the first two compounds into fluoroacetate was observed, but very little isotope incorporation resulted from C-1 of the hydroxypyruvate. Clearly, only the C-2 and C-3 of  $\beta$ -hydroxypyruvate are significantly incorporated into fluoroacetate. It was concluded that the carbon skeleton arises from glycerol, which is converted to  $\beta$ -hydroxypyruvate and is then processed through to fluoroacetate by fluorination and decarboxylation.

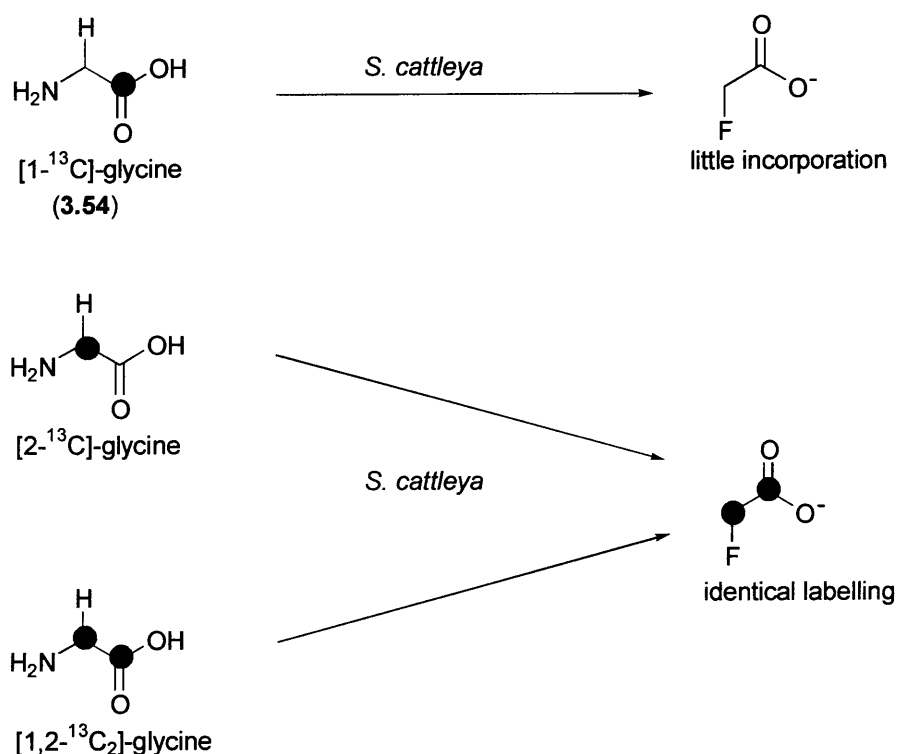


Scheme 3.17 Possible biosynthetic routes to fluoroacetate through  $\beta$ -hydroxypyruvate

In order to explore whether the decarboxylation or fluorination event occurred first, [2- $^{14}\text{C}$ ] and [1,2- $^{13}\text{C}$ ] glycolate were administered to separate cultures of *S. cattleya*. In the event, only low incorporation resulted, and it was concluded that glycolate is not significant in fluoroacetate biosynthesis. However, the workers did not observe any  $\beta$ -fluoropyruvate in the culture broth either, nor was any labelled  $\beta$ -fluoropyruvate administered to the organism. The fact that no  $\beta$ -fluoropyruvate was found in the culture broth is not conclusive evidence that the compound is not the first fluorometabolite on the pathway.  $\beta$ -Fluoropyruvate is rapidly defluorinated *in vivo* by pyruvate decarboxylase, and if it were formed it would either undergo this fate or be rapidly processed towards fluoroacetate and 4-fluorothreonine. Levels of the compound, observable by  $^{19}\text{F}$  NMR, would be unlikely to build up.

To test the hypothesis of Sanada *et al.*,<sup>61</sup> that fluoroacetate and glycine combine to form 4-fluorothreonine, Reid and co-workers incubated resting cell cultures of *S. cattleya* with 4-fluorothreonine and also with fluoroacetate.<sup>63</sup> From these experiments the rates of interconversion were noted to be 20 fold too low to account for the biosynthesis of one metabolite from the other. Incubation of resting cells with glycine had no effect on the relative concentrations of the two metabolites, also supporting this finding. Finally, an experiment was performed by incubating resting cells with  $^2\text{H}_2$ -labelled fluoroacetate. Less than 5% deuterium incorporation was observed, into the 4 position of the 4-fluorothreonine, as judged by  $^{19}\text{F}$  NMR. This low level of interconversion between the fluoroacetate and 4-fluorothreonine, can, most reasonably, be explained in terms of defluorination and then re-incorporation of the

released fluoride by the *de novo* synthesis, similar to previous observations with DL-fluorosuccinate, fluorofumarate, 4-fluoroglutamate and 3-fluoroalanine.

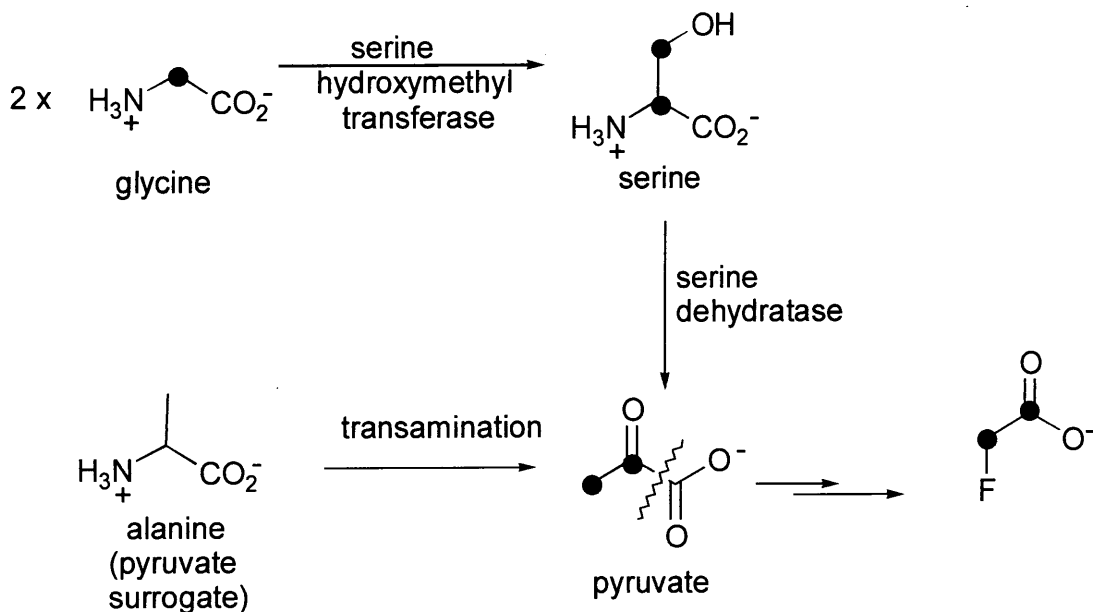


Scheme 3.18 Incorporation of labelled glycine into fluoroacetate

Further experiments, incubating individual resting cell cultures with [1-<sup>13</sup>C], [2-<sup>13</sup>C] and [1,2-<sup>13</sup>C<sub>2</sub>]-glycine (3.54) are revealing. [1-<sup>13</sup>C]-Glycine was incorporated to a level lower than 4%, where as [2-<sup>13</sup>C] and [1,2-<sup>13</sup>C<sub>2</sub>]-glycine both gave rise to incorporations of 40%. A high degree of double labelling was also observed to occur (Scheme 3.18). These results were interpreted in terms of glycine generating serine. Glycine is cleaved with C-2 processed via *N*<sup>5</sup>, *N*<sup>10</sup>-methylene-tetrahydrofolate by serine hydroxymethyltransferase where it is condensed with another molecule of glycine to generate serine. The serine could then be metabolised to pyruvate by serine dehydratase.<sup>65</sup> To further investigate the relationship of pyruvate to the biosynthesis of the two fluorometabolites, resting cells were incubated with labelled pyruvate<sup>66</sup> Although little incorporation of label from [1-<sup>13</sup>C]-pyruvate was detected by GCMS, incubation of individual resting cell cultures with [2-<sup>13</sup>C] and [3-<sup>13</sup>C]-pyruvate separately, resulted in a 37% incorporation of label at C-1 of fluoroacetate and a 21% incorporation into the C-2 of fluoroacetate, respectively. These results are evidence that the C-2 and C-3 of pyruvate, similar to hydroxyppyruvate, are incorporated as an intact unit into fluoroacetate, with C-3 contributing to the fluoromethyl carbon. The



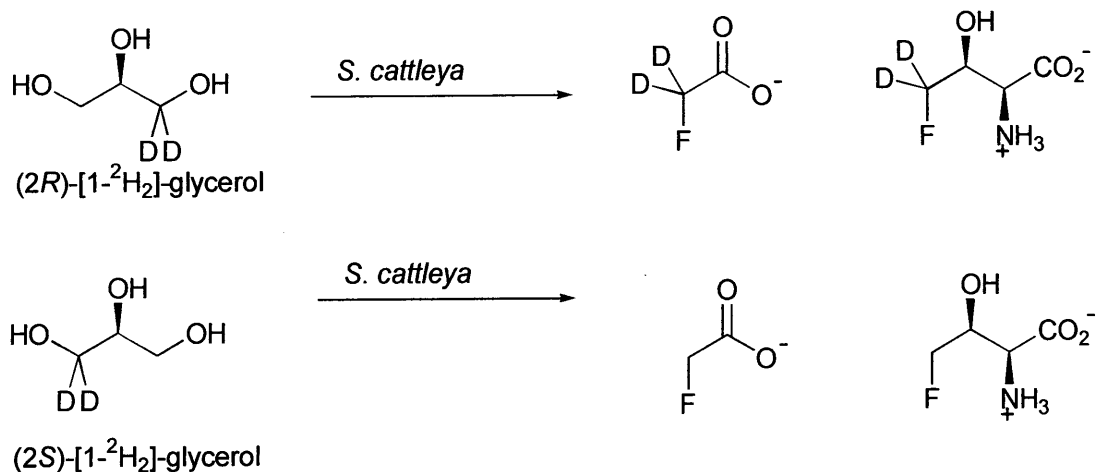
role of pyruvate on the biosynthetic pathway is corroborated by a similar incorporation of L-[3-<sup>13</sup>C]-alanine (a pyruvate surrogate) which is transaminated *in vivo* to release pyruvate.



Scheme 3.19 An explanation for the incorporation pattern resulting from the feeding of labelled glycine

Hamilton *et al.* postulate that pyruvate might have one of two fates.<sup>66</sup> Oxidative decarboxylation to furnish acetyl-CoA would seem an unlikely step to take towards the fluorometabolites as it would result in a methyl group which is no longer activated towards nucleophilic attack. A more likely fate for pyruvate would be conversion to oxaloacetate, mediated by pyruvate carboxylase, followed by the decarboxylation of oxaloacetate to phosphoenolpyruvate. The glycolytic pathway is now entered. There are a range of glycolytic intermediates containing a phosphate group at C-3 which could potentially be replaced by fluoride. The study investigated the possibility of oxaloacetate as a precursor to the fluorometabolites, by incubating resting cells with [<sup>2</sup>H<sub>3</sub>]-aspartate and [<sup>2</sup>H<sub>4</sub>]-succinate (compounds readily metabolised to oxaloacetate *in vivo*). Though aspartate was only incorporated at the 6.5% level, 2% of the fluorometabolites retained both deuteria. The succinate was incorporated at the much higher level of 20% and, consistent with succinate being processed through the Krebs cycle, only one deuterium was retained. These results reinforce the intermediacy of oxaloacetate upon the pathway.

The authors tenaciously suggest that although they have shown pyruvate to be a highly effective precursor of the two fluorometabolites, it can not be postulated that either pyruvate or  $\beta$ -hydroxypyruvate is the substrate for enzymatic fluorination. They carefully stipulate that the high levels of incorporation arising from the feeding of labelled pyruvate could be as much due to the substrate being tightly channelled through the various enzymatic processes, as to its proximity to the fluorination event.<sup>65</sup>



Scheme 3.20 Results from the incubation of (2R)-[1-<sup>2</sup>H<sub>2</sub>]- and (2S)-[1-<sup>2</sup>H<sub>2</sub>]-glycerol with resting cell cultures of *S. cattleya*

Further insight into the problem has been provided by the feeding of both (2R)-[1-<sup>2</sup>H<sub>2</sub>]- and (2S)-[1-<sup>2</sup>H<sub>2</sub>]-glycerol to resting cell suspensions of the bacteria. Deuterium was only incorporated into fluoroacetate from (2R)-[1-<sup>2</sup>H<sub>2</sub>]-glycerol, with two deuteria labelling the fluoromethyl group at a level of 28%. Therefore, the *pro-S* hydroxymethyl of the glycerol must be cleaved during the biosynthesis. The fact that two deuteria are carried through to the fluorinated products places considerable mechanistic limitation upon the subsequent processes leading up to the fluorination event. It may therefore be postulated that the glycerol is phosphorylated at its *pro-R* position to generate *sn*-glycerol-3-phosphate thus activating the carbon atom which may subsequently be attacked by fluoride.<sup>67</sup>

In addition to this, the incorporation of label into the C-1 and C-2 of fluoroacetate mirrors those into C-3 and C-4 of 4-fluorothreonine in terms of magnitude and regiochemistry, from the various feeding experiments. This observation leads the authors to propose that the two sets of carbons share a common biosynthetic origin

and that there is a single fluorinating enzyme operating in *S. cattleya*. With the likelihood being that the substrate to be fluorinated lies between pyruvate and glycerol implicating an intermediate upon the Krebs cycle.

## References

- 1 T. Hayashi and V. A. Soloshonok, *Tetrahedron Asymmetry*, 1994, **5**, xiii.
- 2 J. Fried and E. F. Sabo, *J. Am. Chem. Soc.*, 1954, **76**, 1455.
- 3 C. Heidelberger, N. K. Chaudhuri, P. Danneberg, D. Mooren, L. Griesbach, R. Duschinsky, R. J. Schnitzer, E. Plevin, J. Schneiner, *Nature*, 1957, **179**, 663.
- 4 D. V. Santi, C. S. McHenry, *Proc. Natl. Acad. Sci. USA*, 1972, **69**, 1855.
- 5 Y. Miauno, A. Ichikawa, K. Tomita, *Prostaglandins*, 1983, **26**, 785.
- 6 L. Fowden, *Proc. Roy. Soc.*, 1968, **171**, 5.
- 7 D. J. Faulkner, M. O. Stallard, J. Fayos, J. Clardy, *J. Am. Chem. Soc.* 1973, **95**, 3413.
- 8 T. Murakami, N. Tanaka, *Prog. Chem. Org. Nat. Prod.* 1988, **54**, 1.
- 9 G. W. Gribble, *Chem. Soc. Rev.*, 1999, **28**, 335
- 10 M. Sakuma, H. Fukami, *Tetrahedron Lett.* 1993, **34**, 6059.
- 11 T. F. Spande, H. M. Garraffo, M. W. Edwards, H. J. C. Yeh, L. Pannell, J. W. Daly, *J. Am. Chem. Soc.* 1992, **114**, 3475.
- 12 C. T. Walsh, *Science*, 1993, **261**, 308.
- 13 M. Picard, J. Gross, E. Lübbert, S. Tölzer, S. Krauss, K-H. van Pée, A. Berkessel, *Angew. Chem. Int. Ed. Engl.*, 1997, **36**, 1196.
- 14 O. Kirk, L. S. Conrad, *Angew. Chem. Int. Ed. Engl.*, 1999, **38**, 977.
- 15 S. Kirner, S. Krauss, G. Sury, S. T. Lam, J. M. Ligon, K-H van Pée, *Microbiol.*, 1996, **142**, 2129.
- 16 K. Hohaus, A. Altmann, W. Burd, I. Fischer, P. E. Hammer, D. S. Hill, J. M. Ligon, K-H van Pée, *Angew. Chem. Int. Ed. Engl.*, 1997, **36**, 2012.
- 17 S. O. Thomas, V. L. Singleton, J. A. Lowery, R. W. Sharpe, L. M. Pruess, J. N. Porter, J. H. Mowat, N. Bohonos, *Antibiotics Ann.*, 1957, 716.
- 18 I. D. Jenkins, J. P. H. Verheyden, J. G. Moffatt, *J. Am. Chem. Soc.*, 1976, **98**, 3346.
- 19 D. B. Harper, D. O Hagan, *Nat. Prod. Rep.*, 1994, **11**, 123.

- 20 J. S. C. Marais, *Onderstepoort J. Vet. Sci. Anim. Ind.* 1944, **20**, 67.
- 21 T. Vartiainen, J. Gynther, *Fd. Chem. Toxic.*, 1984, **22**, 307.
- 22 D. O' Hagan, R. Perry, M. J. Lock, J. J. M. Meyer, L. Dasaradhi, J. T. G. Hamilton, D. B. Harper, *Phytochemistry*, 1993, **33**, 1043.
- 23 R. J. Hall, *New Phytol.*, 1972, **71**, 855.
- 24 R. A. Peters, M. Shorthouse, *Phytochemistry*, 1972, **11**, 1337.
- 25 R. A. Peters, R. J. Hall, *Biochemical Pharmacology*, 1959, **2**, 25.
- 26 R. A. Peters, R. J. Hall, P. F. V. Ward, N. Sheppard, *Biochem. J.*, 1960, **77**, 17.
- 27 P. F. V. Ward, R. J. Hall, R. A. Peters, *Nature*, 1964, **201**, 611.
- 28 R. A. Peters, M. Shorthouse, *Nature*, 1967, **216**, 80.
- 29 D. B. Harper, D. O'Hagan, *Nat. Prod. Rep.*, 1994, **11**, 123.
- 30 R. Dummel, E. Kun, *J. Biol. Chem.*, 1969, **244**, 2966.
- 31 R. Keck, H. Haas, J. Retey, *FEBS Lett.*, 1980, **114**, 287.
- 32 M. A. Marletta, P. A. Srere, C. Walsh, *Biochemistry*, 1981, **20**, 3719.
- 33 W. C. Stallings, C. T. Monti, J. F. Belvedere, R. K. Preston, J. P. Gluster, *Arch. Biochem. Biophys.*, 1980, **203**, 65.
- 34 R. A. Peters, R. W. Wakelin, P. Buffa, L. C. Thomas, *Proc. Roy. Soc., B*, 1953, **140**, 497.
- 35 C. Walsh, *Adv. In Enzymology*, 1982, **55**, 197.
- 36 E. Kun, in "Biochemistry Involving Carbon- Fluorine Bonds" , ed. R. Filler, American Chemical Society, Washington, 1976, p. 1.
- 37 E. Kun, E. Kirsten, M. L. Sharma, *Dev. Bioenerg. Biomemb.*, 1978, **2**, 285.
- 38 E. Kirsten, M. L. Sharma, E. Kun, *Mol. Pharmacol.*, 1978, **14**, 172.
- 39 E. Kun, E. Kirsten, M. L. Sharma, *Proc. Nat. Acad. Sci*, 1977, **74**, 4942.
- 40 J. J. M. Meyer, N. Grobbelaar, R. Vleggaar, A. I. Louw, *J. Plant Physiol.*, 1992, **139**, 369.
- 41 J. N. Eloff, B. von Sydow, *Phytochemistry*, 1971, **10**, 1409.

- 42 J. Y. Cheng, M. H. Yu, G. W. Millar, G. W. Welkie, *Environ. Sci. Technol.*, 1968, **2**, 367.
- 43 H. Kawasaki, K. Miyashi, K. Tonomura, *Agric. Biol. Chem.* 1981, **45**, 231.
- 44 P. Goldman, *J. Biol. Chem.* 1965, **240**, 3434.
- 45 C. Kennes, F. Pries, G. H. Krooshof, E. Bokma, J. Kingma, D. B. Janssen, *J. Biochem.*, 1995, **228**, 403.
- 46 K. H. G. Verschueren, F. Seljeé, H. J. Rozeboom, K. H. Kalk, B. W. Dijkstra, *Nature*, 1993, **363**, 693.
- 47 J-Q. Liu, T. Kurihara, S. Ichiyama, M. Miyagi, S. Tsunasawa, H. Kawasaki, K. Soda, N. Esaki, *J. Biol. Chem.*, 1998, **273**, 30897.
- 48 A. S. Seneviratne, L. Fowden, *Phytochemistry*, 1968, **7**, 1039.
- 49 S. Nigam, C. Ressler, *Biochim. Biophys. Acta*, 1964, **93**, 339.
- 50 H. G. Floss, L. Hadwiger, E. E. Conn, *Nature*, 1965, **208**, 1207.
- 51 R. J. Mead, W. Segal, *Aust. J. Biol. Sci.*, 1972, **25**, 327.
- 52 J. J. Meyer, D. O'Hagan, *Phytochemistry*, 1992, **31**, 499.
- 53 R. J. Mead, W. Segal, *Phytochemistry*, 1973, **12**, 1977.
- 54 R. A. Peters, *Fluoride*, 1973, **6**, 189.
- 55 P. H. Jerie, M. A. Hall, *Proc. R. Soc. Lond., B*, 1978, **200**, 87.
- 56 J. H. Dodds, S. K. Musa, P. H. Jerie, M. A. Hall, *Plant Sci. Lett.*, 1979, **17**, 109.
- 57 H. B. Singh, L. J. Salas, H. Shigeishi, E. Scribner, *Science*, 1979, **203**, 899
- 58 J. Russow, in "The Handbook of Environmental Chemistry Vol. 3 Part A. Anthropogenic Compounds", ed. O. Hutzinger, Springer-Verlag, Berlin, 1980.
- 59 P. Goldman, G. W. A. Milne, *J. Biol. Chem.*, 1966, **241**, 5557.
- 60 S. L. Neidleman, J. Geigert, *Trends in Biotechnology*, 1983, **1**, 21.
- 61 S. L. Neidleman, J. Geigert, *Biohalogenation; Principles, Basic Roles and Applications*, 1986, Ellis Horwood Ltd., Chichester, p. 173.
- 62 M. Sanada, T. Miyano, S. Iwadare, J. M. Williamson, B. H. Arison, J. L. Smith, A. W. Douglas, J. M. Liesch, E. Inamine, *J. Antibiot.*, 1985, **39**, 259.

- 63 T. Tamura, M. Wada, N. Esaki, K. Soda, *J. Bacteriol.*, 1995, **177**, 2265.
- 64 K. A. Reid, R. D. Bowden, D. B. Harper, in *Naturally Produced Organohalogenes*, ed. A. Grimvall, E. W. B. de Leer, Kluwer Academic Publishers, Dordrecht, 1995, 269.
- 65 J. T. G. Hamilton, M. R. Amin, D. B. Harper, D. O' Hagan, *Chem. Commun.*, 1997, 797.
- 66 J. T. G. Hamilton, C. D. Murphy, M. R. Amin, D. O'Hagan, D. B. Harper, *J. Chem. Soc., Perkin Trans. 1*, 1998, 759.
- 67 J. Nieschalk, J. T. G. Hamilton, C. D. Murphy, D. B. Harper, D. O'Hagan, *Chem. Commun.*, 1997, 799.

## **CHAPTER 4**

### **The Stereochemical Course of Biological Fluorination in *Streptomyces cattleya***

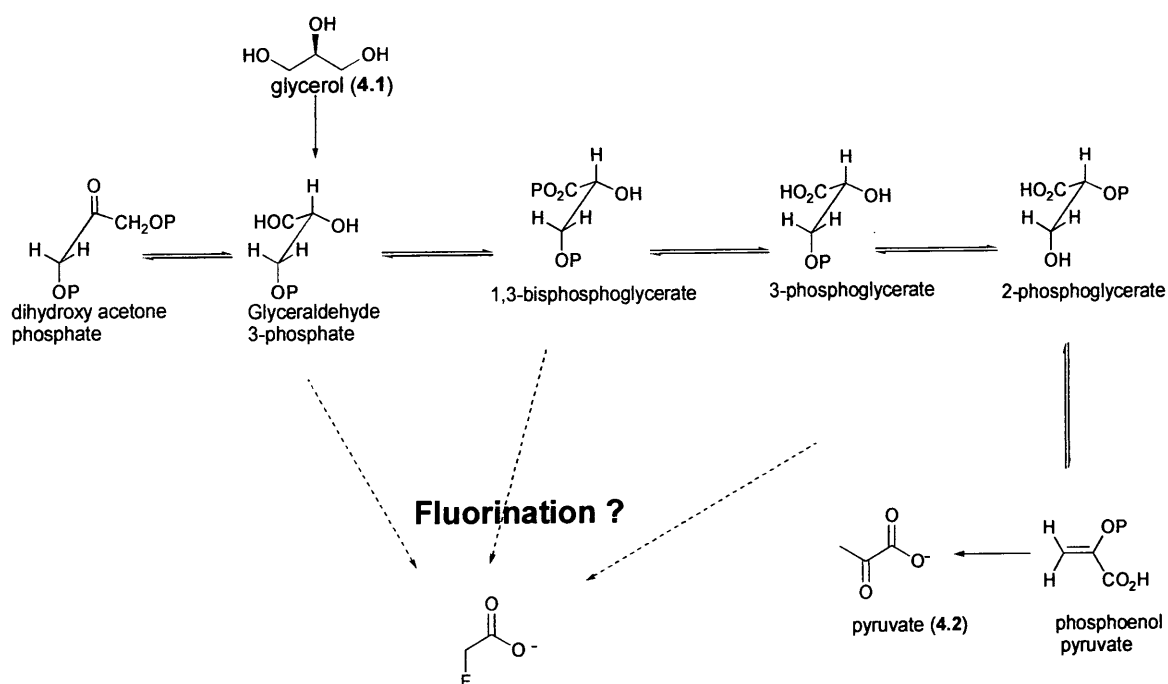


## **CHAPTER 4**

### **The Stereochemical Course of Biological Fluorination in *Streptomyces cattleya***

#### **4.1 Introduction**

To gain further insight into the mechanism of biological fluorination in *Streptomyces cattleya*, a study was undertaken to establish the stereochemical course (retention or inversion) of the fluorination reaction during the biosynthesis of fluoroacetate. From earlier studies (see section 3.11), it has been shown that the most likely substrate for the enzymatic fluorination is a metabolite closely related to glycerol (4.1) or pyruvate (4.2). Clearly, intermediates upon the glycolytic pathway emerge as candidate substrates for this enzyme.



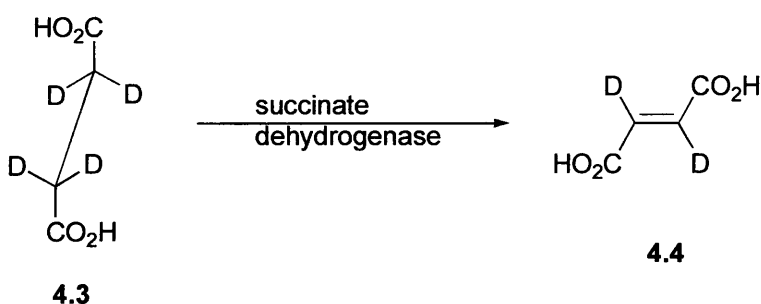
Scheme 4.1 Glycolytic intermediates as candidate substrates for biological fluorination

Previous experiments in which both (2*R*)-[1-<sup>2</sup>H<sub>2</sub>] and (2*S*)-[1-<sup>2</sup>H<sub>2</sub>]-glycerol were administered to resting cell cultures of *S. cattleya*, showed that the *pro-R* hydroxymethyl is retained as the fluoromethyl group, whereas the *pro-S* hydroxymethyl group is cleaved. These experiments also demonstrated that when (2*R*)-[1-<sup>2</sup>H<sub>2</sub>]-glycerol was administered, both deuteria from the *pro-R* hydroxymethyl group were retained (see section 3.11). In order to determine the stereochemical course of the biological fluorination, it is necessary to incubate *S. cattleya* with glycerols bearing stereoselectively deuterated *pro-R* hydroxymethyl groups. One method is to synthesise and feed (1*S*, 2*R*)-[1-<sup>2</sup>H]- and (1*R*, 2*R*)-[1-<sup>2</sup>H]-glycerols. A complementary approach is to administer [2,2,3,3-<sup>2</sup>H<sub>4</sub>]-succinate. The stereochemical processing of succinate through the Krebs cycle and glycolysis is well established (section 4.2) and [2,2,3,3-<sup>2</sup>H<sub>4</sub>]-succinate can be employed to stereoselectively deuterate the *pro-R* hydroxymethyl group of glycerol and other related glycolytic intermediates.

## 4.2 The stereochemical processing of succinate through the Krebs cycle and glycolysis

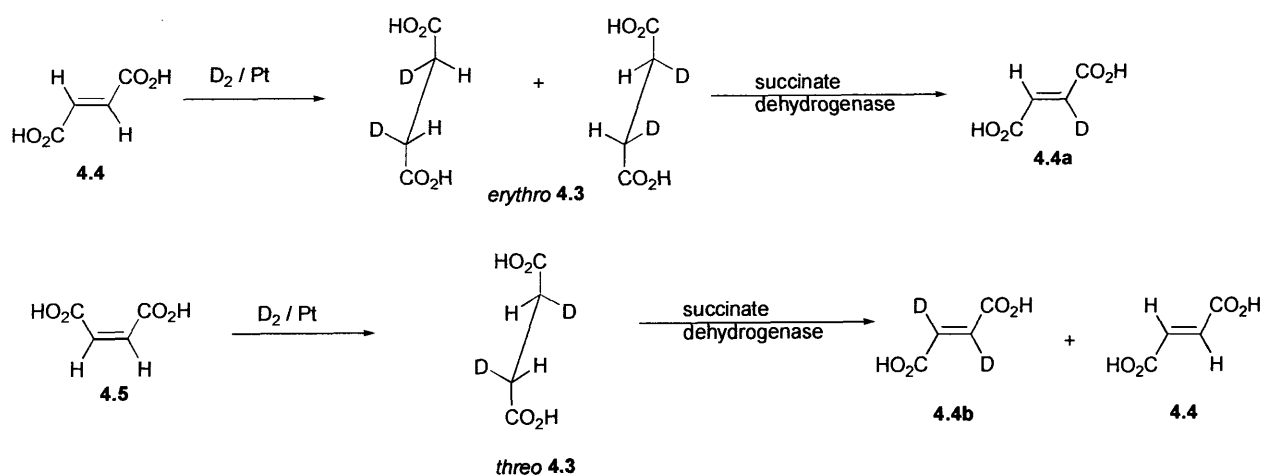
### 4.2.1 The conversion of succinate to fumarate

The enzyme, succinate dehydrogenase, mediates the stereospecific removal of two vicinal hydrogen atoms from succinate (4.3) to generate fumarate (4.4). Accordingly, when [2,2,3,3-<sup>2</sup>H<sub>4</sub>]-succinate is administered to the enzyme, [2,3-<sup>2</sup>H<sub>2</sub>]-fumarate is generated (Scheme 4.2).



Scheme 4.2 The succinate dehydrogenase mediated conversion of [2,2,3,3-<sup>2</sup>H<sub>4</sub>]-succinate(4.3) to [2,3-<sup>2</sup>H<sub>2</sub>]-fumarate (4.4)

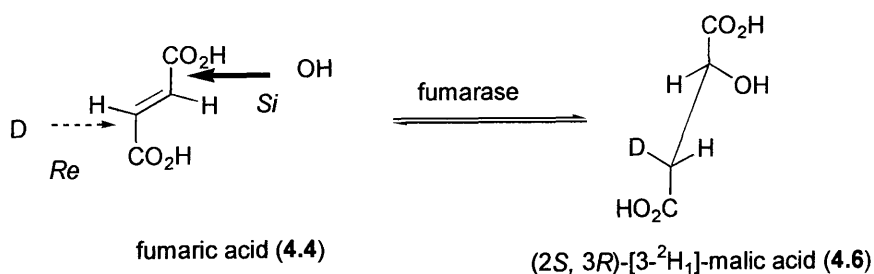
The conversion has been shown to proceed with the *anti*-elimination of one H<sub>Re</sub> and one H<sub>Si</sub> atom, from succinate when held in an *anti*-periplanar conformation.<sup>1</sup> Tchen and van Milligan demonstrated the steric course of the biotransformation by administering *threo* and *erythro* [2,3-<sup>2</sup>H<sub>2</sub>]-succinic acids to a Keilin-Hartree preparation of heart sarcosome<sup>2</sup> that contained succinate dehydrogenase. The *threo* and *erythro* [2,3-<sup>2</sup>H<sub>2</sub>]-succinic acids were afforded by the known *syn* hydrogenation with a platinum catalyst of fumaric (4.4) and maleic acid (4.5) respectively. When *threo* [2,3-<sup>2</sup>H<sub>2</sub>]-succinic acid was administered [2-<sup>2</sup>H]-fumaric acid (4.4 a) resulted; whereas when *erythro* [2,3-<sup>2</sup>H<sub>2</sub>]-succinic acid was administered [2,3-<sup>2</sup>H<sub>2</sub>]-fumaric acid (4.4 b), and unlabelled fumaric acid (4.4) resulted (scheme 4.3). This is consistent with the *anti*-elimination of one H<sub>Re</sub> and one H<sub>Si</sub> atom.



Scheme 4.3 Tchen and van Milligan's demonstration of the steric course of the conversion of succinic acid (4.3) to fumaric acid (4.4), mediated by the enzyme succinate dehydrogenase

#### 4.2.2 The conversion of fumarate to malate

The *anti*-addition of water across the double bond of fumarate (4.4) to afford (*S*)-malate (4.6) is mediated by the enzyme fumarase.<sup>3</sup> Incubation of the enzyme with fumarate and malate in the presence of <sup>2</sup>H<sub>2</sub>O leads to the incorporation of one deuterium at the C-3 position of malate (scheme 4.4). Even after prolonged periods of incubation, no deuteria are incorporated into the fumarate. This indicates that the enzyme operates with very high stereospecificity. A comparison of synthetic ( $\pm$ )-*threo*-[3-<sup>2</sup>H<sub>1</sub>]malic acid with the malic acid derived from the incubation experiment, by <sup>1</sup>H NMR, reveals that the biosynthetic material is *erythro* and that the water is added in an *anti* fashion.<sup>4</sup>

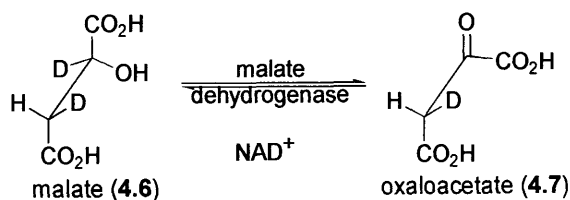


Scheme 4.4 The fumarase mediated conversion of fumaric acid (4.4), in the presence of <sup>2</sup>H<sub>2</sub>O, to (2*S*, 3*R*)-[3-<sup>2</sup>H<sub>1</sub>]-malic acid (4.6)

Consequently, this means that when [2,2,3,3-<sup>2</sup>H<sub>4</sub>]-succinate is administered, the resultant [2,3-<sup>2</sup>H<sub>2</sub>]-fumarate is processed to (2*S*, 3*S*)-[2, 3-<sup>2</sup>H<sub>2</sub>]-malic acid.

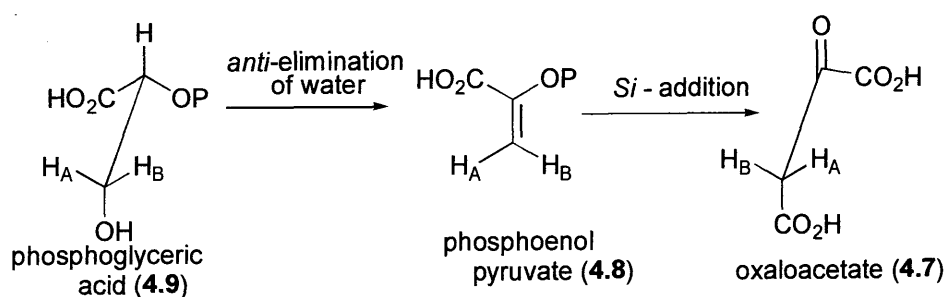
#### 4.2.3 The Conversion of malate to phosphoenol pyruvate

Malate dehydrogenase, in the presence of NAD<sup>+</sup>, mediates the oxidation of the hydroxyl group at the C-2 of malate (4.6) to an  $\alpha$ -keto-acid affording oxaloacetate (4.7). This conversion involves no alteration in the stereochemistry at C-3. (3*S*)-[3-<sup>2</sup>H<sub>2</sub>]-Oxaloacetate results from the processing of [2,2,3,3-<sup>2</sup>H<sub>4</sub>]-succinate around the Krebs cycle (scheme 4.5).



Scheme 4.5 The malate dehydrogenase mediated conversion of malate (4.6) to oxaloacetate (4.7)

The enzyme phosphoenol pyruvate carboxylase mediates the reversible carboxylation of phosphoenol pyruvate (4.8) to oxaloacetate (4.7). The stereochemical course of this biotransformation, as it affects C-3, has been studied by Rose and co-workers.<sup>5</sup> Utilising the known *anti*-elimination of water from phosphoglyceric acid (4.9) to form phosphoenol pyruvate (4.8)<sup>6</sup>, they administered stereospecifically tritiated 2-phosphoglycerates (4.9), of known configuration, to obtain the *E* and *Z*-[3-<sup>3</sup>H] phosphoenol pyruvates (4.8). The position of tritium in the resultant oxaloacetate, demonstrated that CO<sub>2</sub> is added to the *Si*-face of the phosphoenol pyruvate at C-3 (scheme 4.6).

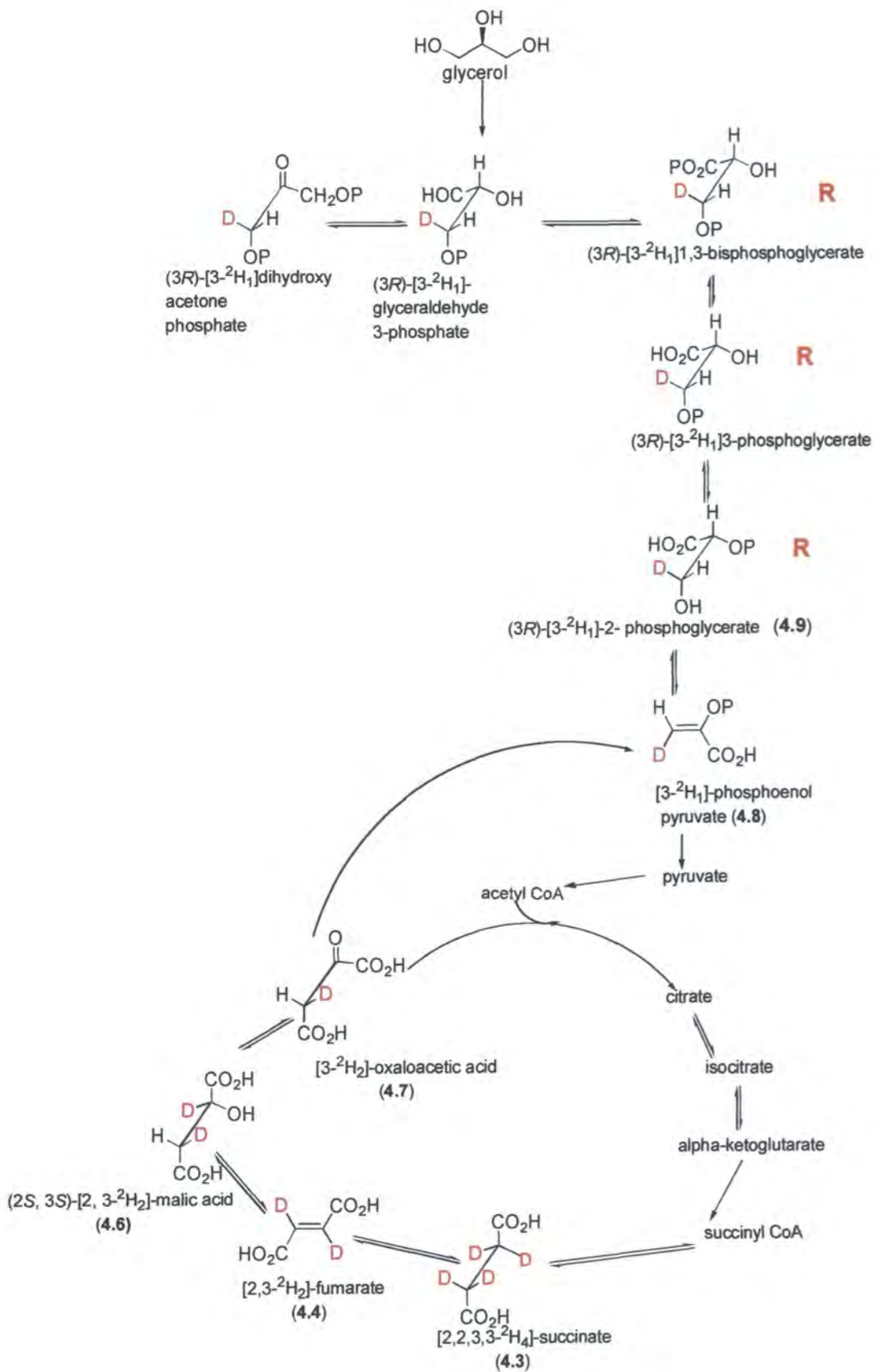


Scheme 4.6 The stereochemical course of the phosphoenol pyruvate carboxylase mediated conversion of phosphoenol pyruvate (4.8) to oxaloacetate (4.7)

Analysis of the configuration of the resultant oxaloacetate was achieved by the use of the known biochemical sequence: oxaloacetate (4.7) → malate (4.6) → fumarate (4.4) (see section 4.3.2).

#### 4.2.4 Metabolic processing of [2,2,3,3-<sup>2</sup>H<sub>4</sub>]-succinate

The processing of [2,2,3,3-<sup>2</sup>H<sub>4</sub>]-succinate through the Krebs cycle to (3*R*)-[3-<sup>2</sup>H<sub>1</sub>]-2-phosphoglycerate is illustrated in scheme 4.7. The stereochemistry is retained at C-3 as the compound for each of the intermediates upon the glycolytic pathway. It follows that upon feeding [2,2,3,3-<sup>2</sup>H<sub>4</sub>]-succinate, the carbon centre to be fluorinated has the *R* stereochemistry by virtue of deuterium substitution (scheme 4.7).



Scheme 4.7 Metabolic processing of [2,2,3,3- $^2\text{H}_4$ ]-succinate

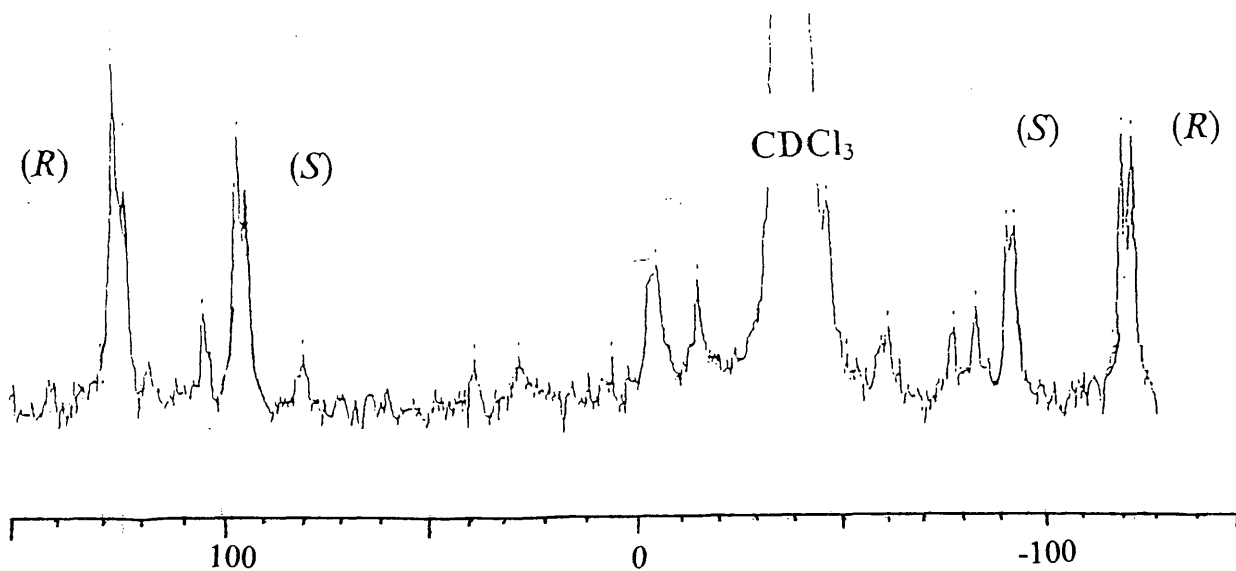
#### **4.2.5 [2,2,3,3-<sup>2</sup>H<sub>4</sub>]-Succinate feeding experiments**

Sodium [2,2,3,3-<sup>2</sup>H<sub>4</sub>]-succinate was administered to 8 day old resting cells of *Streptomyces cattleya* at a final concentration of 8.7 mM. The cells were incubated for 48 hours, after which time the fluoroacetate was harvested by lyophilization of the acidified, freeze-dried supernatant. The experiment was repeated with further resting cells until 7 mg of fluoroacetate had been collected.

The level of labelling in the resultant fluoroacetate was between 10 and 15%. The [<sup>2</sup>H<sub>1</sub>]-fluoroacetate content is chiral by virtue only of deuterium substitution. This is intrinsically a difficult system to resolve by methods of conventional analysis. However, the comparatively new technique of chiral liquid crystalline <sup>2</sup>H NMR<sup>7</sup> had been shown to be capable of resolving (2*S*) and (2*S*)-[2-<sup>2</sup>H]-fluoroacetates as their hexyl ester derivatives (see section 2.5).

The sodium fluoroacetate, derived from the feeding of sodium [2,2,3,3-<sup>2</sup>H<sub>4</sub>]-succinate, was added to a portion of unlabelled commercial fluoroacetate, to ease handling of the material, and derivatised as the hexyl ester. The resulting compound was dissolved in poly  $\gamma$ -benzyl L-glutamate and chloroform, and examined by <sup>2</sup>H NMR (fig 4.1a). By comparing this <sup>2</sup>H NMR spectra with the chiral liquid crystal <sup>2</sup>H NMR spectra of the synthetic (2*S*)-[2-<sup>2</sup>H]-fluoroacetate (fig 4.1b), it is apparent that the biosynthetic material has predominantly the *R*-configuration.





configuration, after incubation of *S. cattleya* with [2,2,3,3- $^2\text{H}_4$ ]-succinate.

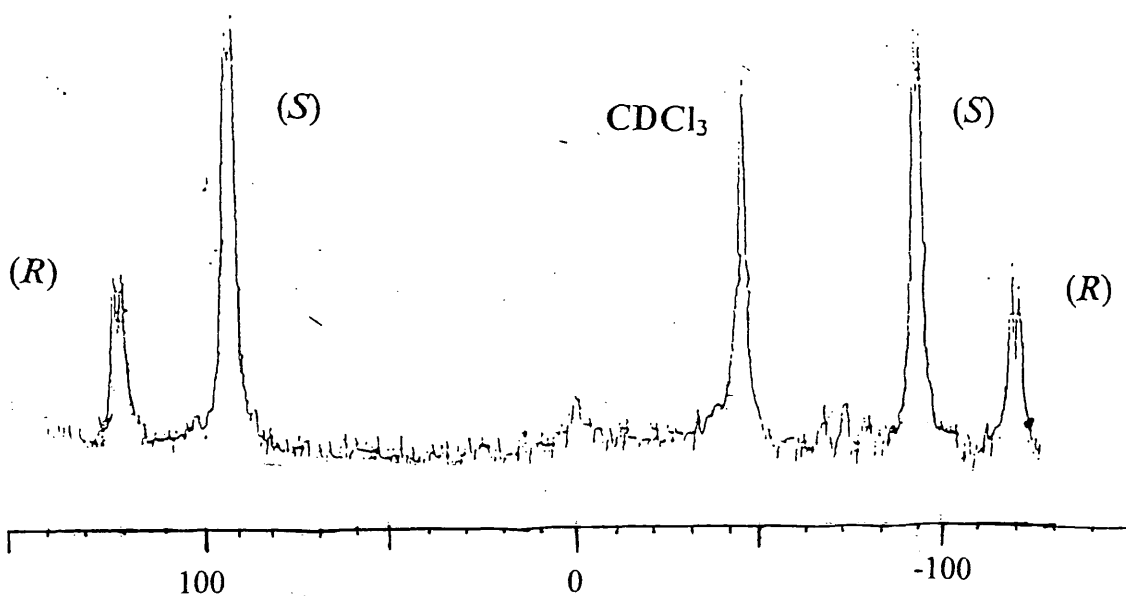


Fig 4.1b  $^2\text{H}$  NMR of synthetic hexyl [2- $^2\text{H}$ ]- fluoroacetate 38 % ee in favour of  $(S)$ - configuration

The spectra are obtained by analysing the compounds in a liquid material composed of PBLG and chloroform on a Bruker AC-250, 250.133 MHz. In addition to relying upon the integrals of the peaks to provide information as to the relative amounts of each enantiomer, the peaks were cut out from the paper that they were printed on and weighed. The two methods of analysis provided the same answer.

Fig 4.1

#### **4.2.6 Conclusion**

The [1-<sup>2</sup>H]-fluoroacetate recovered after incubation of [2,2,3,3-<sup>2</sup>H<sub>4</sub>]-succinate with *S. cattleya*, has predominantly *R*-configuration. As the C-3s of the glycolytic intermediates resulting from the metabolic processing of [2,2,3,3-<sup>2</sup>H<sub>4</sub>]-succinate are known, also, to be in the (*R*)-configuration, it may be deduced that the fluorination event proceeds with retention stereochemistry. Despite a poor signal to noise ratio in the <sup>2</sup>H NMR spectrum, an enantiomeric excess of approximately 25% may be calculated.

The enantiomeric excess is lower than anticipated and several possibilities exist to rationalise this. One reason for the low ee could be that the stereospecificity of the fluorinating enzyme is low. A second explanation could be that one or more of the steps upon the Krebs cycle and the glycolytic pathway operate with poor stereochemical integrity within *S. cattleya*.

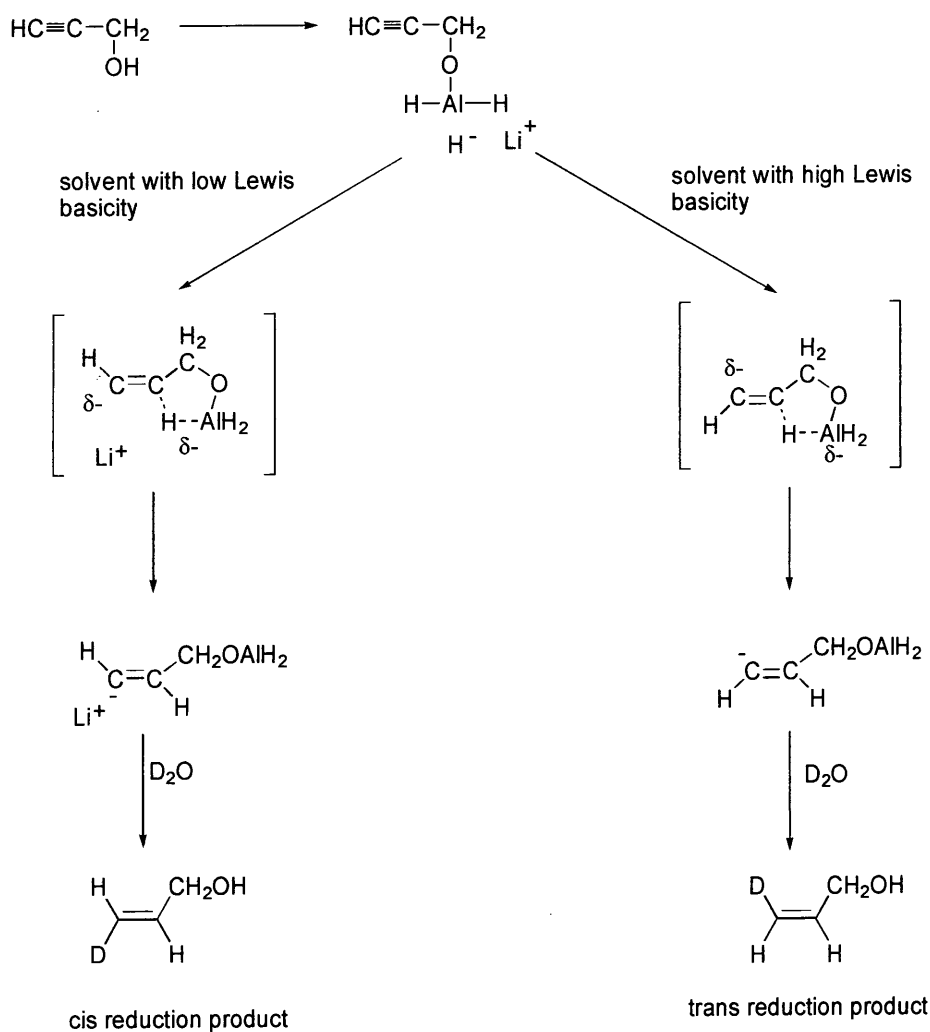
#### **4.3 Experiments with (2*R*)-[1-<sup>2</sup>H<sub>2</sub>]- and (2*S*)-[1-<sup>2</sup>H<sub>2</sub>]-glycerols**

The substrate to be fluorinated is known to be biosynthetically proximate to glycerol. In order to corroborate the information provided by the incubation [2,2,3,3-<sup>2</sup>H<sub>4</sub>]-succinate with resting cells of *S. cattleya* (2*R*)-[1-<sup>2</sup>H<sub>2</sub>]- and (2*S*)-[1-<sup>2</sup>H<sub>2</sub>]-glycerols (4.10, 4.10a) were synthesised and administered to the organism.

Glycerol is processed through glyceraldehyde 3-phosphate and subsequently onto 1,3-bisphosphoglycerate, 3-phosphoglycerate, and 2-phosphoglycerate. These enzymatic transformations affect only the chemistry at C-2 and do not alter the stereochemistry at C-3, the carbon centre that undergoes fluorination. Therefore, it was anticipated that, as glycerol enters the glycolytic pathway by an alternative route to succinate, and is not necessarily processed through the Krebs cycle, it would be possible to assess the stereochemical integrity of the fluorinating enzyme itself.

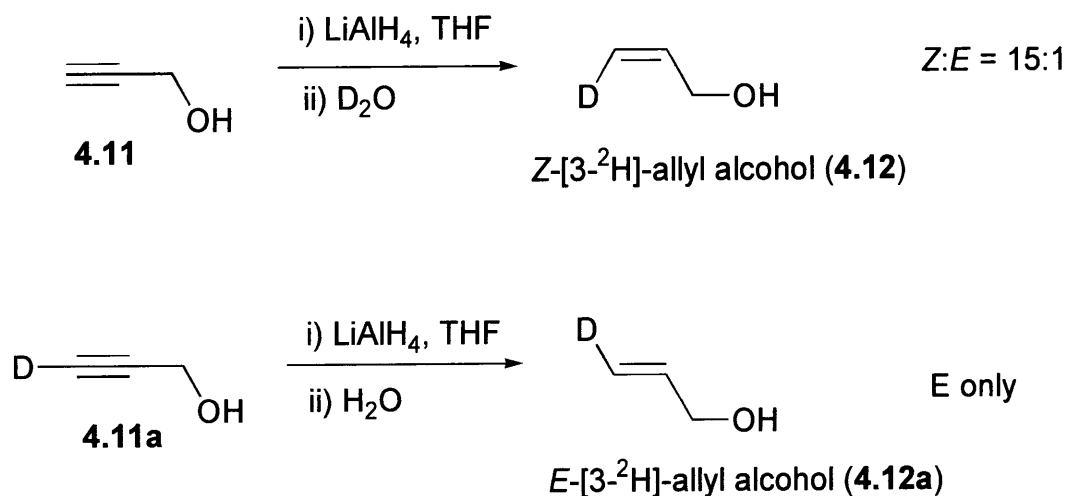


the charges being adopted. Hydrolysis of this transition state complex furnishes the *trans* reduction product. In agreement with this hypothesis, it was demonstrated that when dicyclohexyl-18-crown-6 is used in conjunction with the weakly Lewis basic solvent, isopropyl ether, the level of *trans* reduction increases dramatically. It was also found that lowering the temperature increased the amount of *cis* reduction product.



**Scheme 4.8** The reaction of lithium aluminium hydride with propargyl alcohol in Lewis basic and Lewis acidic solvents

Nieschalk prepared both the *Z*- and *E*-[3-<sup>2</sup>H]-allyl alcohols (**4.12**, **4.12a**) from propargyl alcohol and 3-[<sup>2</sup>H<sub>1</sub>]-propargyl alcohol(**4.11**, **4.11a**), respectively.<sup>14</sup> THF was used as solvent to promote the formation of the *trans* reduction products.



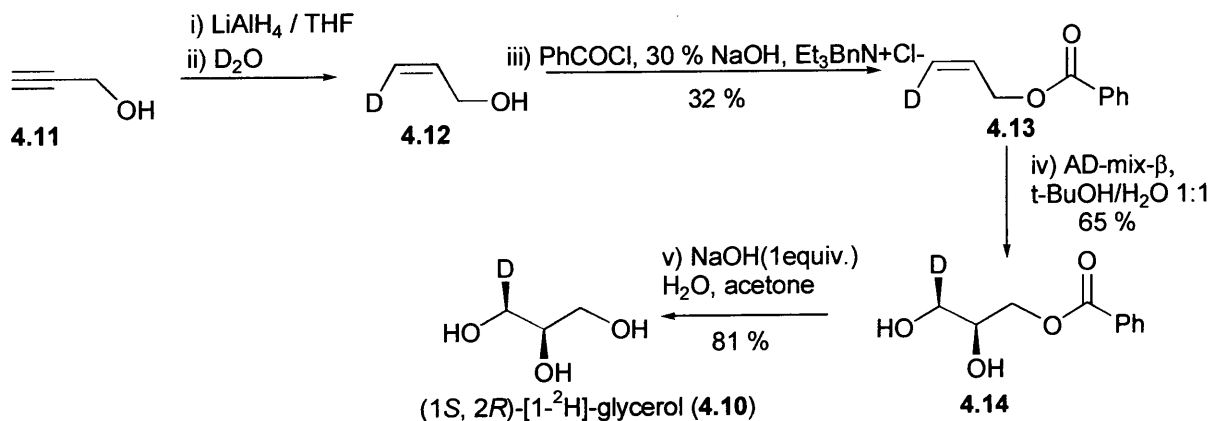
Scheme 4.9 The *trans* reduction of propargyl alcohol and 3-[<sup>2</sup>H<sub>1</sub>]-propargyl alcohol(**4.11**, **4.11a**)

Nieschalk noted that in addition to the *Z*-[3-<sup>2</sup>H]-allyl alcohol produced, following the D<sub>2</sub>O quench, some [2-<sup>2</sup>H]-allyl alcohol was also formed due to hydride attack at the terminal carbon of the acetylene. However, labelling at C-2 was not envisaged to be a problem for feeding experiments, as the proton from the C-2 of glycerol is not incorporated into the fluoroacetate.

The two resultant allyl alcohols were converted to their corresponding benzoate derivatives which were then asymmetrically dihydroxylated using Sharpless methodology<sup>17</sup> and commercially available AD-mix-β. The reaction afforded the 3-hydroxypropyl benzoates with an ee of 74 %. This was raised to 95 % by recrystallisation of the product. The benzoate protected glycerols were hydrolysed with sodium hydroxide to afford both (1*S*, 2*R*)-[1-<sup>2</sup>H]- and (1*R*, 2*R*)-[1-<sup>2</sup>H]-glycerols in high enantiomeric excess.

### 4.3.2 Synthesis and feeding of (1*S*, 2*R*)-[1-<sup>2</sup>H]-glycerol

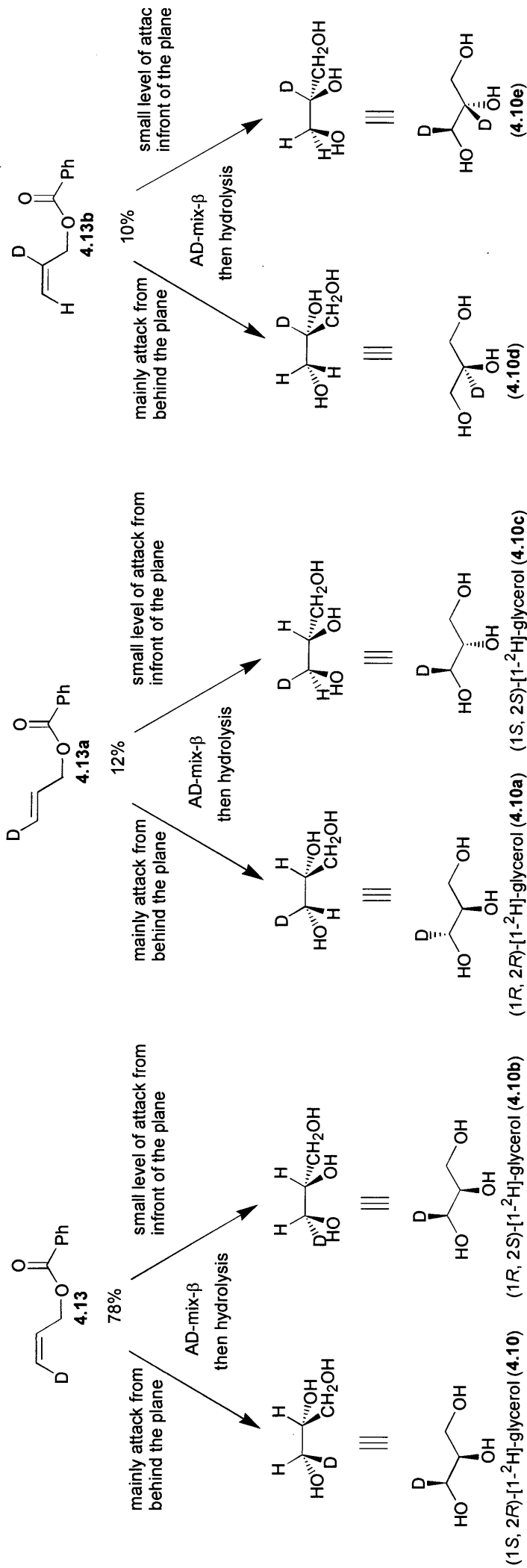
(1*S*, 2*R*)-[1-<sup>2</sup>H]-Glycerol was prepared in gram quantities according to Nieschalk's procedure (scheme 4.10). The reduction of propargyl alcohol (4.11) with lithium aluminium hydride, using the Lewis basic solvent, THF, followed by a D<sub>2</sub>O quench predominantly yielded the *trans* reduction product, Z-[3-<sup>2</sup>H]-allyl alcohol (4.12). The Z-[3-<sup>2</sup>H]-allyl alcohol was esterified to afford Z-[3-<sup>2</sup>H]-allyl benzoate (4.13). <sup>2</sup>H NMR analysis confirmed that the product consisted of 12% *E*-[3-<sup>2</sup>H]-allyl benzoate (4.13a), 78% Z-[3-<sup>2</sup>H]-allyl benzoate (4.13), and 10% of material deuterated at the 2 position (4.13b). The allyl benzoate was reacted with AD-mix-β to furnish [3(*S*)-<sup>2</sup>H]-2(*R*), 3-dihydroxypropyl benzoate (4.14), which initially had the appearance of a pale yellow oil. Purification over silica gel transformed the yellow oil to a white crystalline solid. The enantiomeric excess of the compound was assessed by comparing the integrals of the *ortho* benzoate hydrogen atoms in the <sup>1</sup>H NMR spectra using a europium chiral shift reagent, Eu(hfbc)<sub>3</sub>. Recrystallisation of the material increased the ee from an initial value of 67% to 84%.



Scheme 4.10 The synthesis of (1*S*, 2*R*)-[1-<sup>2</sup>H]-glycerol

Glycerol was afforded by hydrolysis of the ester in aqueous sodium hydroxide and acetone. Six glycerols are contained within the mixture, the major component being the (1*S*, 2*R*)-[1-<sup>2</sup>H]-glycerol (scheme 4.11).

products of first reaction



Scheme 4.11 (1S, 2R)-[1-<sup>2</sup>H]-Glycerol and the other minor components of the glycerol mixture

*Z*-[3-<sup>2</sup>H]-allylbenzoate (**4.13**), resulting from the *trans* reduction of propargyl alcohol with lithium aluminium hydride, is the major product (78%) of the first step of the synthesis. The reaction of *Z*-[3-<sup>2</sup>H]-allylbenzoate with AD-mix-β leads, predominantly, to the addition of two hydroxyl moieties behind the plane of the double bond; following hydrolysis (1*S*, 2*R*)-[1-<sup>2</sup>H]-glycerol (**4.10**) is afforded. A small amount of addition also occurs from in front of the plane of the double bond leading to (1*R*, 2*S*)-[1-<sup>2</sup>H]-glycerol (**4.10b**). The reduction reaction also produced 12% of the *cis* reduction product, *E*-[3-<sup>2</sup>H]-allyl benzoate (**4.13a**); the major and minor compounds formed following dihydroxylation to the back and front faces of the double bond of **4.13a** are glycerols **4.10a** and **4.10c**, respectively. During the reduction some hydride attack occurred at the terminal C-atom of the acetylene this resulted in 10% of the reduction product containing deuterium at C-2 (**4.13b**). Ester **4.13b** is dihydroxylated to afford [2-<sup>2</sup>H]-glycerols **4.10d** and **4.10e** as the major and minor products respectively.

It is known that deuterium from the C-2 of glycerol is not incorporated into fluoroacetate, thus glycerols **4.10d** and **4.10e** are not relevant contaminants. Deuterium labels the *pro-S* hydroxymethyl group of glycerols **4.10b** and **4.10c**, this is known to be cleaved in the biosynthesis of fluoroacetate by *S. cattleya*. Only two of the six glycerols contribute deuteria to the fluoroacetate:- (1*S*, 2*R*)-[1-<sup>2</sup>H]-glycerol (**4.10**) and (1*R*, 2*R*)-[1-<sup>2</sup>H]-glycerol (**4.10a**). If the ratio of dihydroxylation in front and behind the plane of the double bond, with *Z*-[3-<sup>2</sup>H]-allylbenzoate (**4.13**) is equivalent to that with *E*-[3-<sup>2</sup>H]-allylbenzoate (**4.13a**), the resultant (1*S*, 2*R*)-[1-<sup>2</sup>H]-glycerol would have an ee of 73%.

The glycerol was analysed by chiral liquid crystal <sup>2</sup>H NMR using poly-ε-carbobenzoxy-L-lysine (PCBL) in dimethyl formamide as the chiral solvent (Fig 4.3). The analysis showed 3 different components:- 75 % (1*S*, 2*R*)-[1-<sup>2</sup>H]-glycerol (**4.10**), 13% (1*R*, 2*R*)-[1-<sup>2</sup>H]-glycerol (**4.10a**), and 10% of glycerol **4.10d**. These values compare closely to the amounts of the various [3-<sup>2</sup>H]-allylbenzoates ( 78% *cis*, 12% *trans* and 10% deuterated at C-2).

It may be concluded that the AD-mix-β predominantly mediates dihydroxylation from behind the face of the double bond of the [3-<sup>2</sup>H]-allylbenzoate. The stereochemistry of the resultant glycerol is therefore, largely governed by the stereochemistry of the lithium aluminium hydride reduction of the propargyl alcohol. From the Chiral liquid crystal <sup>2</sup>H NMR it may be concluded that the synthetic (1*S*, 2*R*)-[1-<sup>2</sup>H]-glycerol has a 70% ee.



4.10

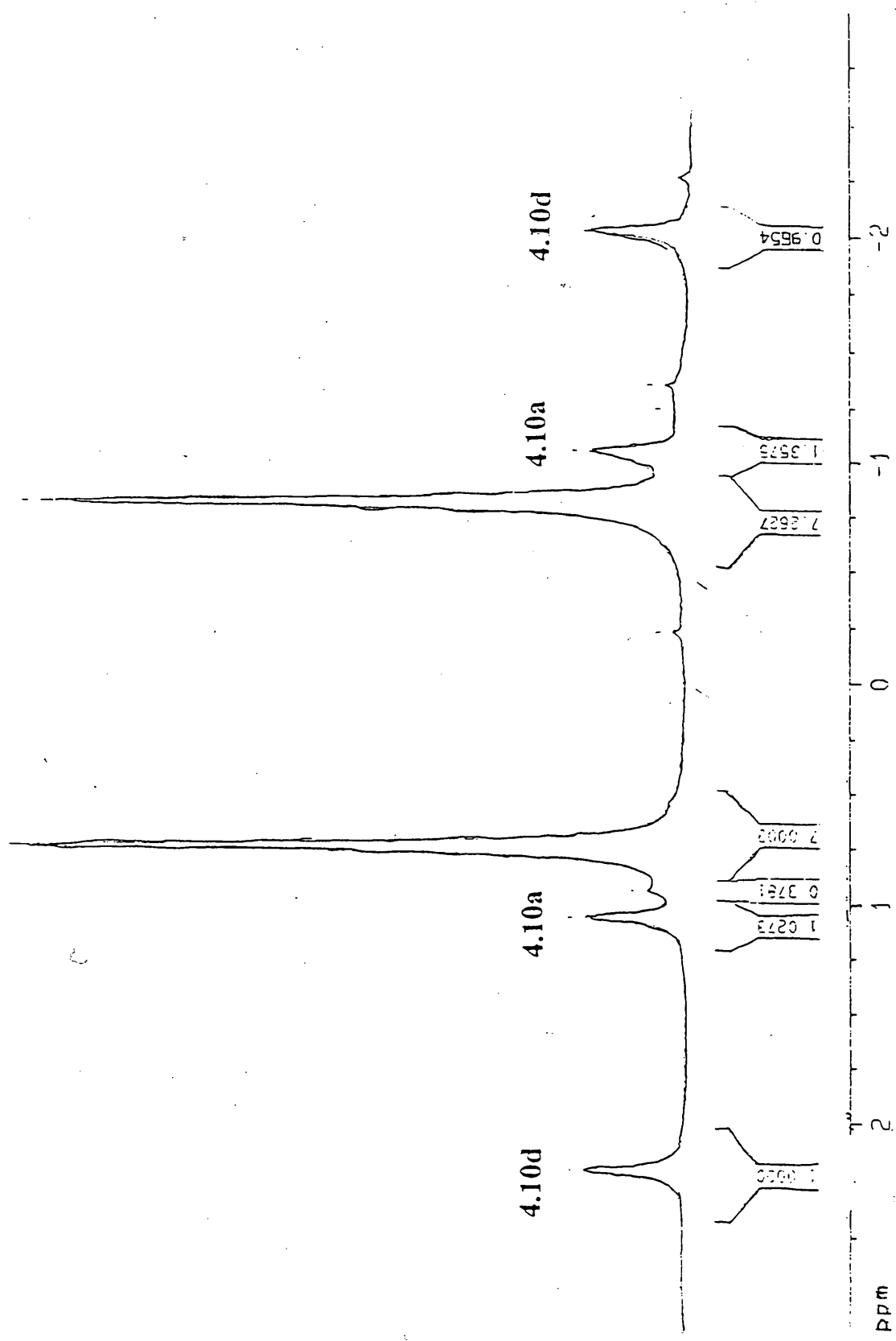


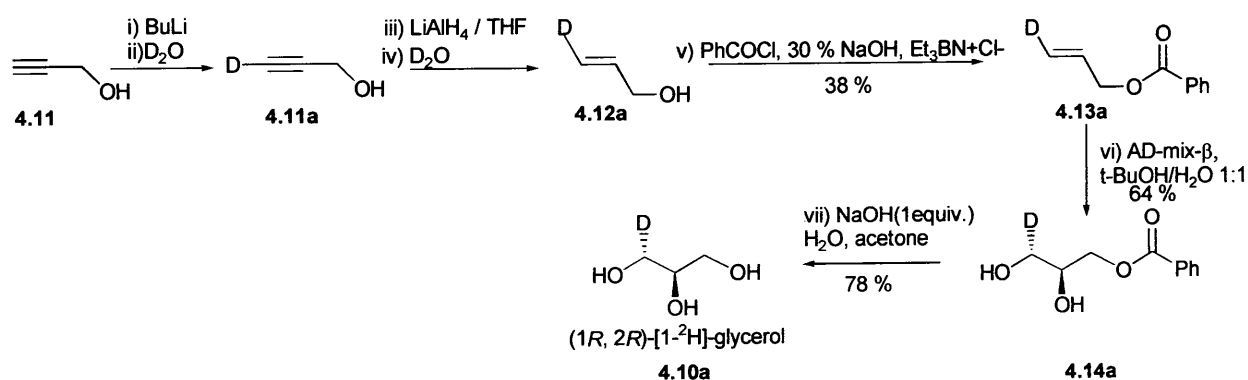
Fig 4.3  $^2\text{H}$  NMR of synthetic (1S, 2R)-[1- $^2\text{H}$ ]-glycerol in dimethyl formamide as the chiral solvent (Bruker AC-250, 250.133 MHz)

The glycerol was administered to 8 day old resting cells of *Streptomyces cattleya* at a final concentration of 8.7 mM. After 48 hours of incubation, the cells were harvested. The resultant [2-<sup>2</sup>H<sub>1</sub>]-fluoroacetate was extracted and analysed in the same manner as the [2-<sup>2</sup>H<sub>1</sub>]-fluoroacetate produced following the feeding of [2,2,3,3-<sup>2</sup>H<sub>4</sub>]-succinate to *S. cattleya* (fig 4.5a).

### 4.3.3 Synthesis of (1*R*, 2*R*)-[1-<sup>2</sup>H]-glycerol

(1*R*, 2*R*)-[1-<sup>2</sup>H]-Glycerol was synthesised following Nieschalk's procedure. The terminal proton of the alkyne was exchanged with deuterium by treating the propargylic alcohol with butyl lithium and quenching the resultant anion with D<sub>2</sub>O. The lithium aluminium hydride, *trans* reduction of the resulting [3-<sup>2</sup>H]-propargyl alcohol (**4.11a**) was then performed and the reaction quenched to afford *E*-[3-<sup>2</sup>H] allyl alcohol (**4.12a**) as the only isomer. The <sup>2</sup>H NMR of the *E*-[3-<sup>2</sup>H]-allylbenzoate (**4.13a**) exhibited a single peak at 5.34 ppm.

The *E*-[3-<sup>2</sup>H]-allylbenzoate was dihydroxylated using AD-mix-β; purification over silica afforded white crystalline [3(*R*)-<sup>2</sup>H]-2(*R*), 3-dihydroxypropyl benzoate (**4.14a**). The enantiomeric excess was increased from 72% to 95% by recrystallisation. The protected glycerol was hydrolysed using aqueous sodium hydroxide and acetone to afford (1*R*, 2*R*)-[1-<sup>2</sup>H]-glycerol (**4.10a**) in gram quantities.



Scheme 4.12 The synthesis of (1*R*, 2*R*)-[1-<sup>2</sup>H]-glycerol

The (1*R*, 2*R*)-[1-<sup>2</sup>H]-glycerol was analysed by chiral liquid crystal <sup>2</sup>H NMR using PCBL in dimethyl formamide as the chiral solvent (Fig 4.4). The resultant spectrum indicated the presence only one glycerol component, the (1*R*, 2*R*)-[1-<sup>2</sup>H]-glycerol (4.10a).

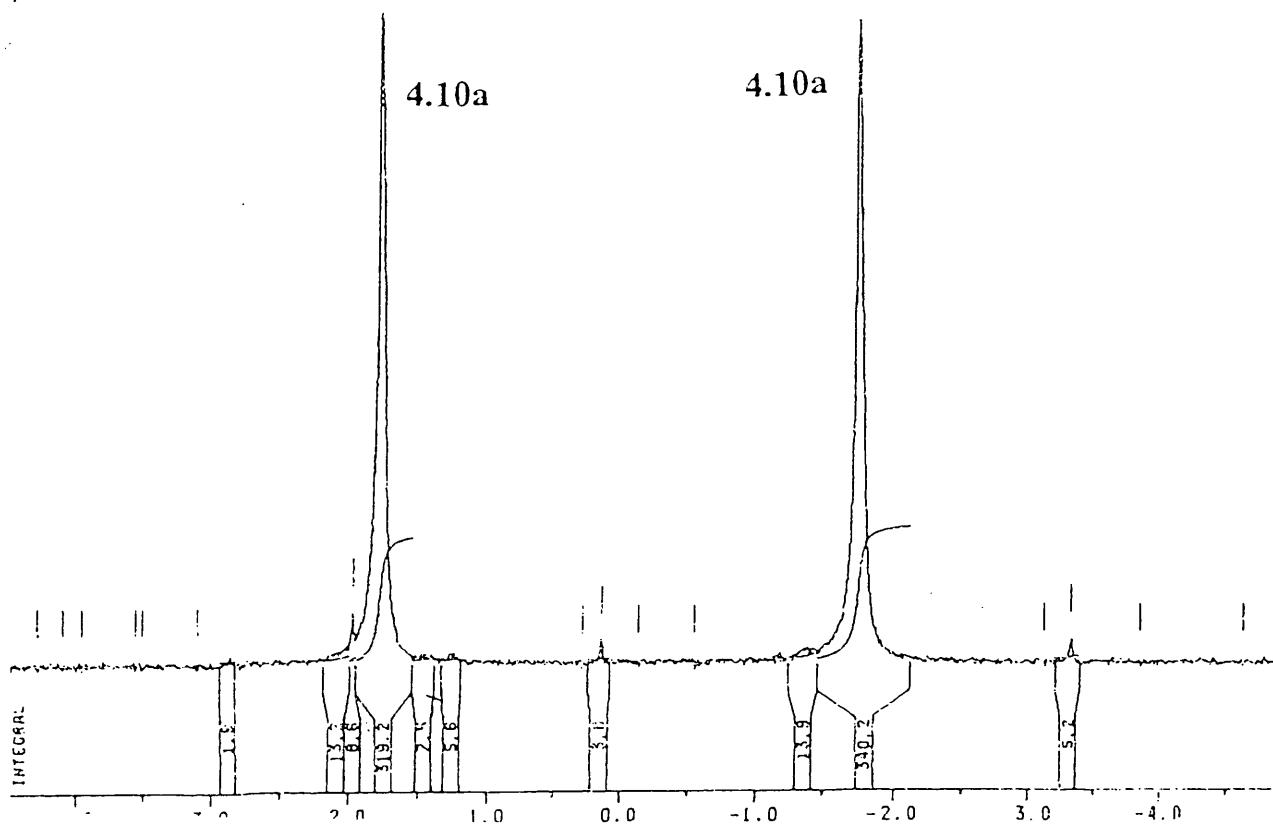


(Fig 4.4) <sup>2</sup>H NMR of synthetic (1*R*, 2*R*)-[1-<sup>2</sup>H]-glycerol using PCBL in dimethyl formamide as the chiral solvent (Bruker AC-250, 250.133 MHz)

The (1*R*, 2*R*)-[1-<sup>2</sup>H]-glycerol was administered to 8 day old resting cells of *Streptomyces cattleya* at a final concentration of 8.7 mM. After 48 hours of incubation, the cells were harvested. The resultant [2-<sup>2</sup>H<sub>1</sub>]-fluoroacetate was extracted and analysed in the same manner as the [2-<sup>2</sup>H<sub>1</sub>]-fluoroacetate produced following the feeding of [2,2,3,3-<sup>2</sup>H<sub>4</sub>]-succinate to *S. cattleya* (fig 4.5b).

#### 4.3.5 Results from the feeding of the chiral glycerols

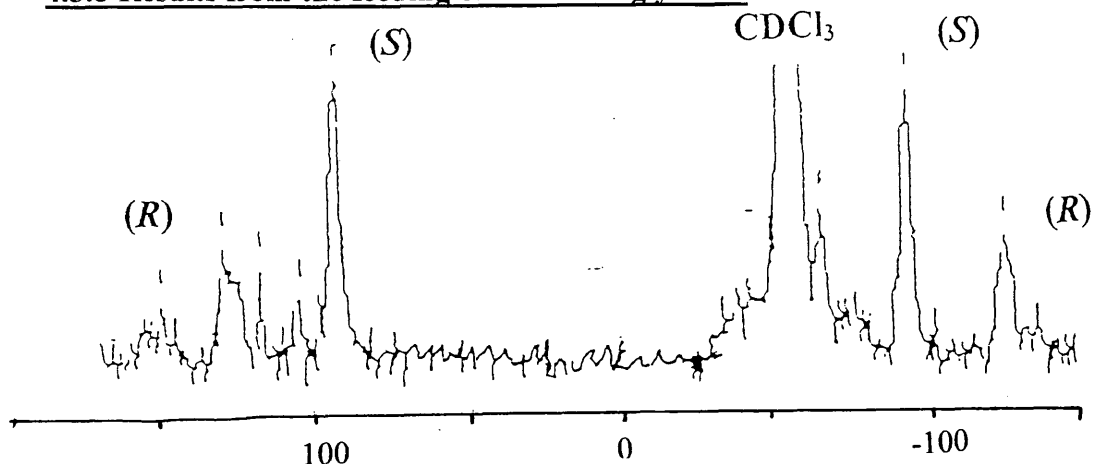


Fig 4.5a  $^2\text{H}$  NMR of  $[2\text{-}^2\text{H}]$ -hexylfluoroacetate, from *S. cattleya* fed (1*S*, 2*R*)- $[1\text{-}^2\text{H}]$ -glycerol

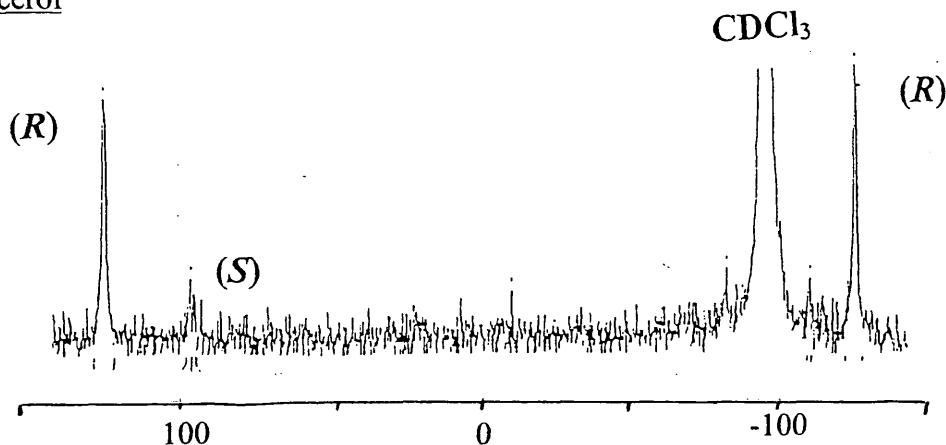


Fig 4.5b  $^2\text{H}$  NMR of  $[2\text{-}^2\text{H}]$ -hexylfluoroacetate, from *S. cattleya* fed (1*R*, 2*R*)- $[1\text{-}^2\text{H}]$ -glycerol

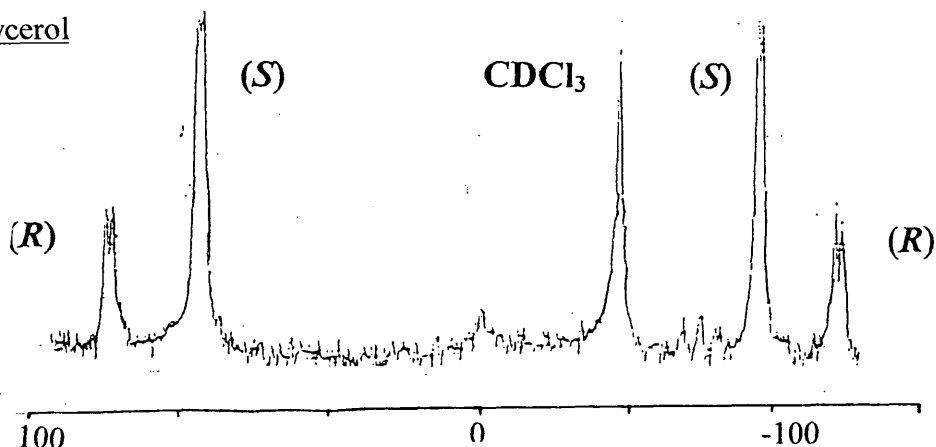


Fig 4.5c  $^2\text{H}$  NMR of synthetic (2*S*)- $[2\text{-}^2\text{H}]$ -hexylfluoroacetate

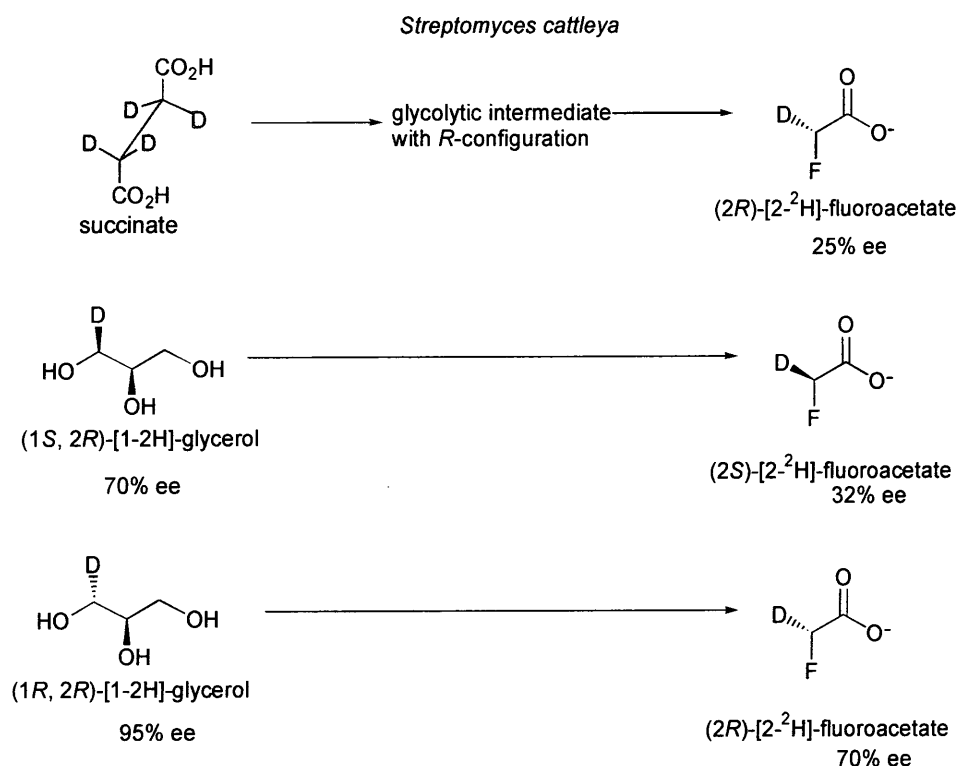
The spectra are obtained by analysing the compounds in a liquid material composed of PBLG and chloroform on a Bruker AC-250, 250.133 MHz.

Fig 4.5

In addition to relying upon the integrals of the peaks to provide information as to the relative amounts of each enantiomer, the peaks were cut out from the paper that they were printed on and weighed. The two methods of analysis provided the same answer.

#### 4.4 Conclusions

Chiral liquid crystal  $^2\text{H}$  NMR shows that (2*S*)-[2- $^2\text{H}$ ]-fluoroacetate is derived from resting cell cultures of *Streptomyces cattleya* that have been fed (1*S*, 2*R*)-[1- $^2\text{H}$ ]-glycerol, whilst cultures that have been fed (1*R*, 2*R*)-[1- $^2\text{H}$ ]-glycerol produce (2*R*)-[2- $^2\text{H}$ ]-fluoroacetate. These results complement the [2,2,3,3- $^2\text{H}_4$ ]-succinate feeding experiment by indicating that the stereochemistry of the carbon centre is retained during the biosynthetic fluorination by *Streptomyces cattleya*.



Scheme 4.13 The stereochemical outcome of administering [2,2,3,3- $^2\text{H}_4$ ]-succinate, (1*S*, 2*R*)-[1- $^2\text{H}$ ]-glycerol and (1*R*, 2*R*)-[1- $^2\text{H}$ ]-glycerol to *Streptomyces cattleya*

The enantiomeric excess of the fluoroacetate resulting from the incubation of [2,2,3,3- $^2\text{H}_4$ ]-succinate with *S. cattleya* is low (25%). This may be attributed to a loss of stereochemistry as the succinate is processed through the Krebs cycle (see section 4.2.6). The fluoroacetate resulting from the feeding of (1*S*, 2*R*)-[1- $^2\text{H}$ ]-glycerol is slightly higher, with a value of 32%. Due to the small amount of [2- $^2\text{H}$ ]-fluoroacetate available for analysis, the spectra for this biosynthetic sample has a low signal to noise ratio. This makes it difficult to measure the ee exactly. Although the enantiomeric excess is low, it is significant that the glycerol fed had an ee of 70%. It

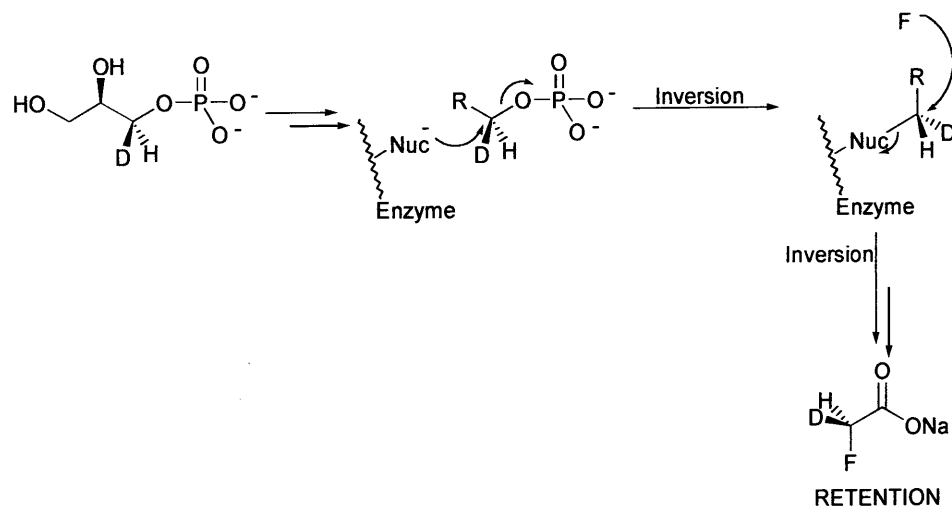
may be interpreted that from a sample of 85% (1*S*, 2*R*)-[1-<sup>2</sup>H]-glycerol the bacteria biosynthesised fluoroacetate of which 66% was in the *S*-configuration.

The incubation of (1*R*, 2*R*)-[1-<sup>2</sup>H]-glycerol with a 95 % ee (98 % of the molecules with *R*-configuration) with *S. cattleya* results in the production of (*R*)-[<sup>2</sup>H]-fluoroacetate with an ee of 70% (85 % of the molecules with *R*-configuration).

It is noteworthy that in each of the feeding experiments a considerable loss of enantiomeric purity is observed. The results indicate that the fluorination proceeds with an overall retention of configuration, with a low level of inversion occurring concurrently.

#### **4.5 Possible mechanisms of fluorination**

From the knowledge that the fluorination occurs with overall retention of configuration, one explanation would be that fluorination occurs *via* two stereochemical inversions. An amino acid residue, such as cysteine, positioned at the active site of the fluorinating enzyme may be envisaged to act as a nucleophile attacking the substrate to be fluorinated. This covalent modification could be followed by nucleophilic attack by a source of fluoride. As fluoride attacks the activated complex the amino acid residue is released (scheme 4.14).



**Scheme 4.14 Possible mechanism of fluorination involving two inversion processes**

## References

- 1 T. T. Tchen, H. van Milligan, *J. Am. Chem. Soc.* 1960, **82**, 4115
- 2 D. Keilin, E. F. Hartree, *Proc Roy. Soc. (London)*, 1940, **B129**, 227.
- 3 S. England, *J. Biol. Chem.*, 1960, **235**, 1510
- 4 O. Gawron, A. J. Glaid, T. P. Fondly, *J. Am. Chem. Soc.*, 1961, **83**, 3634  
F. A. L. Anet, *J. Am. Chem. Soc.*, 1960, **82**, 994.
- 5 I. A. Rose, E. L. O'Connell, P. Noce, M. F. Utter, H. G. Wood, J. M. Willard, T. G. Cooper, M. Benziman, *J. Biol. Chem.*, 1976, **244**, 6130
- 6 M. Cohn, J. E. Pearson, E. L. O'Connell, I. A. Rose, *J. Am. Chem. Soc.*, 1970, **92**, 4095.
- 7 P. Lesot, D. Merlet, A. Loewenstein, J. Courtieu, *Tet. Assym.*, 1998, **9**, 1871.
- 8 J. M. Beale, H. G. Floss, *Angew. Chem., Int. Ed. Engl.*, 1989, **28**, 146.
- 9 C. A. Townsend, S. S. Mao, *J. Chem. Soc., Chem. Commun.*, 1987, 86.
- 10 H. Oikawa, K. Yagi, K. Watanabe, M. Honma, A. Ichihara, *Chem. Commun.*, 1997, 97.
- 11 H. Uzawa, Y. Nishida, S. Hanada, H. Ohru, H. Meguro, *J. Chem. Soc., Chem. Commun.*, 1989, 862.
- 12 K. Kakinuma, Y. Iihama, I. Takagi, K. Ozawa, N. Yamaguchi, N. Imamura, Y. Esumi, M. Uramoto, *Tetrahedron*, 1992, **48**, 3763.
- 13 D. S. Matteson, A. A. Kandil, R. Soundararajan, *J. Am. Chem. Soc.*, 1990, **112**, 3964.
- 14 J. Nieschalk, D. O'Hagan, *Tetrahedron Asymm.*, 1997, **8**, 2325.
- 15 R. A. Raphael, *Acetylinic Compounds in Organic Synthesis*, Butterworth and Co. Ltd., London, 1955, p29.
- 16 B. Grant, C. Djerassi, *J. Org. Chem.*, 1974, **39**, 968.
- 17 K. B. Sharpless, W. Amberg, Y. L. Bennani, G. A. Crispino, J. Hartung, K. S. Jeong, H. L. Kwong, K. Morikawa, Z. M. Wang, D. Xu, X. L. Zhang, *J. Org. Chem.*, 1992, **57**, 2768.

## **CHAPTER 5**

### **The Biosynthesis of Longianone**





## CHAPTER 5

### The Biosynthesis of Longianone

#### Introduction and Background

##### 5.1 Introduction

Longianone (**5.1**) is a secondary metabolite of the fungus *Xylaria longiana*. Longianone was first isolated and purified along with the two known fungal metabolites (R)-(-)-mellein (**5.2**) and 4-hydroxymellein (**5.3**) in 1998 by Edwards.<sup>1</sup> The compound was given the trivial name “eggtimerone” due to its structural resemblance to an eggtimer. Although *longiana* is an uncommon member of the fungal genus *Xylaria*, it is widely distributed, occurring in both tropical and temperate climates. *Xylaria longiana* is a slow growing fungus which lives on dead and decaying wood and has been reported on a number of hosts from *Fagus sylvaticus* (beech tree) in Switzerland to the leaves of *Nicotiana* (tobacco plant) in Georgia, USA.

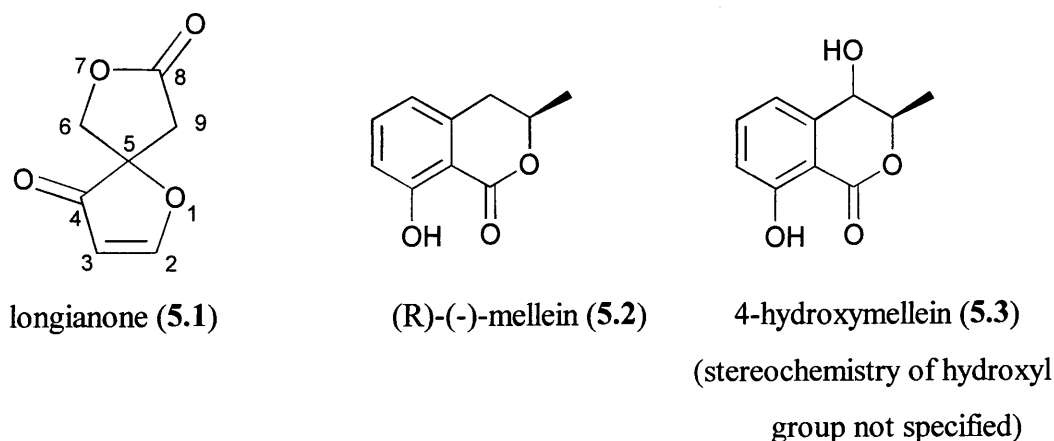


Fig. 5.1 Metabolites of *X. longiana*

Longianone, formally 1,7-dioxaspiro[4,4]non-2-ene-4,8-dione, has an intriguing bicyclic structure consisting of a 2H-furane-3-one nucleus “fused” by a spiro centre to a lactone ring. Edwards confirmed the structure of longianone by a crystal X-ray determination; however, this did not reveal the absolute configuration at the spiro centre C-5, the designation of which remains unassigned.

Longianone is optically active with a strong negative rotation:  $[\alpha]_D^{20} = -85$  ( $c = 1.0$ , EtOH) indicating a high enantiomeric excess.

## 5.2 Naturally occurring analogues of longianone

The 2H-furane-3-one moiety is a common structural feature in a number of natural products. In compounds isolated to date, however, it is only in chilenone A (5.4) and B (5.5) from the red marine alga *Laurencia chilensis* that the 4, 5 positions occur unsubstituted.<sup>2,3</sup> In all other cases, at least one of these sites carries a functional group.

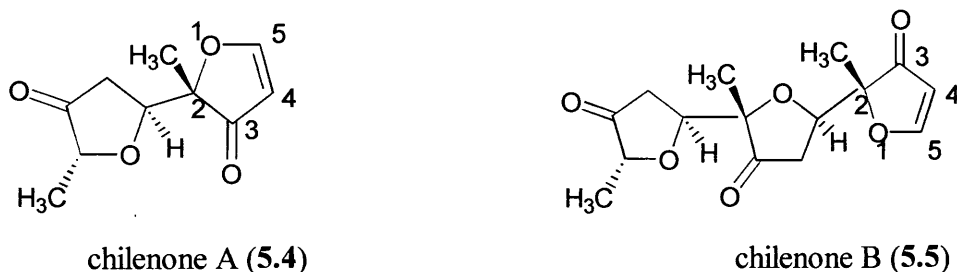


Fig. 5.2 Chilenones

Few naturally occurring spirocyclics containing the furane-3-one have been isolated to date. Pseurotin A (5.6) and its analogues B, C, D and E from cultures of *Pseudeurotium ovalis*<sup>4,5,6,7</sup> contain the furane-3-one system but they also possess substituents at both positions 4 and 5, and the ring is fused to an elaborate lactam rather than a lactone. Hyperlactone (5.7) and its analogues from the stem and leaves of *Hypericum chinensis*<sup>8</sup> are, at first glance, structurally very similar to longianone; however the lactone ring is fused at a different position to a substituted furan-3-one and the side chains are indicative of a terpenoid type biosynthesis.

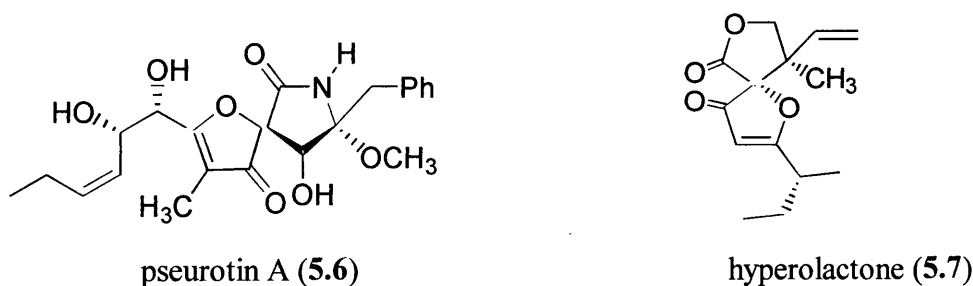
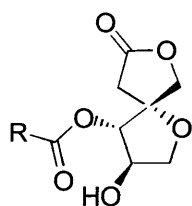
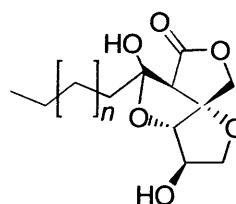
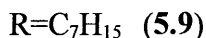


Fig. 5.3 Natural products containing furane-3-one



secosyrin R= C<sub>2</sub>H<sub>11</sub> (5.8)



syringolide n=2 (5.10)

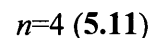
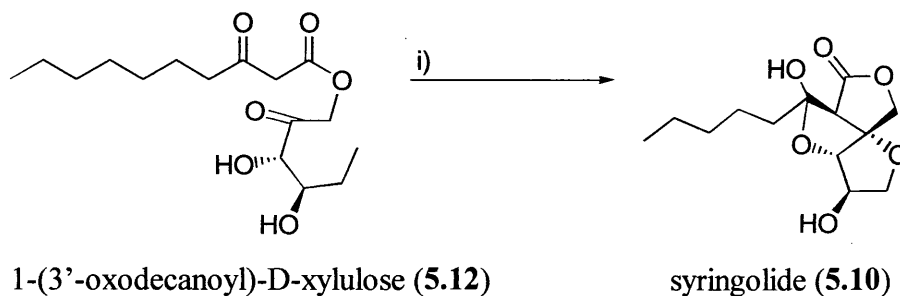


**Fig. 5.4 Secosyrins and syringolides**

The secosyrins (5.8, 5.9) and the syringolides (5.10, 5.11) (Fig 5.4), metabolites of the bacterium *Pseudomonas syringia* pv. *Tomato*,<sup>9,10</sup> have a much greater resemblance to longianone. The only significant structural difference in the former is that the carbon carbon double bond is hydrated and one ketone unit is replaced by an ester moiety. A hypothetical biosynthesis for the secosyrins proposes the combination of a polyketide chain with a pentose sugar. Some support for this hypothesis has been provided in a biomimetic synthesis of the secosyrins, in which 1-(3'-oxodecanoyl)-D-xylulose (5.12) was demonstrated to afford the syringolide (5.10) (scheme 5.1).<sup>11</sup> It is not inconceivable that longianone would share a similar biosynthesis to these metabolites and be of polyketide origin.



1-(3'-oxodecanoyl)-D-xylulose (5.12)

syringolide (5.10)

i) THF, Al<sub>2</sub>O<sub>3</sub>

**Scheme 5.1 Biomimetic study of the formation of syringolide (5.10)**

### **5.3 Fatty acids and polyketides**

Fatty acids and polyketides share a very similar biosynthesis. Both classes of metabolite are assembled by the head to tail condensation of acetate units. Fatty acids are characterised by a long hydrophobic hydrocarbon chain linked to a polar hydrophilic carboxylic acid head. Their resultant amphiphilic quality causes the fatty acids to aggregate together and has been exploited by nature to form micelles and membrane bilayers in almost all living organisms. Fatty acids are also utilised in nature,

in the form of tri-fatty acid esters of glycerol, for long term energy storage. The tri-fatty acid esters may be oxidised to release energy, ultimately available in the form of ATP. Nature's use of fatty acids does not stop with mechanical and energy storage functions. In mammals, prostaglandins, elaborate C<sub>20</sub> unsaturated fatty acids containing a cyclopentane ring system, are used as hormones; such molecules show marked similarity to the biologically active polyketides.

The polyketides are a large family of secondary metabolites. They range from small structurally non-complex molecules such as 6-methylsalicylic acid to large and incredibly intricate structures such as maitotoxin (5.13) (fig. 5.5).<sup>4</sup> Many polyketides have important pharmaceutical properties.

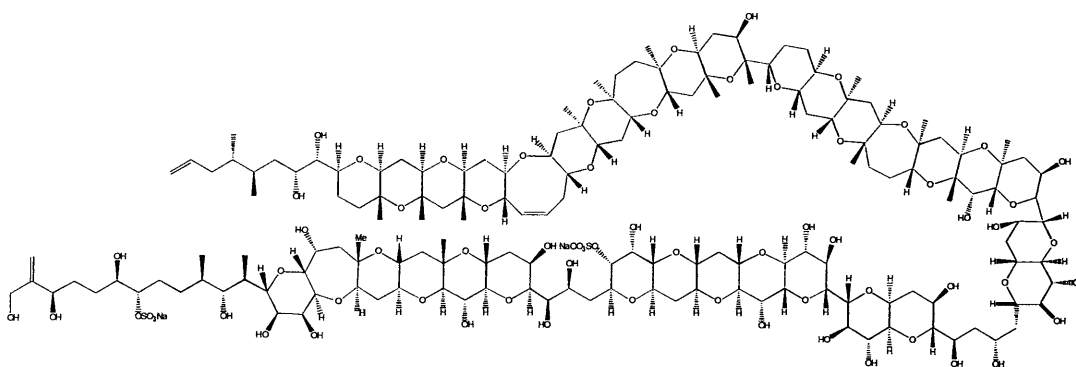


**Fig. 5.5 Maitotoxin (5.13)**

The term polyketide was coined, almost 100 years ago, by John Norman Collie and today refers to natural products containing multiple carbonyl and/or hydroxy groups each separated by a methylene carbon<sup>3</sup>. Polyketides are typically synthesised by the organism at the onset of its stationary growth phase.

#### **5.4 Fatty acid biosynthesis**

As fatty acids are built up by the head-to-tail condensation of acetate units, most naturally occurring examples are straight chains consisting of an even number of carbon atoms (5.14, 5.15). Some fatty acids with odd numbered chain lengths and branching exist, this structural feature is due to the incorporation of non-acetate starter units (5.16, 5.17).

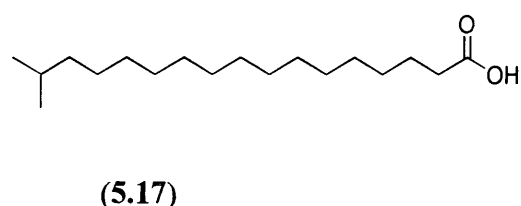
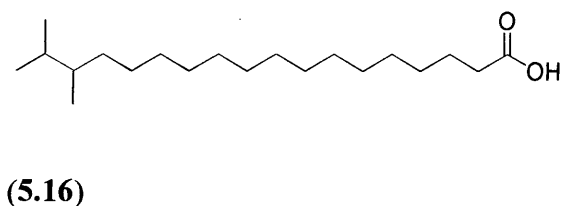
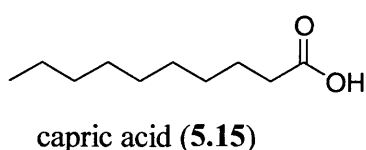
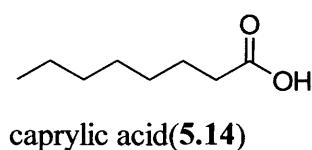
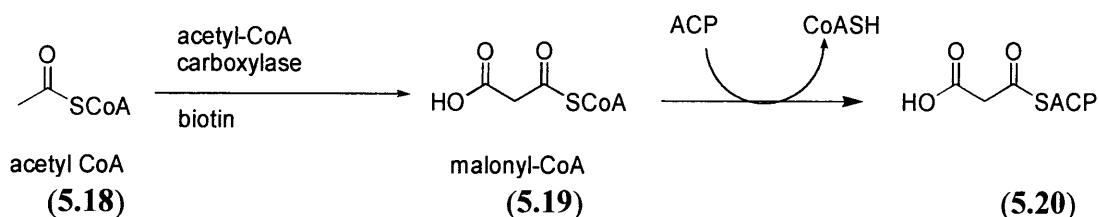


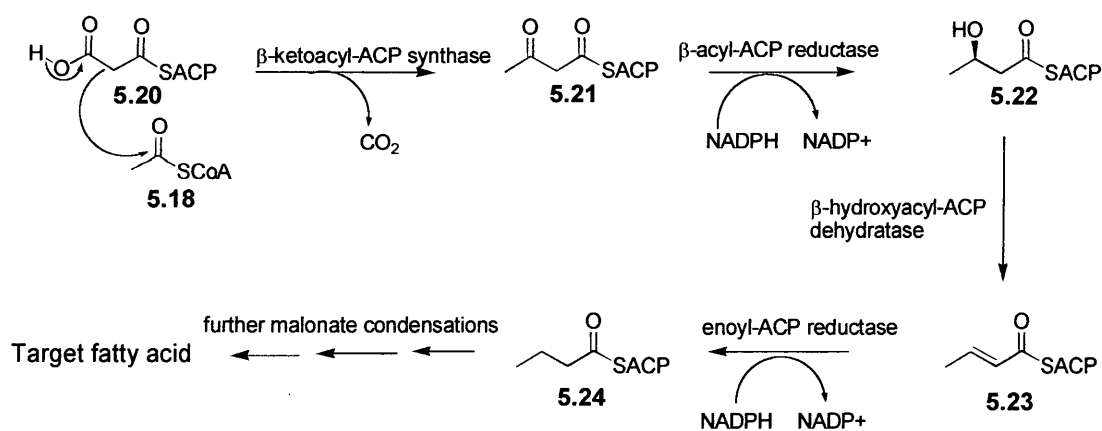
**Fig 5.6 Fatty acids**

Fatty acid biosynthesis involves two steps. The initial process is the activation of acetyl-CoA (5.18), the thioester of co-enzyme A with acetic acid, to generate malonyl-CoA (5.19), a process mediated by the enzyme acetyl-CoA carboxylase. This enzyme requires biotin as a co-factor (scheme 5.2) <sup>12</sup>. The second step is the conversion of acetyl-CoA and malonyl-CoA into the fatty acid, a process mediated by the fatty acid synthase enzyme (FAS) in the presence of the co-factor NADPH.



**Scheme 5.2 Activation of acetyl-CoA to malonyl-ACP**

An acyl carrier protein (ACP), onto which the malonate moiety is transesterified, acts as a chaperone taking the intermediate acyl thioesters around the catalytic sites of the FAS. The malonyl-SACP (5.20) is first led to a site in the synthase, here it undergoes a decarboxylative condensation with a molecule of acetyl-CoA which has entered the active site of the FAS (Scheme 5.3).



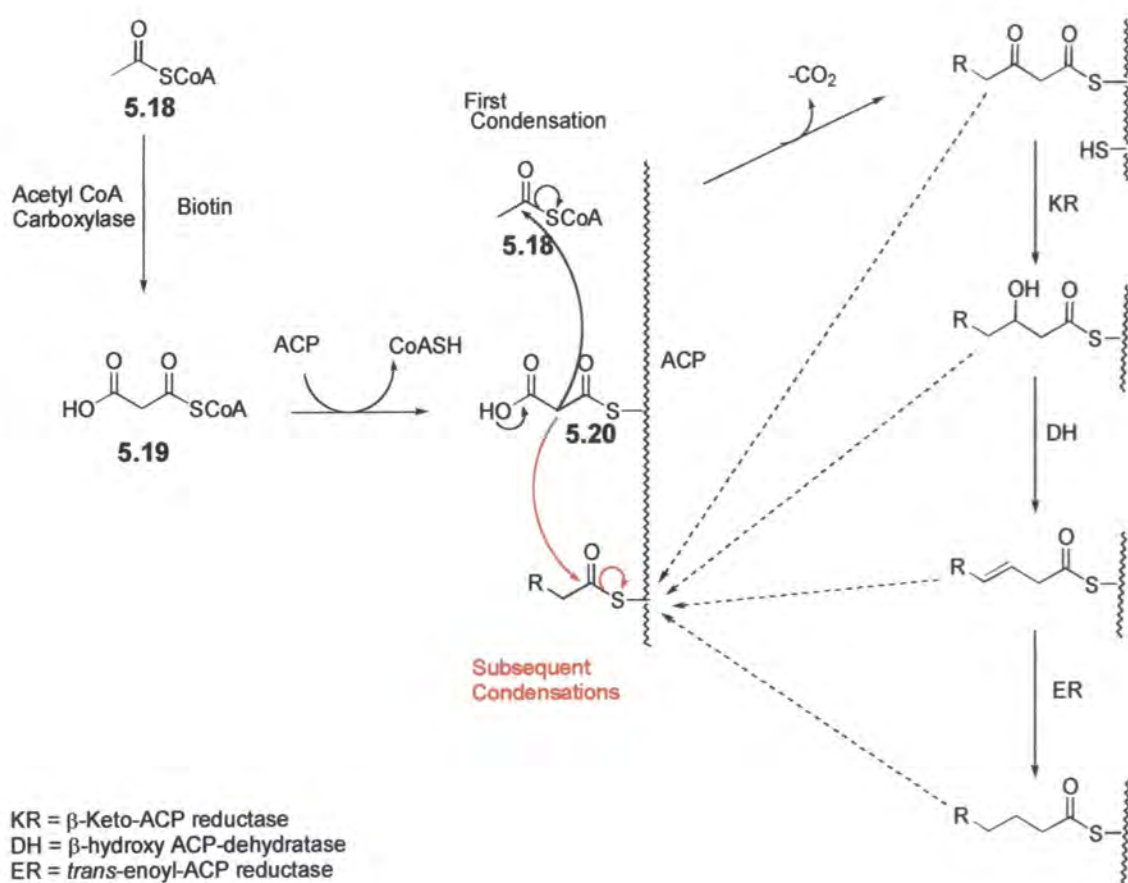
**Scheme 5.3 Fatty acid biosynthesis**

The resultant  $\beta$ -ketobutyryl-ACP (5.21) is then passed from the active site of one enzyme to another undergoing a sequence of enzymatic operations; first by a  $\beta$ -keto-ACP reductase, then by a  $\beta$ -hydroxy-ACP dehydratase and finally by a *trans*-enoyl-ACP reductase. Finally, the acyl moiety of the resulting butyryl-ACP (5.24) is transesterified to a free thiol residue at the active site of the condensing enzyme. It may now re-enter the cycle to condense with another molecule of malonyl-ACP and extend the chain further .

FASs are amongst the most highly sophisticated enzyme complexes identified to date and a wide range of structural diversity exists between the FASs of different organisms. The most primitive examples may be found in bacteria and plants (Type II FAS) where the synthase exists as a collection of dissociated enzymes. A more highly developed family of synthases exist in mammals, which possess almost all of the necessary individual enzymatic activities on two multifunctional proteins (Type I FAS). Typically, in all systems, the fatty acid is synthesised in its entirety without the release of any intermediates. It would appear that in fatty acid assembly there is a high level of commitment for the first few condensation reactions, as chain lengths below  $\text{C}_{14}$  are rare.

## 5.5 Polyketide biosynthesis

Polyketides are constructed in a very similar way to fatty acids. The enzymes mediating the synthesis are not the same but almost certainly evolved by mutation of the genes responsible for the FAS. The main difference between the biosynthesis of polyketides and that of fatty acids is that polyketide chains are “progressively assembled”: that is, the functionality residual in the polyketide chains is introduced as the chain is assembled. For example a carbonyl group is introduced by not performing any of the reductive steps at all, an alcohol by reducing once only, and an alkene generated by missing out the final reduction step (scheme 5.3). A large family of complex polyketides exist whose structural variations depend upon differences in chain length and levels of reduction, mediated entirely by the PKS<sup>3</sup>.

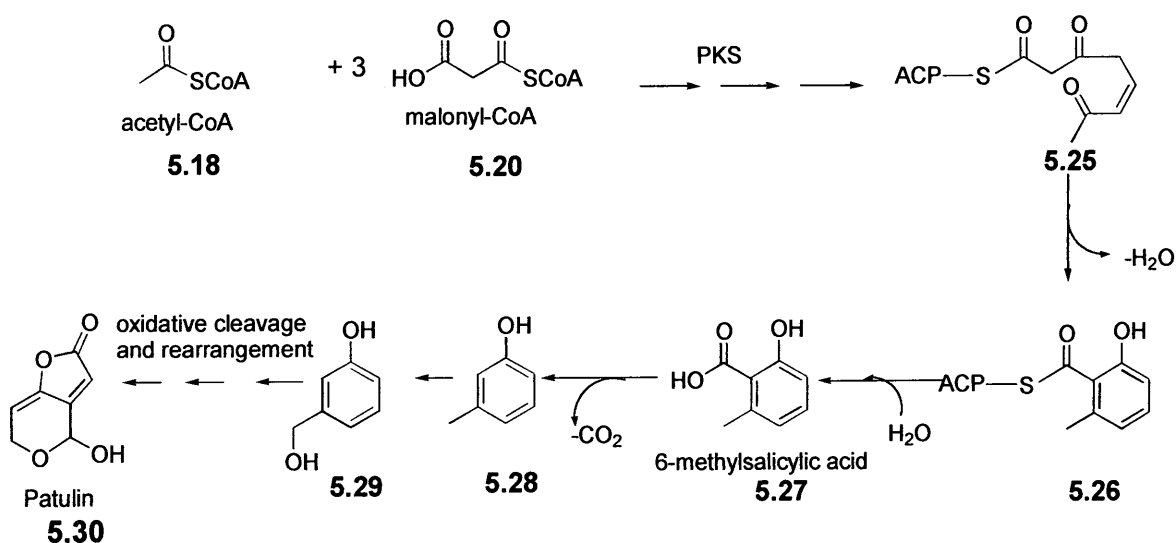


Scheme 5.4 Polyketide biosynthesis

## 5.6 Patulin and its biosynthesis

It is noteworthy that fungal metabolites of the formula  $C_7H_6O_4$  are restricted to aromatic compounds like gentisic acid, gramicin, and quinones such as terreic acid, in addition to the two lactones patulin and isopatulin. Patulin, a hemi-acetal lactone, is produced by *Penicillium* and *Aspergillus* fungi. When first isolated in 1938, from *Penicillium expansum*, the molecule attracted much interest due to its potent antibiotic and antibacterial properties. There are reports of the use of patulin in the treatment of the common cold.<sup>13</sup> Enthusiasm for the use of patulin as a medicine soon dwindled when it was subsequently found to be toxic to mammals. The compound has most recently risen to notoriety as a contaminant in food arising from the fruit used being infected by fungi. Strict quality control procedures are used to screen for trace levels of patulin in products such as apple juice.<sup>14</sup>

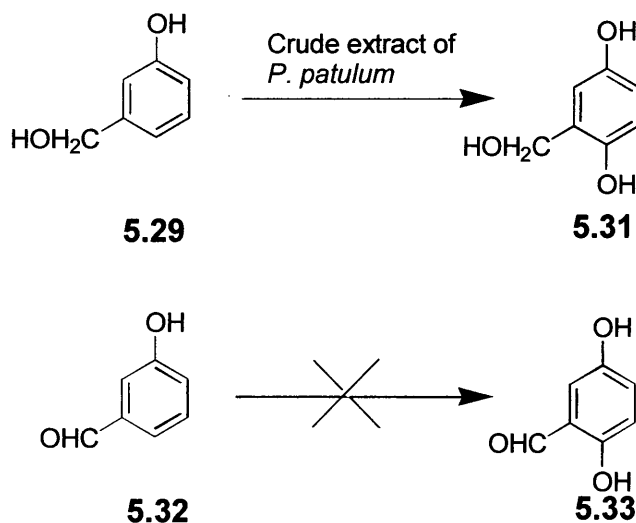
As a consequence of the high levels of interest shown towards patulin, its biosynthesis has been extensively studied. Initial biosynthetic investigations were conducted by Tanenbaum and Bassett who demonstrated its acetogenic origin. They also determined, by the feeding of labelled biosynthetic 6-methylsalicylic acid (6-MSA), that 6-MSA is converted to patulin.<sup>15</sup> Studies by Scott showed the incorporation of deuterated m-cresol.<sup>16</sup> This corroborated the idea that patulin is derived from 6-MSA which is decarboxylated to m-cresol and then oxidatively cleaved.



Scheme 5.5 The biosynthesis of patulin

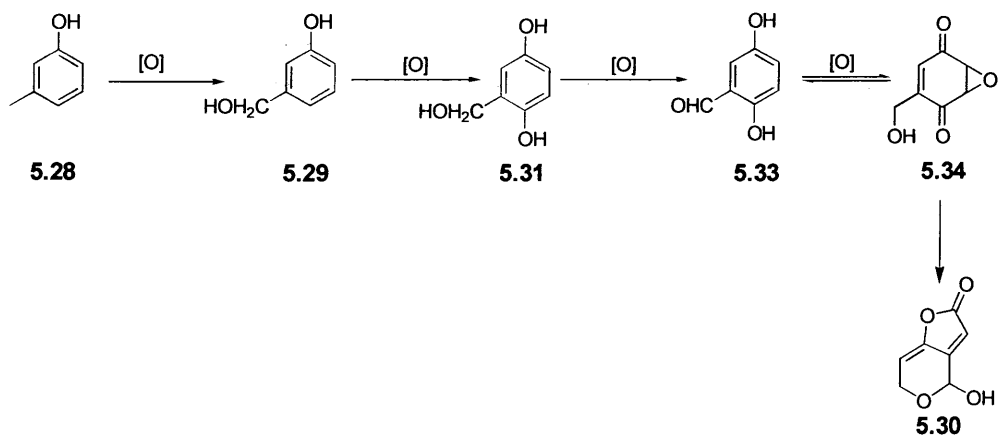


Through experiments using cell free preparations of *P. patulum*, the conversion of *m*-cresol (5.28) to *m*-hydroxybenzyl alcohol (5.29) was shown. This biotransformation required both NADPH and molecular oxygen. The hydroxylase, mediating this transformation, was shown to be inhibited by carbon monoxide, an effect which could be reversed by light at 450 nm. This evidence implicated a mixed function oxidase involving an NADPH dependent reductase and a pigment such as cytochrome P-450.<sup>17</sup> In turn, the conversion of *m*-hydroxybenzyl alcohol (5.29) to gentisyl alcohol (5.31) was demonstrated in a crude enzyme extract of the fungus. This biotransformation also relied upon the presence of molecular oxygen and NADPH. The enzyme was shown to be very substrate specific, and would not ring hydroxylate *m*-hydroxybenzaldehyde (5.32) (Scheme 5.6).<sup>18</sup>



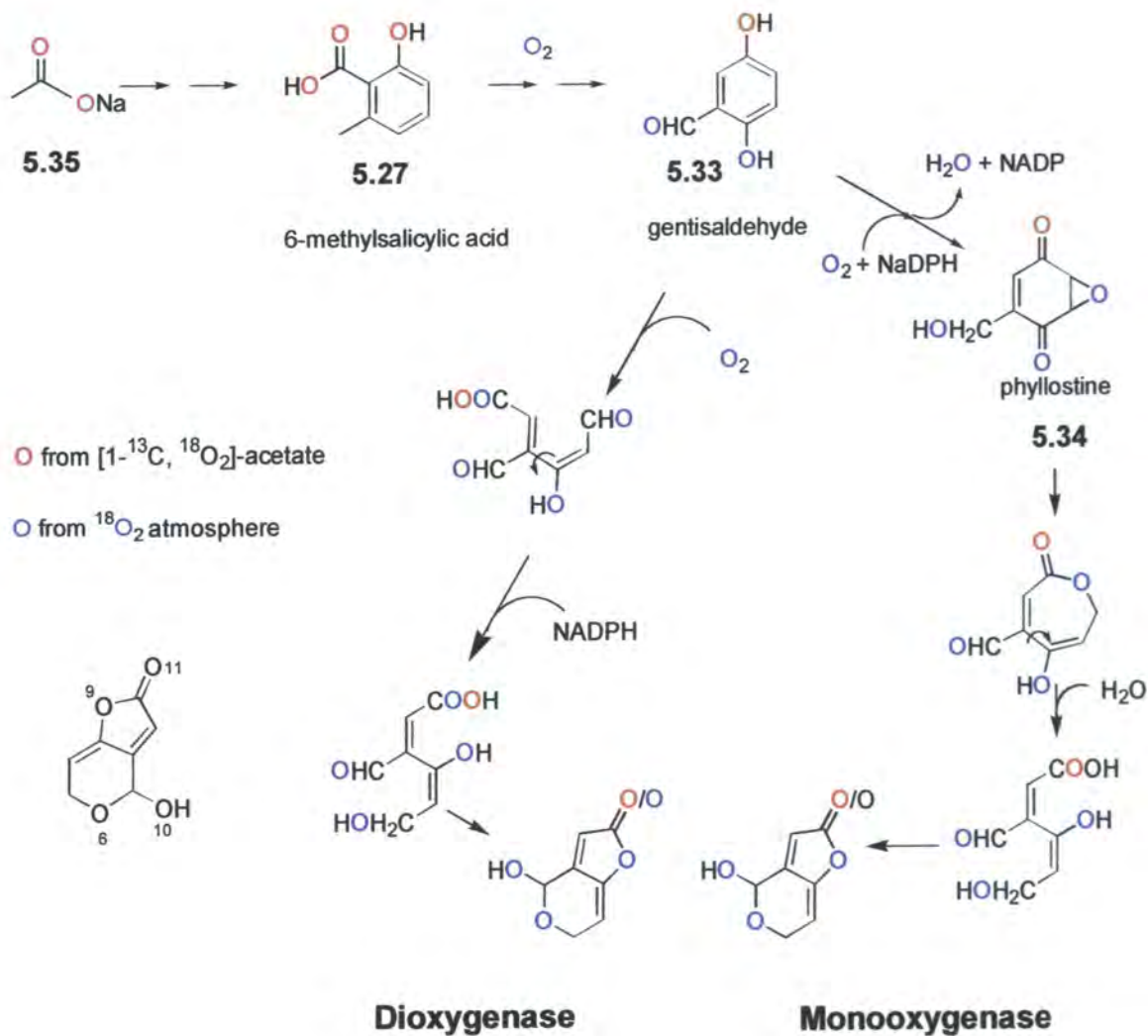
Scheme 5.6 Ring hydroxylation in the biosynthesis of patulin

Another intermediate, phyllostine (5.34), was isolated from *P. patulum* culture medium. Experiments showed that [2-<sup>14</sup>C] acetate and tritiated gentisaldehyde is readily incorporated into phyllostine and that [<sup>14</sup>C] phyllostine is incorporated into patulin.<sup>19</sup> This finding provided some clues as to the nature of the aromatic oxidation and ring cleavage during patulin biosynthesis (Scheme 5.7).



Scheme 5.7 Processing of the aromatic ring in the biosynthesis of patulin

Further investigations were performed to determine how the aromatic ring system is oxidised and then rearranged. Two mechanisms for ring cleavage were postulated: Scott suggested a dioxygenase process<sup>20</sup> whilst Gaucher favoured a monooxygenase route.<sup>18</sup> Sankawa explored this issue by using an  $^{18}\text{O}_2$  atmosphere during feeding experiments with  $[1-^{13}\text{C}]$ -acetate and  $[2-^{13}\text{C}]$ -acetate. By examining the  $^{13}\text{C}$  NMR of the resultant patulin, the incorporation of  $^{18}\text{O}$  was detected, at specific sites, by the upfield isotope shift of  $^{13}\text{C}$  directly bonded to  $^{18}\text{O}$ . Sankawa compared these results to those obtained when  $[1-^{13}\text{C}, ^{18}\text{O}_2]$ -acetate was fed as the only source of label.<sup>21</sup> Were the biosynthesis to proceed *via* the dioxygenase mechanism, growing the fungus under an  $^{18}\text{O}_2$  enriched atmosphere would lead to incorporation of label at each of the four oxygen sites in the resultant patulin. If the mechanism were to proceed *via* the monooxygenase route, there would be  $^{18}\text{O}$  incorporation into all of the oxygen sites except the O-11. (Scheme 5.8).



Scheme 5.8 <sup>18</sup>O<sub>2</sub> Labelling experiments

In the event, the resultant patulin gave rise to <sup>18</sup>O incorporations at O-6, O-9 and O-10: no <sup>18</sup>O was observed at O-11. The cultures that had been fed [1-<sup>13</sup>C, <sup>18</sup>O<sub>2</sub>]-acetate produced patulin with <sup>18</sup>O incorporated at the O-11 position alone. These results were consistent with a monooxygenase mechanism.

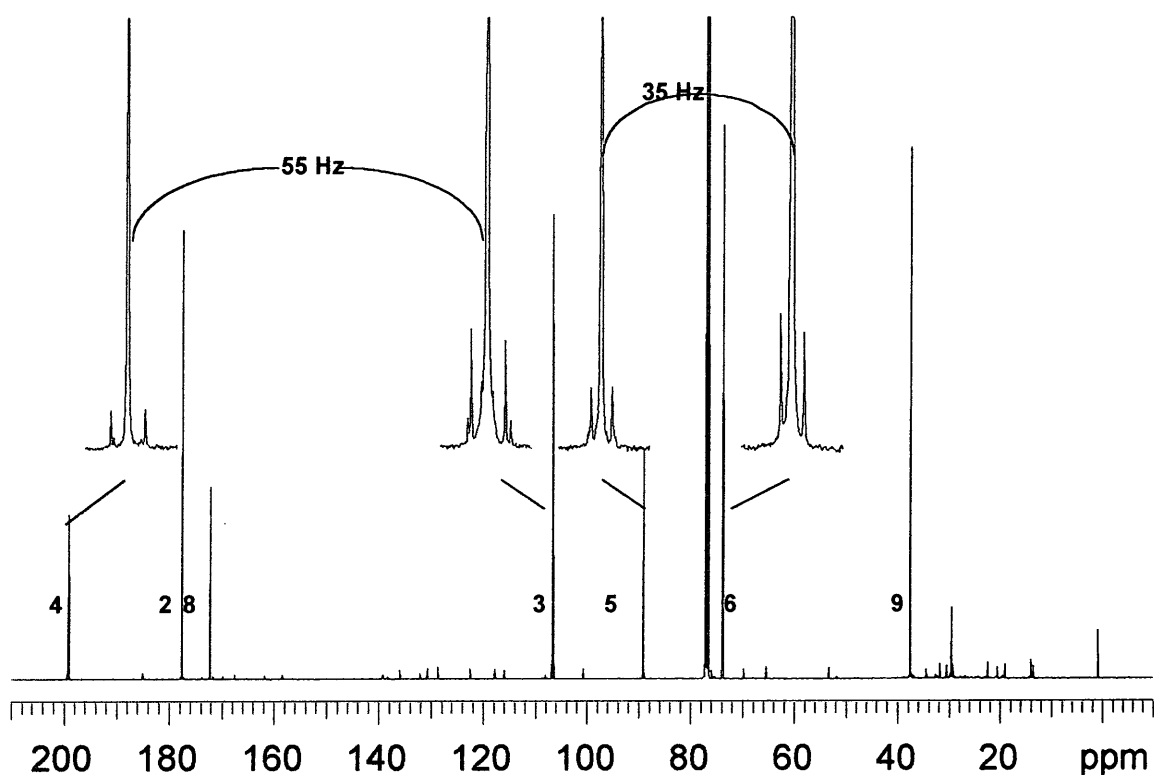
### **5.7 Initial investigations into the biosynthesis of longianone in *X. longiana***

No previous biosynthetic work has been performed on longianone, however longianone is an isomer of patulin and the two molecules share some common structural features. The well known biosynthetic pathway to patulin, through 6-MSA may therefore hold some clues to the biosynthesis of longianone.

An initial investigation into the biosynthesis of longianone was conducted by feeding [1,2-<sup>13</sup>C<sub>2</sub>]-acetate at a final concentration of 7 mM to a four week old culture of *X. longiana*. The culture was grown in a medium of 3 % malt extract (Oxoid) and 6 % glucose and maintained at 28 °C. The cultures were maintained under constant illumination from a low wattage lamp. After a further 4 weeks growth the culture was harvested and the longianone extracted into ethyl acetate and purified by column chromatography.

Analysis of the resulting longianone by <sup>13</sup>C NMR, confirmed an incorporation of [1,2-<sup>13</sup>C<sub>2</sub>]-acetate of 0.035 % (Fig. 5.7). The low incorporation is most probably a result of the high levels of glucose required by the fungal culture to insure production of the longianone.<sup>1</sup> The glucose is processed by glycolysis to acetate and thus the [1,2-<sup>13</sup>C<sub>2</sub>]-acetate administered to the fungus, is much diluted by the endogenous acetate pool.

Fig. 5.7  $^{13}\text{C}$  NMR of [1,2- $^{13}\text{C}_2$ ]-acetate fed longianone



Carbon	Coupling constant /Hz
2	
3	55
4	56
5	35
6	34
8	

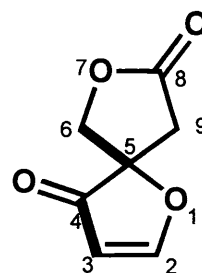
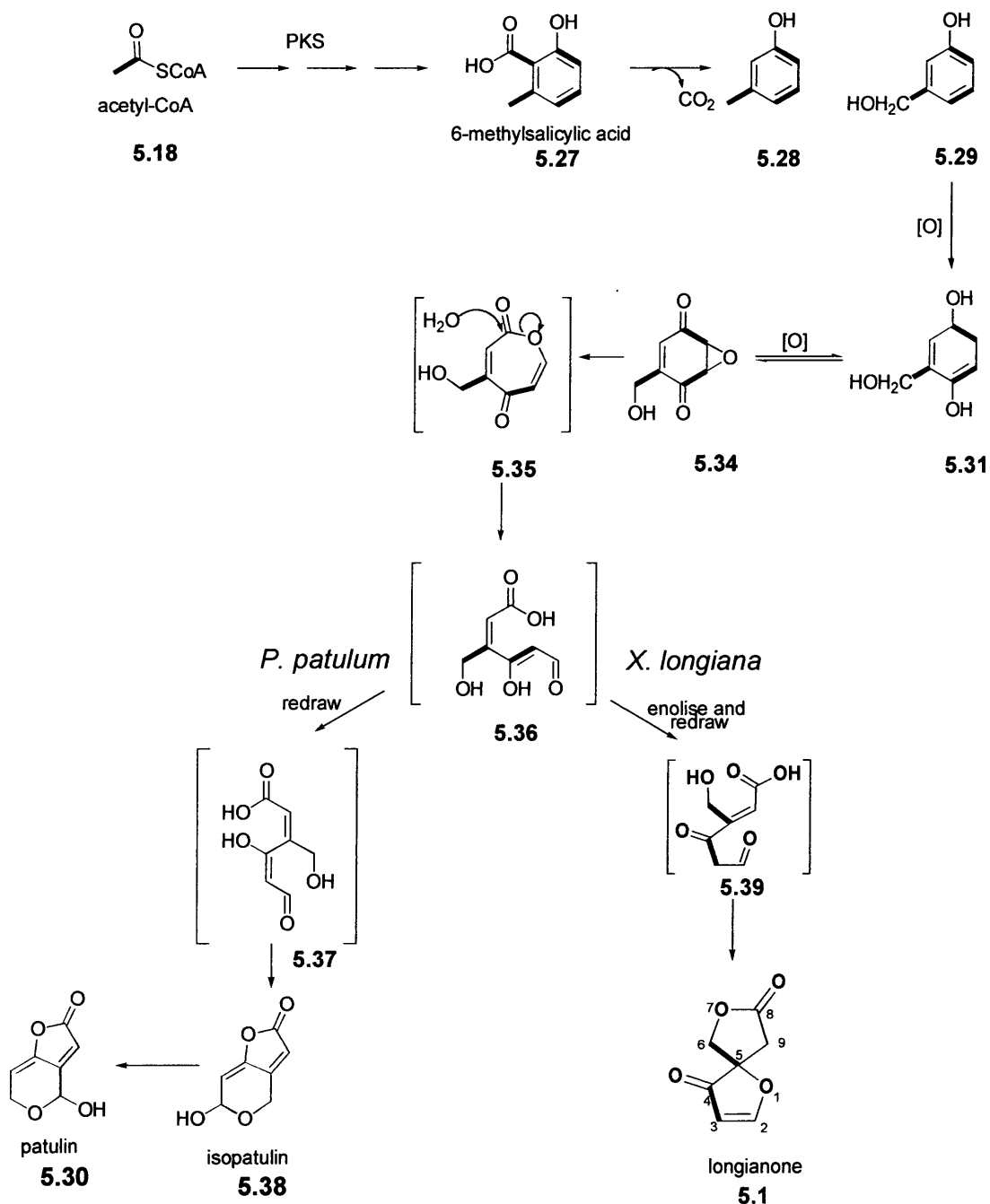


Table 5.1 Incorporation of [1,2- $^{13}\text{C}_2$ ]-acetate into longianone

Intact incorporation of [1,2- $^{13}\text{C}_2$ ]-acetate was observed at the C3/C4 and C5/C6 positions, due to the reciprocal couplings between the  $^{13}\text{C}$  nuclei.

This result indicates longianone to be acetogenic in its origin. Incorporations into C1, 2, 8 and 9 could not be detected, presumably, as these carbons had become divorced from their original  $^{13}\text{C}$  partners in the acetate, no coupling is apparent. The level of incorporation is too low to detect the presence of a single  $^{13}\text{C}$  on top of the natural abundance peak (1.11%). The labelling pattern is consistent with a biosynthesis similar to that of patulin derived from 6-MSA (Scheme 5.9).

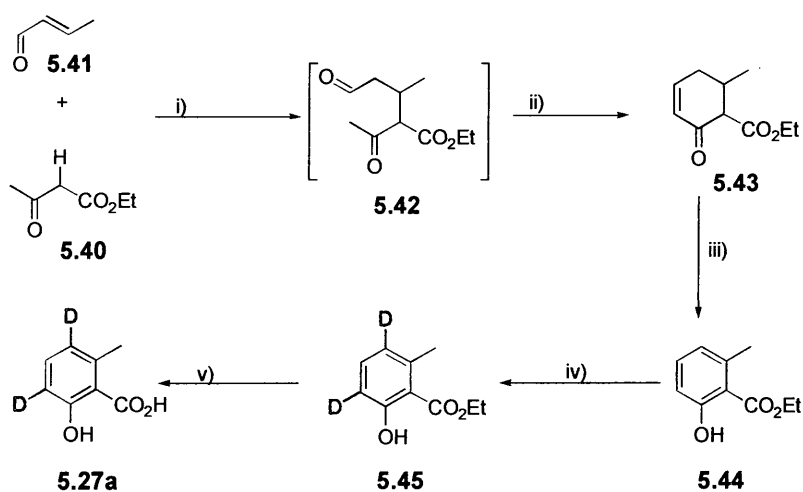


Scheme 5.9 A hypothetical biosynthesis of longianone which accounts for the observed labelling pattern following the feeding of [1,2- $^{13}\text{C}_2$ ]-acetate

To further investigate the biosynthesis of longianone and its relationship to patulin, a series of known intermediates on the patulin pathway were synthesised carrying an isotopic label. Deuterium was selected as the isotope of choice as it can be readily exchanged into aromatic ring systems and is relatively inexpensive. Deuterium also has the advantage of a lower natural abundance ( $1.5 \times 10^{-2} \%$ ), than  $^{13}\text{C}$  (1.11 %) and therefore low levels of incorporation may be more easily observed by using  $^2\text{H}$  NMR analysis. The isotopically labelled intermediates synthesised were [3,5- $^2\text{H}_2$ ]-6-methylsalicylic acid, [2,4,6- $^2\text{H}_3$ ]*m*-cresol, [7,7- $^2\text{H}_2$ ]*m*-hydroxybenzylalcohol and [2,4,6,7,7- $^2\text{H}_5$ ] *m*-hydroxybenzylalcohol.

### 5.8 Synthesis of [3,5- $^2\text{H}_2$ ]-6-methylsalicylic acid

Ethyl 2-hydroxy-6-methylbenzoate (**5.44**) was synthesised *via* a route previously described by Hauser *et al.*<sup>22</sup> The sodium salt of ethyl acetoacetate (**5.40**) was generated after treatment with sodium ethoxide, and was used as a nucleophile for a Michael type addition with crotonaldehyde (**5.41**) This generated the keto-aldehyde intermediate (**5.42**). Without isolation of the product, dry HCl gas was bubbled through the mixture to promote an aldol condensation to form ethyl 5-methyl-3-oxocyclohexene-4-carboxylate (**5.43**). The progress of the cyclisation was monitored by the diminution of the large singlet corresponding to the acetyl group in the  $^1\text{H}$  NMR spectrum. On occasion that the reaction had not proceeded to completion, further HCl was introduced.



i) EtOH, Na, ii) HCl, iii) Br<sub>2</sub>, AcOH, iv) DCl, D<sub>2</sub>O, MeOD, v) KOH MeOH.

Scheme 5.10 The synthesis of [3,5- $^2\text{H}_2$ ]-6-methylsalicylic acid

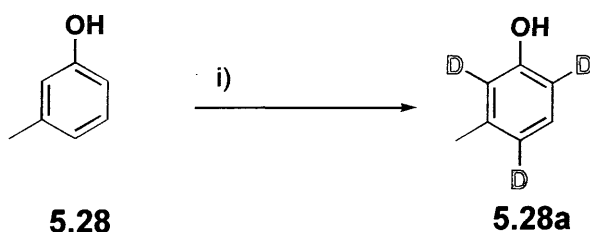
Following distillation, the resultant ethyl 5-methyl-3-oxocyclohexene-4-carboxylate (**5.43**) was treated with a mixture of bromine and acetic acid, a method first described by Lacey.<sup>23</sup> The resultant ethyl 2-hydroxy-6-methylbenzoate (**5.44**) was purified by steam distillation.

Various methods of preparing [3,5-<sup>2</sup>H<sub>2</sub>]-6-methylsalicylic acid (**5.27a**) from the white crystalline ester were investigated. It was anticipated that ring deuteration and ester hydrolysis of the ethyl 2-hydroxy-6-methylbenzoate (**5.44**) could be achieved in one step by refluxing the ester in DCl/D<sub>2</sub>O. Unfortunately, following the experiment, the <sup>1</sup>H NMR indicated that although deuterium had been exchanged into the aromatic ring, there was no evidence that any hydrolysis of the ester had occurred. The ester is fairly sterically hindered, positioned on the aromatic ring between a methyl and a hydroxyl moiety, and it is possible that steric constraints that disfavour acid hydrolysis. In an alternative experiment the material was refluxed in a solution of NaOD and D<sub>2</sub>O. Abstrusely, under these conditions, there was no exchange of deuterium into the ring but the ester was readily hydrolysed. This offered a way forward.

6-Methylsalicylic acid, acquired by the hydrolysis of ethyl 2-hydroxy-6-methylbenzoate under alkaline conditions, was refluxed in D<sub>2</sub>O and DCl. In this case, although deuterium was exchanged into the ring, the material readily decarboxylated, under the acidic conditions generating *m*-cresol. Finally, it proved that deutering the ester in acidic media followed by hydrolysis in a basic solution was the most effective method of preparing [3,5-<sup>2</sup>H<sub>2</sub>]-6-methylsalicylic acid. The resultant 6 MSA was found to be 45 % monodeuterated, 21 % dideuterated and 5 % trideuterated, by mass spectral analysis. Proton NMR showed the material to be almost completely deuterated at positions 3 and 5, and only slightly deuterated at position 4.



### 5.9 Synthesis of [2,4,6-<sup>2</sup>H<sub>3</sub>]m-cresol

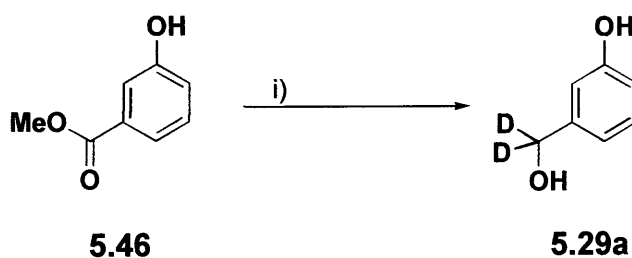


i) D<sub>2</sub>O, PBr<sub>3</sub>

Scheme 5.11 Synthesis of [2,4,6-<sup>2</sup>H<sub>3</sub>]m-cresol

[2,4,6-<sup>2</sup>H<sub>3</sub>]m-Cresol (**5.39**) was prepared following the method of Ojanpera *et al.*<sup>24</sup> The synthesis involved the addition of phosphorous tribromide to deuterium oxide to generate DBr *in situ*. m-Cresol (**5.28**) was added and the mixture refluxed. <sup>2</sup>H NMR and mass spectrometry confirmed the product to be almost entirely deuterated at positions 2,4 and 6.

### 5.10 Synthesis of [7,7-<sup>2</sup>H<sub>2</sub>]m-hydroxybenzyl alcohol



i) LiAlD<sub>4</sub>

Scheme 5.12 Synthesis of [7,7-<sup>2</sup>H<sub>2</sub>]m-hydroxybenzyl alcohol

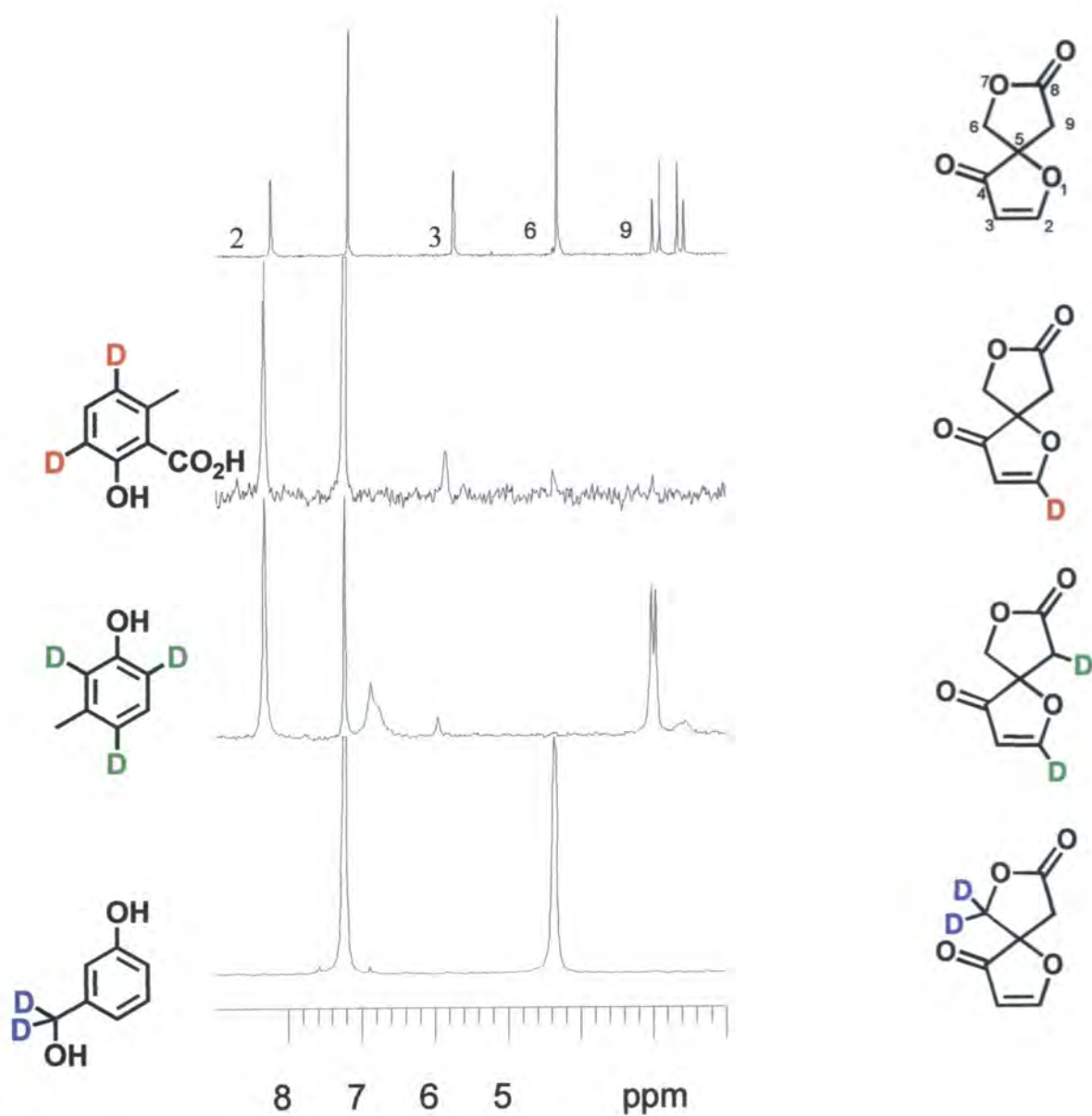
[7,7-<sup>2</sup>H]m-Hydroxybenzyl alcohol (**5.29a**) was prepared by the lithium aluminium deuteride reduction of methyl m-hydroxybenzoate (**5.46**). <sup>1</sup>H NMR and mass spectrometry confirmed that the methylene group was almost entirely dideuterated.

### 5.11 Feeding experiments with [3,5-<sup>2</sup>H<sub>2</sub>]- 6-methylsalicylic acid, [2,4,6-<sup>2</sup>H<sub>3</sub>]m-cresol and [7,7-<sup>2</sup>H<sub>2</sub>]m-hydroxybenzyl alcohol

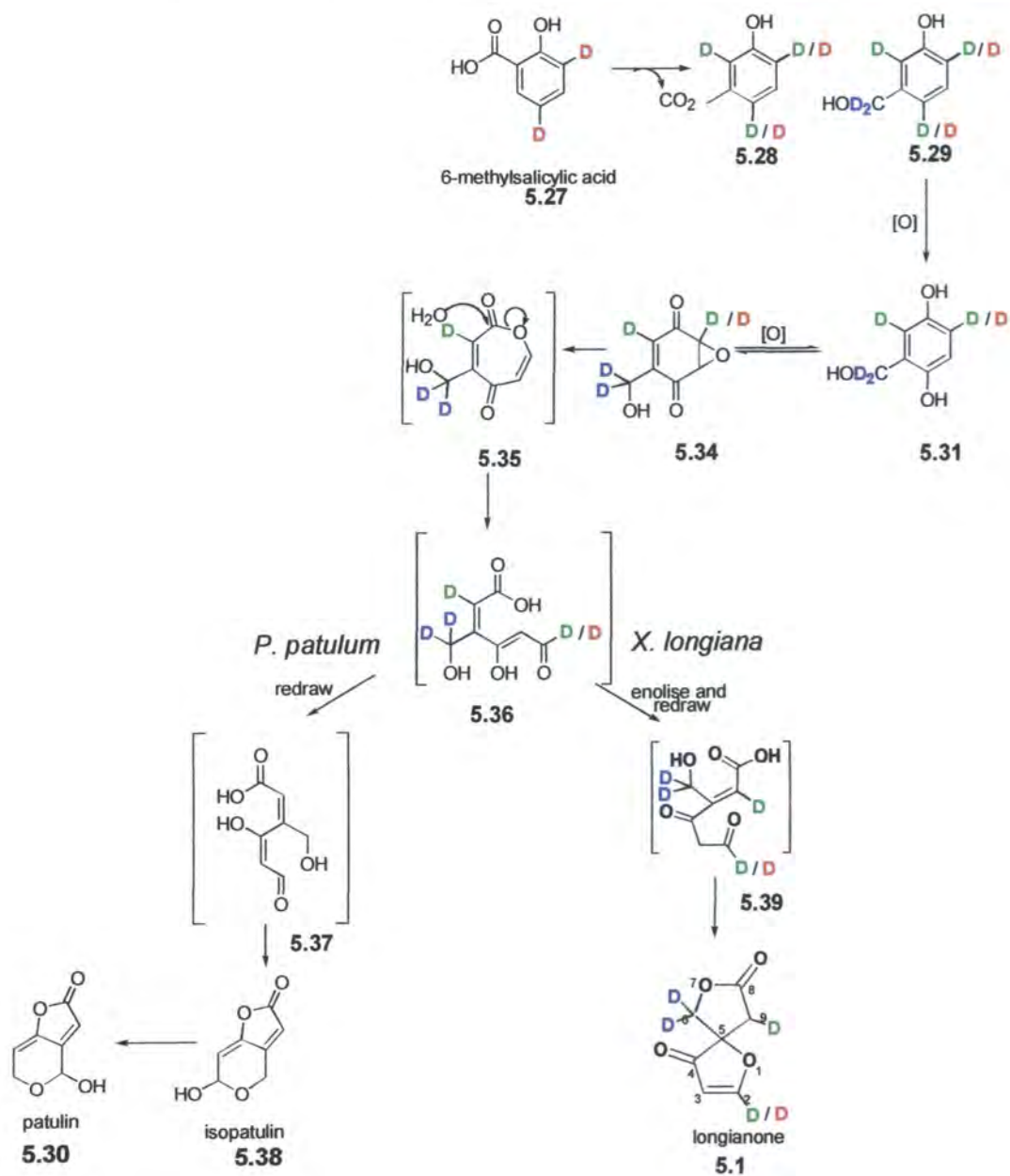
In separate experiments, four week old cultures of *X. longiana* were supplemented with [3,5-<sup>2</sup>H<sub>2</sub>]- 6-methylsalicylic acid (**5.27a**), [2,4,6-<sup>2</sup>H<sub>3</sub>]m-cresol (**5.28a**) and [7,7-

$^2\text{H}_2$ ] *m*-hydroxybenzyl alcohol (**5.29a**) each to a final concentration of 7 mM over a period of 3 days. The longianone produced from each experiment was purified over silica with and the resultant material was subjected to  $^2\text{H}$  NMR analysis. In each case deuterium incorporation into the longianone could be observed indicating that the three compounds are all true intermediates on the biosynthetic pathway to longianone.

**Fig 5.8**  $^2\text{H}$  NMR Results from the feeding of the labelled aromatics



Additionally, the labelling patterns in the resultant longianone, from the three intermediates, is consistent with a close biosynthetic relationship to patulin.

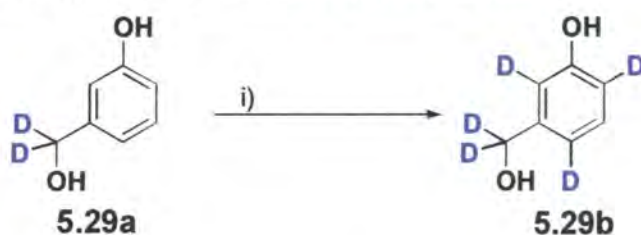


Scheme 5.13 Biosynthetic pathway to longianone accounting for the observed labelling patterns

In the experiments with  $[7,7-^2\text{H}_2]m$ -hydroxybenzylalcohol it proved impossible to determine if both deuteria had become incorporated, as the C-6 diastereotopic deuteria are not resolved by  $^2\text{H-NMR}$ . It was not possible to solve this problem by mass

spectral analysis as a consistent fragmentation pattern for unlabelled longianone could not be obtained by either electronic or chemical methods of ionisation. It was therefore necessary to find an alternative method to determine whether one or both of the deuteria were incorporated. The solution to this problem was to feed *m*-hydroxybenzyl alcohol that was dideuterated at the methylene position and also in the ring. The deuterons in the resultant longianone arising from positions in the aromatic ring could thus be used as an internal calibration and their signals in the  $^2\text{H}$  NMR spectrum integrated against those arising from the methylene group.

### 5.12 Synthesis of [2,4,6,7,7- $^2\text{H}_5$ ]*m*-hydroxybenzyl alcohol



i)  $\text{D}_2\text{SO}_4$ ,  $\text{D}_2\text{O}$  carius tube  $120^\circ\text{C}$ , 150 atmos, for 3 hours

Scheme 5.14 Synthesis of [2,4,6,7,7- $^2\text{H}_5$ ]*m*-hydroxybenzyl alcohol

Attempts to synthesise [2,4,6,7,7- $^2\text{H}_5$ ]*m*-hydroxybenzyl alcohol (**5.29b**) by first exchanging deuterium into the aromatic ring of methyl *m*-hydroxybenzoate (**5.46**) and then reducing the ester with lithium aluminium deuteride failed. Although hydrolysis to the acid occurred, no exchange of deuterium into the electron deficient ring of the aromatic ester could be observed by  $^1\text{H}$  NMR after the material had been refluxed under either acidic or basic conditions.

Deuterium exchange into the ring of *m*-hydroxybenzyl alcohol was witnessed in the  $^1\text{H}$  NMR. This exchange could be optimised by increasing the pressure at which the reaction was performed.

Accordingly [2,4,6,7,7- $^2\text{H}_5$ ]*m*-hydroxybenzyl alcohol (**5.29b**) was afforded by heating [7,7- $^2\text{H}_2$ ]*m*-hydroxybenzyl alcohol (**5.29a**) in a weak solution of  $\text{D}_2\text{SO}_4$  with  $\text{D}_2\text{O}$ , in a Carius tube, to  $120^\circ\text{C}$  with a theoretical maximum pressure of 150 atmos. The resultant material was shown to be 75 % deuterated at positions 2,4 and 6 of the ring. This proved acceptable for the required feeding experiment.

### 5.13 Feeding experiment with [2,4,6,7,7-<sup>2</sup>H<sub>5</sub>]m-hydroxybenzyl alcohol

A four week old culture of *X. longiana* was supplemented with [2,4,6,7,7-<sup>2</sup>H<sub>5</sub>]m-hydroxybenzyl alcohol (5.29b) to a final concentration of 7 mM, over a period of 3 days. The longianone isolated from this experiment was purified and then analysed by <sup>2</sup>H NMR.

The resultant <sup>2</sup>H NMR showed three clear enrichments at C-2, C-6 and C-9 with similar intensities. As the intensities are similar it is clear that only one deuterium atom from the hydroxymethyl group had become incorporated into the C-6 methylene group of longianone.

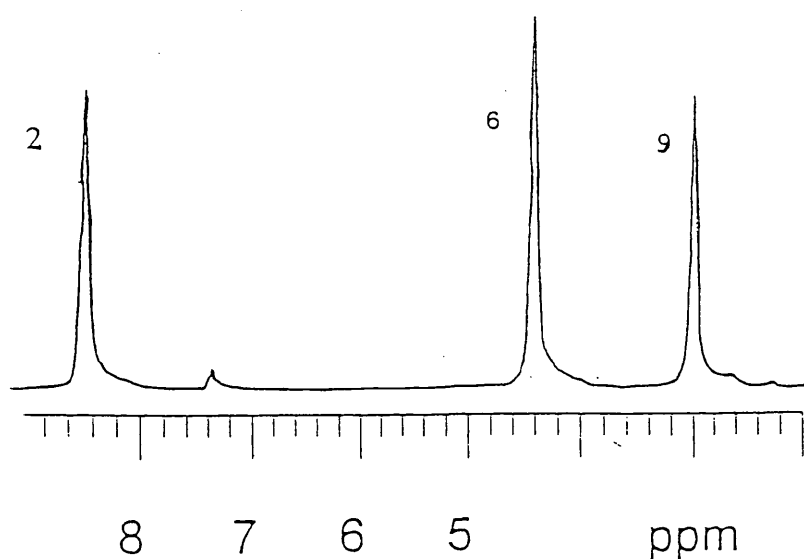


Fig 5.9 <sup>2</sup>H NMR After feeding [2,4,6,7,7-<sup>2</sup>H]m-hydroxybenzyl alcohol

Clearly, if both deuterons had become incorporated into the methylene group, the signal at 4.4 ppm would have had twice the intensity. It follows that the hydroxymethyl group must be oxidised to an aldehyde at some stage during the biosynthesis.

### 5.14 Levels of incorporation of the deuterated intermediates

$$\text{Specific incorporation} = \frac{\text{no. moles of deuterated metabolite produced}}{\text{no. moles of deuterated precursor fed}}$$

Eqn. 5.1

Deuterated Precursor	Specific Incorporation (%)
[1,2- <sup>13</sup> C]-acetate	0.34
[3,5- <sup>2</sup> H]- 6-methylsalicylic acid	0.08
[2,4,6- <sup>2</sup> H]- <i>m</i> -cresol	0.45
[7,7- <sup>2</sup> H]- <i>m</i> - hydroxybenzyl alcohol	5.62

Table 5.2 Incorporation levels of the deuterated intermediates

### 5.15 Discussion

Through the feeding of appropriate isotopically labelled compounds it has been shown that the biosynthesis of longianone is acetogenic and proceeds through the intermediates 6-MSA, *m*-cresol and *m*-hydroxybenzyl alcohol. These compounds are known intermediates on the biosynthetic pathway to patulin (5.30), an isomer of longianone (5.1). It is apparent that the two compounds share a very similar biosynthesis which diverges at a late stage. In the case of both patulin and longianone the biosynthesis starts with the polyketide assembly of 6-MSA which then undergoes considerable oxidation and eventual cleavage to afford intermediate 5.36. The manner in which intermediate 5.36 cyclises determines whether patulin or longianone is formed as the final product.

In biological screening longianone has shown only moderate cytotoxic activity in contrast to patulin. It is possible that longianone is the result of an evolutionary "mistake" by a related organism which may once have synthesised the fungal toxin.

The extremely high levels of production of the metabolite (100 mg in 100 ml of culture medium) lead one to feel that the fungus must benefit in some way from the production of this highly functionalised, intriguing molecule.

## References

- 1 R. L. Edwards, D. J. Maitland, C. L. Oliver, M. S. Pacey, L. Shields and A. J. Whalley, *J. Chem. Soc., Perkin Trans. 1*, 1999, 715.
- 2 A. San-Martin, J. Rovirosa, O. Munoz, M. H.M. Chen, R. D. Guneratne and J. Clardy, *Tetrahedron Lett.*, 1983, **24**, 4063.
- 3 A. San-Martin, J. Rovirosa, C. Xu, H. S. M. Lu and J. Clardy, *Tetrahedron Lett.*, 1987, **28**, 6013.
- 4 P. Bloch, C. Tamm, P. Bollinger, T. J. Petcher and H. P. Weber, *Helv. Chim. Acta*, 1981, **59**, 133.
- 5 P. Bloch and J. C. Tamm, *Helv. Chim. Acta*, 1981, **64**, 304.
- 6 W. Breitenstein, K. K. Chexal, P. Mohr and C. Tamm, *Helv. Chim. Acta*, 1981, **64**, 379.
- 7 M. Dolder, X. Chao and C. Tamm, *Helv. Chim. Acta*, 1990, **73**, 63.
- 8 M. Tada, M. Nagai, C. Okumura, J. Osano and T. Matsuzaki, *Chem. Lett.*, 1989, 683.
- 9 S. L. Midland, N. T. Keen and J.J. Sims, *J. Org. Chem.*, 1995, **60**, 1118.
- 10 S. L. Midland, N. T. Keen, J.J. Sims, M. M. Midland, M. M. Stayton, M. J. Smith, E. P. Mazzola, K. J. Graham and J. Clardy, *J. Org. Chem.*, 1993, **58**, 2940.
- 11 J. P. Henschke, and R. W. Rickards, *Tetrahedron Lett.*, 1996, **37**, 3557.
- 12 R. B. Herbert, *The Biosynthesis of Secondary Metabolites*, 1989, 2<sup>nd</sup> Ed., Chapman and Hall, London and New York.
- 13 J. H. Birkinshaw, A. Bracken, S. E. Mitchell and H. Raistrick, *The Lancet*, 1943, 625.
- 14 P. M. Scott, and B. P. C. Kennedy, *J. Ass. Off. Anal. Chem.*, 1973, **56**, 813.
- 15 S. W. Tanenbaum and E.W. Bassett, *J. Biol. Chem.*, 1959, **234**, 1861.
- 16 A. I. Scott and M. Yalpani, *J. Chem Soc., Chem. Comm.*, 1967, 945.
- 17 G. Murphy, G. Vogel, G. Krippahl and F. Lynen, *Eur. J. Biochem.* 1974, **49**, 443.
- 18 G. Murphy, F. Lynen, *Eur. J. Biochem.* 1975, **58**, 467.
- 19 J. Sekiguchi and G. M. Gaucher, *Biochemistry*, 1978, **17**, 1785.

- 20 A. I. Scott and L. Beadling, *Bioorg. Chem.*, 1974, **3**, 281.
- 21 H. Iijima, H. Noguchi, Y. Ebizuka, U. Sankawa, H. Seto, *Chem. Pharm. Bull.*, 1983, **31**, 362.
- 22 F. M. Hauser, S. A. Pogany, *Synthesis*, 1980, 814.
- 23 R. N. Lacey, *J. Chem. Soc.*, 1960, 1625.
- 24 K. Wahala, I. Ojanpera, L. Hayri, T. A. Hase, *Synth. Commun.*, 1987, **17**, 137.



## **CHAPTER 6**

### **Experimental**

## **CHAPTER 6**

### **Experimental**

#### **6.1 Chemical Synthesis**

##### **6.1.1 General**

NMR spectra were recorded on Varian Mercury 200 MHz ( $^1\text{H}$  at 199.992 MHz,  $^{13}\text{C}$  at 50.30 MHz), Varian Unity 300 MHz ( $^1\text{H}$  at 299.908 MHz,  $^{13}\text{C}$  at 75.450 MHz) or Unity Inova 500 MHz ( $^1\text{H}$  at 499.779 MHz,  $^{13}\text{C}$  at 125.669 MHz) machines. Samples were run in deuteriochloroform, unless stated otherwise, with chemical shifts reported in parts per million quoted relative to  $\text{CDCl}_3$  at  $\delta_{\text{H}} = 7.27$ ,  $\delta_{\text{C}} = 77.0$ . The deuterated solvent was used as a lock. Coupling constants are reported in hertz.

Melting points were measured on a Gallenkamp variable heater and are uncorrected.

Infra red spectra were recorded with absorption values in  $\text{cm}^{-1}$  using a Perkin Elmer fitted with a golden gate attachment.

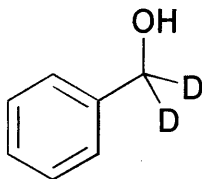
Mass spectral analysis was performed using electron ionisation on a Micromass Autospec, Electrospray Fisons Platform mass spectrometer equipped with a H.P.1 capillary column (25 m long, 0.22 mm i.d., 0.2  $\mu\text{m}$  film thickness) connected to a H.P. 5890 series II oven, unless stated otherwise.

Reaction glassware was dried in an oven at 120 °C and cooled in a dry atmosphere of nitrogen. The solvents used in reactions were dried and distilled prior to use: tetrahydrofuran (THF) and diethyl ether (sodium, benzophenone, under nitrogen), ethyl acetate (calcium chloride, under nitrogen), dichloromethane and diisopropylamine (calcium hydride). Petroleum ether refers to the 40-60°C boiling fraction. Non-aqueous reactions were carried out under an atmosphere of dry nitrogen unless otherwise stated.

Thin layer chromatography was carried out on Merck, Kieselgel 60,  $F_{254}$  glass backed plates. Flash chromatography was carried out using Fluka silica gel-60 (35-70 mm).

### **6.1.2 Preparation of (S)-hexyl-[<sup>2</sup>H]-fluoroacetate (2.17a)**

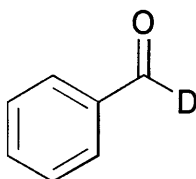
#### **[7,7-<sup>2</sup>H<sub>2</sub>]-Benzyl alcohol (2.19)**



**2.19**

To a stirred solution of lithium aluminium deuteride (1.41 g, 33.67 mmol) in THF (80 ml), cooled to 0 °C, was added ethyl benzoate (6.92 g, 46.16 mmol) dissolved in THF (25 ml). The mixture was heated under reflux for 2 h then cooled once more to 0 °C before quenching the reaction using Micovic and Mihailovic's basic work up procedure.<sup>1</sup> The mixture was filtered and the insoluble material washed with diethyl ether (60 ml). The solvent was evaporated under reduced pressure to yield [7,7-<sup>2</sup>H<sub>2</sub>]-benzyl alcohol (4.90 g, 97 %) as a clear, colourless oil. *v max* (neat): 3307, 3027, 2975, 1495; *m/z* (EI+) 110 (M<sup>+</sup>, 100 %), 109 (56 %);  $\delta_{\text{H}}$  (CDCl<sub>3</sub>): 7.4 (6H, m, Ar-H).  $\delta_{\text{C}}$  (CDCl<sub>3</sub>): 64.2 (pentet, J 23, CD<sub>2</sub>OH), 127, 128, 129 (C-Ar).

#### **[7-<sup>2</sup>H]-Benzaldehyde (2.20)**

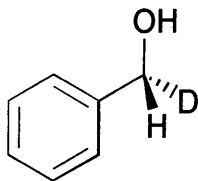


**2.20**

[7,7-<sup>2</sup>H<sub>2</sub>]-Benzyl alcohol (4.75 g, 43.19 mmol) was added to a vigorously stirred mixture of pyridinium chlorochromate (PCC) (16.01 g, 74.27 mmol) and 3 Å ground molecular sieves (75 g) in dichloromethane (DCM) (100 ml). The progress of the reaction was followed by thin layer chromatography (TLC) (DCM, silica plates). After 4 h, the mixture was filtered through a plug of silica and the residue washed with DCM (100 ml). The DCM was evaporated and the remaining material distilled (atmospheric pressure, 178 °C) to yield [7-<sup>2</sup>H]-benzaldehyde (3.67 g, 77 %) as a clear colourless, almond scented liquid. *v max* (neat): 3061, 2108, 1679, 1596, 1583; *m/z* (EI+) 108 (M<sup>+</sup>+1, 5 %),

107 (62 %);  $\delta_{\text{H}}$  ( $\text{CDCl}_3$ ): 7.6 (6H, m, Ph-H).  $\delta_{\text{C}}$  ( $\text{CDCl}_3$ ): 129.1, 129.8, 134.6 (C-Ph), 192.1 (t, J 27, CDO) .

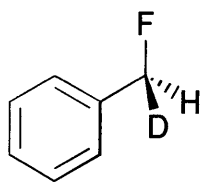
**(R)-[7- $^2\text{H}$ ]-Benzyl alcohol (2.21)<sup>2</sup>**



**2.21**

(1S)-(-)- $\alpha$ -Pinene (3.7 ml, 23.5 mmol) was added to a solution of 9-borabicyclo[3.3.1]nonane (9-BBN) in THF (0.5 M, 43.8 ml, 21.9 mmol), stirred. The mixture was gently heated under reflux for 2 h then cooled to room temperature before the addition of [7- $^2\text{H}$ ]-benzaldehyde (1.81 g, 17.57 mmol). The mixture was, once again, heated under reflux for 2 h, cooled to room temperature, quenched with acetaldehyde (2 ml, 36 mmol) and stirred for 10 minutes. The THF was removed under reduced pressure and the residual material heated to 65 °C under a vacuum of 0.01 mbar for 3 h to remove the  $\alpha$ -pinene. Diethyl ether (20 ml) was added to the resultant viscous oil and the mixture stirred until the oil dissolved. 8-Hydroxyquinoline (3.20 g, 22.05 mmol) in diethyl ether (30 ml) was added to the mixture producing a vibrant yellow/green precipitate, the precipitate was filtered and washed with diethyl ether, the diethyl ether removed under reduced pressure and the resultant material distilled using a Kugelrohr apparatus. The crude material obtained from this distillation was further purified by distillation using a vigreux column to yield (R)-[7- $^2\text{H}$ ]-benzyl alcohol (1.33 g, 69 %) as a clear colourless oil. B.p. 205 °C,  $V_{\text{max}}$  (neat): 3316, 3019, 2960, 1495;  $m/z$  (EI+) 110 ( $\text{M}^{\dagger}+1$ , 5 %), 109 (49 %), 108 (99 %), 80 (84 %), 79 (60 %), 78 (55 %), 77 (81 %), 51 (100 %).  $\delta_{\text{H}}$  ( $\text{CDCl}_3$ ): 4.6 (1H, s, CDHOH), 7.3 (6H, m, Ph-H).  $\delta_{\text{C}}$  ( $\text{CDCl}_3$ ): 64.8 (t,  $J_{\text{CD}}$  22, CDHOH), 127.1, 127.7, 128.6 (C-Ph).

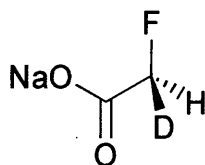
**(S)-[7-<sup>2</sup>H]-Benzyl fluoride (2.22)<sup>3</sup>**



**2.22**

(*R*)-[7-<sup>2</sup>H]-Benzyl alcohol (0.49 g, 4.5 mmol) was added to a stirred solution of diethylaminosulphur trifluoride (DAST) (0.7 ml, 5.8 mmol) in DCM (40 ml) cooled to -78 °C. The reaction was stirred at room temperature for 10 h then heated under reflux for 30 minutes to ensure completion of the reaction. Water (50 ml) was added to quench the reaction and the organic phase washed with water (3 x 30 ml). The organic phase was dried over magnesium sulphate, filtered and most of the DCM removed under reduced pressure, with caution taken not to allow the temperature to exceed 20 °C so as to minimise evaporation of the benzyl fluoride. The benzyl fluoride was not further purified.  $\delta_F$  (CDCl<sub>3</sub>): -207.2 (1F, d.t,  $J_{HF}$  48,  $J_{DF}$  7, CDHF)  $\delta_H$  (CDCl<sub>3</sub>): 5.4 (1H, d,  $J_{HF}$  48, CDHF) 7.4 (6H, s, Ph-H).  $\delta_C$  (CDCl<sub>3</sub>): 8.4 (dt,  $J_{FC}$  165,  $J_{DC}$  23 CDF), 127.8, 128.9, 129.0 (C-Ph)

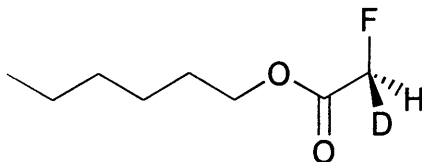
**(S)-[<sup>2</sup>H]-Fluoroacetate (2.17a)**



**2.17**

(*S*)-[7-<sup>2</sup>H]-Benzyl fluoride (398 mg, 2.22 mmol), prepared above, was added to a stirred solution of potassium permanganate (105 mg, 0.67 mmol) and potassium periodate (39.2 g, 170.3 mmol) in water (200ml). The mixture was stirred at room temperature for 48 h and then, most of the water removed under reduced pressure. The remaining solution was acidified with sulphuric acid (2 M), and the material lyophilised. The lyophilised solution was neutralised using sodium hydroxide (0.1 M) and the water removed by freeze drying to furnish (*S*)-[<sup>2</sup>H]-fluoroacetate as a white solid.  $\delta_F$  (CDCl<sub>3</sub>): -217.4 (1F, d.t,  $J_{HF}$  48,  $J_{DF}$  7, CDHF).

**(S)-Hexyl-[<sup>2</sup>H]-fluoroacetate (2.26)**



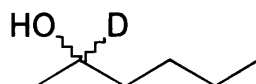
**2.26**

Thionyl chloride (0.5ml, 5 mmol) was added to a mixture of (*S*)-[<sup>2</sup>H]-fluoroacetate (10 mg, 0.01 mmol) and commercial sodium fluoroacetate (400 mg, 4 mmol) cooled to 0 °C. The mixture was gently heated under reflux for 2 h, then cooled to 0 °C, once more, before the remaining excess thionyl chloride was quenched by the addition of a further portion of commercial sodium fluoroacetate (200 mg, 2 mmol). Hexanol (2 ml, 16.0 mmol) was added to quench the fluoroacetyl chloride that had been generated, and the mixture stirred for a further 30 minutes. The material was purified by columning over silica using DCM as the eluant to give hexyl fluoroacetate (98 %) and (*S*)-hexyl-[<sup>2</sup>H]-fluoroacetate as a colourless oil (405 mg, 50%).  $\delta_F$  (CDCl<sub>3</sub>): -230.4 (1F, d.t,  $J_{HF}$  47,  $J_{DF}$  7, CDHF, 1%), -229.9 (1F, t,  $J$  48, CH<sub>2</sub>F, 99 %),  $\delta_H$  (CDCl<sub>3</sub>): 0.8 (3H, t,  $J$  6, CH<sub>3</sub>), 1.2 (6H, m), 1.6 (2H, m), 4.1 (2H, t,  $J$  7, CH<sub>2</sub>O), 4.7 (2H, d,  $J$  47, CH<sub>2</sub>F).  $\delta_C$  (CDCl<sub>3</sub>): 13.8, 22.4, 25.3, 28.4, 31.3, 65.3, 77.4 (d,  $J$  182, CH<sub>2</sub>F) 168 (C=O).

## **6.1.3 Preparation of various fluoro-deutero-alkanes**

### **6.1.3.1 Preparation of 2-fluoro[2-<sup>2</sup>H]-hexane (2.28)**

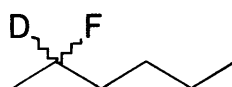
#### **[2-<sup>2</sup>H]-Hexan-2-ol (2.27)**



**2.27**

Hexan-2-one (3.99 g, 39.8 mmol) was added to a suspension of lithium aluminium deuteride (0.93 g, 22.1 mmol) in THF (40 ml) cooled to 0 °C, and stirred. The mixture was left to warm to room temperature then heated under reflux for 3 h. After cooling the reaction mixture, once again, to 0 °C, quenching was performed using Micovic and Mihailovic's basic workup procedure.<sup>1</sup> The mixture was filtered and the insoluble material washed with diethyl ether. The solvent was evaporated under reduced pressure to yield [2-<sup>2</sup>H]-hexan-2-ol as a clear colourless oil (3.10 g, 97 %).  $\nu_{max}$  (neat): 3343, 2959, 2928, 2859, 2364.  $m/z$  (CI+, NH<sub>3</sub>) 104 (M+1, 0.13 % )  $\delta_H$  (CDCl<sub>3</sub>): 0.9 (3H, m), 1.2 (3H, m), 1.3 (6H, m), 1.8 (1H, OH).  $\delta_C$  (CDCl<sub>3</sub>): 13.9, 22.6, 23.1, 27.8, 38.8, 67.4 (t, J 22, CDOH)

#### **2-Fluoro[2-<sup>2</sup>H]-hexane (2.28)<sup>3</sup>**

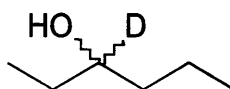


**2.28**

[2-<sup>2</sup>H]-Hexan-2-ol (0.90 g, 8.74 mmol) was added to a solution of diethylaminosulphur trifluoride (DAST) (1.2 ml, 9.08 mmol) in DCM (20 ml) cooled to -78°C. The reaction mixture was heated under reflux for 3 h with stirring. The mixture was cooled to 0 °C and quenched by the addition of water. The organic phase was washed with water (3 x 20 ml) and dried over magnesium sulphate. The solvent was cautiously removed under reduced pressure and the product purified by vacuum line distillation to yield 2-fluoro[2-<sup>2</sup>H]-hexane (0.56 g, 61 %) as a colourless liquid.  $\delta_F$  (CDCl<sub>3</sub>): -189.9 (m)  $\delta_H$  (CDCl<sub>3</sub>): 0.9 -1.0 (6H, m), 1.4-1.7 (6H, m),  $\delta_C$  (CDCl<sub>3</sub>): 9.3 (d, J 6), 14.0, 18.3 (d, J 5), 27.9 (d, J 21), 36.7 (d, J 21), 95.0 (dt, J<sub>FC</sub> 166 J<sub>DC</sub> 23, CDF).

### 6.1.3.2 Preparation of 3-fluoro[3-<sup>2</sup>H]-hexane (2.30)

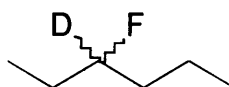
#### [3-<sup>2</sup>H]-Hexan-3-ol (2.29)



2.29

Hexan-3-one (4.34 g, 43.4 mmol) was added to a suspension of lithium aluminium deuteride (0.97 g, 23.1 mmol) in THF (40 ml), cooled to 0 °C, and stirred. The mixture was left to warm to room temperature then heated under reflux for 3 h. After cooling the reaction mixture, once again, to 0 °C quenching was performed using Micovic and Mihailovic's basic workup procedure.<sup>1</sup> The mixture was filtered, and the insoluble material washed with diethyl ether. The solvent was evaporated under reduced pressure to yield [3-<sup>2</sup>H]-hexan-3-ol as a clear colourless oil (4.06 g, 91 %).  $\nu_{max}$  (neat): 3326, 2958, 2927, 2873, 1462.  $m/z$  (CI+, NH<sub>3</sub>) 135 (M+1, 14 %)  $\delta_H$  (CDCl<sub>3</sub>): 0.9 (6H, m), 1.4 (6H, m), 1.8 (1H, OH)  $\delta_C$  (CDCl<sub>3</sub>): 9.7, 14.0, 18.7, 29.9, 38.9, 72.3 (t, J 22, CDOH).

#### 3-Fluoro[3-<sup>2</sup>H]-hexane (2.30)<sup>3</sup>



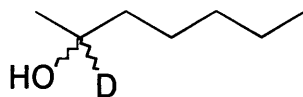
2.30

[3-<sup>2</sup>H]-Hexan-3-ol (0.93 g, 8.98 mmol) was added to a solution of diethylaminosulphur trifluoride (DAST) (1.2 ml, 9.08 mmol) in DCM (20 ml), cooled to -78°C. The reaction mixture was heated under reflux for 3 h with stirring. The mixture was cooled to 0 °C and quenched by the addition of water. The organic phase was washed with water (3 x 20 ml) and dried over magnesium sulphate. The solvent was cautiously removed under reduced pressure and the product purified by vacuum line distillation to yield 3-fluoro[3-<sup>2</sup>H]-hexane (0.55 g, 58 %) as a colourless liquid.  $\delta_F$  (CDCl<sub>3</sub>): -189.9 (m)  $\delta_H$  (CDCl<sub>3</sub>): 0.9-1.0 (6H, m), 1.4-1.7 (6H, m),  $\delta_C$  (CDCl<sub>3</sub>): 9.3 (d, J 6), 14.0, 18.3 (d, J 5), 28.0 (d, J 21), 36.7 (d 20.5), 95.0 (dt, J<sub>FC</sub> 166, J<sub>DC</sub> 22, CDF).



### 6.1.3.3 Preparation of 2-fluoro[2-<sup>2</sup>H]-heptane (2.32)

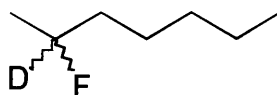
#### [2-<sup>2</sup>H]-Heptan-2-ol (2.31)



2.31

Heptan-2-one (3.39 g, 29.8 mmol) was added to a suspension of lithium aluminium deuteride (0.66 g, 15.8 mmol) in THF (40 ml), cooled to 0 °C and stirred. The mixture was left to warm to room temperature then heated under reflux for 3 h. After cooling the reaction mixture, once again, to 0 °C quenching was performed using Micovic and Mihailovic's basic workup procedure.<sup>1</sup> The mixture was filtered, and the insoluble material washed with diethyl ether. The solvent was evaporated under reduced pressure to yield [2-<sup>2</sup>H]-heptan-2-ol as a clear colourless oil (3.23 g, 93 %).  $\nu_{max}$  (neat): 3350, 2955, 2929, 2859, 1459.  $m/z$  (CI<sup>+</sup>, NH<sub>3</sub>) 136 (M+NH<sub>4</sub><sup>+</sup>+1, 5 %), 135 (M+NH<sub>4</sub><sup>+</sup>, 66 %), 118 (M+1, 1 %), 117 (M, 6 %).  $\delta_H$  (CDCl<sub>3</sub>): 0.8-0.9 (3H, m), 1.1 (3H, m), 1.2-1.4 (6H, m), 1.8-1.9 (2H, m) 2.4 (1H, OH)  $\delta_C$  (CDCl<sub>3</sub>): 13.9, 22.5, 23.1, 25.3, 31.7, 39.0, 67.3 (t, J 37, CDOH).

#### 2-Fluoro[2-<sup>2</sup>H]-heptane (2.32)<sup>3</sup>

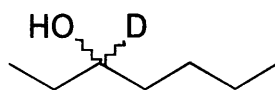


2.32

[2-<sup>2</sup>H]-Heptan-2-ol (1.10 g, 9.40 mmol) was added to a solution of diethylaminosulphur trifluoride (DAST) (1.2 ml, 9.08 mmol) in DCM (20 ml) cooled to -78°C. The reaction mixture was heated under reflux for 3 h with stirring. The mixture was cooled to 0 °C and quenched by the addition of water. The organic phase was washed with water (3 x 20 ml) and dried over magnesium sulphate. The solvent was cautiously removed under reduced pressure and the product purified by vacuum line distillation to yield 2-fluoro[2-<sup>2</sup>H]-heptane (0.58 g, 52 %) as a colourless liquid.  $\delta_F$  (CDCl<sub>3</sub>): -180.5 (m)  $\delta_H$  (CDCl<sub>3</sub>): 0.9 (3H, t, J 6), 1.3 (3H, s), 1.3-1.4 (8H, m),  $\delta_C$  (CDCl<sub>3</sub>): 13.7, 20.6 (d, J 23), 22.4, 25.1, 31.6, 36.7 (d, J 21), 90.4 (dt, J<sub>FC</sub> 163, J<sub>DC</sub> 23, CDF).

### 6.1.3.4 Preparation of 3-fluoro[3-<sup>2</sup>H]-heptane (2.34)

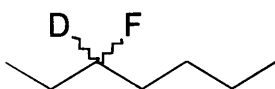
#### **[3-<sup>2</sup>H]-Heptan-3-ol (2.33)**



**2.33**

Heptan-3-one (3.23 g, 28.4 mmol) was added to a suspension of lithium aluminium deuteride (0.66 g, 15.8 mmol) in THF (40 ml), cooled to 0 °C, and stirred. The mixture was left to warm to room temperature then heated under reflux for 3 h. After cooling the reaction mixture, once again, to 0 °C, quenching was performed using Micovic and Mihailovic's basic workup procedure.<sup>1</sup> The mixture was filtered, and the insoluble material washed with diethyl ether. The solvent was evaporated under reduced pressure to yield [3-<sup>2</sup>H]-heptan-3-ol as a clear colourless oil (2.20 g, 66 %).  $\nu_{max}$  (neat): 3322, 2957, 2925, 2858, 1458.  $m/z$  (CI+, NH<sub>3</sub>) 133 (M+NH<sub>4</sub><sup>+</sup>+1, 8 %), 132 (M+NH<sub>4</sub><sup>+</sup>, 100 %), 115 (M+1, 10 %), 114 (M, 10 %).  $\delta_H$  (CDCl<sub>3</sub>): 0.8-0.9 (6H, m), 1.2-1.5 (8H, m), 2.5 (CDOH),  $\delta_C$  (CDCl<sub>3</sub>): 9.7, 13.9, 22.6, 27.7, 29.7, 36.3, 72.7 (t, J 21)

#### **3-Fluoro[3-<sup>2</sup>H]-heptane (2.34)<sup>3</sup>**

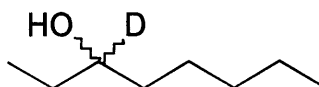


**2.34**

[3-<sup>2</sup>H]-Heptan-3-ol (0.93 g, 8.98 mmol) was added to a solution of diethylaminosulphur trifluoride (DAST) (1.2 ml, 9.08 mmol) in DCM (20 ml), cooled to -78°C. The reaction mixture was heated under reflux for 3 h with stirring. The mixture was cooled to 0 °C and quenched by the addition of water. The organic phase was washed with water (3 x 20 ml) and dried over magnesium sulphate. The solvent was cautiously removed under reduced pressure and the product purified by vacuum line distillation to yield 3-fluoro[3-<sup>2</sup>H]-heptane (0.55 g, 58 %) as a colourless liquid.  $\delta_F$  (CDCl<sub>3</sub>): -182.4 (m)  $\delta_H$  (CDCl<sub>3</sub>): 0.9-1.0 (6H, m), 1.3-1.7 (8H, m),  $\delta_C$  (CDCl<sub>3</sub>): 9.3 (d, J 6), 13.9 (d, J 10), 22.6, 27.2 (d, J 5), 27.9 (d, J 21), 34.3 (d 24), 95.3 (dt, J<sub>FC</sub> 166, J<sub>DC</sub> 23, CDF).

### **6.1.3.5 Preparation of 3-fluoro[3-<sup>2</sup>H]-octane (2.36)**

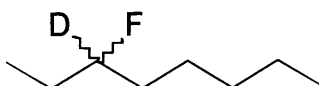
#### **[3-<sup>2</sup>H]-Octan-3-ol (2.35)**



**2.35**

Octan-3-one (6.79 g, 53.1 mmol) was added to a suspension of lithium aluminium deuteride (1.40 g, 33.4 mmol) in THF (40 ml), cooled to 0 °C, and stirred. The mixture was left to warm to room temperature then heated under reflux for 3 h. After cooling the reaction mixture, once again, to 0 °C quenching was performed using Micovic and Mihailovic's basic workup procedure.<sup>1</sup> The mixture was filtered, and the insoluble material washed with diethyl ether. The solvent was evaporated under reduced pressure to yield [3-<sup>2</sup>H]-octan-3-ol as a clear colourless oil (4.68 g, 67 %).  $\nu_{max}$  (neat): 3322, 2957, 2925, 2858, 1458.  $m/z$  (CI+, NH<sub>3</sub>) 150 (M+NH<sub>4</sub><sup>+</sup>+1, 3 %), 149 (M+NH<sub>4</sub><sup>+</sup>, 23 %), 131 (M, 3 %).  $\delta_H$  (CDCl<sub>3</sub>): 0.9-1.0 (6H, m), 1.2-1.5 (10 H, m), 1.9 (1H, OH)  $\delta_C$  (CDCl<sub>3</sub>): 9.9, 14.1, 22.7, 25.4, 30.1, 32.0, 36.9, 72.8 (t, J 21, CDOH).

#### **3-Fluoro[3-<sup>2</sup>H]-octane (2.36)<sup>3</sup>**

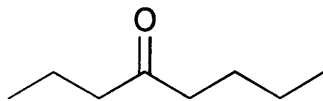


**2.36**

[3-<sup>2</sup>H]-Octane-3-ol (2.17 g, 16.53 mmol) was added to a solution of diethylaminosulphur trifluoride (DAST) (2.4 ml, 18.16 mmol) in DCM (20 ml) cooled to -78°C. The reaction mixture was heated under reflux for 3 h with stirring. The mixture was cooled to 0 °C and quenched by the addition of water. The organic phase was washed with water (3 x 20 ml) and dried over magnesium sulphate. The solvent was cautiously removed under reduced pressure and the product purified by Kugelrohr distillation to yield 3-fluoro[3-<sup>2</sup>H]-octane (0.55 g, 58 %) as a pale yellow liquid.  $\delta_F$  (CDCl<sub>3</sub>): -182.5 (m)  $\delta_H$  (CDCl<sub>3</sub>): 0.9-1.0 (6H, m), 1.3-1.7 (10 H, m),  $\delta_C$ (CDCl<sub>3</sub>): 9.5 (d, J 6), 14.1, 22.8, 25.0 (d, J 5), 28.1 (d, J 22), 31.9, 34.7 (d 20.9), 95.3 (dt, J<sub>FC</sub> 166, J<sub>DC</sub> 23, CDF).

### 6.1.3.6 Preparation of 4-fluoro[4-<sup>2</sup>H]-octane (2.39)

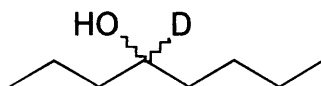
#### 4-Octanone (2.37)



2.37

4-Octanol (4.94 g, 37.98 mmol) was added to a vigorously stirred mixture of PCC (12.4 g, 57.6 mmol) and 3 Å ground molecular sieves (40 g) in DCM (200ml). The progress of the reaction was followed by TLC (DCM, silica plates). After 5 h, the mixture was filtered through a plug of silica and the residue washed with DCM (100 ml). The DCM was evaporated under reduced pressure to yield 4-octanone (3.72 g, 77 %) as a clear, colourless liquid.  $\nu_{max}$  (neat): 2874, 1709, 1461.  $m/z$  (CI<sup>+</sup>, NH<sub>3</sub>) 147 (M+NH<sub>4</sub><sup>+</sup>+1, 7 %), 146 (M+NH<sub>4</sub><sup>+</sup>, 100 %), 129 (M+1, 15 %), 128 (M, 7 %).  $\delta_H$  (CDCl<sub>3</sub>): 0.7-0.8 (6H, m), 1.0-1.2 (2H, m), 1.2-1.5 (4H, m), 2.1-2.3 (4H, m).  $\delta_C$  (CDCl<sub>3</sub>): 13.3, 13.4, 16.9, 22.0, 25.6, 42.1, 44.2, 210.6.

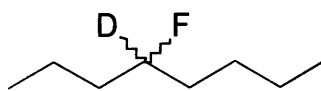
#### [4-<sup>2</sup>H]-Octan-4-ol (2.38)



2.38

Octan-4-one (3.57 g, 27.9 mmol) was added to a suspension of lithium aluminium deuteride (0.65 g, 15.5 mmol) in THF (40 ml), cooled to 0 °C and stirred. The mixture was left to warm to room temperature then heated under reflux for 3 h. After cooling the reaction mixture, once again, to 0 °C, quenching was performed using Micovic and Mihailovic's basic workup procedure.<sup>1</sup> The mixture was filtered, and the insoluble material washed with diethyl ether. The solvent was evaporated under reduced pressure to yield [4-<sup>2</sup>H]-octan-4-ol as a clear colourless oil (2.38 g, 65 %).  $\nu_{max}$  (neat): 3314, 2956, 2928, 2872, 1456.  $m/z$  (CI<sup>+</sup>, NH<sub>3</sub>) 150 (M+NH<sub>4</sub><sup>+</sup>+1, 3 %), 149 (M+NH<sub>4</sub><sup>+</sup>, 40 %), 131 (M+1, 2 %), 130 (M, 3 %).  $\delta_H$  (CDCl<sub>3</sub>): 0.8-0.9 (6H, m), 1.2-1.3 (10H, m), 2.6 (1H, broad, OH).  $\delta_C$  (CDCl<sub>3</sub>): 13.8, 13.9, 18.6, 22.6, 27.6, 36.8, 39.3, 70.7 (t, J 22, CDOH).

### 4-Fluoro[4-<sup>2</sup>H]-octane (2.39)<sup>3</sup>

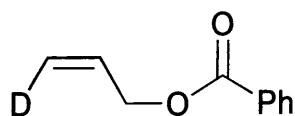


2.39

[4-<sup>2</sup>H]-Octane-4-ol (0.89 g, 6.81 mmol) was added to a solution of diethylaminosulphur trifluoride (DAST) (1 ml, 7.56 mmol) in DCM (20 ml) cooled to -78°C. The reaction mixture was heated under reflux for 3 h with stirring. The mixture was cooled to 0 °C and quenched by the addition of water. The organic phase was washed with water (3 x 20 ml) and dried over magnesium sulphate. The solvent was cautiously removed under reduced pressure and the product purified by Kugelrohr distillation to yield 4-fluoro[4-<sup>2</sup>H]-octane (0.42 g, 46 %) as a pale yellow liquid.  $\delta_F$  (CDCl<sub>3</sub>): -181.7 (m)  $\delta_H$  (CDCl<sub>3</sub>): 0.9-1.3 (6H, m), 1.3-1.6 (10 H, m),  $\delta_C$  (CDCl<sub>3</sub>): 13.8 (d, J 3), 18.4 (d, J 5), 22.6, 27.3(d, J 5), 34.8 (d, J 21), 37.1, 37.3, 93.6 (dt,  $J_{FC}$  166,  $J_{DC}$  20, CDF).

### **6.1.4 Preparation of (1*S*, 2*R*)-[1-<sup>2</sup>H]-glycerol (4.10) and (1*R*, 2*R*)-[1-<sup>2</sup>H]-glycerol (4.10a)<sup>4</sup>**

#### **Z-[3-<sup>2</sup>H]-(2-Propenyl) benzoate (4.13)<sup>4</sup>**

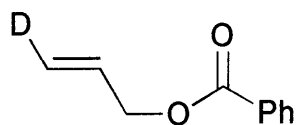


**4.13**

Propargyl alcohol (5.01 g, 91.0 mmol) was added dropwise to a suspension of lithium aluminium hydride (4.25 g, 132 mmol) in THF (110 ml) cooled to 0 °C and stirred. The mixture was left to warm to room temperature and stirred for 3 h. The reaction was quenched by slowly adding a mixture of THF (10 ml) and deuterium oxide (5 ml) until hydrogen gas ceased to be evolved. The mixture was filtered, the insoluble material washed with dichloromethane (200 ml) and the filtrate added to an aqueous sodium hydroxide solution (30 %, 50 ml), which contained benzyl triethyl ammonium chloride (2.03 g, 9 mmol), with vigorous stirring. A solution of benzoyl chloride (16.90 g,) in dichloromethane (40 ml) was added to this mixture, and gradually a dense white precipitate formed. After 2 h, water was added to dissolve the precipitated material. The organic phase was separated, and the aqueous extracted with dichloromethane. Washing of the combined organic phase with water until neutral and drying over magnesium sulphate, afforded the crude product after solvent removal.

Purification over silica (ethyl acetate/ petroleum ether 1:8) gave Z-[3-<sup>2</sup>H]-(2-Propenyl) benzoate (4.78 g, 32 %) as a colourless oil.  $\nu_{max}$  (neat): 3063, 2943, 1716, 1601, 1451.  $m/z$  (EI+) 163 ( $M^+$ , 22 %), 162 (4 %), 85 %D.  $\delta_H$  (CDCl<sub>3</sub>): 4.9 (2H, d, J 6 Hz, CH<sub>2</sub>), 5.3 (1H, d, J 10 Hz, 3'-H *trans*), 6.0-6.2 (1H, m, 2'-H), 7.4-7.5 (2H, m, 3-H, 5-H), 7.5-7.6 (1H, m, 4-H), 8.0-8.1 (2H, m, 2-H, 6-H).  $\delta_D$  (CHCl<sub>3</sub>): 5.3 (1D, s, 3'-D *trans*, 12 %), 5.5 (1D, s, 3'-D *cis*, 78 %), 6.1 (1D, s, 2'-D, 10 %)  $\delta_C$  (CDCl<sub>3</sub>): 65.3 (C-1'), 117.7 (t, J 24 Hz, C-3'), 128.2 (C-3, C-5), 129.5 (C-2, C-6), 130.1 (C-1), 132.1 (C-2'), 132.8 (C-4), 166.0 (CO<sub>2</sub>Ph).

***E*-[3-<sup>2</sup>H]-(2-Propenyl) benzoate (4.13a)<sup>4</sup>**

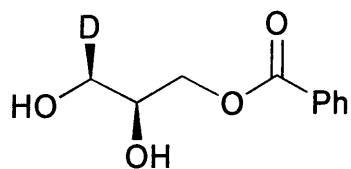


**4.13a**

A solution of propargyl alcohol (6.50 g, 116 mmol) in dry THF (150 ml) was treated with *n*-butyl lithium (125 ml, 1.6M in hexane, 200 mmol) at -78 °C, and left to warm to room temperature. Deuterium oxide (8.0 ml, 400 mmol) was added, the mixture filtered, to remove precipitate, dried over magnesium sulphate, filtered once more and concentrated by distilling off the solvents through a vigreux column at atmospheric pressure. The remaining solution was slowly added to a solution of lithium aluminium hydride (6.89 g, 181 mmol) in dry THF (105 ml) at 0 °C and stirred at this temperature for 3 h. A 2:1 water THF mixture was added carefully until fizzing ceased and the crude *E*-[3-<sup>2</sup>H]-allyl alcohol was benzoylated and purified as described above to give *E*-[3-<sup>2</sup>H]-(2-propenyl) benzoate (7.21 g, 38 %) as a colourless oil.

*v max* (neat): 2942, 2360, 2345, 1718 (C=O), 1602 (C=C), 1451. *m/z* (EI+) 163 (M<sup>+</sup>, 4.84 %), 162 (3.58 %), 57 %D.  $\delta_{\text{H}}$  (CDCl<sub>3</sub>): 4.8 (2H, d, J 6 Hz, CH<sub>2</sub>), 5.4 (1H, d, J 17 Hz, 3'-H *cis*), 6.0-6.2 (1H, m, 2'-H), 7.4-7.5 (2H, m, 3-H, 5-H), 7.5-7.6 (1H, m, 4-H), 8.1 (2H, m, 2-H, 6-H).  $\delta_{\text{D}}$  (CHCl<sub>3</sub>): 5.3 (1D, s)  $\delta_{\text{C}}$  (CDCl<sub>3</sub>): 65.5 (C-1'), 118.0 (t, J 24 Hz, C-3'), 128.3 (C-3, C-5), 129.6 (C-2, C-6), 129.7 (C-1), 132.1 (C-2'), 132.9 (C-4), 166.2 (CO<sub>2</sub>Ph).

### [3(*S*)-<sup>2</sup>H]-2(*R*), 3-Dihydroxypropyl benzoate (4.14)<sup>4</sup>

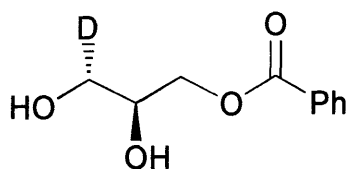


#### 4.14

AD-mix- $\beta$  (43.01 g) was added to a mixture of water (144 ml) and tert-butyl alcohol (144 ml). The mixture was stirred for 30 minutes until all of the AD-mix- $\beta$  was in solution, the solution was then cooled to 0 °C and stirred for a further 30 minutes. Z-[3-<sup>2</sup>H]-2-Propenyl) benzoate (5.24 g, 32.1 mmol) was added and the mixture stirred for 4 h. Sodium disulphite (50.1 g, 262 mmol) was added and the mixture allowed to warm to room temperature and stirred for a further hour. The aqueous phase was extracted into ethyl acetate (4 x 100 ml) and the combined organics dried over magnesium sulphate. Evaporation of the solvent under reduced pressure gave the crude product, which was purified by column chromatography (ethyl acetate/petroleum ether 2:1). The resultant material was recrystallised from diethyl ether and petroleum ether to yield [3(*S*)-<sup>2</sup>H]-2(*R*), 3-dihydroxypropyl benzoate (4.13 g, 65 %) as a fine white powder. mp. 55-56 °C (lit 61 °C)<sup>4</sup>,  $[\alpha]_D^{25} = +28.8$ , (*c* 2.5, EtOH)  $\nu_{max}$  (neat): 3362 (OH), 2882 (CH), 1698 (C=O), 1268 (C-O). *m/z* (CI<sup>+</sup>NH<sub>3</sub>) 198 (M<sup>+</sup>+1, 46 %), 180 (100 %).  $\delta_H$  (CDCl<sub>3</sub>): 2.2 (1H, br, OH), 2.6 (1H, br, OH), 3.8 (1H, br, 3'-H), 4.1 (1H, br, 2'-H), 4.4 (2H, m, 1'-H), 7.4-7.5 (2H, m, 3-H, 5-H), 7.5-7.6 (1H, m, 4-H), 8.0-8.1 (2H, m, 2-H, 6-H).  $\delta_D$  (CHCl<sub>3</sub>): 3.7 (1D, s)  $\delta_C$  (CDCl<sub>3</sub>): 63.1 (t, J 20 C-3'), 65.6 (C-2'), 70.1 (C-1'), 128.3 (C-3, C-5), 129.5 (C-1, C-2, C-6), 133.1 (C-4), 132.9 (C-4), 166.8 (CO<sub>2</sub>Ph).



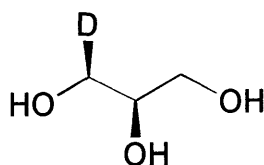
### [3(*R*)-<sup>2</sup>H]-2(*R*), 3-Dihydroxypropyl benzoate (4.14a)<sup>4</sup>



4.14a

[3(*S*)-<sup>2</sup>H]-2(*R*), 3-Dihydroxypropyl benzoate (4.33 g, 67 %) was obtained from *E*-[3-<sup>2</sup>H]-2-propenyl benzoate (5.35 g, 32.81 mmol) as described above for 4.14. Recrystallisation afforded a fine white powder of m.p. 56-57 °C (lit 63 °C)<sup>4</sup>.  $[\alpha]_D^{25} = +5.3$ , (*c* 2.5, EtOH) *v max* (neat): 3499 (OH), 3459 (OH) 2928 (CH), 1697 (C=O), 1271 (C-O). *m/z* (Cl<sup>+</sup>+NH<sub>3</sub>) 198 (M<sup>+</sup>+1, 100 %), 180 (72 %).  $\delta_H$  (CDCl<sub>3</sub>): 2.3 (1H, br, OH), 2.8 (1H, br, OH), 3.7 (1H, br, 3'-H), 4.1 (1H, br, 2'-H), 4.4 (2H, m, 1'-H), 7.4-7.5 (2H, m, 3-H, 5-H), 7.5-7.6 (1H, m, 4-H), 8.0-8.1 (2H, m, 2-H, 6-H).  $\delta_D$  (CHCl<sub>3</sub>): 3.80 (1D, s)  $\delta_C$  (CDCl<sub>3</sub>): 63.2 (t, J 19, C-3'), 65.9 (C-2'), 70.5 (C-1'), 128.6 (C-3, C-5), 129.7 (C-1, C-2, C-6), 133.5 (C-4), 132.9 (C-4), 167.1 (CO<sub>2</sub>Ph).

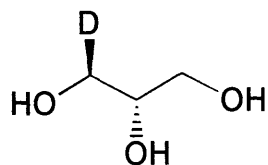
### (1*S*, 2*R*)-[1-<sup>2</sup>H]-Glycerol (4.10)<sup>4</sup>



4.10

[3(*S*)-<sup>2</sup>H]-2(*R*), 3-Dihydroxypropyl benzoate (4.13 g, 20.1 mmol) was dissolved in acetone (151 ml) and an aqueous sodium hydroxide solution (0.5 M, 42 ml, 21 mmol). The mixture was heated to 65 °C with stirring for 1 h. The solvents were evaporated to dryness, under reduced pressure, and the resultant solid ground up, washed with dry analar acetone and the filtrate combined and concentrated. The crude material was purified over silica (water/acetone 5:95) to afford glycerol (2.55 g, 81 %) as a viscous oil. *v max* (neat): 3250 (OH), 2932, 2885 (CH), 1646, 1408. *m/z* (ES<sup>+</sup>) 94 (M<sup>+</sup>+1, 5 %).  $\delta_H$  (D<sub>2</sub>O): 3.3-3.4 (1H, m, 3-Ha), 3.4 (2H, m, 1-Hb, 3-Hb), 3.6 (1H, m, 2-H).  $\delta_D$  (H<sub>2</sub>O): 3.4 (1D, s) and 3.6 from 15 % [2-<sup>2</sup>H<sub>1</sub>]-glycerol.  $\delta_C$  (D<sub>2</sub>O): 66.6 (t, J 22 C-1), 66.9 (C-3) 76.4 (C-2).

**(1*R*, 2*R*)-[1-<sup>2</sup>H]-Glycerol (4.10a)<sup>4</sup>**



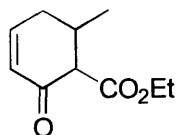
**4.10a**

(1*R*, 2*R*)-[1-<sup>2</sup>H]-Glycerol (1.93 g, 75 %) was obtained from [3(*R*)-<sup>2</sup>H]-2(*R*), 3-dihydroxypropyl benzoate (5.43 g, 27.6 mmol) as described above for 4.10.  $\nu_{max}$  (neat): 3260 (OH), 2884 (CH), 1684, 1404.  $m/z$  (ES+) 94 ( $M^+ + 1$ , 2 %).  $\delta_H$  (D<sub>2</sub>O): 3.4 (2H, dd,  $J$  6,  $J$  11, 1-Ha, 3-Ha), 3.5 (1H, dd,  $J$  4,  $J$  11, 3-Hb), 3.6 (1H, m, 2-H).  $\delta_D$  (H<sub>2</sub>O): 3.5 (1D, s).  $\delta_C$  (D<sub>2</sub>O): 62.3 (t,  $J$  22 C-1), 62.6 (C-3), 72.1 (C-2).

## 6.1.5 Preparation of deuterated compounds with which to investigate the biosynthesis of longianone

### 6.1.5.1 Preparation of [3,5-<sup>2</sup>H<sub>2</sub>]-6-methylsalicylic acid (5.27a)<sup>5</sup>

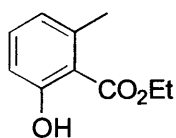
#### **Ethyl 5-methyl-3-oxocyclohexene-4-carboxylate (5.43)<sup>5</sup>**



**5.43**

Ethyl acetoacetate (35 ml, 280 mmol) was added to a stirred solution of sodium (204 mg, 9.87 mmol) dissolved in ethanol (50 ml). The mixture was cooled to 0 °C and crotonaldehyde (23 ml, 280 mmol) was added, over the course of 1 h, with stirring. The reaction was left to stir at room temperature for 16 h. The resultant yellow, turbid solution was cooled to 0 °C, saturated with dry hydrogen chloride gas then stirred at room temperature for a further 24 h. It was seen, by <sup>1</sup>H NMR, that the reaction had not gone to completion. The reaction was saturated with dry hydrogen chloride gas, once more, and stirred for a further 24 h. The solvent and some biproduct were removed on the water aspirator at 50 °C, and the mixture was purified by distillation (90 °C, 27 kgm<sup>-1</sup>s<sup>-2</sup>) to yield ethyl 5-methyl-3-oxocyclohexane-4-carboxylate (32 g, 68 %) as a pale yellow oil. b.p. 90 °C, 27 Pa, *v max*: 2963, 1734, 1673. *m/z* (EI+) 183 (M<sup>+</sup>+1, 18 %), 131 (100 %), 123 (36 %), 85 (29 %).  $\delta_{\text{H}}$  (CDCl<sub>3</sub>): 1.1 (3H, d, J 6, C5-CH<sub>3</sub>), 1.3 (3H, t, J 7, CO<sub>2</sub>CH<sub>2</sub>CH<sub>3</sub>), 2.1 (1H, m, C5H), 2.5 (2H, m, C6H<sub>2</sub>) 3.1 (1H, d, J 12, C4H), 4.1 (2H, q, J 7, CO<sub>2</sub>CH<sub>2</sub>CH<sub>3</sub>), 6.1 (1H, dom, J 9, C2H).  $\delta_{\text{C}}$  (CDCl<sub>3</sub>): 14.4 (CO<sub>2</sub>CH<sub>2</sub>CH<sub>3</sub>), 20.0 (C5CH<sub>3</sub>), 33.1 (C6), 33.6 (C5), 61.3 (C4), 61.9 (CO<sub>2</sub>CH<sub>2</sub>CH<sub>3</sub>), 129.0 (C2), 149.9 (C1), 170.1 (CO<sub>2</sub>Et), 194.7 (C3).

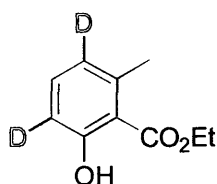
## Ethyl 2-hydroxy-6-methylbenzoate (5.44)<sup>5</sup>



**5.44**

Bromine (4.3 ml, 850 mmol) in acetic acid (10 ml) was added slowly to a stirred solution of ethyl 5-methyl-3-oxocyclohexane-4-carboxylate (14.30 g, 846 mmol) in chloroform (100 ml) at 0 °C. The mixture was allowed to warm to room temperature, stirred for 1 h, and was then heated to reflux for 16 h. The dark orange/brown reaction mixture was cooled to room temperature, dichloromethane added (75 ml) and the organics washed with water (3 x 100 ml) and saturated sodium hydrogen carbonate solution (1 x 50 ml). The solvent was removed, under reduced pressure, and the resulting brown tar purified by steam distillation. Ethyl 2-hydroxy-6-methylbenzoate (9.86 g, 69 %) was recovered as a white solid with needle like crystals having a strong phenolic smell. m.p. 38-40 °C (lit. 42 °C)<sup>5</sup>,  $\nu_{max}$  2978.5, 1738.7, 1642.0, 1600, 1459.  $m/z$  (EI+) 181 ( $M^+ + 1$ , 7 %), 180 (54 %), 135 (37 %), 134 (100 %), 106 (18 %), 77 (27 %), 51 (24 %).  $\delta_H$  (CDCl<sub>3</sub>): 1.5 (3H, t, J 7, CO<sub>2</sub>CH<sub>2</sub>CH<sub>3</sub>), 2.6 (3H, s, CH<sub>3</sub>-Ph), 4.5 (2H, q, J 7, CO<sub>2</sub>CH<sub>2</sub>CH<sub>3</sub>), 6.8 (1H, d, J 7, C3H), 6.9 (1H, d, J 8, C5H), 7.3 (1H, d.d, J 8, C4H), 11.4 (1H, s, OH, disappears on shaking with <sup>2</sup>H<sub>2</sub>O).  $\delta_C$  (CDCl<sub>3</sub>): 14.4 (CO<sub>2</sub>CH<sub>2</sub>CH<sub>3</sub>), 24.2 (CH<sub>3</sub>-Ph), 61.7 (CO<sub>2</sub>CH<sub>2</sub>CH<sub>3</sub>), 112.5 (C1), 115.7 (C3), 123.0 (C5), 134.2 (C4), 141.5 (C6), 163.0 (C2), 171.9 (CO<sub>2</sub>Et).

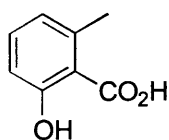
## Ethyl [3,5-<sup>2</sup>H<sub>2</sub>]-2-hydroxy-6-methylbenzoate (5.45)



**5.45**

Deuterium chloride (2 ml) and deuterium oxide (2 ml) were added to ethyl 2-hydroxy-6-methylbenzoate (1.00 g, 5 mmol), which had been previously treated by stirring with deuterium oxide. The mixture was heated under reflux for 16 h, cooled and the product removed by filtration through a sinter. <sup>1</sup>H NMR indicated that only a third of the protons had been exchanged by deuterons. The material was heated under reflux for a further 16 h with deuterium chloride (2 ml) and deuterium oxide (2 ml). The resulting product was collected by filtration, through a sinter funnel, and dried under reduced pressure to yield 2-hydroxy-6-methylbenzoate (0.81 g, 81 %) that was 27 % mono, 55 % di and 7% trideuterated. m.p. 38-40 °C (lit. 42 °C)<sup>5</sup>, *v max*: 2980, 1739, 1643, 1598, 1460. *m/z* (EI+) 183 (M<sup>+</sup>+1, 4 %), 182 (31 %), 181 (12 %), 180 (4 %), 137 (22 %), 136 (100 %) 135 (37 %), 134 (12 %).  $\delta_{\text{H}}$  (CDCl<sub>3</sub>): 1.5 (3H, t, J 7, CO<sub>2</sub>CH<sub>2</sub>CH<sub>3</sub>), 2.6 (3H, s, CH<sub>3</sub>-Ph), 4.5 (2H, q, J 7, CO<sub>2</sub>CH<sub>2</sub>CH<sub>3</sub>), 6.7 (0.12 H, d, J 4, Ph), 6.9 (0.12 H, d, J 6, Ph), 11.4 (1H, s, OH, disappears on shaking with <sup>2</sup>H<sub>2</sub>O).  $\delta_{\text{C}}$  (CDCl<sub>3</sub>): 14.4 (CO<sub>2</sub>CH<sub>2</sub>CH<sub>3</sub>), 24.2 (CH<sub>3</sub>-Ph), 61.7 (CO<sub>2</sub>CH<sub>2</sub>CH<sub>3</sub>), 112.5 (C1), 115.7 (t, J 27, C3), 123.0 (t, J 31, C5), 134.0 (t, J 11, C4), 141.2 (C6), 162.9 (C2), 171.9 (CO<sub>2</sub>Et).

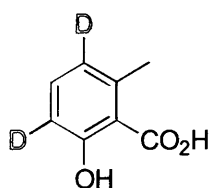
## 6-Methylsalicylic acid (5.27) <sup>5</sup>



**5.27**

A solution of ethyl 2-hydroxy-6-methylbenzoate (1.01 g, 6 mmol) in aqueous sodium hydroxide (5 ml, 1 M) was heated under reflux for 8 h. After cooling, the reaction mixture was acidified with aqueous hydrogen chloride (1 M) and extracted into ethyl acetate (3 x 20 ml). The combined ethyl acetate was dried over magnesium sulphate and removed by rotary evaporation to yield 6-methylsalicylic acid (0.82 g, 90 %). Mp 169-170 °C (lit. 170-171 °C)<sup>6</sup>,  $\nu_{max}$ : 3422, 3050, 2977, 2848, 2595, 1646, 1599.  $m/z$  (EI+) 152 (16 %), 151 (88 %), 150 (100 %) 149 (34 %).  $\delta_H$  (CDCl<sub>3</sub>/CD<sub>3</sub>OD): 2.6 (3H, s, CH<sub>3</sub>-Ph), 6.7 (1H, d, J 7, C3H), 6.8 (1H, d, J 8.4, C5H), 7.4 (1H, d.d, J 8, C4H).  $\delta_C$  (CDCl<sub>3</sub>/CD<sub>3</sub>OD): 23.6 (CH<sub>3</sub>-Ph), 112.3 (C1), 115.0 (C3), 122.7 (C5), 133.7 (C4), 142.0 (C6), 162.7 (C2), 174.1 (C=O<sub>2</sub>H).

## [3,5-<sup>2</sup>H<sub>2</sub>]- 6-Methylsalicylic acid (5.27a)

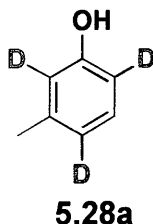


**5.27a**

Using the procedure detailed above, ethyl [3,5-<sup>2</sup>H]-2-hydroxy-6-methylbenzoate (1.02 g, 6 mmol) was converted to [3,5-<sup>2</sup>H<sub>2</sub>]- 6-methylsalicylic acid (0.84 g, 91 %). m.p. 167-169°C (lit. 170-171 °C, undeuterated)<sup>6</sup>,  $\nu_{max}$ : 3420.9, 3048.9, 2974.7, 2847.0, 2593.66, 1645.25, 1598.84.  $m/z$  (EI+) 154 (7 %), 153 (29 %), 152 (62 %) 151 (40 %), 150 (24 %), 149 (17 %), 148 (4 %).  $\delta_H$  (CDCl<sub>3</sub>/CD<sub>3</sub>OD): 2.6 (3H, s, CH<sub>3</sub>-Ph), 6.7 (0.1H, d, J 8, C3H), 6.8 (0.1H, d, J 8, C5H), 7.4 (0.9H, d.d, J 8, C4H).  $\delta_C$

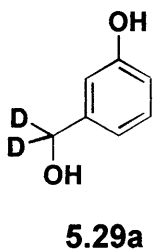
(CDCl<sub>3</sub>/CD<sub>3</sub>OD): 23.6 (CH<sub>3</sub>-Ph), 112.0 (C1), 115.0 (t, J 19, C3), 122.7 (t, C5), 133.7 (C4), 142.0 (C6), 162.7 (C2), 174.1 (C=O<sub>2</sub>H).

### **6.1.5.2 Preparation of [2,4,6-<sup>2</sup>H<sub>3</sub>]m-cresol (5.28a)**<sup>7</sup>



A suspension of phosphorus tribromide (1.2 ml) in deuterium oxide (10 ml) was stirred at 0 °C. After 30 minutes, *m*-cresol (1.10 g, 10.3 mmol) was added. The mixture was stirred for a further 30 minutes, at 0 °C, then heated under reflux overnight. After cooling, the mixture was extracted into diethyl ether (3 x 50 ml) the organic extracts were combined and then dried over magnesium sulphate. The solvent was removed under reduced pressure to yield [2,4,6-<sup>2</sup>H<sub>3</sub>]m-cresol (1.11 g, 98 %).  $\nu$  max: 3316.0, 2357.4, 1587.9, 1489.8.  $m/z$  (EI+) 112 (M<sup>+</sup>+1, 15 %), 111 (100 %), 110 (99 %), 109 (52 %).  $\delta_H$  (CDCl<sub>3</sub>): 2.3 (3H, s, CH<sub>3</sub>-Ph), 7.1 (1H, s, C5H).  $\delta_C$  (CDCl<sub>3</sub>): 21.3 (CH<sub>3</sub>-Ph), 112.1 (t, J 21), 115.8 (t, J 22), 121.5 (t, J 22), 129.3 (C5), 139.8 (C3), 155.1 (C1).

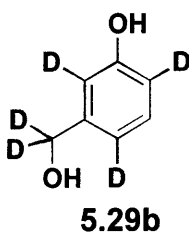
### **6.1.5.2 Preparation of [7,7-<sup>2</sup>H<sub>2</sub>]m-hydroxybenzyl alcohol (5.29a)**



To a stirred solution of lithium aluminium deuteride (0.82 g, 19.61 mmol) in THF (50 ml) cooled to 0 °C, was added *m*-hydroxy methyl benzoate (4.00 g, 26.32 mmol) dissolved in THF (10 ml). The mixture was allowed to warm gradually to room temperature and then heated under reflux for 48 h. The reaction was quenched using Micovic and Mihailovic's basic workup procedure.<sup>1</sup> The mixture was filtered, and the insoluble material washed with ethyl acetate. The solvent was evaporated under reduced

pressure to yield [7,7-<sup>2</sup>H<sub>2</sub>]*m*-hydroxybenzyl alcohol (2.32 g, 70 %). m.p. 69-70 °C (lit. non. deuterated 67-68 °C)<sup>8</sup>,  $\nu_{max}$ : 3357, 3053, 2947, 1587, 1496.  $m/z$  (EI+) 127 ( $M^+ + 1$ , 9 %), 126 (100 %), 125 (19 %), 124 (8 %).  $\delta_H$  (D<sub>2</sub>O): 6.6-6.7 (3H, m, 2-H, 4-H, 6-H), 7.0-7.2 (1H, m, H-5).  $\delta_C$  (D<sub>2</sub>O): 63.2 (p, J 44, CD<sub>2</sub>OH), 115 (C4), 116 (C6), 119 (C2), 130 (C5), 142 (C3), 158 (C1).

#### **6.1.5.4 Preparation of [2,4,6,7,7-<sup>2</sup>H<sub>5</sub>]*m*-hydroxybenzyl alcohol (5.29b)**



[7,7-<sup>2</sup>H<sub>2</sub>]*m*-Hydroxybenzyl alcohol (0.61 g, 4.87 mmol), deuterium oxide (5 ml) and conc. deuteriosulphuric acid (1 drop) were placed in a carius tube which was heated to 120 °C, 1.52 x 10<sup>7</sup> Pa, for 3 h. The material was filtered and neutralised with aqueous sodium hydroxide (0.01 M), and the water removed on a freeze drier. Purification over silica (ethyl acetate / dichloromethane 9 : 1) gave [2,4,6,7,7-<sup>2</sup>H<sub>5</sub>]*m*-hydroxybenzyl alcohol as a white solid, (0.51 g, 83 %) m.p. 69-70 °C (lit. non. deuterated 67-68 °C)<sup>8</sup>,  $\nu_{max}$ : 3358, 3053, 2946, 1587, 1497, 1390, 1283, 1244, 1084, 1077, 779.  $m/z$  (EI+) 130 ( $M^+ + 1$ , 94 %), 129 (30 %), 128 (48 %), 127 (36 %), 126 (17 %), 125 (5 %).  $\delta_H$  (D<sub>2</sub>O): 6.6-6.7 (3H, m, 2-H, 4-H, 6-H, 20 % of signal remains), 7.0-7.2 (1H, m, H-5, 100 % of signal remains).  $\delta_D$  (H<sub>2</sub>O): 4.4 (2D, CD<sub>2</sub>OH), 6.7 (2.4 D, 2-D, 4-D, 6-D, 81% deuterated)  $\delta_C$  (D<sub>2</sub>O): 63.2 (p, J 44, CD<sub>2</sub>OH), 114.7 (t, J 23, C4), 115.2 (t, J 24, C6), 119.5 (t, J 25, C2), 130.5 (C5), 142.6 (C3), 156.2 (C1).



## **6.2 Biological**

### **6.2.1 General details**

The manipulation of both micro-organisms, *Streptomyces cattleya* and *Xylaria longiana*, was carried out in a Galenkemp flow hood. Surfaces were washed with 70 % ethanol, 30 % water (v/v), and all flask rims flame sterilised. Glassware, media and consumables were sterilised in a portable gas heated autoclave at 121°C and  $1.46 \times 10^9$  Pa for 20 minutes. Liquid volumes greater than 100 ml were sterilised for 50 minutes. Supplementation of extraneous materials to culture broths was performed through sterilised 0.2 µm filters.

### **6.2.2 *Streptomyces cattleya***

An authentic culture of *Streptomyces cattleya* NRRL 8057 was obtained from Professor D. Harper, The Queen's University of Belfast, microbial Biochemistry Section, Food Science Department, Belfast (originally from United States Department of Agriculture, Agricultural Research Service, Midwest Area Northern Regional Research Laboratories, Peoria, Illinois, USA).

#### **6.2.2.1 Agar**

Cultures were maintained on agar slants containing soybean flour (2% w/v), mannitol (2% w/v), agar (1.5% w/v) and deionised water. The slants were grown for 14 days at 28 °C before the static cultures were sealed and stored at 4 °C.

### **6.2.2.2 Starter and batch cultures**

Starter and batch cultures of *S. cattleya* were grown on chemically defined media, which was prepared by combining previously mixed and sterilised stock solutions.

**Ion solution**, sterilised by autoclaving

NH<sub>4</sub>Cl (6.75 g), NaCl (2.25 g), MgSO<sub>4</sub>·7H<sub>2</sub>O (2.25 g), CaCO<sub>3</sub> (1.13 g), FeSO<sub>4</sub>·7H<sub>2</sub>O (0.11 g) CoCl<sub>2</sub>·6H<sub>2</sub>O (45 mg), ZnSO<sub>4</sub>·7H<sub>2</sub>O (45 mg) and distilled water (900 ml)

**Carbon source solution**, sterilised by filtration (Nalgene filter sterilisation units) in 75 ml portions into presterilised Schott bottles.

Glycerol (45 g), monosodium glutamate (22.5 g), *myo*-inositol (1.8 g), *para*-aminobenzoic acid (450 µl of freshly prepared 1 mg / 1 ml solution) and distilled water (450 ml).

**Phosphate buffer solution**, sterilise by autoclaving.

KH<sub>2</sub>PO<sub>4</sub> (20 g / l), pH adjusted to 7.00 (± 0.02) with KOH (2 M)

**Fluoride solution**, sterilised by autoclaving.

NaF (0.5 M)

The prepared and sterilised solutions (ion solution (150 ml), carbon source solution (75 ml), phosphate buffer solution (75 ml), fluoride solution (3 ml)) were mixed with distilled water (450 ml) that had been sterilised in a 1 l Erlenmeyer flask. An aliquot of the resultant solution (90 ml) was decanted into a 500 ml Erlenmeyer flask and subsequently inoculated with a loop of vegetative mycelium from an agar slant. The remainder of the medium was stored at 4 °C until required. The starter culture was incubated at 28 °C for four days, on an orbital shaker at 175 rpm. Portions of the remaining defined medium (90 ml) were decanted into sterile 500 ml Erlenmeyer flasks and warmed to 28 °C. The flasks were inoculated from the starter culture (0.3 ml) and then incubated for 8 days at 28 °C on an orbital shaker at 175 rpm.

### **6.2.2.3 Resting cell experiments with *S. cattleya***

Resting cell experiments were performed under aseptic conditions. All the equipment and solutions were sterilised prior to use. All manipulations were carried out in a laminar flow hood. Cells were harvested by centrifugation (25 minutes, 14,000 rpm, 25 °C) and the pellet washed three times by resuspension in 100 ml of 50 mM MES (morpholineethanesulphonic acid monohydrate) buffer at pH 6.50 ( $\pm 0.02$ ) followed by centrifugation and further resuspension. Once fully washed, the bacterial pellet was resuspended in 50 mM MES buffer at a concentration of 0.18 g/ ml (wet weight). 45 ml of the resultant cell suspension was pipetted into a 500 ml Erlenmeyer flask. Sodium fluoride solution (3 ml, 40 mM) and further MES buffer (48 ml) were added to the flask. The deuterated precursor (3 ml, 200 mM), sterilised by membrane filtration, was then added to the cell suspension and the cells then incubated at 28 °C for 48 h on an orbital shaker at 175 rpm.

#### **[2,2,3,3-<sup>2</sup>H<sub>4</sub>]-Succinate**

A solution of [2,2,3,3-<sup>2</sup>H<sub>4</sub>]-succinate (200 mM in sterile 50 mM MES buffer and adjusted to pH 6.50  $\pm 0.02$  with 2M KOH) was filter sterilised and administered to resting cells of *S. cattleya* at a final concentration of 8.7mM.

#### **(1S, 2R)-[1-<sup>2</sup>H]-Glycerol**

A solution of (1S, 2R)-[1-<sup>2</sup>H]-glycerol (200 mM in sterile 50 mM MES buffer) was filter sterilised and administered to resting cells of *S. cattleya* at a final concentration of 8.7mM.

#### **(1R, 2R)-[1-<sup>2</sup>H]-Glycerol**

A solution of (1R, 2R)-[1-<sup>2</sup>H]-glycerol (200 mM in sterile 50 mM MES buffer) was filter sterilised and administered to resting cells of *S. cattleya* at a final concentration of 8.7mM.

### **6.2.2.4 Harvesting fluoroacetate**

After 48 h of incubation with the deuterated precursors, the fluoroacetate produced by the cells was harvested by centrifuging the cells at 14,000 rpm at 25 °C for 25 minutes, decanting off the supernatant and freeze drying it. The pH or the freeze dried supernatant

was first adjusted to pH  $3.00 \pm 0.02$  with 2 M H<sub>2</sub>SO<sub>4</sub>, and the material lyophilised to remove most of the sodium fluoride (pK<sub>a</sub> = 3.45). The residual material was then further acidified to pH 2.5 and lyophilised once more to extract the fluoroacetate (pK<sub>a</sub> 2.59), the fraction containing the fluoroacetic acid was adjusted to pH  $6.00 \pm 0.02$  using 0.02 M NaOH and the resultant solution freeze dried once more.

### **6.2.3 *Xylaria longiana***

An authentic culture of *X. longiana* was obtained from Raymond L. Edwards (University of Bradford) and initiated onto agar slants. Aqueous cultures were maintained in 200 ml of medium, prepared (as indicated below) from commercially available materials, in 400 ml Thompson bottles, stoppered with tightly wound cotton wool. Cultures were kept in a constantly illuminated incubator at 28°C, and harvested after 4 weeks growth. Inoculation was achieved by adding aqueous solution containing fungal mycelia (1 ml) to the culture medium, under sterile conditions.

#### **6.2.3.1 Agar**

Warm distilled water (250 ml) was added to malt extract (7.5 g, Oxoid) and agar powder (3.75 g). The powder was fully dissolved, stirring and heating the mixture as required. The pH of the medium was not adjusted. The sterilised agar gel was allowed to cool to  $\approx 60^\circ\text{C}$  before pouring into sample bottles and allowing it to set at an angle. *Xylaria longiana* was inoculated onto the cooled slant by first scraping the agar, to produce a rough surface, and then by adding 0.2 ml of starter culture medium from an existing culture of 8 weeks of age, or more. The *Xylaria longiana* was stored on the agar slants at 28°C until required to inoculate a starter culture.

#### **6.2.3.2 Culture medium**

Distilled water (200ml) was added to malt extract (6 g, Oxoid) and glucose (12 g) The pH of the medium was not adjusted. The medium was placed into a Thompson bottle and sterilised. Cultures were inoculated from an existing starter culture, that was at least 8 weeks old, by the addition of 1 ml of the culture medium. The cultures were incubated at a temperature between 23 and 28°C.

### **6.2.3.3 Feeding of labelled precursors to *X. longiana***

#### **[1,2-<sup>13</sup>C<sub>2</sub>]-Acetate**

A 23 day old culture of *X. longiana* was pulse fed [1,2-<sup>13</sup>C<sub>2</sub>]-acetate, on 3 consecutive days, to a final concentration of 7 mM. The culture was incubated for a further 27 days before harvesting.

#### **[2,4,6-<sup>2</sup>H<sub>3</sub>]*m*-Cresol (5.28 a)**

A culture of *X. longiana* was pulse fed [2,4,6-<sup>2</sup>H<sub>3</sub>]*m*-cresol at an age of 23 days and at 29 days to a final concentration of 7 mM. The fungus looked very unhealthy for a considerable period of time following the feeding of the *m*-cresol, and was thus incubated for a further 88 days before work up.

#### **[3,5-<sup>2</sup>H<sub>2</sub>]- 6-Methylsalicylic acid (5.27 a)**

A culture of *X. longiana* (in 200 ml of culture medium) was pulse fed [3,5-<sup>2</sup>H<sub>2</sub>]- 6-methylsalicylic acid dissolved in methanol (0.5 ml) at an age of 23 days and at 29 days to a final concentration of 7 mM. Again the fungus appeared unhealthy and stopped growing for a considerable period of time, and was thus incubated for a further 60 days before harvesting.

#### **[7,7-<sup>2</sup>H<sub>2</sub>]*m*-Hydroxybenzylalcohol (5.29 a)**

A 23 day old culture of *X. longiana* was pulse fed [7,7-<sup>2</sup>H<sub>2</sub>]*m*-hydroxybenzylalcohol, on 3 consecutive days, to a final concentration of 7 mM. The culture was incubated for a further 27 days before harvesting.

#### **[2,4,6,7,7-<sup>2</sup>H<sub>5</sub>]*m*- Hydroxybenzylalcohol (5.29 b)**

A 23 day old culture of *X. longiana* was pulse fed [2,4,6,7,7-<sup>2</sup>H<sub>5</sub>]*m*-hydroxybenzylalcohol, on 3 consecutive days, to a final concentration of 7 mM. The culture was incubated for a further 27 days before harvesting.

### **6.2.3.4 Extraction of longianone from *X. longiana***

The fungal mycelia were removed from the culture broth by reduced pressure filtration, and washed with ethyl acetate (2 x 25 ml). The filtrate was extracted into

ethyl acetate (3 x 300 ml), the ethyl acetate portions were combined, dried over magnesium sulphate and the solvent removed under reduced pressure, taking care that the temperature of the extract should never exceed 35°C. The sticky brown components from the fungal broth, which coated the crude crystals of longianone, were removed by dissolving the entire extract into DCM (20 ml) loading the solution onto a dry column of silica gel and eluting with DCM (20 ml), and then with ethyl acetate (20 ml). The second fraction containing longianone (on average, 150 mg). The solvent was removed under reduced pressure and the longianone left to crystallise at room temperature.

$\nu_{max}$  (KBr): 1790, 1709.  $m/z$   $\delta_H$  (CDCl<sub>3</sub>): 2.71 (1H, d, J 18.3), 3.04 (1H, d, J 18.3), 4.40 (2H, s), 5.83 (1H, d, J 2.6), 8.32 (1H, d, J 2.6).  $\delta_C$  (CDCl<sub>3</sub>): 37.7, 74.0, 89.5, 106.9, 172.4, 177.7, 199.2.

### **6.3 The preparation of samples for analysis by chiral liquid crystal**

#### **<sup>2</sup>H-NMR**

PBLG (120 mg, DP~800, MW 150,000-350,000) was weighed into an NMR tube (5mm in diameter). The deuterated sample was weighed into the NMR tube (for hexyl fluoroacetate 3 mg was used, for the fluoroalkanes 30 mg was used). Chloroform (803 mg, dried over molecular sieves) was finally added to the NMR tube. The tube was left for 2 h to allow the PBLG to dissolve. The contents of the tube were mixed thoroughly by drawing the material from one end of the NMR tube to the other, 40 times, by application of a centrifugal force. Following centrifugation the NMR tubes were weighed and sealed. The <sup>2</sup>H-NMR of the samples were run immediately after mixing, before homogeneity could be lost. Experiments were performed at the Institut de Chimie Moléculaire d'Orsay, Université de Paris Sud, France on a Bruker AC-250, and some repeated at the University of Durham on a Unity Inova 500 MHz. Gradient shimming was employed to increase the resolution of the spectra.

## References

- 1 V. M. Mićović and M. L. Mihailović *J. Org. Chem.*, 1953, **18**, 1190.
- 2 M. M. Midland, S. Greer, A. Tramontano, S. A. Zderic, *J. Am. Chem. Soc.*, 1979, **101**, 2352.
- 3 W. J. Middleton, *J. Org. Chem.*, 1975, **40**, 574
- 4 J. Nieschalk, D. O'Hagan, *Tetrahedron Asymm.*, 1997, **8**, 2325
- 5 F. M. Hauser, S. A. Pogany, *Synthesis*, 1980, 814
- 6 Anslow, Raistick, *Biochem J.*, 1931, **25**, 39
- 7 K. Wahala, I. Ojanpera, L. Hayri, T. A. Hase, *Synth. Commun.*, 1987, **17**, 137.
- 8 P. Haberfield, J. Kivuls, M. Huddad, T. Rizzo, *J. Phys. Chem.*, 1984, **88**, 1913.

## Appendix I: List of conferences attended

December 1997	Post-graduate Bioorganic symposium, Cardiff
July 1998	Polyketides II: Chemistry, Biochemistry and Molecular Genetics, Bristol ( <i>poster presentation</i> )
December 1998	Cambridge Polyketides meeting
January 1999	Post-graduate Bioorganic symposium, Leicester
July 1999	Cambridge Polyketides meeting ( <i>spoken presentation</i> )
December 1999	Cambridge Polyketides meeting
December 1999	Post-graduate Bioorganic symposium, Oxford ( <i>poster presentation</i> )
February 2000	Queen's University Belfast ( <i>spoken presentation</i> )
August 2000	RSC Natural Products meeting, Nottingham ( <i>poster presentation</i> )



## **Appendix II: Publication**

**Biosynthesis of longianone from *Xylaria longiana*: a metabolite with a biosynthetic relationship to patulin**

R. J. M. Goss, J. Fuchser, D. O'Hagan, *Chem. Comm.*, 1999, 2255.

# Biosynthesis of longianone from *Xylaria longiana*: a metabolite with a biosynthetic relationship to patulin

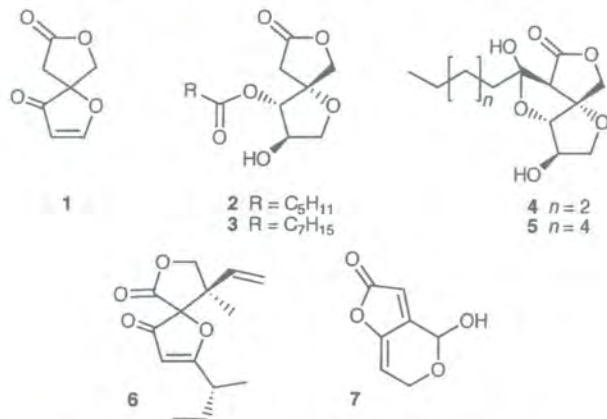
Rebecca J. M. Goss, Jens Fuchser and David O'Hagan\*

Department of Chemistry, Science Laboratories, South Road, Durham, UK DH1 3LE.  
E-mail: david.o'hagan@durham.ac.uk

Received (in Cambridge, UK) 9th September 1999, Accepted 1st October 1999

Longianone, a metabolite of *Xylaria longiana*, is an isomer of the well known fungal toxin, patulin; it is demonstrated that longianone is biosynthesised from 6-methylsalicylic acid in a pathway closely related to that found in patulin biosynthesis.

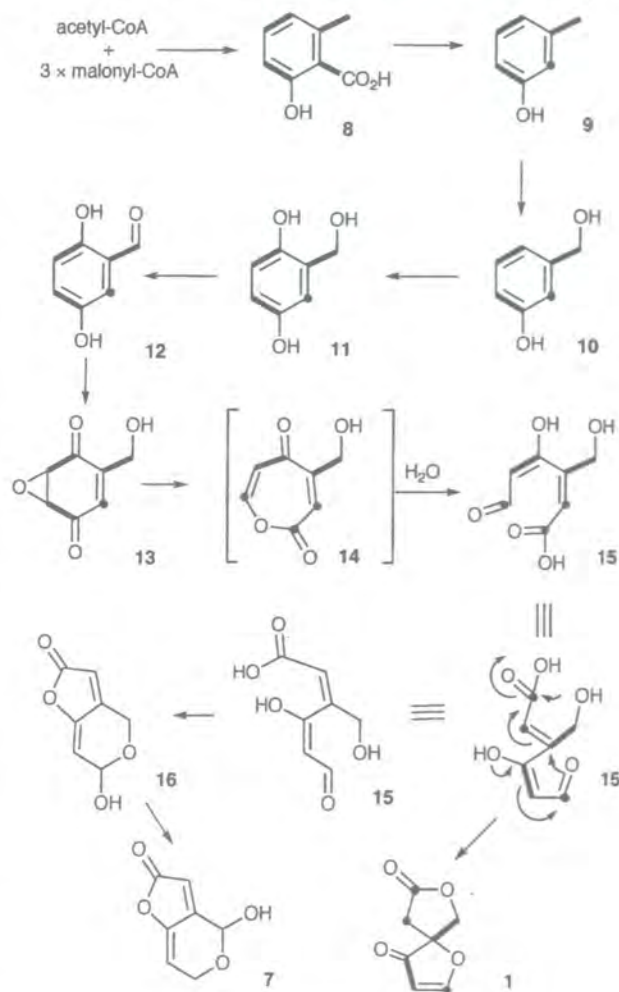
The isolation and structure of the metabolite longianone **1** was recently reported from *Xylaria longiana*.<sup>1</sup> Longianone **1** possesses an intriguing spiro-bicyclic ring structure (1,7-dioxaspiro[4,4]non-2-ene-4,8-dione).



It is optically active, however the absolute configuration of the natural product is unknown at present. Structurally, longianone **1** represents a rare parent ring system. The only related bicyclic ring systems are the secosyrins **2** and **3** and their more elaborated co-metabolites, the syringolides **4** and **5**, metabolites of the bacterium *Pseudomonas syringia* pv. *tomato*.<sup>2,3</sup> A biosynthesis has been proposed<sup>3</sup> for the secosyrins **4** and **5** which involves the combination of a polyketide chain with a pentose sugar moiety, however this is not based on experimental evidence. Another related ring system is found in the hyperlactones A–C **6** isolated from *Hypericum chinensis*.<sup>4</sup> However, in that case the ester functionality occupies a different site in the ring system and the hyperlactones are clearly terpenoid in origin and have no biosynthetic relationship to longianone **1** or the secosyrins. It is noteworthy that longianone **1** has a structural formula (C<sub>7</sub>H<sub>6</sub>O<sub>4</sub>) which is isomeric with the fungal mycotoxin, patulin **7**. Patulin **7** has an intriguing biosynthetic origin derived from oxidative ring opening of the aromatic polyketide metabolite, 6-methylsalicylic acid (6-MSA) **8**<sup>5–8</sup> and the pathway to patulin biosynthesis is illustrated in Scheme 1. The interesting structure of longianone **1** and its constitutional relationship to patulin **7** stimulated us to initiate a biosynthetic investigation of **1** from *X. longiana*.

An initial experiment involved feeding [1,2-<sup>13</sup>C<sub>2</sub>]acetate to static cultures of *X. longiana*.<sup>1</sup> This resulted in a low (0.4%) but detectable incorporation of isotope into the resultant longianone **1**. <sup>13</sup>C NMR analysis revealed reciprocal couplings between C-3/C-4 (*J*<sub>13C-13C</sub> = 55 Hz) and C-5/C-6 (*J*<sub>13C-13C</sub> = 34 Hz) of **1**, indicating the incorporation of two intact acetate units. This was the first indication of a polyketide origin, and the labelling

pattern was consistent with the intermediacy of 6-MSA **8** and a similarity to patulin biosynthesis, as illustrated in Scheme 1. In order to reinforce this hypothesis an experiment with [3,5-<sup>2</sup>H<sub>2</sub>]-6-MSA **8a** was conducted. A sample of ethyl 2-hydroxy-6-methylbenzoate was synthesised following an established route,<sup>9</sup> then deuterium was exchanged into the aromatic nucleus by refluxing with DCl, D<sub>2</sub>O and MeOD for 24 h and the ester was hydrolysed to [3,5-<sup>2</sup>H<sub>2</sub>]-6-MSA **8a** by refluxing with NaOH. The subsequent feeding experiment resulted in a sample of longianone which was enriched with deuterium (<sup>2</sup>H NMR analysis) at C-2 [Fig. 1(b)]. There was a minor enrichment at C-3 arising from some exchange into the aromatic precursor **8a** at C-4 during isotope exchange [Fig. 1(b)]. *m*-Cresol **9** and *m*-hydroxybenzyl alcohol **10** are established intermediates in patulin biosynthesis<sup>7</sup> and in order to assess if they have a role in longianone biosynthesis they were each prepared enriched with deuterium, and fed in separate experiments to *X. longiana* cultures. An experiment with [2,4,6-<sup>2</sup>H<sub>3</sub>]-*m*-cresol **9a**, prepared



Scheme 1

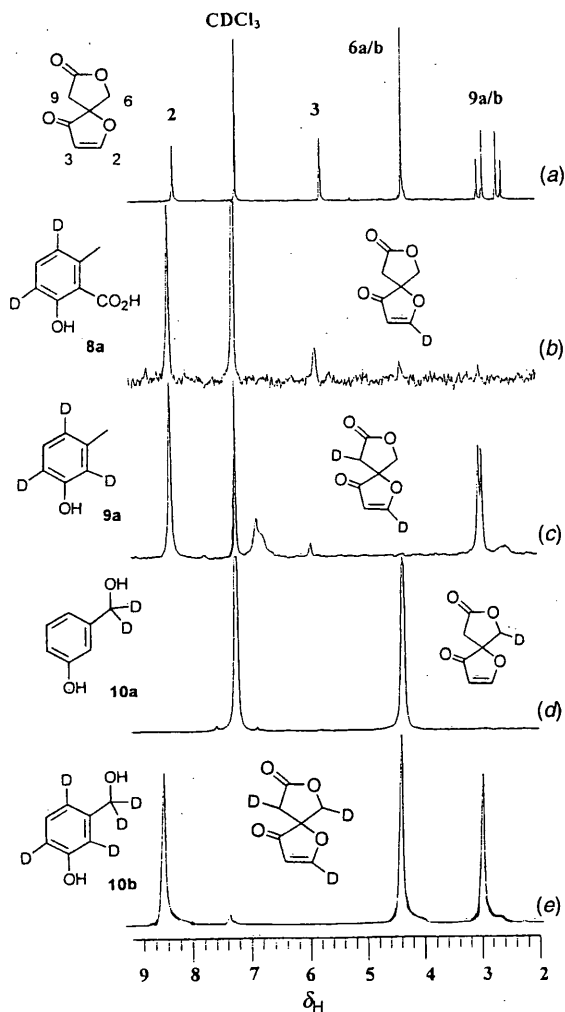
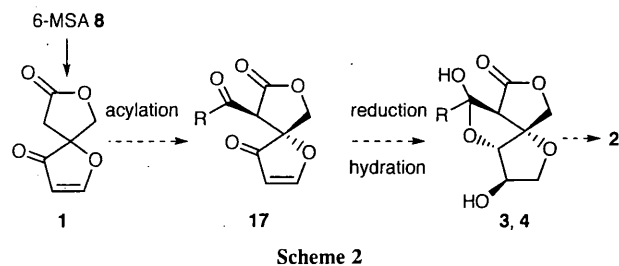


Fig. 1 (a)  $^1\text{H}$  NMR ( $\text{CDCl}_3$ ) spectrum and assignment of longianone 1; (b)  $^2\text{H}$  NMR ( $\text{CHCl}_3$ ) spectrum of 1 after feeding 8a; (c)  $^2\text{H}$  NMR ( $\text{CHCl}_3$ ) spectrum of 1 after feeding 9a; (d)  $^2\text{H}$  NMR ( $\text{CHCl}_3$ ) spectrum of 1 after feeding 10a; (e)  $^2\text{H}$  NMR ( $\text{CHCl}_3$ ) spectrum of 1 after feeding 10b.

by reaction with  $\text{PBr}_3$  and  $\text{D}_2\text{O}$ ,<sup>10</sup> resulted in deuterium incorporation into 1 at C-2 and C-9 as determined by  $^2\text{H}$  NMR [Fig. 1(c)]. The methylene hydrogens at C-9 are diastereotopic and well resolved by NMR, and the resulting  $^2\text{H}$  NMR spectrum after feeding 9a indicated a stereospecific enrichment into C-9, however upon storage (3 months) a slow racemisation was witnessed. Incorporation of 3-hydroxy[ $\alpha,\alpha\text{-}^2\text{H}_2$ ]benzyl alcohol 10a, prepared by reducing methyl 3-hydroxybenzoate with  $\text{LiAlD}_4$ , resulted in labelling at C-6 in 1 [Fig. 1(d)]. It was not clear from this latter experiment whether both deuterium atoms were processed through to the C-6 methylene group of longianone 1 as these deuterium atoms, which are formally diastereotopic, have nonetheless similar chemical shifts in the resultant  $^2\text{H}$  and  $^1\text{H}$  NMR spectra. In order to gain information on this issue a second experiment was carried out using 10b, which was prepared with deuterium atoms located both at the hydroxymethyl group and at C-2, C-4 and C-6 of the aromatic ring. The resultant  $^2\text{H}$  NMR spectrum [Fig. 1(e)] of longianone 1 showed three clear enrichments at C-2, C-6 and C-9, with similar intensities. We have drawn the conclusion therefore that only one deuterium atom from the methylene group of 3-hydroxybenzyl alcohol 10b became incorporated into the C-6 methylene group of longianone and therefore the hydroxymethyl group is oxidised up to the aldehyde level during the biosynthesis.

The isotopic labelling experiments reveal a common biosynthetic pathway to both longianone 1 and patulin 2 which



diverges at a late stage. Both metabolites are derived from 6-MSA 8 and have 9 and 10 as common biosynthetic intermediates. Also oxidation of the hydroxymethyl group to the aldehyde level is revealed as common to both cases and the aromatic ring is cleaved across the same bond. The conversion of gentisaldehyde 12 to phyllostine 13 is a biochemically characterised step<sup>11</sup> in patulin biosynthesis and the intermediacy of neopatulin (also termed isopatulin) has been established from mutant studies,<sup>8</sup> so reasonably the pathway progresses through 14<sup>12</sup> with hydrolysis to 15. Different *E/Z* isomers of 15 emerge as the likely branchpoint of the two pathways, with straightforward ester and intramolecular Michael-type cyclisations to generate both rings of longianone. An alternative cyclisation of 15 (ester and hemiacetal formations) generates neopatulin 16 which is a precursor to patulin 7 requiring an oxidation and a reduction. Perhaps longianone 1 is a shunt metabolite of an organism which has lost the capacity to complete patulin 7 biosynthesis.

In view of the above experimental evidence an alternative hypothesis to that recently proposed<sup>2,3</sup> emerges for the biosynthesis of the secosyrins 2 and 3 and the syringolides 4 and 5. This would involve an origin from a longianone skeleton derived from 6-MSA, followed by acylation  $\alpha$  to the lactone to generate intermediate 17, as illustrated in Scheme 2. Elaborations such as reduction and hydration would generate 4 and 5 and a retro-aldol reaction would generate 2 and 3. It remains to be determined whether this or the previous proposal<sup>3</sup> is the more valid for the biosynthesis of those metabolites.

We thank Dr Raymond L. Edwards of the University of Bradford for providing a strain of *Xylaria longiana* and Ian McKeag of the University of Durham for  $^2\text{H}$  NMR analysis. The EU and Isle of Man Education Authority is gratefully acknowledged for a Studentship (R. J. M. G.).

## Notes and references

- R. L. Edwards, D. J. Maitland, C. L. Oliver, M. C. Pacey, L. Shields and A. J. S. Whalley, *J. Chem. Soc., Perkin Trans. 1*, 1999, 715.
- S. L. Midland, N. T. Keen and J. J. Sims, *J. Org. Chem.*, 1995, 60, 1118.
- S. L. Midland, N. T. Keen, J. J. Sims, M. M. Midland, M. M. Stayton, M. J. Smith, E. P. Mazzola, K. J. Graham and J. Clardy, *J. Org. Chem.*, 1993, 58, 2940.
- M. Tada, M. Nagai, C. Okumura, J. Osano and T. Matsuzaki, *Chem. Lett.*, 1989, 683.
- H. Iijima, H. Noguchi, Y. Ebizuka, U. Sankawa and H. Seto, *Chem. Pharm. Bull.*, 1983, 31, 362.
- S. W. Tanenbaum and E. W. Bassett, *J. Biol. Chem.*, 1959, 234, 1861.
- A. I. Scott and M. Yalpani, *J. Chem. Soc., Chem. Commun.*, 1967, 945.
- J. Sekiguchi, G. M. Gaucher and Y. Yamada, *Tetrahedron Lett.*, 1979, 41.
- F. M. Hauser and S. A. Pogany, *Synthesis*, 1980, 814.
- K. Wähälä, I. Ojanperä, L. Häyri and T. A. Hase, *Synth. Commun.*, 1987, 137.
- J. Sekiguchi and G. M. Gaucher, *Biochemistry*, 1978, 17, 1785.
- M. Bennet, G. B. Gill, G. Pattenden, A. J. Shuker and A. Stapleton, *J. Chem. Soc., Perkin Trans. 1*, 1991, 929.

Communication 9107311F

